Green synthesis of Carbon Nanodots and its Theranostic and Bio-sensing Applications

Dissertation submitted in partial fulfilment of the requirements for the degree of

Doctor of Philosophy
In

MATERIALS ENGINEERING
By
SOMEDUTTA MAITY

(16ETPM03)

Under the guidance of

Dr. PRADIP PAIK &
Prof. M. GHANASHYAM KRISHNA



SCHOOL OF ENGINEERING SCIENCES AND TECHNOLOGY UNIVERSITY OF HYDERABAD HYDERABAD-500046 INDIA

March 2023

Dedicated

To

Maa, Baba, husband

&

Grandfather

DECLARATION

I declare that the thesis entitled "Green synthesis of Carbon Nanodots and its Theranostic

and Bio-sensing Applications" submitted to the University of Hyderabad for the award of

Doctor of Philosophy (Ph.D) in Materials Engineering is original and the work was carried out

by me during my tenure as a Ph.D scholar under the supervision of **Dr.Pradip Paik**, Associate

Professor presently at IIT-BHU and Prof. M. Ghanashyam Krishna, Professor at the

University of Hyderabad, INDIA. This dissertation has not submitted for the award of any

other degree, diploma, membership or similar title of any university or institution. Finally,

plagiarism of this dissertation has been checked and satisfied the requirements.

SOMEDUTTA MAITY

SCHOOL OF ENGINEERING SCIENCES AND TECHNOLOGY,

UNIVERSITY OF HYDERABAD,

HYDERABAD-500046

INDIA.

Place: HYDERABAD

Date:

CERTIFICATE



This is to certify that the dissertation entitled "Green Synthesis of Carbon Nanodots and its Theranostic and Bio-Sensing Applications" submitted by SOMEDUTTA MAITY bearing Reg. No. 16ETPM03 in partial fulfilment of the requirements for the award of Doctor of Philosophy in the School of Engineering Sciences and Technology in Materials Engineering, is a Bonafide record of research work carried out by her under my supervision and guidance.

The contents of this dissertation have been filled patents or published in peered reviewed journals with following references:

A. Patent filed:

- [1] A method of synthesizing carbon dots and a product thereof, (Application No.:202011018557, Dated: 30th April, 2020).
- [2] New therapeutic Nano medicine for the treatment of breast cancer Application No:

202111060434, Dated: 23rd December 2021.

B. Publication in journal:

- [3] Maity, Somedutta *et.al.*, *ACS Biomaterial*. *Sci. Eng*. 2022, 8, 8, 3608–3622. (doi.org/10.1021/acsbiomaterials.2c00463).
- [4] Maity, Somedutta et.al., "Green synthesis of Carbon Nano dots from Kernel part of *Azadirachta Indica* seeds: selective detection of biologically relevant metal ions and drug delivery applications (communicated, year 2023)

C. Presentation in conferences:

- [5] <u>Somedutta Maity</u>, Presented (Poster) in "Nanotechnology for Better Living" April 6-7, 2019 **IIT Kanpur.**
- [6] <u>Somedutta Maity</u>, Presented (Poster) Third International Conference on Advanced Materials (ICAM 2019) 9-11 August 2019 at Mahatma Gandhi University, Kottayam, Kerala, India.

[7] <u>Somedutta Maity</u> Presented (Poster) Advances in polymer science and rubber technology, September 24-27, 2019 (APSRT,) IIT Kharagpur, India.

Prof. M. GHANASHYAM KRISHNA
Centre for Advanced Studies in

Electronics Science & Technology
School of Physics, University of Hyderabad
PHYSICARPAD SCA 046 Telangana, India

Posadif Paik

Further, the student has passed the following courses towards the fulfillment of coursework required for Ph.D.

SLNo	Course No	Title of the Course	Credits	Pass/Fail
1	MT-801	Thermodynamics and Phase Equilibria	04	Pans
2	MT-802	Characterization of Materials - Microscopy	04	Pass
3	MT-803	Introduction to Nanoscience& Engineering	04	Pass
4	MT-804	Composites	04	Pass
5	MT-805	Mechanical Behabiour of Materials	02	Pass
6	MT-806	Concepts in Materials Science and Engineering	04	Pass
7	МТ-807	Materials processing and Characterization Laboratory	04	Pass
8	MT-808	Advanced Engineering Mathematics	04	Pass
9	MT-854	Materials Characterization-	04	Pass
10	MT-855	Materials Processing and Characterization Laboratory	04	Pass
11	MT-860	Nano Biomaterials/ Nano Biotechnology	04	Pass
12	MT-801	Research Methodology	04	Pass

Supervisor Taik

Dr Pradip Paik

M. Thomashyam. Supervisor

Prof. M. GHANASHYAM KRISHNA Prof. Ghanashyam Krishnaies in Electronics Science & Technology School of Physics, University of Hyderabad HYDERABAD-500 046. Telangana, India.

Prof. Dibakar Das

School of Engineering Sciences and Technology University of Hyderabad 500 046.

ACKNOWLEDGEMENTS

I am grateful to many people for their assistance and encouragement prior to and throughout my Ph.D tenure. My achievement in research is in no small part due to their input and feedback on many occasions.

First and foremost, I would like to express my sincere gratitude to my supervisor Dr. Pradip Paik Associate Professor for the continuous support during my Ph.D study and research, for his motivation, enthusiasm, and immense knowledge and continuous guidance helped me in all the time of research and writing of this thesis. I am equally grateful to Prof. Ghanashyam Krishna for the dynamism, vision, sincerity and motivation has deeply inspired me.

My doctoral review committee member Dr. Swati Ghosh Acharyaa (SEST) has also been helpful and supportive over this period. I am extremely grateful to Dean of the School of Engineering Sciences and Technology (Prof. Dibakar Das) and the other faculties in the Department for providing me the facilities and the guidance to carry out my research work.

I feel fortunate enough to have had the opportunity to collaborate my research work with Dr. Munendra Singh Tomar and Singh, Monika Post Doc IIT (BHU).

I thank my seniors from University of Hyderabad specially Dr. Himadri Medhi, Dr. Santosh Kumar, Dr. Monami Das Modak for being my support system and encouragement. I am also indebted to my lab mates from IIT (BHU) Kirti Wasnik, Prem Shankar Gupta, Sukanya Patra, Divya Pareek, Gurmeet Singh and Desh Deepak yadav. I am thankful for them to help me during my long time spending at IIT (BHU) to carry out the work.

I would also like to thank the technicians and non-teaching staff of SEST.I would like to thank Dr. Sunil, Dr. Kamal, Ms Supriya, Ms Nabanita for their encouragement and help.

Special and profound thanks to Dr. Gargi Saha always showed light in the dark.

Last but not the least, I would like to thank my family: my parents Mrs.Suravi Maity and Mr.Kashi Nath Maity, for their love, prayers, caring and sacrifices for educating and preparing me for my future.

I am very much thankful to my husband Ramesh Koduru for understanding, prayers and his continuous support to complete this research work. My Special thanks goes to my aunty, sister, and brother in law, friend specially Rajshekher, Arpita, Suvhoshree for their keen interest shown to complete this thesis successfully.

Finally, my thanks go to all the people who have supported me to complete the research work directly or indirectly.

CONTENTS

Title page	Page No.
Acknowledgments	
Contents	viii-xiii
List of Figures	xiv-xvii
List of Tables	xviii-xix
Abbreviations	xx-xxi
List of Publications	xxii-xxiv
Abstract	xxv-xxix
CHAPTER-I INTRODUCTION AND LITERATURE REVIEW	1
1.1. Background	2
1.2. Different types of nanoparticles and their synthesis	3
1.2.1 Polymer nanoparticles	3
1.2.2 Metallic nanoparticles and Metal oxide nanoparticles	5
1.2.3 Quantum dots	8
1.2.4 Carbon dots (CDs)	9
(Only basic of CDs)	
1.3. Nano particles for biomedical applications	10
1.3.1 Drug delivery	10
1.3.2 Cancer therapy	12
1.3.3 Imaging and Diagnosis	13
1.3.4 Theranostic applications	14
1.3.5 Molecular detection	15
1.3.6 Biosensors	15
1.3.7 Antibacterial effects	16
1.4. Special emphasized on Carbon dots, and their application in biology a uses	

1.4.1 Synthesis, characterization, methods of reported CDs and drawback of t method	_
1.4.2 CDs for Nanomedicine	18
1.4.3 CDs for Nanotoxicity	19
Factors affecting toxicity of CD nanomaterials and other nanomaterials	
1.5 Overview of cancer	20
1.5.1 Types of cancer	21
1.5.2 Path physiology of cancer	21
1.5.3 Causes of Cancer	
1.5.4.Cancer statistics (Indian & Global scenarios)	24
1.6 Carbon dots nanomaterials for therapy	
1.6.1 Carbon dot for imaging	28
1.6.2 Carbon dots for Treatment of cancer	29
1.6.3 Carbon dot for Biosensor	29
1.6.4 Carbon dot for Selective detection of biologically relevant metal ions	30
Sodium	30
Potassium	31
Calcium	31
Iron	32
Zinc	32
1.6.5 Selective detection of heavy metal detection	32
Cadmium	33
Arsenic	34
Manganese	34
Aluminium	35
Copper	35
Cobalt	35
Nickol	26

1.7	Antimicrobial	activity	and	basic	mechanism
-----	---------------	----------	-----	-------	-----------

Use of carbon materials for Antibacterial activities	
1.8 Motivation and problem definition of this dissertation based review	
1.9 Objective and scopes of the dissertation	38
Justification of the objectives	
1.10 Organization of thesis	39
CHAPTER II: MATERIALS METHOD & EXPERIMENTAL PROCE	ESS 41
2.1. Materials and Methods	42
2.1.1 List of chemicals used	42
2.1.2 List of solvents used	43
2.1.3 List of Drug used.	44
2.1.4 List of glassware and consumables	44
2.1.5 List of material used in cell culture.	45
2.1.6 List of cells used	46
2.1.7 Bacteria used for antibacterial activity	47
2.2. Experimental section	48
2.2.1. Collection of Neem seed and barks	48
2.2.2. Preparation of cake powder from seed & barks	48
2.2.3. Biohazards and their handling	49
2.3. Instrumentation	50
2.3.1. Synthesis of carbon dots was confirmed by	50
2.3.1.1.FTIR (Fourier transform infrared) spectrometer	51
2.3.3.2. NMR (Nuclear magnetic resonance) (¹ H)	51
2.3.2. Morphology and other physical properties	51

Cont	ents 2.3.2.1. FE-SEM (Field emission scanning electron microscope)	2
	2.3.2.2. TEM (Transmission electron microscopy)	
	2.3.2.3 AFM (Atomic force microscope)	
	2.3.2.4 BET (Brunauer-Emmett-Teller)	
	2.3.2.5 DSC (Differential scanning calorimetry)	
	2.3.2.6 TGA (Thermogravimetric analysis)	
	2.3.2.7 XRD (X-ray diffraction)	
	2.3.2.8 DLS & Zeta Potential	
	2.3.2.9 Multimode plate reader	
	2.3.2.10 Fluorescence Sprectoscoy (FL)	
	2.3.3. Biological studies	
	2.3.3.1. UV-Visible	
	2.3.3.2. LSCM(Laser scanning confocal microscopy)	9
	2.3.3.3 MTT: Cytotoxicity and cell viability	
	2.3.3.4. Flow cytometry (FC)	
	2.3.3.5 Cell culture	
CH A	APTER III: RESULTS AND DISCUSSION6	3
of	1 Azadirachta indica seed-derived carbon Nano capsules:Cell imaging, Depolarization f mitochondrial membrane potential and dose-dependent control death of breas ancer.	t
3.	1.1 Introduction 6	5
3.	1.2 Results and discussions6	8
	3.1.2.1. Morphological characterization	8
	3.1.2.2. Study the Chemical Functionality and Thermal stability	О
	3.1.2.3. BET Surface Area Analysis and Surface Zeta Potential	4
	3.1.2.4. Absorbance and Optical characterization	0
	3.1.2.5. Cytotoxicity and living cell imaging	2
	3.1.2.6. Mitochondrial apoptosis analysis	5

3.1.2.7. Effect of Carbon Nanocapsules on Apoptotic Cell Death through Flow Cytometry	
3.1.3. Summary9	2
3.2. Plant-derived Carbon Nano dots for sensor-based detection of metal ions and it implementation in multiple logic gates	
3.2.1. Introduction	4
3.2.2. Results and discussions9	8
3.2.2.1. Structural confirmation	8
3.2.2.2. Chemical functionality & thermal stability	9
3.2.2.3. Surface properties	0
3.2.2.4. Optical and photoluminescence properties	12
3.2.2.5. Fluorescence quenching	15
3.2.2.6. Biologically relevant metal ion sensing activity	19
3.2.2.7. Drug loading & release study	1
3.2.2.8. Biocompatibility studies	2
3.2.2.9 The synergic effect of CDs with DOX decreases the mitochondrial membran potential (MMP)	
3.2.2.10 The synergic effect of CDs with DOX enhances the apoptotic cell death of MCF-breast cancer cells	
3.2.2.11 Cell Imaging and study the cell morphology	7
3.2.3. Summary	8
3.3 Absorption of metal ions on the high-temperature synthesized metal ions 11	9
3.3.1. Introduction	9
3.3.2. Results and discussions	20
3.3.2.1. Morphology Structural characterization 12	0
3.3.2.2. Chemical Functionality	:3
3.3.2.2. Thermal stability of Carbon dots	:4
3.3.2.4. Structural Properties.	:5
3.3.2.5 BET (Adsorption-desorption) surface area analysis pore size analysis 12	27

Contents 3.3.2.6. Zeta potential and Zeta size	127
3.3.2.7 UV-Vis absorption	
3.3.2.8. Fluorescence heavy metal quenching of carbon dots	
3.3.2.9. Biocompatibility studies	
3.3.3. Summary	
3.4. Revealing the structures of cellulose from bark <i>Azadirachta indic</i> activity, and Their Application: An in vitro study	
3.4.1. Introduction	136
3.4.2. Results and discussions	137
3.4.2.1. Morphology confirmation	
3.4.2.2. Chemical functionality & thermal stability	139
3.4.2.3. Structural & surface zeta potential	140
3.4.2.4. Surface area analysis and pore size	141
3.4.2.5. <i>In vitro</i> antibacterial activity of cellulose nanofibers	142
3.3.3. Summary	143
CHAPTER IV: Summary & conclusions	145
4.1. Conclusions	146

LIST OF FIGURES

CHAPTER -1

Figure 1.1: Schematic representation of Factors affecting the development of cancer
Figure 1.2 Estimated numbers of new cases in 2018, worldwide, including females, and all ages
Figure 1.3: Different types of carbon dots and their example
Figure 1.4: Schematic overview of the thesis work with details and description in each Chapter
CHAPTER: 3
Figure 3.1.1 (A)-(B) TEM micrographs of the mCNCs (SN4), (C) particle size distribution of the mCNCs, and (D) EDAX spectrum of mCNCs
Figure 3.1.2 Particle size and morphology studied through the TEM for the samples: (a) SN-1, (b) SN-2, and (c) SN-369
Figure 3.1.3 (A) FT-IR spectrum for mCNCs (SN4), (B) TGA thermogram for mCNCs (SN4), (C) DSC thermogram of mCNCs (SN4) and (D) XRD pattern of the mCNCs (SN4)
Figure 3.1.4 Schematic shows the FTIR spectrum of the samples: (a) SN-1, (b) SN-2, and (c) SN-3
Figure 3.1.5 Thermal stability studied through TGA for the samples: (a) SN-1, (b) SN-2, and for sample (c) SN-3
Figure 3.1.6 DSC thermograms for the samples: (a) SN-1, (b) SN-2 and (c) SN-3
Figure 3.1.7 XRD pattern for the samples: (a) SN-1, (b) SN-2, and (a) SN-3
Figure 3.1.8 (A) BJH adsorption—desorption isotherm and (B) pore size distribution profile calculated from desorption isotherm, (C) zeta potential profile acquired in a water medium, (D) effect of pH on zeta potential (for sample SN-4), (E) particle size obtained from DLS in a water medium, and (F) Raman spectra of mCNCs, respectively
Figure 3.1.9 BET experiments: BJH adsorption–desorption isotherm for the samples: (A) SN-1, (B) SN-2, and (C) SN-3
Figure 3.1.10 Pore size distribution profile for the samples. Pore size was calculated from BET for (a) SN-1, (b) SN-2, and (c) SN-3
Figure 3.1.11 Zeta potential profile for the samples: (a) SN-1, (b) SN-2, and (c) SN-377
Figure 3.1.12 Effect of pH on zeta potential for the sample (a) SN-1, (b) SN-2, and (c) SN-378
Figure 3.1.13 Particle size obtained from DLS for (a) SN-1, (b) SN-2, (c) SN-3

_		-		-	
\mathcal{C}	~	٠ +	_	↑ +	_
	,,,	"	$\boldsymbol{\mu}$	11	۰.

Figure 3.1.14 Raman spectra for the samples, (a) SN-1, (b) SN-2, (c)SN-3
Figure 3.1.15 (A) UV-vis spectra, (B) PL variation with concentration, (C) effect of pH in luminescent, of the mCNCs (SN4). (D) Fluorescence behavior of the mCNCs (SN4) obtained with an excitation wavelength of 340–420 nm
Figure 3.1.16 UV-Vis spectra for the samples, (a) SN-1, (b) SN-2, (c) SN-3
Figure: 3.1.17 Showing the interaction Nano formulated SN-1, SN-2, SN-3 and SN-4 samples on (A) MCF-7 cells and (B) MDA-MB-231 cells. The red arrows represent the capsules, under fluorescent microscopy.
Figure 3.1.18 (A) Cell viability of normal splenocytes at different concentrations of anocapsules (SN-1, SN-2, SN-3, and SN-4) and (B) cytotoxicity of the mCNCs (SN4) against the MDA-MB-231 and MCF-7
Figure 3.1.19 FACS study for quantifying the depletion of mitochondrial membrane potential by using Rh123. For MCF-7 cells
Figure 3.1.20 FACS study for quantifying the depletion of mitochondrial membrane potential by using Rh123. MDA-MB-231 cells
Figure 3.1.21 Quantitative estimation of mitochondrial membrane potential by using Rh123.MDA-MB-231 and MCF-7 cells
Figure 3.1.22 MCF-7 Cancer cells were treated with carbon nanocapsules (comparison of apoptosis index of SN-1, SN-2, SN-3, and SN-4)
Figure 3.1.23 MDA-MB-231 Cancer cells were treated with carbon nanocapsules (comparison of apoptosis index of SN-1, SN-2, SN-3, and SN-4)
Figure 3.1.24 comparison of apoptosis index of nanocapsules with the MDAMB- 231 & MCF-7 cells
Figure 3.2.1 TEM results of CDs (KS-1),(a)-(c) TEM micrographs at different magnifications, (d) SAED pattern, (e) particle size distribution, and (f) EDAX spectrum of CDs
Figure 3.2.2 (a) FT-IR spectrum, (b) TGA thermogram, (c) DSC, and (d) XRD pattern of the CDs
Figure 3.2.3. Shows the (a) BJH adsorption–desorption isotherm acquired in N ₂ gas, Fig. (b) Pore size distribution of CDs obtained from desorption isotherm, Fig. (c) Particle size results obtained from DLS, Fig. (d) Raman spectra of solid CDs sample and Fig. (e) Zeta Potential results for the CDs in water medium and Fig. (f) ¹ H-NMR spectrum for CDs acquired in CDCl ₃ , 400Hz (KS-1), respectively.
Fig 3.2.4 Figure shows (a) UV-Vis absorption spectrum in water, (b) Fluorescence spectra in different solvents, (c) Photoluminescence variation with differences in pH from 2 to 12, and (d) Fluorescence intensity dependency on temperature variance for synthesized CDs

	tρ	

Figure 3.2.5 (a) Fluorescence spectra of CDs of (100 μg. mL ⁻¹) with different concentrations of Fe ⁺³ . b) Shows the dependence of fluorescence intensity on the CDs at 0-140 μM solution of Fe ⁺³ , Fig.(c) Shows the fluorescence intensity ratios (F-F ₀)/F ₀ of the CDs solution in presence of various metal ions
Figure 3.2.6: Fluorescence spectra of CDs of at 0-140 μM solution with different concentrations of a) Ca ²⁺ b) Na ⁺ c) K ⁺
Figure 3.2.7. (a) Fluorescence spectra of CDs of (100 μg. mL ⁻¹) with different concentrations of Zn ²⁺ .b) Shows the dependence of fluorescence intensity on the CDs at 0-140 μM solution of Zn ²⁺ , Fig.(c) Shows the fluorescence intensity ratios (F-F ₀)/F ₀ of the CDs solution in presence of various metal ions.
Figure 3.2.8. a) Scheme of a simple 'YES' logic gate, b) Scheme of a simple 'NOT' logic
gate
Figure 3.2.9 Cumulative DOX released from the CDs-DOX formulation
Figure 3.2.10: Cell viability values (%) estimated by MTT assay for different concentrations of CDs. (a) Cell viability for CDs alone and (b) Cell viability of the DOX loaded CDs (CDs-DOX) and DOX alone
Figure: 3.2.11 . Flow cytometry study to calculate the diminution of mitochondrial membrane potential by using fluorescent potentiometric probes Rh123. MCF-7 breast cancer cells.
Figure 3.2.12. MCF-7 cells were treated with CDs enhances the apoptotic cell death assay
Figure 3.2.13. The representative photomicrographs of MCF-7 cells were shown as typical 2D morphology
Figure 3.3.1 Particle size and morphology studied through the TEM for the samples: (a) typical image of KN-1, (b) Particle size distribution of KN-1,(c) SAED generated by TEM for KN-1 (d) EDAX of KN-1 (e) TEM images of higher temperature of KN-2 (f) Particle size distribution of KN-2 (g)corresponding SAED patterns of the specimens processed KN-2 (h) EDAX elemental analysis of synthesized CDs, (i-j) AFM images of synthesized CDs for KN-1 and KN-2 121
Figure 3.3.2 FT-IR spectrum of the samples: (a) KN-1, (b) KN-2 & NMR data for (c) KN-1(d) KN-2
Figure 3.3.3: Thermal stability studied through TGA for the samples: (a) KN-1, (b) KN-2, DSC thermal graph for the samples: (c) KN-1, (d) KN-2
Figure 3.3.4: XRD pattern for the samples: (a) KN-1 and (b) KN-2 Raman spectroscopy (c) KN-1 and (d) KN-2

	_	_	n	+	ρ	n	+	_
1		()	rı	•	μ	rı	•	ς

Figure 3.3.5: BET experiments: BJH adsorption-desorption isotherm for the samples: (a) KN-1 and (b) KN-2. Pore size distribution profile for the samples. Pore size calculated from BET for (c) KN-1 and (d)KN2
Figure 3.3.6: Zeta potential profile for the samples: (a) KN-1, (b) KN-2.Particle size obtained from DLS for (c) KN-1, (d) KN-2
Figure 3.3.7: UV-Vis spectra for the samples (a) KN-1, (b) KN-2
Figure 3.3.8: a) Fluorescence spectra of KN-1 carbon dots of (100 μg/mL) with different concentrations of different metal ions (Al ³⁺ , Cd ²⁺ , Mn ²⁺ , Ni ²⁺ , Co ⁺² , Cu ²⁺ , Cu ⁺ , and As ⁺³) concentrations (0-140 μM).
b) Fluorescence spectra of KN-2 carbon dots of (100 μg/mL) with different concentrations of different metal ions(Al ³⁺ , Cd ²⁺ , Mn ²⁺ , Ni ²⁺ , Co ⁺² , Cu ²⁺ , Cu ⁺ , and As ⁺³) concentrations (0-140 μM)
Figure 3.3.9: Fluorescence spectra with different concentration, fluorescence intensity percentage ratios (F-F ₀)/F ₀ with different ions (Al ³⁺ , Cd ²⁺ , Mn ²⁺ , Ni ²⁺ , Co ⁺² , Cu ²⁺ , Cu ⁺ and As ⁺³)
Figure 3.3.10 Illustrate the Cell viability values (%) estimated by MTT assay versus incubation concentration of CDs at different concentrations (0, 15. 62, 31. 25, 62. 5, 125,250, 500, 1000 μg/mL) at 37°C for 24 h. for two different samples i.e (a) KN-1 and (b) KN-2 in normal splenocytes without any drug molecule
Figure 3.4.1 Transmission electron microscope (TEM) images of nanofiber formation in different magnifications.(a-d) High-magnification TEM image of neem bark nanocellulose nanofiber,(e) FESEM images NC of nanofibers scale bar is ~1μm,(f) SAED pattern of neem bark NC nanofiber
Figure 3.4.2 (a) AFM images of nanofiber (b) Corresponds to 3D image of NC
Figure 3.4.3 (a) Differential scanning calorimetry (DSC) figures showing the difference in dehydration and melting point temperature (b) TGA curve of nanofiber heating rate of 10 °C/min (c) A manufactured nanofiber's FT-IR spectrum. (d) UV-VIS spectrum
Figure 3.4.4 (a) Raman spectra of carbon nanofibers derived from a regenerated cellulose nanofiber,(b) The zeta potential values of cellulose nanofibres derived from neem bark. (c) The diameter size distribution of neem nanofibers particles (d) XRD patterns of the nanofibers 140
Figure 3.4.5 (a) BET-data of the investigated carbon nanofibers (b) pore size distribution (c) Graph of Dynamic Viscosity Vs Temperature of nanofiber. It is evident from the graph, as temperature increases, the density decreases. (d) The plot of viscosity vs. shear rate of nanofiber.
Figure 3.4.6. Images of antibacterial activities of discs of different concentrations of Neem bark nanofiber antibiotics on (A) Escherichia coli (B) <i>candida albicans</i> (C) <i>stephylococcus aureus</i> (D) <i>klebsiella pneumonia</i> 142

LIST OF TABLES

CHAPTER: 1

Table 1.1: Different types of Polymeric nanoparticles and their different applications. 4
Table 1.2: Various types of metallic nanoparticles and its different application 5
Table 1.3: Table of several kinds of metal oxide nanoparticles & their different application
Metal oxide
Table 1.4: Highlighted on the carbon quantum dots (CQDs) and various synthesis routes
Using precursors and uses of CQDs
Table 1.5 : Table of Different synthesis routes with precursor of CDs 9
Table 1.6: General view of NPs for the cancer treatment development on research stage 11
Table 1.7: Gist of NPs for Imaging and Diagnostics that are in the development or research stages 13
Table 1.8: Outline of NPs in the stage of development or study for Theranostic applications. 14
Table 1.9: Different synthesis methods Related to CDs, their unique benefits and
draw backs
CHAPTER: 2
Table: 2.1 Shows the list of chemicals required for the synthesis of different types of carbon dots and the fabrication of mesoporous carbon nanocapsules
Table: 2.2. Shows the list of solvents required for the synthesis of different types of carbon dots and the fabrication of mesoporous carbon nanocapsules
Table: 2.3. Shows the list of anticancer drugs used to load inside the pores of capsules to treat various cancers
Table: 2.4. Show the list of glassware and apparatus required for the experimental procedure to synthesize carbon dots and the fabrication of mesoporous carbon nanocapsule
Table: 2.5. Show the list of Materials required for cell culture and other cell-based studies 46
Table: 2.6. Show the list of cells used for the cell culture and other cell-based studies
Table: 2.7. Show the list of bacteria used for the antibacterial activity

CHAPTER: 3

Table 3.1 Comparison of Apoptosis Index SN-1, SN-2, SN-3 and SN-4 with MCF-7 breas cancer cells 8
Table 3.2 Comparison of Apoptosis Index SN-1, SN-2, SN-3 and SN-4 with MDA-MB-23 breast cancer cells 8
Table 3.3: Shows the effects of pH on photo luminance on synthesized CDs. 10
Table 3.4: Effect of temperature on the fluorescence intensity of synthesized CDs

LIST OF ABBREVIATIONS, ACRONYMS AND SYMBOLS

AFM Atomic force microscope

BET Brunauer-Emmett-Teller

BJH Barrett-Joyner-Halenda

BSA Bovine Serum Albumin

CD Carbon Dots

CLSM Confocal laser scanning microscope

DLS Dynamic Light Scattering

DMEM Dulbecco's Modified Eagle's medium

DOX Doxorubicin Hydrochloride

DSC Differential scanning calorimetry

FBS Fetal Bovine Serum

FESEM Field Emission Scanning Electron Microscope

FL Fluorescence Spectroscopy

HRTEM High Resolution Transmission Electron Microscopy

LSCM Laser scanning confocal microscopy

MCF-7 Michigan Cancer Foundation-7

MDA-MB-231 Human Mammary Carcinoma

MIC Minimum inhibitory concentration

MTT [3-(4,5-Dimethylthiazol-2-yl)-2,5-Diphenyltetrazolium Bromide

PBS Phosphate Buffer Saline

PL Photoluminescence

SEM Scanning Electron Microscope

TEM Transmission Electron Microscope

TGA Thermo gravimetric analysis

UV-VIS Ultraviolet Visible Spectroscopy

XRD X Ray Diffraction

λ Wavelength

Dh Hydrodynamic Diameter

Dt Translational Diffusion Coefficient

kB Boltzmann's Constant

η Dynamic Viscosity

LIST OF PATENT FILED/PUBLICATIONS/CONFERENCES

Patent Filed:

- [1] A method of synthesizing carbon dots and a product thereof, Application No.:202011018557, Dated: 30th April, 2020.
- [2] New therapeutic Nano medicine for the treatment of breast cancer Application No: 202111060434, Dated: 23rd December 2021.

Publications:

[3] Maity, Somedutta; Tomar, Munendra; Paik, Pradip.et.al *Azadirachta Indica* seed derived carbon nanocapsules: cell imaging, depolarization of mitochondrial membrane potential and dose dependent control death of breast cancer. *ACS Biomater. Sci. Eng.* 2022, 8, 8, 3608–3622.

(doi.org/10.1021/acsbiomaterials.2c00463)

- [4] Maity Somedutta; Pradip Paik Green synthesis of Carbon Nano dots from Kernel part of Azadirachta Indica seeds: selective detection of biologically relevant metal ions and drug delivery applications. (Manuscript for submission)
- [5] Maity Somedutta; Pradip Paik Detection and Separation of heavy metals by Carbon nanoparticles (CDs) synthesized from Kernel part of *Azadirachta Indica*. (Manuscript for submission)
- [6] Revealing the structures of cellulose from bark *Azadirachta indica*, antimicrobial activity and Their Application: An in vitro study. (**Manuscript for submission**)

Other Publications

- [7] Medhi, Himadri; Maity, Somedutta; Suthram, Niranjan; Chalapareddy, Suresh; Bhattacharyya, Mrinal; Paik, Pradip Hollow mesoporous polymer capsules with Dihydroartemisinin and Chloroquinediphosphate for knocking down Plasmodium falciparum infection, Biomed. Phys. Eng. Express, 2018, 4, 035006.
- [8] SumbulAfroz, HimadriMedhi, Somedutta Maity, GillipsieMinhas, SrikanthBattu, JeevanGiddaluru, Koushi Kumar, Pradip Paik and Nooruddin Khan; ZnOnanocapsules for the induction of enhanced antigen-specific immunological responses, Nanoscale.

- [9] Monami Das Modak, Ganesh Damarla, **Somedutta Maity**, Anil K. Chaudhary and Pradip Paik, "Self- assembled Pearl-necklace patterned upconverting nanocrystals with highly efficient blue and ultraviolet emission: femtosecond laser based upconversion properties", RSC Adv., 2019, 9, 38246-38256 **RSC Adv.**
- [10] Pradip Paik, K. Santhosh Kumar, Monami Das Modak, Koushi Kumar U and Somedutta Maity, UCN–SiO₂– GO: a core shell and conjugate system for controlling delivery of doxorubicin by 980 nm NIR pulse, RSC Adv., 2018,8, 37492-37502. RSC Adv.
- [11] Monami Das Modak, Ganesh Damarla, K. Santhosh Kumar, **Somedutta Maity**, Anil K. Chaudhury and Pradip Paik, Upconverting nanodots of nayf4yb3er3 synthesis characterization and UV visible luminescence study through tisapphire 140 femto second laser pulses,arXiv:2008.06783, (2020), 18th August, 2020, (http://arxiv.org/abs/2008.06783).
- [12] Pandey, Monica; Wasnik, Kirti; Gupta, Shubhra; Singh, Monika; Patra, Sukanya; Gupta, Prem Shankar; Pareek, Divya; Maity, Somedutta; Tilak, Ragini; Paik, Pradip, "Target specific inhibition of bacterial and Candida species by mesoporous Ag/Sn-SnO₂ composite nanoparticles: in silico and in vitro investigation" c
- [13] Pandey, Monica; Singh, Monika; Wasnik, Kirti; Gupta, Shubhra; Patra, Sukanya; c; Pareek, Divya; ChaitanyaNyshadhamsai Naga; **Maity, Somedutta**; Reddy, Aramati; Tilak, Ragini; Paik, Pradip, "Targeted and Enhanced Antimicrobial Inhibition of MesoporousZnO–Ag₂O/Ag, ZnO–CuO, and ZnO–SnO₂ Composite Nanoparticles".
- [14] Gopabandhu Panigrahi; Himadri Medhi; KirtiWasnik; SukanyaPatra; Premshankar Gupta; DivyaPareek; **Somedutta Maity**; Monica Pandey. Hollow Mesoporous SiO2-ZnO Nanocapsules and effective in vitro delivery of anticancer drugs against different cancers with low doses of drugs.

Book Chapter:

[15] Monika Singh^a, Sukanya Patra^a, Divya Pareek^a, Kirti Wasnik^a, Prem Shankar Gupta^a, Somedutta Maity^b, Monica Pandey^b and Pradip Paik^a* Polymer Nanoparticles and their Biomedical applications.

[16] Gupta, Prem Shankar; Wasnik, Kirti; Patra, Sukanya; Pareek, Divya; Singh, Monika; Maity, Somedutta; Pandey, Monica; A Review on Biodegradable Polymeric Materials for Bone Tissue Engineering (BTE) Applications.

ABSTRACT

Every year, an estimated 14.1 million cancer cases are diagnosed worldwide, with this figure expected to rise to 24 million by 2035. Cancer is a major cause of mortality globally, accounting for roughly 10 million fatalities in 2020, with breast cancer accounting for 2.26 million cases and lung cancer accounting for 2.21 million cases. Breast cancer is the most common cancer in the UK, with 50,000 new cases diagnosed each year. Because most present anticancer therapies have limits and adverse effects, there is an urgent need to create novel anticancer medicines. Nanotechnology has made significant progress in various areas of cancer treatment, including in vitro diagnostics, imaging, and therapy. The first generation of novel nanomaterials (NMS) as anticancer drugs has effectively reached widespread usage. MDA-MB-231, an estrogen receptornegative and highly invasive breast cancer cell line, and MCF-7, an estrogen receptor-positive and non-metastatic cell line, were employed. The intracellular uptake of the carbon nano sample was studied and compared using several correlative microscopy methods such as transmission electron microscopy (TEM), confocal microscopy, and scanning electron microscopy (SEM), among others. Cell death exhibited necrosis and apoptosis characteristics, as well as mitochondrial structural alterations.

PART —I: Synthesis of seed-derived carbon nanocapsules cell imaging, depolarization of mitochondrial membrane potential and dose-dependent control death of breast Cancer.

In this part, a series of mesoporous carbon nanocapsules (mCNS) of size below 10 nm have been prepared from *Azadirachta indica* seeds with a very easy and cost-effective approach. These nanocapsules can emit red and green light and are effective for cell imaging. Further, these carbon nanocapsules are biocompatible with normal healthy cells, however, they possess modest cytotoxicity against the MCF-7 (human breast cancer) and MDA- MB-231 (triple-negative

breast cancer) and the rate of killing cancer. Cells strongly depend on the dose of mCNCs. Further, the mitochondrial membrane potential and apoptosis assay were performed to analyze the therapeutic significance of these nano-capsules to kill breast cancer. Results showed that these carbon nano capsules can depolarize the mitochondrial membrane potential alone (without using conventional drugs) and can change the physiological parameters and cellular metabolic energy of the cancer cells and kill them. The apoptosis results confirmed the death of breast cancer cells in the form of apoptosis and necrosis. Moreover, the results suggested that the porous carbon nano capsules (mCNCs) reported herein can be used as a potential candidate and useful for theranostic applications such as cancer cell detection and therapy without using any conventional drugs.

PART-II: Synthesize of carbon dots for kernel part of seed: Photoluminescence mechanisms and applications in detection of biologically relevant metal ions

In this part, a facile cost-effective green synthesis approach was used to synthesize carbon-dot (CDs) of size \sim 4 nm, from the Kernel part of the *Azadirachta Indica* seeds and investigated their fluorescent and metal ions sensing capability based on the fluorescence OFF-ON, ON-OFF device mechanism and also used for the delivery of drugs. Metallic ions such as Ca^{2+} , K^+ , Na^+ , Fe^{3+} , and Zn^{2+} which are biologically important for many reactions have been used to explore the selective sensitivity of these CDs for detection. The resultant dot size with an average diameter of 4 nm has been used to eliminate the "Achilles heel" problems, which are associated with the Zn^{2+} in the body and its detection is a very challenging task. It is found that the sensitivity of detection of the Zn^{2+} can be regulated by using a different solvent. This material can also be used as a sensing probe for the selective detection of Fe^{3+} at a very low concentration of the solution (\sim 5 μ M). The synthesis method of CDs reported here is cost-effective, very fast, and ecofriendly and it is highly selective towards Fe^{3+} and Zn^{2+} . Due to the fast response capability and

the high sensitivity of these CDs to achieve logic operations, it provides a new understanding to construct potential next-generation molecular devices for the detection of different bio molecules with high selectivity. Further, these CDs are biocompatible against normal healthy cells, capable of loading small bio molecules and drugs that reassembled its use in drug delivery and therapeutic applications such as for breast cancer therapy and we observed significant synergic cytotoxic effects of CDs loaded with DOX against breast cancer cells. CDs especially in combination with DOX have been exhibited to be effective against MCF-7 (breast cancer) and should be deemed secure and effective approaches in cancer prevention and therapy. Thus, the CDs reported herein in this work have been synthesized from the green synthesis approach and can be used as a molecular probe for the detection of metal ions as well as for drug delivery applications.

PART-III: High-temperature synthesized carbon dots and their absorption of heavy metal ions.

Carbon nanodots (CNDs) are well-known as one of a new family of zero-dimensional nanomaterials. In the present development, carbon dots are considered the highest research field because of their biocompatibility, attractive fluorescent activities, ease of functionality, chemical stability, and photo stability. There are several ways to produce carbon dots, however, expected sustainable carbon sources can produce CNDs on a large scale. This can be a significant advantage for researchers to explore their versatile applications. Carbon nano dots have been heavy metal quenchers as discerning and sensitive fluorescent even at micromolar ranges. Although we focus on the fluorescence-sensing mechanism of heavy metal ions using green-recourses CNDs as a detection tool. We give a brief outline of green resources utilized in the CND synthesis, its property, and the fluorescence mechanism of CNDs. Additionally, related problems and possible solutions to rising above the outlook path of CNDs in this quencher field

are discussed. Further, in present days heavy metal pollution is expected in the process of emission and mass production. It is already reported heavy metal ions will cause permanent damage to the human body as well as other organisms. Even at low concentrations, it is non-degradable nature of exposure and ingestion. Therefore, it can be of great importance for the ecological and human health environment to extend high accuracy and understanding as well as a steady process for detecting heavy metal ions. In the above lines, this work systematically sums up the quenching mechanism of heavy metal ions to demonstrate the related green CND-based quencher and the capability of separation of them from the water-based solution.

PART IV: Revealing the structures of nano cellulose from Neem bark antimicrobial activity and their application: an in vitro study

Azadirachta indica (A.indica) is an naturally available, entirely biodegradable source of "nanocellulose" (NC). For the potential biomedical application and for the developing the antibacterial activities in various polymeric nanofibers and scaffolds, neem extract blended with the Nanofiber. And hence, in the present study we first time explored A. indica bark as a natural source for the development of antibacterial properties contain cellulose nanofibers. However, seeds, leaves are widely used for the biological application and a Tree bark is generally considered a useless raw resource. As Tree bark are rich in chemical components which could be commercially useful if used effectively. With the objective of to develop the antibacterial potential containing nanofibers, we synthesized and studied the a the physicochemical parameters in soil, thicknesses, moisture content, water holding capacity, expansion, porosity, and biodegradability of the cellulose nanofibers. Majorly, the integration of A. indica extract demonstrated an enhanced shelf life due to its significant antibacterial action, and this remaining nanocellulose was destroyed in the soil with little environmental impact. Impact of Nanocellulose fiber were tested on gram negative and gram positive bacteria via disc diffusion

process shows the statistically significant antibacterial activity. Further, our study concludes these nano cellulose fibres poses the antibacterial potential and will be useful in various biomedical applications.

CHAPTER-1

INTRODUCTION AND LITERATURE REVIEW

CHAPTER-1

INTRODUCTION AND LITERATURE REVIEW

Chapter 1 Introduction establishes the background of nanotechnology in medicine and biology and its applications including breast cancer treatment. This section also elaborated and highlights the various nanomaterials, their synthesis, characterizations and applications in various biomedical fields.

1.1. Background

Nano-biomaterials have become an important tool for medical applications for a variety of reasons, including biocompatibility and unique effects owing to their nanoscale. The ability to include biomaterials in the production of nanostructures has opened the door to novel applications in a variety of sectors. One of the most significant is contemporary medicine, which has extremely difficult challenges to tackle. Nanotechnology has been applied to two main issues of general interest in modern medicine, tissue engineering and antimicrobial activities, which have been chosen for this study owing to large examples and effects.

Over the past decades, the nanotechnology field gain interest as the most active and innovative research area.³ It has diverse applications in various interdisciplinary areas like basic Chemistry, Physics, Biology, Material Engineering and science. Due to the unique property of the material (aspect ratio) nano range, nanotechnology had proven its potential in the areas of agriculture⁴, the food industry, ⁵ pharmaceutical, ⁶ electronics, textiles, ⁷ diagnostic, ⁸ etc. Out of the above mentioned application areas, the major success has been achieved in the medicinal field. ⁹ This includes the motive of a drug delivery system with maximum therapeutic efficacy. Research has been carried out with various research groups on various types of nanoparticles such as, polymeric nanoparticles, liposomes, dendrimers, carbon dots, nanofibers, carbon

nanotubes, and metallic nanoparticles. Among these, the metal-based materials are widely being explored for theranostic applications, ¹⁰ using their optical, biological, and physical chemical properties. In this content, the present dissertation focused on non-metal-based nanoparticles and their applications in biomedical and therapeutic applications. ¹¹

1.2. Different types of nanoparticles and their synthesis

1.2.1 Polymer nanoparticles

In this part, different types of polymer particles used for the therapeutic applications has been highlighted in the tabulated form (Table:1.1). The uses are focused on the anti-glioma activity, drug delivery, theranostic, or cell imaging, anti-inflammatory activity, cancer treatment etc. Such as, a novel class of bio-polymeric core-shell nanoparticles (PCL, PLA and PLGA) have been reported. These polymeric nanoparticles were synthesized using emulsification solvent evaporation (SESE) technique. These polymeric core-shell NPs are known as viable platforms for the future nanomedicine, particularly in targeted drug delivery, can be as theranostic, and medical bio imaging. Inhibiting the PI3K/Akt/mTOR signalling pathway these polymeric nanoparticles are also useful for the treatment of the different cancers, such as particularly glioblastoma. ¹²⁻¹³ Furthermore, encapsulation of the drugs with different properties such as, extremely hydrophobic hyper for in, a 5-LO lipophilic inhibitor, with in AcDex-related NPs provides used for effective suppression 5-LO function in neutrophil in the presence of albumin. ¹⁴ In an another study, it is reported that the Polycaprolactone (PCL) nanoparticles loaded with Amp B are useful for the treatment of leishmanial infections. ¹⁵⁻¹⁶

Table 1.1:Table of different types of Polymeric nanoparticles and their different applications

Sr. No.	Application Purpose	Types of Polymeric Nanoparticles/met hod	Types of polymers	Ref.
1	Drug delivery, theranostics, or bioimaging	C-6-loaded polymers core-shell Nanoparticles produced spontaneous solven t evaporation emulsification	PCL, PLA, PLGA	[12]
2	Anti-glioma activity	Polysorbate 80- coated PLGA NPs with rapamycin	PLGA	[13]
3	Anti inflammation properties	Hyperforin-loaded AcDex-based related NPs were synthesized using ethyl acetate & water in solvent evaporation process.	AcDex	[14]
4	Antifungal activity	By nanoprecipitation process PCL-NCs loaded with Amp B.	Biopolymer of PCL	[15]
5	Severe combined immunodeficiency disease	PEG NCs with Pegademase bovine- loaded colloidal nanocapsules	PEG	[16]
6	Undefined Oral Delivery	By using nanoprecipitation method loadedwithEudragit L 100 NCs,	Anionic based copolymers using methacrylic acic and methyl methacrylate	[17]
7	Lung cancers in combination with chrono-modulated chemotherapy	Paclitaxel-loaded PCL-PEG-PCL NCs	PCL-PEG-PCL	[18]

1.2.2 Metallic nanoparticles and Metal oxide nanoparticles:

In this section, Table 1.2 highlighted on the several types of nano structured materials and their applications different applications, namely Imaging therapy, photo thermal therapy, radio sensitizer applications, skin penetration and effect on cells, chemotherapies, photo thermal therapies, biosensing applications etc. Such as, platinum nano particles were reported in the direction of triggering breaking in DNA strands in the human colon cancer cell type (HT29) in a intensity, time, and in a size-dependent basis. A quick and simple method for attaching thiolated DNA to AuNPs based on mPEG-remarkable SH's stabilizing impact on AuNPs. SiNPs and their variations are reported as a strong tool for antimicrobial targeted delivery, which potentially can decrease the consequences of a high medication dose and related adverse effects. Self-assembled Au core-shell NPs with biocompatible polymers for biological thermo - responsive polymers, pH-responsive polymeric materials, conductive polymeric material, anti bio-fouling polymers, and numerous nature derived polymers are also reported for their biomedical uses that are tabulated in Table 1.2. MNPs have piqued the interest of the researchers due to their potential as magnetic resonance imaging (MRI) contrast agents and heat regulators in cancer therapy.

Table 1.2: Various types of metallic nanoparticles and its different applications

Sr No	Type of Nanomparticles	Specific sites	Targeted sides	Ref.
1	Gold or Silver nanoparticles	Cancer cell	Photo thermal treatment and imaging	[19]
2	Nanoparticles of platinum	Cancer	Toxic effects study	[20]
3	AuNPs	Cancer	Through Radio sensitizer	[21]
4	Au NPs	Skin	Skin penetration study	[22]
5	Pt NPs@PVA	Brain	Toxicity study	[23]

6	Ag NPs	Anti-microbial agent	Toxicity study	[24]
7	Ag NPs	Wound healing	Therapeutic study	[25]
8	Au-branched shell nanostructures	Breast cancer	Imaging and photo thermal therapy	[26]
9	MagneticNPs	Cancer	Biosensor, Chemotherapies, and molecular bio-imaging	[27]
10	Magnetic NPs	fertilizers, pesticides	Sensor, coating, packaging, remote sensing,	[28]
11	Core-shellFeONPs@Si/Au	cancer (Head and neck)	Photo thermal therapy	[29]

Further Table-1.3 highlighted on the different varieties of metal oxide nanoparticles & their different applications in biomedical applications such as for antibacterial, gene treatments, drug delivery, tissue engineering, and imaging, bio imaging and surgical devices, etc. such as, using citrate-intercalated layers double hydroxide (LDH) as a substrates and Ag⁺ as a precursor, silver oxide NPS with controlled particle size were effectively synthesized and they are potentially used in the antibacterial, medication delivery, gene therapy, tissue development, imaging etc.³⁰⁻³¹ Cerium oxide nanoparticles have demonstrated tremendous promise as antioxidant and radio protective compounds for use in cancer treatment, Bio imaging and making surgical devices.³² The manufacture of neem-assisted zinc oxide (ZnO-neem) particles assists in determining neem's function in thermo-hydraulic behaviour as nano fluids and use for the skin treatment.³³ Sodium titanium oxide bronze has the fascinating qualities of high electric conductivity and strong chemical stability, as well as a novel one-dimensional tunnel crystal structure that may be used for cation storage and they have also potential use as Antimicrobial coating material and for the sterilization.³⁴ Nickel oxide NPs alter the physiology, phyto-chemistry, and molecular structure of

Chinese Cabbage Seedlings and can be used in the Biomedical applications such as for anticancer effects.³⁵ Copper oxide wire nanoparticles are used as an antibiotic, antiviral, antimicrobial, antifouling, and antifungal activities.³⁶ The pulsed laser ablation in liquid laser creation of gold/oxide nanocomposites has been implemented to ensure one-step synthesis of different gold/oxide nanocomposites with consistent shape and excellent dispersibility, and used in antibacterial, cell imaging, photodynamic therapy, therapeutic agents, surgical devices.³⁷ However, bacterial resistance to antibiotics is among the most significant current biomedical issues, with the quest for novel medicines to tackle bacterial diseases being prioritized.³⁸

Table-1.3: Table of several kinds of metal oxide nanoparticles & their different applications Metal oxide.

Serial	Nano particle	Applications	Ref.
number			
1	Fe ₂ O ₃	Image and environmentally remediation	[30]
2	Ag ₂ O	Tissue developments, Delivery of drugs, gene therapeutics, bactericidal, imaging, and other applications	[31]
3	CeO	Surgical devices, Bio imaging etc.	[32]
4	ZnO	Skin treatment and care, etc.	[33]
5	TiO ₂	Coating material, sterilization, Antimicrobial,	[34]
6	NiO	Anticancer	[35]
7	CuO	Antiviral, ,Antibiotic, Antimicrobial, Antifouling, and Antifungal treatment,	[36]
8	Au	Drug delivery, Cellular imaging, Antimicrobial, Surgical devices, Cancer treatment, Photodynamic therapies, etc.	[37]
9	Al_2O_3	Antimicrobial	[38]
10	Fe/Fe ₂ O ₃	Tissue repairing, Cellularlabeling, Drug delivery, Hyperthermia, etc	[39]
11	CaO	Antimicrobial	[40]
12	MgO	Antimicrobial	[41]

1.2.3 Quantum dots

Because of their unique optical adsorption properties, photo-induced transfer of electrons, photoluminescence, and electrons reservoir qualities, carbon CQDs (quantum dots) have emerged as a promising new material viable contender for photo catalysis applications. ⁴²⁻⁴³ Carbon quantum dots (CQDs) have now been shown toward good photo sensitizers when combined using a molecular catalyst in aqueous solution with solar-powered hydrogen generation. ⁴⁴ A green and simple approach for extremely sensitive and accurate dopamine detection was devised by manufacturing a cuo dots/Nafion composite film (Cu2O-CDs/NF). ⁴⁵A facial and green hydrothermal approach was used to create carbon dots (CDs) with high fluorescence utilizing biomass quinoa as the carbon source. ⁴⁶ Quantum Dot Synthesis of Carbon iron from jujubes (III) from jujubes. ⁴⁷ The produced CDs emit strong green light with a highest quantum yield for greenemitting materials is roughly 46.4%. CDs. ⁴⁸ Hydrothermal treatment of orange juice yielded extremely PL quantum output of 26% in luminescence carbon quantum dots a single step. ⁴⁹ Many other CQD utilization and various synthesis routes using precursors are tabulated in Table 1.4.

Table-1.4: Highlighted on the carbon quantum dots (CQDs) and various synthesis routes using precursors and uses of CQDs.

Serial				
Number	Process	Precursors	Applications	Ref.
	A sol-gel technique with an		Degradation of	
1	electrochemical method	Graphite rods, Ti(OBu) ₄	MB,Photocatalysis	[42]
		TiO2, HQC, and		
2	Hydrothermal	Fe(HQC) ₃	Phenol degradation	[43]
3	Thermolysis	citric acid nanoparticle	Water molecule break	[44]
		PVP, carbohydrate,		
4	Ultrasonic	and CuSO ₄	CO ₂ transformation	[45]
5	Hydrothermal	Coffee ground	Sensing	[46]
6	Hydrothermal	Juju bees	Sensing	[47]
		Ammonia, diammonium		
7	Solid state reaction	hydrogen citrate	Bioimaging, sensor	[48]

8	Hydrothermal	Orange juice	Bioimaging	[49]
9	Microwave- assisted pyrolysis	Arginine and glucose	Non-viral gene delivery	[50]
		Branched PEI,		
10	Hydrothermal	ammonium persulfate	Gene Delivery	[51]

1.2.4 Carbon dots (CDs)

Carbon dots (CDs) are very much fascinating. On a gram scale, high quantum productivity (QY) CDs, 53%, made by heating a formamide solution of citric acid and ethylene diamine.⁵² Malic acid carbon dots are excellent for super-resolution fluorescence specificity microscopy under a range of circumstances, as demonstrated in preserved and living trout gill epithelial cells.⁵³ Using complimentary nucleotide sequence as ligands on surfaces, they selectively enable two separate "Dual-color" carbon dots are dispersed to associate *in situ & in vitro*.^{54,55}

Using folic acid as a precursor, researchers created nitrogen-doped CDs in an aqueous phase method. So Using a one-step hydrothermal technique, carboxymethyl chitosan & hyaluronic acid had been employed to synthesize unique specifically aimed carbon dots nano carrier photoluminescence. Nitrogen and Sulphur co-doped photoluminescence CDs can be synthesized from waste *Allium sativum* peel. Using Fluorescent CDs, cell microenvironment can be detected. It was also shown a totally green synthetic process for manufacturing luminous nitrogen-doped carbon dots using milk.

Table 1.5: Table of Different synthesis routes with precursor of CDs.

Sr No	Synthesis Method	Solvent(s)	Carbon Precursor(s)	Ref.
	Hydrothermal			
1	Carbonization	Formamide	Citric acid	[52]
2	Microwave	Water	Malic acid	[53]

	Hydrothermal			
3	Carbonization	Nitrobenzene	Sucrose	[54]
	Hydrothermal		Urea and p-	
4	Carbonization	Water	phenylenediamine	[55]
	Hydrothermal			
5	Carbonization	Water	Folic Acid	[56]
	Hydrothermal			
6	Carbonization	Water	K-carrageenan	[57]
			Allium sativum	
7	Pyrolysis	Water	peels (garlic)	[58]
	Hydrothermal	Ethylenediamine in	Agaricus Bisporus	
8	Carbonization	Water	(mushroom)	[59]
	Hydrothermal			
9	Carbonization	Water	Milk	[60]

1.3. Nano particles for biomedical applications

1.3.1 Drug delivery

Nanoparticles provide a novel level in engineering with control towards the area of medicine which allowing for the modification of factors such as medication and diagnostic agent toxicity, pharmacology, solubility, diffusivity, half-life, bio distribution. The uses of nanoparticles are numerous and are anticipated to expand as technology advances. Numerous investigations in recent years have proved their capacity to function as sensors⁶¹, medication transporters ⁶²⁻⁶³ as therapeutic ⁶⁴ targets. Recent attempts have succeeded in integrating therapies and diagnostics into a unified platform, giving rise to "theranostic" procedures.

Utilizing nanoparticles as medication delivery mechanisms is justified by a minimum of three mechanisms (i) improved penetrating nanoparticles' uptake and retention (EPR) in solid malignancies; (ii) the ability to transport stable colloidal systems to deliver blood insoluble

medications; and (iii) regulated release. The potential benefits of each of these topics will be addressed in this section. Paclitaxel (PTX), a commonly accepted pharmacological option used for the treatment of many To create a theranostic technique for treating cancer, human malignancies were co-loaded in lipid nanostructure carriers using CdTe@ CdS@ZnS QDs. (see Table 1.6).⁶⁵

Table 1.6: General view of NPs for the cancer treatment development on research stage

Sl,No.	Target malignancy	Therapies involved	Payload	Modificatio n	Outcome	Ref.
1	model Human prostate cancer lines PC3	Chemother apy	PTX	PLGA NP	Compared to free PTX, drug delivery effectiveness was significantly increased.	[66]
1	Cells K562 from chronic myelogenous leukaemia and PC3 from human prostate cancer	Nucleic- acid-based therapy	Nucleic acids	PEG, transferrin modified NP	showed greater effectiveness when transfecting K562 leukemia cells than untargeted particles.	[67]
2	human HER2- positive cells and MCF7 human HER2- negative cells	Targeted therapy, chemother apy	Docetaxe 1	Tmab modified NP	HER2-positive BT474 cells exhibit increased cytotoxicity, however HER2-negative MCF7 cells do not	[68]
3	BT474, SK-BR-3, and MDA-MB-231 are human HER2-positive breast cancer cell lines; HER2-negative cell lines	Targeted therapy, chemother apy	Paclitaxel	Tmab modified NP	Improved therapeutic effectiveness and reduced cytotoxicity to human breast epithelial cells were seen.	[69]

4	PANC-1 and Patu8988T are human pancreas cancer cell lines.	Targeted therapy	Alantolac tone Erlotinib	PLGA NP	The created NP significantly increased cancer cell death and shown an anticancer impact.	[70]
5	Breast and ovarian cancer mice models, human breast cancer MDA- MB-231 cells, and mice ovary cancer cells	Chemother apy	Doxorubi cin	Exosome	Doxorubicin's capacity to penetrate cells was improved, and drug aggregation in mice hearts was prevented.	[71]
6	melanoma tumours B16- F10 transplanted into C57BL/6	PTT	IONPs/A	Au NP encapsulate d IONPs/Ag cores	The Au NP complex worked effectively as a PTT compound as well as a T2 MRI contrast agent.	[72]

1.3.2 Cancer therapy

A group of researchers presented the creation of a cyclodextrin polymer-based gene delivery system that was based on the transferring.⁶⁷ Lipid-polymercoated with Trastuzumab (Tmab) fusion nanomaterials comprised PLGA, polyethyleneimine (PEI), poly (d, 1-lactide-co-glycolide), and lipids were created in this study.⁶⁸ In this work, pure anti-cancer drug nanorods (NRs) are combined in the core of antibody-drug nanoparticles (ADNs) with a therapeutic Trastuzumab, monoclonal antibody, mostly was situated on exterior part of NRs and used for definite targeting with synergistic therapy of HER2 positive breast cancer cells.⁶⁹ Further, they have created a nano platform to deliver ERL and ALA simultaneously to suppress both EGFR and STAT3 for improved Pancreatic Cancer therapy.⁷⁰ Exosomes improve doxorubicin's therapeutic index in ovarian and breast cancer mice models.⁷¹ The design and production of a unique magnetic hollow gold nano shell complex with iron oxide nanoparticles in the hollow interior are also reported for the treatment of melanoma tumors.⁷²

1.3.3 Imaging and Diagnosis

A group of researchers demonstrated on the SWNTs, Au NPs, and Au NRs functionalized with polymers, they are exceptional stable in aqueous medium, at various pH, high temperatures, with in serum. Dendrimer nanoparticles loaded with gadolinium can be used in cancer magnetic resonance contrast enhancement. The manufacture and development of cutting-edge QD probes are used for the cell and molecular bio imaging. Authors also looked in the nanoparticles bio distribution, pharmacokinetics, and toxicity as they relate to in vivo imaging and treatment. They tested the cellular absorption of Non-phagocytic T cells carrying SPIO throughout selection of particle sizes between 33 nm and approximately 1.5 micron, with precisely regulated surface characteristics and without the use of transfection agents. Gold nanoparticles are used in disease detection and therapy as mentioned earlier, and the systems must be biocompatible and able of becoming functionalized for identification of particular target areas in the body following systemic delivery. Because of the great X-Ray attenuation, non-toxicity, and ease of synthesis and surfaces synthesis process for colloidal stability and selective distribution, gold nanoparticles (AuNPs) have recently gained attention as an X-Ray contrast agent. Many more detail uses of the NPs in Imaging and Diagnostics have been shown in Table 1.7.

Table 1.7: Gist of NPs for Imaging and Diagnostics that are in the development or research stages

Sr. No.	Nanoparticle	Application	Ref.
1	Perfluorocarbon	Imaging of angiogenesis, cancer metastases and blood clots.	[73]
2	Gd complexes	CT imaging	[74]
3	Fullerenes	MRI to enhance contrast.	[75]

4	CDs	Cellular imaging.	[76]
5	Silicon particles	MRI.	[77]
6	Iron oxide	Imaging of tumours	[78]
7	Au NPs	Ultrasound.	[79]
8	Au NPs	X-ray/CT scan.	[80]

1.3.4 Theranostic applications

Hollow manganese oxide particles with surface functionalization are used for the delivery of siRNAs with a cancer target cell among magnetic resonance imagingn. Magnetic nanoparticles with target-cell specificity for simultaneously molecular imaging and siRNA delivery. Magnetic resonance images and treatment for cancer treatment utilizing nanoparticles loaded with docetaxel and super para magnetic iron oxide. The inherent near-infrared photoluminescence of luminous porous silicon nanoparticles (LPSiNPs) allows monitoring both of accumulation and degradation *in vivo*. Chemically Single-walled nanotubes (SWNT) that have been chemically functionalized demonstrated assure within tumour-targeted accumulating in rats, as well as bio viability, elimination, in addition to low toxicity. **Single-Valle 1.8**)

Table 1.8: Outline of NPs in the stage of development or study for Theranostic applications

Sr. No	Applications	Drug used	Nanoparticles used	Ref.
1				
	MRI plus RNA delivery	siRNA	Mn2O3	[81]
2				
	Targeting, MRI and therapy	siRNA, DOX, docetaxel	Fe2O3	[82- 83]
3	Diagnosis, tumour targeting and			
	PTT	DOX	Au NPs	[84- 85]
4				
	Photodynamic therapies, X-ray/CT	Pyropheophorbide		
	imaging, but also drug carrier	(HPPH), DOX	SiO2	[86-87]

5	Diagnosis, DNA and drug delivery	DNA plasmid, DOX, PTX	CNTs	[88-89]
6	Imaging, therapy and sensing	DOX, MTX	QDs	[90-91]

1.3.5 Molecular detection

Many significant technological improvements have been achieved in the applications of nanoparticles for bio molecular detection over the last decade. 92-93 Nanoparticles, in particular, have been widely employed in nucleic acid and protein bio affinity sensors. 94 Because of their nanoscale size, these particles have a selective reactivity with advantageous physical character (optical, electrical, magnetic and electrochemical) that be chemically tailorable. 95 Thus, the nanoparticles seemed effectively utilized for example, in nucleic acid 96 in addition to protein detection. 97 Recently, evanescent-wave-induced light scattering-based colorimetric detection has been established. 98.99 Gold nanoparticle labels include employed in conjunction by in addition to the electrochemical and optical detection; there are various platforms for detecting. Initially, quantum dots (QDs) be utilized as fluorescent biological labelling. 100,101 Furthermore, photo chemically stable semiconductor nanoparticles feature limited, symmetric, size-tuneable emissions spectrum. Core-shell structured QDs are preferable in fluorescence-based applications. 102,103 Since Tan and colleagues first employed dye-doped silica nanoparticles as labels in DNA detection, they have received increased attention.

1.3.6 Biosensors

A nano biosensor type of sensor that is used to watch, compute, with evaluate biological phenomena utilizing sensors produced using nanotechnology methods. They are typically made from quantum dots, nano particles, nano wires, and nano films. The nano scale regime is where most occurs naturally biological systems include membranes, protein complexes, and viruses, as well as their relations. This makes nanoscale devices attractive potential biomedical and bio

analytical applications that need upper levels sensitivity, particularity, and quicker reaction period than standard bio-sensing approaches. 104,105

1.3.7 Antibacterial effects

The increasing usage of nanoparticles in medicine has resulted in an increase in the number of research investigating potential antibacterial actions of nanoparticles. ¹⁰⁶ Metal nanoparticles, for example, can alter the metabolic activity of bacteria. ¹⁰⁷. This capability is a big benefit when it comes to eradicating microorganisms to heal illnesses. The capacity of NPs to infiltrate bio films also provides a feasible way for inhibiting bio film development based on gene expression inhibition caused by Ag. ¹⁰⁸

To perform their antibacterial action, bacterial cells must come into contact with NPs. Electrostatic attraction, ¹⁰⁹ van der Waals forces, ¹¹⁰ and hydrophobic interactions, receptor-ligand interactions, and recognized kinds of attachment. Then NPs enter bacteria membrane congregate alongside the metabolic route, ¹¹¹ affecting the cell membrane's structure and function. Following that, NPs react with the fundamental characteristics of bacterial cells, including DNA and lysosomes, ribosomes, with enzymes, causing oxidative stress, heterogeneous changes, cell membrane permeability changes, abnormalities in electrolyte balance, and enzyme inhibition, protein deactivation, and gene expression changes. ^{112,113} The most often postulated processes incorporate oxidative stress in current research stress, ¹¹⁴ metal ion, ¹¹⁵ in addition to non-oxidative mechanisms. ¹¹⁶

1.4. Special emphasized on Carbon dots, and their application in biology and medicinal uses

1.4.1 Synthesis, characterization, methods of reported CDs and drawback of the existing methodChemical ablation is a process in which powerful oxidizing acids, carbonize biological compounds carbonaceous materials, which may then be there sliced in small sheets by controlled oxidation. It was shown that surface passivation was the crucial movement for the PL kind of

CDs. Furthermore, the CDs emission wavelengths may be changed via altering the number of treatments and the fundamental elements. The CDs manufactured using different methods are ideal for the biological applications because to their multi colour emission and harmlessness.

Table 1.9: Different synthesis methods Related to CDs, their unique benefits and drawbacks.

Approache s	Synthesis methods	Quantum Yield %	Disadvantage	Advantage	Ref.
Bottom-up	Chemical ablation	4.34–28	Multiple stages, demanding processing conditions, and inadequate control of oversize	a variety of beginning materials, the most effective technique	[117]
Bottom-up	Hydrothermal/solv othermal treatment	1.1–94.5	Ineffective size control and low production yield	inexpensive, green, and non- toxic	[118-119]
Bottom-up and Top Down	Solid-state thermal treatment	9–69	Poor control oversize	cheap, sustainable, and non-toxic	[120- 121]
Bottom-up	Microwave irradiation	2–44.9	Poor control oversize	Quick, economical, and environmentally friendly	[122- 123]
Top Down	Laser ablation	4–36	Low QY & poor size control	Tuneable surface conditions, a efficient process, as well as a high output yield	[124]

Because its cheap cost, non-toxicity, and environmental friendliness, hydrothermal technique is probably one of the special approaches utilized towards produce novel carbon-related nano materials. Typically, an organic pioneer solution is enclosed within a high-temperature hydrothermal reactor. CDs may be made from a variety of organic resources, together with cysteine (cys) in addition to citric acid, glucose, chitosan, food waste, banana extract, and numerous natural polymers, using hydrothermal carbonization (HTC).

Electrochemical carbonization is a process for producing CDs without the need of heat by employing a variety of bulk carbon sources as the carbonous precursor. Unlike more modern electrochemistry approaches that employ carbon-based electrodes as a source of carbon for CD manufacturing, electrochemical carbonisation converts the solution to CDs.

One of the most enticing features of this ultrasonic irradiation for CD manufacturing is its extremely fast reaction time. Microwave irradiation is regarded as a quick, easy, and low-cost approach for decomposing chemical bonds and carbonizing precursors generating electromagnetic radiation with such a wavelength between one millimetre and one metre.

When, short-wavelength such as laser light interacts through attenuating material, the result is laser ablation (photo ablation). The condition of ligands on the surface of CDs affects the light emitted. As a result, the exterior properties CDs may be modified to achieve the appropriate light release features.

1.4.2 CDs for Nanomedicine

CDs, in addition to being carriers, exhibit therapeutic properties such as antibacterial activity ^{125,126} anticancer activity, ^{127,128} antiviral activity, ^{129,130} and antioxidant activity ¹³¹ Typically, Because of the preservation of pharma cophores in existing structures or the creation of new active structures, as-prepared CPDs exhibit therapeutic performances that are comparable to or better than those of pristine pharmaceuticals when drug molecules (like metronidazole, ¹²⁵ gentamicin sulphate, ¹²⁶

glycyrrhizic acid ¹³⁰ can be used as starting material. Quantum dots are tiny crystals that have been created to transport electrons and convert a spectrum of light into distinct colours. Quantum dots enable the study of cell processes and have the potential to significantly enhance the detection and treatment of illnesses such as cancer. ^{132,133} QDs have been shown in certain studies to have impacts on reproductive dysfunction, TH signalling, estrogen receptor activation, and endocrine compromising activities. ^{134,135}

1.4.3 CDs for Nanotoxicity

Carbon nanoparticles, which are made up of fullerenes and nanotubes, are the most often employed materials for drug administration because fullerenes have several attachment sites that allow for tissue binding and nanotubes have excellent electrical conductivity and strength. 136,137

Factors affecting toxicity of CD nanomaterials and other nanomaterials The dimensions, surface charge, shape, in addition to solubility of nanoparticles are among the factors that influence their interaction with proteins. The exclusive method of NP contact with biological system is primarily determined by the dimension with surface part of the NP. NPs have a relatively huge specific exterior area, which accounts for their high reaction ability and catalytic activity. 138 NPs have diameters that are equivalent to protein globules, diameter DNA helix (2) nm), in adding to cell membrane width (10 nm), allowing towards easily go through cell organelles. 139

NPs have the following forms includes cylinders, spheres, sheets, cubes, even rods. The toxic effects of NPs is highly dependent on their form. This has been demonstrated for a variety of NPs with varying geometries and chemical compositions. ^{140,141} Carbon nanotubes with only one wall have been shown on the way to inhibit calcium channels additional efficiently than spherical fullerenes. ¹⁴² The surface charge of NPs is significant within their toxicity, since it influences their connections by biological system. ^{143,144} It is necessary to apply a coating to the outside of

NPs to changing optical, magnetic, electrical, and is utilised to enhance NP biocompatibility and solubility both biological and water-based fluids by lowering their aggregation potential and raising their stability and so on. As an outcome, the coating reduces the toxic effect of NPs, while in addition allowing them to interact accurately with different types of cells in addition to biological molecules. Furthermore, the shell has significant impact on NP pharmacokinetics, altering trends of NP dispersion and gathering in the body.¹⁴⁵

1.5 Overview of cancer

Cancer is a disease characterized by uncontrolled cell proliferation or abnormal development of cells. Cancer cells have evolved from normal cells in the body. Cancer cells infiltrate neighbouring cells and spread to distant organs. 146 Cancer is defined by the International Union against Cancer as a disturbance of excessive cell growth and proliferation with no obvious relationship to the physiological needs of organs. Cancer cells have a multifaceted genesis. 146,147 They comprise genetics, physical, chemical, metabolic, hormonal, environmental, and enzymatic variables. Cancer is the greatest cause of mortality worldwide, killing about 6 million people each year. Cancer is classified as breast, skin, colon, lung, blood cancer, uterus, and prostate cancer based on cell transfect ion and infection. Most crucially, the body's environmental interface and the repercussions of direct exposure to a range of xenobiotics can contribute to the development of cancer 146-148. Cancer can be cured and treated with innovative drugs using treatments such as a) surgery, b) chemotherapy, c) photodynamic therapy, and d) radiotherapy. However, these approaches are accompanied by several negative side effects, including vomiting, nausea, Cytotoxicity, disruption of body metabolism, weakening of the body's immune system, and bone marrow suppression. 148,149

1.5.1 Types of cancer

Normal cells develop predictably. However, when cancer develops, a collection of cells begins to multiply haphazardly and uncontrollably, generating lumps or tumours. A cancerous tumour grows indefinitely can extended to other portion of the body. Broadly, cancers generally related to life style. Breast cancer, cervical cancer, oral cancer, cancer of the bladder, eyes, pancreas, colorectal, kidney, Esophageal, liver, lung, ovarian, prostrate, skin, stomach, thyroid, uterine, laryngeal, testicular, etc. Among them Breast cancer is one of the largely frequent found cancer in addition to triple negative breast cancer (TNBC) be the riskiest, because triple-negative breast cancer cells absence of estrogens or progesterone receptors (ER or PR) and in addition absence of HER2 protein.

1.5.2 Path physiology of cancer

Cancer is a genetic disorder characterized by the complex combination of genetic and environmental variables that regulate carcinogenesis. ¹⁵⁰ It is one of the most deadly illnesses affecting the global population, accounting for 13% of all dead in 2008. ¹⁵¹ Cancer is a disease in which standard cellular performance are disrupted. ¹⁵² Cancer develop as a result of the gathering of numerous genetic abnormalities and mutation that cause the loosening of signal control pathways that control cell growth, death, and differentiation. Cancerous situations are caused by the development of several gene mutations, which carried to the deregulation of signalling systems that control cell division, death, with DNA repair. ¹⁵³ Tumour cells can divide and extend in the lack of regular constraints one time these pathways be altered to eliminate the impacts of cellular control. Common cells be capable of become tumour through a variety of definite process. Almost all malignant cells have a modest number of acquired molecular, metabolic, and cellular features that result from modifications in critical pathways, oncological research in the latter half of the 20th century showed. ¹⁵³ Continued discovery of a specific mutation sites adding

to the universal nature of cancer are based on the human genome that are common in many different forms of cancer. Cancer can be results of oncogene activation or inactivation of tumour suppressing genes, then impart the abnormal description that differentiate malignant cells¹⁵⁴ Proto-oncogenes, which are progenitors of oncogenes, are changed by dominant mutations, imparting a gain of function to a normal cell such as proliferation. Fundamental cellular functions such as metabolism, development, proliferation, and death in tumour cells are changed as an effect of mutations in both gene type. ^{155,156} Henceforth, altered pathways allowing cancerous cells to proliferate and form tumours nearby location. Cells can proliferate uncontrolled by evading the regulatory effects many processes present in a cell, which are controlled by essential tumour suppressor genes and proto-oncogenes. ¹⁵⁷ When local tumours spread and infect external tissues in the body, they develop into carcinomas.

1.5.3 Causes of Cancer

As previously stated, several malignancies have been associated to repeated exposures or risk factors, particularly in adults. A real threat factor is something so increases an individual's likelihood of contracting an infection. A cancer risk has not always reasoned the disease, but it might decrease the body's resistance near it. Tumour is thought to be caused by the below mentioned risk reason and mechanisms:

Lifestyle aspects: Tobacco intake, high-fat contains diet, as well as exposure to harmful chemicals be all examples of way of life decisions that could be major risk factor for a diverse reason of adult cancers. However, mainly kids with cancer are as well young to have been exposed to these way of life variables for a long period.¹⁵⁸

Some paediatric malignancies may be influenced by family background, heredity, conditions: This is conceivable meant for cancers various types to occur several times in a

family. In some cases, this is uncertain but the sickness is the result of a genetic abnormality, along with exposure to toxins, and mixed of reason, or cleanly happenstance.¹⁵⁸

Some genetic disorders: Beckwith-Wiedemann and Wiskott-Aldrich diagnoses, for example, have been linked to immune system dysfunction. The immune system is a vital organ sophisticated method that protects. The bone marrow produces cells that grow and function as part of the body's immune system. One theory holds that stem cells found in the bone stem become damaged or defective, and when they double to make new cell, they generate cancer cells. An inherent genetic defect or interaction to a pathogen or toxin might be the cause of stem cell insufficiency. ¹⁵⁹

Exposures to certain viruses: Certain paediatric malignancies, example Hodgkin's and non-Hodgkin lymphoma, were found related to the Epstein-Barr virus & HIV, the virus that cause AIDS. Then affected cell reproduces an altered cell, and these modifications eventually transform into a malignancy cell that produces additional cancer cells.¹⁶⁰

Environmental hazards: Herbicides, fertilizers, and electrical wires were all been linked to paediatric malignancies. Cancer has been reported among unrelated in some areas and/or cities. It is uncertain if prenatal or new-born contact to these substances causes malignancy or coincidence. ¹⁶¹

Some high-dose radiation and chemotherapy treatments: who have been subjected to these substances may provoke second cancer in certain situations. The effective anticancer drugs Cells or the immune response can be modified. Cancer is a second type of malignancy develops as a effect of treatment for another cancer.¹⁶²

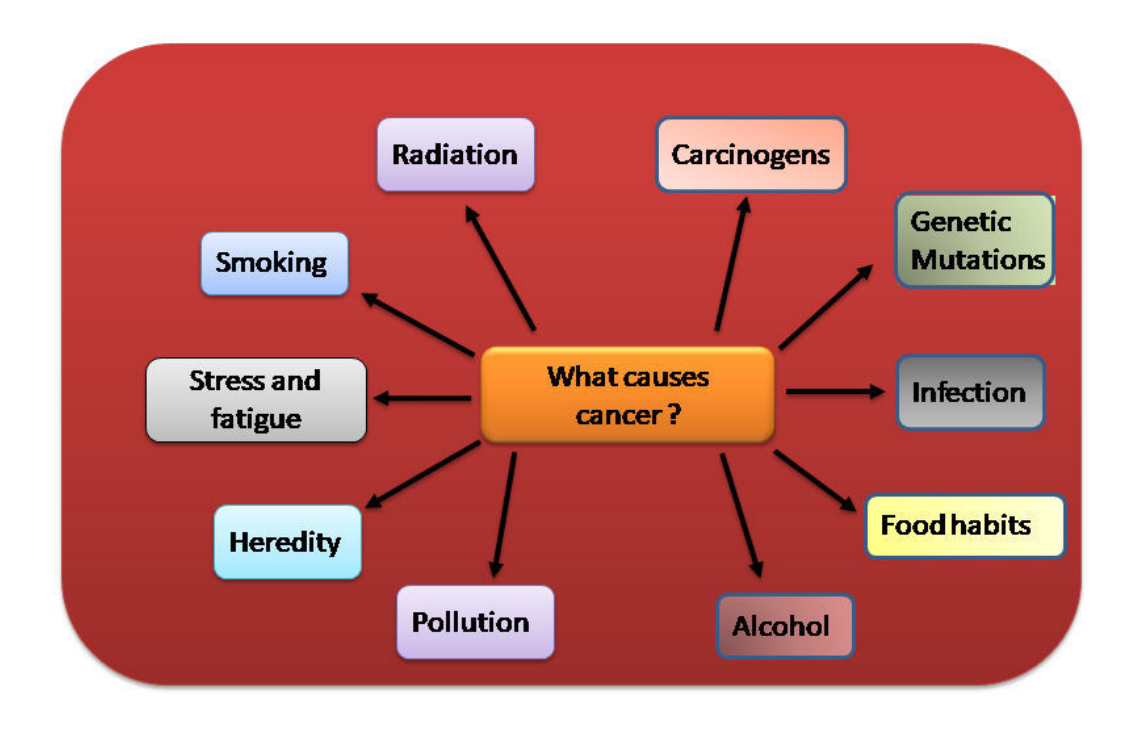


Figure 1.1: Schematic representation of Factors affecting the development of cancer

1.5.4. Cancer statistics (Indian & Global scenarios)

First and for most, the graph depicts the global incidence of female breast cancer. Different malignancies are colour-coded on the chart. Breast cancer is denoted by the colour pink.' Breast cancer is the most frequent malignancy among females globally. In 2018, an estimated 20.8 lakh (2.08 million) women worldwide were diagnosed with breast cancer. In addition, breast cancer accounted for around 24.2% of all malignancies in women. Breast cancer accounted for about one-quarter of all cancers in women.¹⁶³

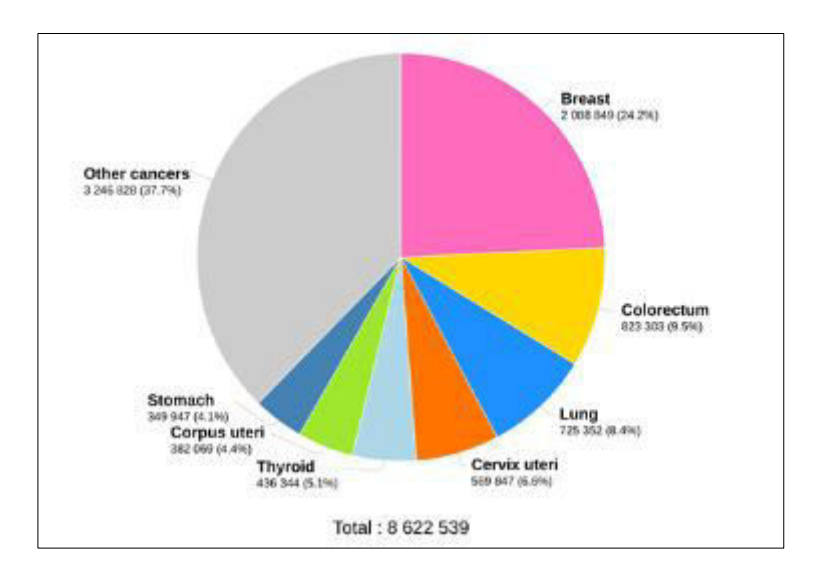


Figure 1.2: Estimated numbers of new cases in 2018, worldwide, including females, and all ages 164 (https://www.breastcancerindia.net/statistics/statglobal.html).

Treatment strategies for cancer

Radiotherapy is among the most used systemic therapies for early-stage breast cancer, as well as its usage has improved the mortality of women who have been diagnosed. Non-specific systemic administration, on the other hand, causes harm to normal unaffected tissue, resulting for both short- and long-term poor outcomes such as heart problems and infertility. Considering this nonspecific form and the issues that arise, there is an obvious and pressing need to develop novel medicines that selectively target and kill cancer cells. The drug's homing, precisely to cancer cells, decreases toxicity while increasing anticancer activity.

The cancer therapy alternatives are:

Surgery: The goal of surgery is to remove tumour or to remove as much it as possible.

Radiation therapy: Radiation therapy involves strong high - energy been of radiation including such X-rays or protons to eliminate cancer cells. Radiation therapy can be given from one device without the person (external radiation) or from inside the person (internal beam radiation). Bone marrow transplant: Bone marrow is the material found within your

bones that generates leukocytes from blood stem cells. A stem cell transplant, in form of bone marrow transplant, individual or a donor's bone marrow bone marrow. Higher doses of chemotherapy to cure your cancer followed by a bone marrow transplant. It has the potential to be used to treat disease bone marrow.

Immunotherapy: Immunotherapy, also referred to as biological treatment, uses patients own body's immune system to fight cancer. Cancer may spread uncontrollably in your body when your immune system fails to recognize it as an invader. Immunotherapy can help your immune system detect and battle cancer. ¹⁶⁵

Hormone therapy: Hormone levels in your body can cause some malignancies. Two examples are breast and prostate cancer. If such hormonal is withdrawn as from system or their activities are prevented, cancer cells may stop growing.

Radiofrequency ablation: Electrical energy is used in this therapy to kill cancerous cells by burning them. When radiofrequency ablation, a doctor will insert a thin needle through the skin or an incision into the cancer tissue. High-frequency radiation passes through the needle, scorching and killing the surrounding tissue.

Targeted drug therapy: The therapy using targeted drugs focuses on particular defects inside cancer cells that allow them to survive.

Carbon nano dot synthetic techniques and characteristics

The processes used in the CDs synthesis of may be separated into two parts: top-down and bottom-up techniques. The features of CDs' physicochemical and optical features, including particle diameter, surface functional groups, doped, and PL emission, are governed by synthetic techniques and materials. Top-down techniques focus on shrinking the beginning materials created by plasma treatment, los laser ablation, electrochemical oxidation, los and arc discharge. los

Bottom-up methods rely on generating CDs from precursors in a inhibited environment to make the CDs. Where most prevalent methods is pyrolysis, ^{169,170} hydrothermal pyrolysis, and microwave pyrolysis are examples of bottom-up approaches. ¹⁷¹

1.6 Carbon dots nanomaterials for therapy

Carbon dots (CDs), initially found in 2004, are a recent addition to the useful nonmaterial category that comprises fullerene, ¹⁷² nanotubes & grapheme. ¹⁷² These part provide a quick review of the CD structure and classification, followed by a description of the various methods used to produce CDs and their advantages as well as disadvantages. Moreover, the part analyses the conceivable processes discovered to describe photoluminescence, one of CDs' most valued features. Then there are recent advancements in CD function such as sensing, ¹⁷³ imaging, ¹⁷⁴ nano medicine, ⁷⁹ photo catalysis, ¹³⁶ photovoltaics, ¹⁷⁵ along with optoelectronics ¹⁷⁴ are explored. The nano-sized luminous CDs are carbon-based nanoparticles with a surface passivation with a diameter of less than 10 nm. ¹⁷⁶ They have regarded novel kind of nanoparticle capable of replacing semiconductor-related QDs. ¹⁷⁷ Their adjustable emission spectra, chemical inertness, and low toxicity contribute to this. Several investigations have shown that 8-10nm CDs have great optical performance and are preferable in terms of low toxicity. ^{178–180}

The shape of a CD is greatly impacted by the source content as well as the processing method. ¹⁷³ CDs are often separated into three distinct zones depends on photoluminescence emission, as illustrated. The Core part of CD is located in the centre and made up of sp² hybridized graphene-like carbon atoms. ¹⁸¹ Difference of the core sp² structure, as shown in Figure 1.12, have additional categorized Carbon dots may be converted as graphene quantum dots, graphene CDs, and amorphous CDs. ¹⁸²

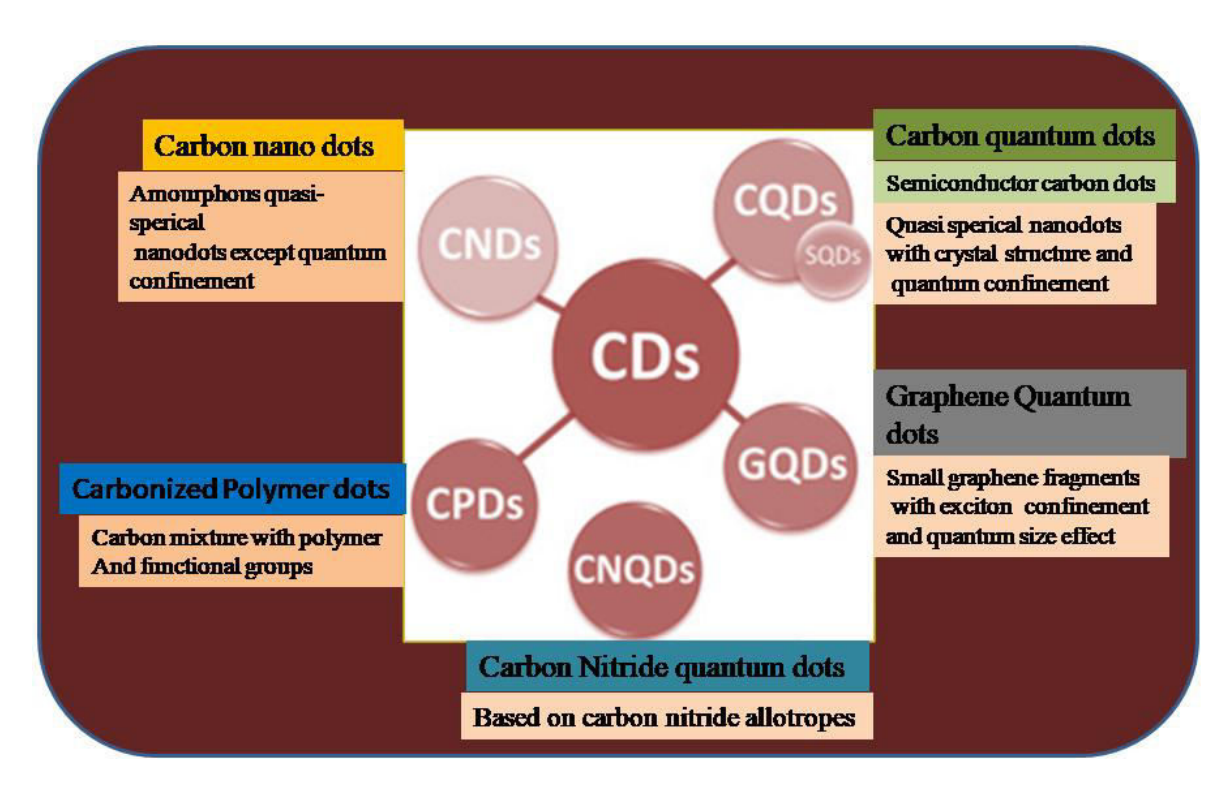


Figure 1.3: Different types of carbon dots and their example

Graphene is an two-dimensional material with a single layer of carbon atoms linked by sp² hybrid bonding, ¹⁸³ graphitic core carbon dots is constructed from layers of sp² hybridized carbon. In addition to crystalline graphitic cores, other groups have produced carbon dots having extremely elevated N doping level, implying that their cores are Carbon nitride formations that are graphitic or crystalline in nature. On the other side amorphous carbon is a very common material carbon dot structures and the topic of this study. ¹⁸⁴ Variable quantities of a structure resulting in structural chaos. In general, these amorphous CDs dimension below 10 nm in length and 0.5 to 5 nm in height. ¹⁸⁵ The lattice gap between layers is typically 0.34 nm. ^{185,186}

1.6.1 Carbon dot for imaging

CDs have demonstrated significant promise as probes for studying biological systems due to their unique properties such like their surface tuning abilities functions, superior photostability, brightness, Cytotoxicity, and impulsive penetration capabilities, making them particularly attractive for biological imaging-related applications. ¹⁸⁷ Different types of cells or tissues, on the

other hand, have distinct forms as well as structures associated biomarkers in the cytoplasmic or on the membrane, resulting in different reaction to foreign particles. As a result, diverse cell membrane lipids, proteins, targeted ligands, and biomarkers were used to manufacture specific functional CDs for creating impacting ways in imaging applications. Therefore in section, we first concentrate on three distinct important types CD-based cell imaging *in vitro*, especially cancerous cells imaging ^{190,191} stem cell therapy, ¹⁹² & neuron imaging, ¹⁸⁹ which enable the use of CDs for that in vivo models, particularly in investigating cancer and neurological disease research, diagnosis, and therapy, as discussed in the section on *in vivo* biomedical applications of CDs. Furthermore, the imaging of organelles, like nucleus imaging, ^{193,194} imaging of mitochondria and endoplasmic reticulum, and so on, ¹⁹⁵ were reviewed, which will be useful in understanding and studying organelle-related disorders.

1.6.2 Carbon dots for Treatment of cancer

Numerous studies investigated the potential use of CDs for cancer theranostic purposes, including targeted anticancer drug delivery, ¹⁹⁶ photodynamic treatment, ¹⁹⁷ photo thermal therapy, ¹⁹⁷ and gene transfer. ¹⁹⁸ This section highlights several *in vitro* as well as *in vivo* CDs for malignancy applications.

1.6.3 Carbon dot for Biosensor

CDs may function as superb electron donors or electron acceptors. CDs were used to detect chemicals such as DNA, ¹⁹⁹ thrombin, ²⁰⁰ nitrite, ²⁰¹ glucose, ²⁰² biothiol ²⁰³ and pH ²⁰⁴ by measuring alterations in their fluorescence intensity under external physical or chemical stimuli. The surface functional groups on CDs show unique affinities to various target ions, resulting in PL intensity quenching via an electron or energy transfer mechanism and excellent selectivity to other ions. Aside from using CD fluorescence as an analytical signal, current research has showed that CDs have good chemi-luminescence (CL) and electro chemi-luminescence (ECL). ²⁰⁵ CDs produced

from onion juice and lemon to detect riboflavin (vitamin B2) in another investigation. The selectivity of CDs for riboflavin detection was investigated with several compounds, demonstrating that CDs were selective for riboflavin. ²⁰⁶

1.6.4 Carbon dot for selective Detection of biologically relevant metal ions

Presence of metal ions are abundant in living organisms as well as engage for numerous key as an example material movement, conversion of energy, transmission of information, and metabolic control, rendering them necessary ingredients into human bodies. When there is a deficit or an excess, they might create health difficulties. To comprehend, it is critical to detect and detect metal ion accumulation in individual cells, organs, as well as complete organisms to improve illness diagnosis and numerous metabolic processes.²⁰⁷ Among the different technologies fluorescent sensors using organic dyes have been developed for metal ion detection gotten a lot of interest because of their many benefits, including large quantum yield, simple alteration procedures, and bio viability, as well as their simplicity of operation, enhanced sensitivity, quick sensing speed, and also real-time detection.²⁰⁸ Here covers current advances in metal ion detection and imaging in biological systems, such as Na⁺, Cu²⁺, K⁺, Mg²⁺,Ca²⁺, Zn²⁺, Fe²⁺/Fe³⁺and, and offers an view on the remaining obstacles in this field.

Sodium

In extracellular fluid, sodium is the most common cation. It helps to regulates blood volume, pulse pressure, osmotic balance, and pH levels, also maintaining fluid and electrolyte balance.²⁰⁹ The differential in sodium and potassium ion concentrations between external as well as internal fluid produces cell membrane potential, allowing the cell towards create an act potential.²¹⁰ Neurotransmission, Muscular contraction, and Heart function are all dependent on action potential.²¹¹ Sodium absorption in the small intestine is critical for chloride, amino acid, glucose, and moisture content. Na is also a crucial a component of the gastric juice²⁰⁹, this is beneficial for

digestion and absorption of nutrition. As a result, detecting Na+ ions are critical for both clinical diagnosis and research.

Potassium

Whereas sodium one of the most abundant cations of mammalian cells, potassium also most abundant cation within them, in animal potassium plays an important part in Balance of fluids and electrolytes, acid-base homeostasis, and systemic blood pressure management, hormone production and action, glucose and insulin metabolism, and neurotransmission. Potassium deficit and abundance can both cause a variety of symptoms such as an irregular heart rhythm and different electrocardiographic abnormalities. ²¹² It is critical to develop highly targeted and sensitive detecting and image of physiological K⁺ required for observing K⁺-related disorders and comprehension of physiological and patho physiological processes involving K⁺.

Calcium

Calcium is the fifth most prevalent element and the most common metal in human anatomy. The 99% of the calcium in the body is found in bones and teeth, with the balance of 1% present in the bloodstream & soft tissue. They function as electrolytes for secondary messenger in cell-signalling pathways ²¹³ modulating blood vessel constriction and relaxation, the transmission of nerve impulses, muscular contraction & hormone production such as insulin. Furthermore, calcium ions are required as a cofactor by several enzymes, including various coagulation factors. ²¹⁴ Ca²⁺ions, for example, are essential to activate seven "vitamin K-dependent" coagulation proteins that regulate blood clotting. For optimal physiological functioning, calcium contents in the blood or extracellular fluid are strictly regulated by the parathyroid glands and vitamin D.²¹⁴ Because calcium's rise and fall is the biological clock that regulates the execution of critical activities measuring [Ca²⁺] changes at the cellular level is critical. ²¹³

Iron

The most abundant element is iron prevalent metal with transition in the human body. It can exist in two physiologically significant states: There are two stable states: ferrous and ferric (Fe²⁺) and (Fe³⁺). Iron is required for several biological activities, ²¹⁵ including transport of oxygen, energy generation, Cell development and replication, as well as DNA synthesis via iron-dependent proteins. Heme containing enzymes (cytochromes a, b, and f oxidase, for example) contribute with electron transportation and/or oxidase activity. Iron-sulphur cluster proteins (Fe-S) have critical functions in energy production, nucleic acid synthesis, replication, and repair. ²¹⁶

Zinc

Zinc, among second most prevalent essential metal in humans after iron, is essential for increasing and development, Immune function, neuro transmission, eyesight, fertility, and intestinal ion transport are all affected.²¹⁷ The single metal ion is zinc among six enzyme families, where zinc is required for the operation of nearly 300 catalysts.²¹⁸ In addition to 1000 transcription factors.²¹⁹ Furthermore, zinc helps in structural role in numerous proteins, nuclear receptors, for example, contain zinc finger binding sequences in their structure, allowing them to bind to DNA and act as transcription factors to control gene expression. Zinc has been proven to influence hormone production.²²⁰ Zinc deficiency in the diet has been linked to decreased child growth and development, pregnancy difficulties, and immune system dysfunction.²¹⁸

1.6.5 Selective detection of heavy metal detection

Anthropogenic heavy metal pollution has resulted in the polluting as well as oceans, waterways, lake, and drinkable water an increasing care about one's health and safety.⁴ This study concentrates on the unique carbon dot optical nano probe for metal detection in water. And those environmentally friendly CDs created from a variety of origins and are typically recognized minimal chemical and biocompatibility characteristics.¹⁰ Certain heavy metal cations in water have

high selectivity and nanomolar detection limits.²²¹ These low-cost C-dots have the capacity to be useful to be used for *In-situ* environmental assessments. As a result, they can a huge favourable impact on environmental monitoring. Heavy metal ions present in aqueous systems above acceptable limits are hazardous to humans and aquatic life example Al +3, Mn+2, Co+2, Cu+2, Cu+2, Ni⁺, Cd⁺², As⁺³ etc. Previously mentioned heavy metals cannot be broken down. They accumulate in living creatures either directly or indirectly through the food chain.²²² Metal ions in the body can be transformed into more harmful forms or directly interfere with metabolic processes.²²³ Metal toxicity has resulted in a variety of illnesses and damage caused by oxidative stress caused by metal ions. 224 The toxic consequences of metallic pollution, along with the necessity for pure water for survival and sanitation, have driven researchers to take every feasible action to maintain water quality.²²² Various ways of detecting and removing metal ions from aqueous systems have been explored in this respect.²²⁵ We will look at metal-free water and the methods utilized for quick detection at low levels. The use of benign materials and methods for metal removal from aquatic systems is also covered in detail. For detection, electrochemical techniques, particularly stripping and cyclic voltammetry, are widely utilized, ²²⁶ but adsorption and ion exchange methods are extremely successful for removal.

Cadmium

Cadmium (Cd) is mostly found in nature as a compound in various minerals. Cadmium has been progressively manufactured since its discovery in the early twentieth century.²²⁷ Cadmium very commonly worn in the chemicals, electrochemical, electrical, and nuclear industries.^{228,229} Cadmium is produced as zinc smelting by product. It mostly used for batteries, dyes, and its absorbed crops more easily than some other heavy crops metals.²³⁰ Where Adequate amount of cadmium released into the surroundings as waste gas,²³¹ wastewater which resulting in contamination. Cadmium is mostly released into the surroundings via exhaust gas & sewerage.

Cadmium reaches the body through the bloodstream and rapidly accumulates in the liver and kidneys. 134 Cadmium is a known carcinogen that affects the function the number of catalysts involved in DNA repair, multiplying cell mistakes and genetic mutations and ultimately leading to cancer. 4

Arsenic

Arsenic commonly abundant element in nature, with variety of arsenic minerals identified. Natural arsenic is mostly derived through the overuse sewage, arsenic-containing additives and pesticides discharged from main industrial locations, and the oxidation of pyrite and arsenopyrite. The arsenic molecule found in nature, whereas arsenate is primarily found in, soil, food and water. Arsenic is extremely toxic to the human body. It immediately affects the human body's tiny artery and capillary walls and interferes with the vasomotor centre. Furthermore, high levels of arsenic can disrupt cell metabolism, alter cell damage is caused by the respiration and oxidation processes. Arsenic enters body via skin contact or wound. Long-term exposure to arsenic can increase the risk of cancer, particularly melanoma, lung cancer, urinary cancer, and liver cancer. 233

Manganese

Manganese (Mn) is a trace metal that is required by all forms of life. As a result, everyone requires it for appropriate development, growth, and functioning.²³⁴ Manganese traces are part of a healthy diet. Excessive exposure, on the other hand, might cause hazardous effects.²³⁵

Keeping manganese in check might be difficult. Toxic levels for certain processes are advantageous to others.²³⁶ Excess manganese is more common in people than deficiency, since it is present almost everywhere. Manganese is mostly deposited in the bones (40%) as well as the liver, kidneys, adrenal and pituitary glands. ²¹⁴ Some can be distributed throughout circulation and easily penetrate the placental and blood-brain barriers.²³⁷

Aluminium

In earth's crust aluminium is the third most abundant element in the nature.²³⁸Aluminum is found naturally in the atmosphere, water, and soil. Many parameters, including water pH and organic matter concentration, have a significant impact on aluminium toxicity. Its toxicity rises as the pH decreases.²³⁹ The mobilization of harmful aluminium ions as a result of pH changes in soil and water induced by acid rains and rising acidity of the surrounding atmosphere harms the ecosystem. This is represented by forest drying, plant poisoning, agricultural decrease or failure, aquatic animal mortality, and different imbalances in the functioning of human and animal systems.²⁴⁰

Copper

Most living organisms require copper (Cu) as a redox-active ion.²⁴¹ Indeed, nature has used redox cycle of Cu⁺ and Cu²⁺ to carry out essential biological activities including Electron transfer oxygen transport, and redox catalysis are all examples of redox catalysis.²¹⁴ The usual sumof Cu⁺ content in human blood plasma is around 1 mg/L, or around 16 M.²⁴² Total serum Cu levels in humans are deemed normal in the range of 12.7-22.2 M.²⁴³ The majority of Cu in plasma coupled with four separate carriers, generating discrete Cu²⁺ pools.²⁴³

Cobalt

Cobalt (Co) is a naturally occurring hard, gray metal. It may be found in rocks, soil, water, plants, animals, and humans. It can cause damage to the vision, the epidermis, the heart, and the airways. Sometimes cobalt exposure may result in cancer.¹⁹¹ The dose, time, and task done all influence the extent of harm. Cobalt is utilized in a variety of industries. It is found in instrument for grinding and cutting, pigments and paints, colour glass, and surgical implants, batteries, and certain electroplating. Its radioactive isotope is employed in medical imaging as well as food irradiation.²⁸

Nickel

Nickel is the 24 th most prevalent element in the Earth's crust and the 5th most plentiful element by mass after iron, oxygen, magnesium, and silicon.²⁴⁴ Nickel and nickel-containing compounds have several industrial and commercial applications because to their chemical characteristics, gloss, and inexpensive cost. Nickel is employed in a variety of applications due to its unique mix of remarkable physicochemical features.²⁴⁶ The widespread usage of nickel in different sectors, as well as occupational exposure, has a detrimental influence on human health.²⁴⁷

1.7 Antimicrobial activity and basic mechanism use of carbon materials for Antibacterial activities

There has been an increase in latest years a desire to find and manufacture new antibacterial compounds derived as of diverse sources of information overcome microorganism's resistance. ¹³⁰ As a consequence, screenings for antibacterial activity and assessing approaches contain attracted greater attention. Several bioassays are well-known, including disk-diffusion, well diffusion, or broth or agar dilution recognized and extensively used. While others, including flow to fluorometric and luminescent techniques generally utilized. Because they need specific equipment and next examination for repeatability and uniformity, even if they are possible offer immediate findings actions of the antibacterial agent and a deeper knowledge of their influence on cell viability and damage done to cells. ²⁵

1.8 Motivation and problem definition of this work based on the literature review

Retaining the carbon dots bio-safe is a challenge in imaging, biological metal ion detection, drug delivery, and heavy metal ions detection system. The preparation of carbon dots by synthetic approaches and the development of nonporous capsules with porosity is not an easy assignment.²⁴⁸ Extensive study work has been carried out on the synthesis of carbon dots based biological application system and nano porous capsules with desired size and shape. Synthesis has

been followed through without using any harmful surfactant or precursor. Synthesis of harmless precursor-based carbon dots in a green synthesis approach 245 to develop potential carrier capsules as a payload for anticancer drugs and nano medicine. The development of capsules with significant and superior qualities such as a wide and huge range of porosity has been ignored and it's a grand challenge to the scientific community to develop nano porous capsules with good viability and with minimum side effects and less Cytotoxicity. Very few reports are available on the capsules with target specific or organ-specific drug delivery and its degradation or removal from the body after completion of its assigned work. To address this, the current research work has been undertaken and discussed in the respective chapters.

Because of their enormous potential, nano-materials have been investigated for a variety of biological applications, one of which is their usage as an antibacterial component.²⁴⁶ There has been continuous research to identify appropriate antibiotic medicines. 90 Because of their antibacterial qualities, metals and metal oxides such as Cu and Ag have been used for a long time. Nanoparticles based on polymer, metal, metal oxide, and other materials are now gaining traction for usage in this industry. Antimicrobial properties of NPs such as ZnO ²⁴⁷ (zinc oxide), GO (Graphene oxide) ¹⁷², CuO ³⁶ (copper oxide), chitosan, ¹³¹ SnO₂ (tin oxide), ²⁴⁸ Ag₂O (silver oxide), ²⁴⁹ and others have been documented and exploited. NPs, on the other hand, have unique features and have been seen to interact with the thiol group of enzymes, inactivating the biological activity of the proteins. ²¹⁶ It is also observed that the oxide nanoparticles promote the production of reactive oxygen species (ROS), which is thought to be the basis for their method of action against microorganisms. However, most NPs are synthesized using a capping agent/surfactant for stability, which sometimes reduces efficiency, increases cost, and lengthens the synthesis time. Antibiotics are currently crucial tools during the fight against infectious illnesses. Although, the spread antibiotic tolerance, along with a lack of freshly developed antimicrobial drugs, endangers to human and animal health.²⁵⁰ The rational use of antibiotics is one of the most important techniques for combating antimicrobial resistance.²⁵¹

Factors influencing antibacterial activity have also been examined in this review. Consideration bacterial status, inoculums size, antibiotic dosages, serum effect, or association with the patient gut micro biota are among these considerations. Antibiotic host dispositions, including metabolism, transport mechanisms, and diffusion between various hosts. These conclusions may be valuable in developing higher potent clinical antibiotic treatment.

1.9. Objective and scopes of the dissertation

With the above-mentioned status and motivation, the objectives of the research are as follows:

Objective 1: Synthesis of seed derived carbon nanocapsules for cell imaging, depolarization of mitochondrial membrane potential, and dose-dependent control death of breast Cancer.

Objective 2: Synthesize of carbon dots from kernel part of seed and study the Photoluminescence mechanisms and applications in detection of biological relevant metal ions.

Objective 3: High temperature synthesized carbon dots and its absorption of heavy metal ions.

Objective 4: Revealing the structures of nano cellulose from Neem bark antimicrobial activity and their application: an *in vitro* study.

1.10. Justification of the objective

- ❖ Carbon nano-capsules derived from neem seeds never been reported. These seed-derived carbon nano capsules used for the cell imaging, depolarization of mitochondrial membrane potential, and dose-dependent regulation of breast cancer have never been reported. Therefore, the proposed work is novel. .
- ❖ Carbon dots for biological metal ion detection: Synthesize of carbon dots from kernel part of seed: Photoluminescence mechanisms and applications in detection of biological relevant metal ions also never been reported and the work reported here is novel.
- Carbon dots derived from Neem seeds and their uses in detection of heavy metal ion also new.

❖ Antimicrobial activity of the of the carbon materials obtained from Neem bark possess antimicrobial activity and their applications reported is for the first time.

1.11 Organization of thesis

The thesis is categorized into five chapters namely, **Chapter I** Introduction & Literature review; **Chapter II** Materials method & experimental process; **Chapter III** Results and discussion which included another four sub-chapter **Chapter IV** Conclusion and future aspects.

Considering the overall thesis, the introductory **Chapter I** briefly describes the use of carbon dots in various applications with a brief note on nanotechnology, applications of carbon dots, nano medicine, and drug delivery system. Additionally, an overview of breast cancer, cell imaging, breast cancer mortality is controlled by mitochondrial membrane potential and dose-dependent control. Illustrate the existing literature on different types of carrier capsules for cell imaging, mitochondrial potential, metal ion detection, and antimicrobial activity. **Chapter II** discusses materials and procedures for undertake the reported study work; also consists of experimental details for the preparation of carbon dots, nanocapsules, in addition to development and characterization through the various instrumentation methods **Chapter III**

<u>Part 1:</u> Synthesis of carbon source from seeds nano capsules cell imaging, depolarization of mitochondrial membrane potential, and dose-dependent control death of breast Cancer.

<u>Part 2</u>: Synthesize of carbon dots for kernel part of seed: Photoluminescence mechanisms and applications in detection of biologically relevant metal ions.

<u>Part 3</u>: High-temperature synthesized carbon dots and their absorption of heavy metal ions.

<u>Part 4</u>: Revealing the structures of nano cellulose from Neem bark antimicrobial activity and their application: an *in vitro* study.

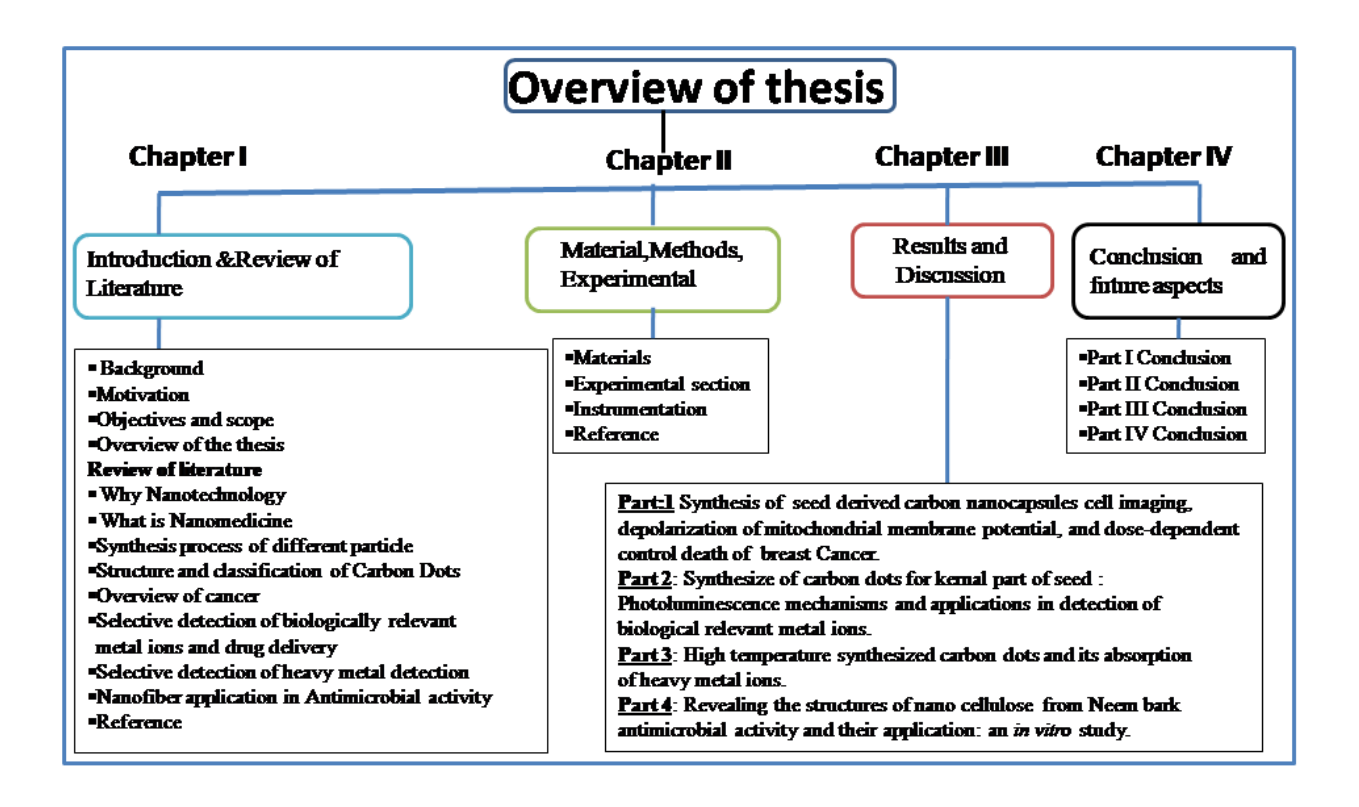


Figure 1.4: Schematic overview of the thesis work with details and description in each chapter

CHAPTER: 2

MATERIALS, SYNTHESIS METHODS, AND CHARACTERIZATION TECHNIQUES

CHAPTER: 2

MATERIALS, SYNTHESIS METHODS, AND CHARACTERIZATION TECHNIQUES

In this chapter, materials, methods used to synthesize the samples, and experimental techniques utilized to characterize the samples have been explained in detail.

2.1 Materials and Methods

2.1.1 List of chemicals used

The chemicals required for the synthesis of carbon dots were purchased from different suppliers and used without further purification. The high-purity (99.8%) chemicals were used for the synthesis of mesoporous carbon nanocapsules and carbon dots. Following is the list of chemicals used to synthesize different types of mesoporous carbon nanocapsules and carbon dots for drug loading and delivery.

Table: 2.1. Shows the list of chemicals required for the synthesis of different types of carbon dots and the fabrication of mesoporous carbon nanocapsules.

S. No	Name of the chemical	Make	Purity
1	MTT (Methylthiazol tetrazolium)	Sigma Aldrich	-
2	FTTC Annexin V Apoptosis Detection Kit I	Sigma Aldrich	-
3	PBS (Phosphate buffer saline)	Sigma Aldrich	-
4	DEA(Diethyl amine)	Sigma Aldrich	98%
5	Acetic acid	SDFCL	99.5%
6	Hydrogen gas cylinder	-	-

2.1.2. List of solvents used

Aside from the chemicals listed above, the following solvents are also necessary for the synthesis of various types of carbon dots and the fabrication of mesoporous carbon nanocapsules. For ¹H NMR characterizations, CDCL₃ (Deuterated chloroform) was used as a reference solvent. The anticancer medication (DOX) molecules were dissolved in dimethyl sulfoxide (DMSO). Some solvents may contain impurities and must be purified using simple steam distillation and fractional distillation procedures before being used in processes.

Table: 2.2. Shows the list of solvents required for the synthesis of different types of carbon dots and the fabrication of mesoporous carbon nanocapsules.

S.NO	Name of the solvent	Make	Purity
1	CH ₃ OH(Methanol)	SDFCL	>99%
2	Acetone(CH ₃ COCH ₃)	SDFCL	> 99.5%
3	Ethanol(CH ₃ CH ₂ OH)	Merck	≥ 99.9 %
4	DMSO (Dimethyl sulfoxide)	Sigma Aldrich	99.9%
5	IPA (Isopropanol)	SRL	99%
6	CDCL ₃	Sigma Aldrich	99.96%
7	PTA	Sigma Aldrich	99.995%
8	diethylamine	Sigma Aldrich	≥99.5%
9	Distilled Water	-	-
10	MQ water	-	-

2.1.3 List of Drug used

Aside from the solvent listed above, the drugs are also necessary for study the biological activity of the synthesized carbon dots and mesoporous carbon nanocapsules and their cumulative effect on the cancer cells and comparatively normal cells.

Table: 2.3. Shows the list of anti cancer drugs used to load inside the pores of capsules to treat various cancers.

S.No	Name of the anticancer drug	Make	Purity
1	Doxorubicin hydrochloride (DOX)	Sigma Aldrich	98.0-102.0%

2. 1. 4 List of glassware and consumables used

To synthesize the carbon dots and fabricate mesoporous carbon nanocapsules, several reactions needtobeperformed and forthat, some apparatus and glass wares are required.

Table: 2.4. Show the list of glassware and apparatus required for the experimental procedure to synthesize carbon dots and the fabrication of mesoporous carbon nanocapsules

S. No	Glassware/Apparatus	Make/Purpose
1	3 Neck round bottom flask	Borosil/reactions
2	THF distillation setup	Borosil/solvent purification
3	Reflux mantle -	
4	Water circulating pump	-
5	Rubber septums	-
6	Magnetic bead	-
7	Hot plate cum stirrer	-
8	Inert gas cylinder (Ar/N ₂)	-
9	Stoppers(L-Shape)	-
10	Conical flasks	Borosil
11	Syringes	-
12	Micropipettes	-

13	Beakers	Borosil
14	Whatman filter papers	-
15	Glass slides	-
16	Copper grids	-
17	Balloons	-
18	P ^H Paper/meter	-
19	Support stand	-
20	Funnels	Borosil
21	Spatulas	-
22	Tissue rolls	-
23	Aluminum foil	-
24	Coverslips	-
25	Para film	-
26	NMR tubes	Proton
27	FACS tubes	-

Most importantly, beakers, conical flasks, stirrers, inert gas cylinders, hydrogen gas cylinders, magnetic beads, etc as mentioned in the following (Table 2.4). Since some reactions are complicated to perform for that fume hood and others safety precautions need to be taken.

2.1.5 List of materials used in cell culture

Aside from the glass wares and apparatus mentioned above, some of the following chemicals (media) and consumables such as glassware, Petri dishes, etc. are required to conduct biological experiments, such as for cell culture, cell treatment, apoptosis and cell cycle studies, including western blotting analysis for protein expression and cellular imaging before and after cancer cell treatment (Table 2.5).Cell-based experiments were extremely sensitive and accomplished without contamination by employing a CO₂ incubator (at 37.4 °C and 5% CO₂ volume).

Table: 2.5. Show the list of Materials required for cell culture and other cell-based studies.

S. No	Materials for cell culture	Make
1	Liquid nitrogen	-
2	60 mm Petri plates	Sigma
3	100 mm Petri plates	Sigma
4	Glass culture dishes 35 mm diameter	Sigma
5	RPMI Media(Gibco) 1640(1X)	Gibco
6	DMEM(1X)	Gibco
7	FBS	Gibco
8	Antibiotic Antimycotic solution 100XLiq. Endotoxin tested	Gibco
9	PBS (Cell culture)	-
10	Alcohol (Cell culture)	-
11	6 Well plates	Eppendorf
12	24 Well plates	Eppendorf
13	Alcohol Spray bottle	-
14	Cryo vials	-
15	Syringe(1mL)	-
16	0. 5 Micron filters	-
17	Annexin-V	
18	PI	
19	Rhodamine 123	
20	1× Binding buffer	

2.1.6 List of cells used

Following list (Table 2. 6) cells are cultivated and utilized to test the killing efficacy and cellular inhibition of anticancer medicines released from specially designed carrier capsules.

Table: 2.6. Show the list of cells used for the cell culture and other cell-based studies.

S. No	Name of the cell	Type of cell
1	MCF-7	Breast cancer metastatic adeno carcinoma.
2	MDA-MB-231	An epithelial, human breast cancer cell line.
3	Normal splenocytes	From normal mice cell spleen.

2.1.7 Bacteria used for antibacterial activity

Following listed (Table 2.7) bacteria are grown and utilized for the antibacterial activity of the synthesized mesoporous carbon nanocapsules and carbon dots to test the killing efficacy of bacteria.

Table: 2.7. Show the list of bacteria used for the antibacterial activity

S. No	Bacteria	Supplier
1	E. Coli	ATCC 25922
2	Candida Albicans	ATCC 24433
3	Staphylococcus Aureus	ATCC 25923
4	Klebsiella Pneumoniae	ATCC 700603

2. 2. Experimental section

2.2.1. Collection of Neem seed and barks

The raw *Azadirachta Indica* (Neem) seeds and Kernel were collected from the plant of our Institute's Farm House. The neem bark used in this study was obtained from a local market in the adjacent biodiversity hotspot of Hyderabad, Telangana, India.

2.2.2. Preparation of cake powder from seed, kernel & bark

Preparation of Mesoporous Carbon Nanocapsules (mCNCs).

The raw *Azadirachta indica* seeds were collected from the Institute campus and then cleaned, dried, and kept in a hot plate for 24 hrs at 60 °C. The kernel part has been separated from the seed part and grinded properly followed by calcinations at different temperatures (e. g., 250, 300, 350, and 400 °C), and then the calcinated samples were homogenized properly using a 1:1:1 ratio of sodium meth oxide, diethyl amine, and methanol solution. 10 gram of the calcined sample was taken in 50 mL of solution for homogenization. The mixture was thoroughly stirred for 24 hrs (300 rpm) at 120 °C of bath temperature. After 24 hrs, the mixture was filtered, and the solute part was dried at 80 °C. Then the samples were characterized through different tools. It can be noted that the samples were designated as follows: SN-1, SN-2, SN-3, and SN-4 which were calcined at the temperatures of 250°C, 300°C, 350°C and 400°C, respectively. The detail of the synthesis method has been filed for Indian patents (application no.: 202011018557, dated 30 April 2020).

Development of carbon-dots from Kernel part of Neem seed:

The raw kernel part of Neem seeds and CDs were synthesized by the pyrolysis method. As received Neem seed's kernel parts were separated and then kept in a hot plate for 24 h dried properly followed by calcinations at 350°C (KS-1),400°C (KN-1), and 450°C (KN-2). Carbonization of the kernel part of Neem seeds was then grinded properly. Then purified Carbon dots CDs were transferred to the vial and stored for further characterization. It can be noted that the details synthesis method has been filed for Indian patents (Ref No: 202111060434, Dated: 23 rd December 2022).

Preparation of nanocellulose nanofibers from the Neem bark:

Azadirachta indica in its natural state bark was washed, dried, and stored on a hot plate at 60 °C for 24 hours. By mixing lingo cellulosic bio-mass at 70-80 °C using distilled water, sodium chlorite salt, and acetic acid for 10-12 hours bulk of lignin and other components was extracted by adjusting the pH With Acetic acid, and sodium chlorite in each hour. After the overnight stirring, the mixture is washed with distilled water until it reaches a neutral pH And the obtained product was dried at 50°C in hot air oven and the solid products was collected. Acid hydrolysis is a common technique for obtaining nano cellulose from cellulosic material. Sulphuric acid is the most often utilized acid.

2.2.3. Biohazards and their handling

Carcinogenic and hazardous materials must be handled with caution following the material safety data sheet (MSDS). Because phosphotungstic acid (PTA) is detrimental to health, proper care must be followed while adding it to carbon capsules and neem seed and bark-derived samples. All chemicals and samples that were temperature and light-sensitive were protected with in aluminum foil and stored in a dark room. Inside the fume hood, reactions involving carcinogenic and dangerous substances were transmitted to reaction chambers. Following the immediate delivery of chemicals from suppliers, the chemical bottles were put in a plastic freezer bag and kept in the freezer at -4 °C and -20 °C (per storage instructions). To avoid contamination, gloves and an apron were used during the experiment.Contact items are thrown away in biohazard garbage. Chemical waste and unwanted solutions and solvents were properly disposed out in according to local authorities' guidelines.

2.3 Instrumentation

Below is mentioned list of equipment to characterize the samples.

2.3.1. Synthesis of carbon dots was confirmed by

- 2.3.1.1. FTIR: Functional groups identification
- 2.3.1.2 NMR (Nuclear magnetic resonance) (¹H) chemical structure.

2.3.2. Morphology and other physical properties

- 2. 3. 2. 1. FE-SEM (Field emission scanning electron microscope)
- 2. 3. 2. 2 TEM (Transmission electron microscope)
- 2. 3. 2. 3 AFM (Atomic force microscope)
- 2. 3. 2. 4 BET (Brunauer-Emmett-Teller)
- 2. 3. 2. 5 DSC (Differential scanning calorimetry)
- 2. 3. 2. 6 TGA (Thermo gravimetric analysis)
- 2. 3. 2. 7 XRD (X-ray diffraction)
- 2. 3. 2. 8 DLS & Zeta Potential
- 2. 3. 2. 9 Multimode plate reader
- 2. 3. 2. 10 Fluorescence Spectroscopy (FL)

2. 3. 3. Biological studies

- 2. 3. 3. 1 UV-Visible: (Drug loading and release)
- 2. 3. 3. 2 LSCM (Laser scanning confocal microscopy)
- 2. 4. 3. 3 MTT: Cytotoxicity and cell viability studies
- 2. 3. 3. 4 Flow cytometry (FC) cell cycle and apoptosis
- 2. 3. 3. 5. Fluorescence microscopy
- 2. 3. 3. 6 Cell culture

2.3.1.1. FTIR: (Fourier transform infrared) Spectrometer

The functional groups of mesoporous Carbon Nanocapsules and carbon dots were described using the Nicolet model Impact-410 model, Infrared spectroscopy, which operates in the infrared area of the electromagnetic spectrum. Based on absorption, IR may be used to discover and study inter-conversions, exchanges, and the synthesis of new functional groups in chemical compounds. It is a typical laboratory device that is extensively used for early confirmation of reactions' beginning or results. It has a substantial advantage over a dispersive spectrometer, which measures intensity over a limited range of wavelengths at one time. The purpose of absorption spectroscopy is to determine how efficiently a sample absorbs light at different wavelengths. The most basic method is dispersive spectroscopy, which involves shining a monochromatic light beam at a sample, measuring how much of the light is absorbed, and repeat for each different wavelength.

2.3.1.2 NMR (Nuclear magnetic resonance ¹H)

The chemical structure and formula of organic and polymer samples were characterized using Bruker DPX¹H NMR. The NMR samples were dissolved in moisture-free CDCl₃ at 25 °C. The type and position of photons were confirmed through ¹H NMR, more broadly speaking for the chemical structure and formula of compounds. However, spectroscopic techniques are categorized which define the interaction between electromagnetic radiation and matter. The ¹H NMR spectra include several signals which mean how many different types of hydrogen atoms are there in a molecule. Relative areas under signals represent about how many hydrogen's of each type are there in the compound and the splitting pattern gives information about how many neighbouring hydrogen atoms are present in the chemical compound. The NMR activity towards the element or molecule completely depends on the nuclear spin. NMR spectroscopy is a physicochemical investigation technique based on the interaction of radiofrequency radiation delivered externally

with atomic nuclei. During this contact, there is a net exchange of energy, which causes a shift in nuclear spin, an inherent feature of atomic nuclei. During this contact, there is a net exchange of energy, which causes a shift in nuclear spin, an inherent feature of atomic nuclei.

2.3.2.1. FE-SEM (Field emission scanning electron microscope)

The morphology, size, and form of carbon dots and mesoporous nanocapsules were examined using an FE-SEM at 15 kV accelerating voltage. The installation of an energy-dispersive X-ray detector (EDAX) in conjunction with digital image processing is a valuable tool for studying the material's elemental composition analysis. The FE-SEM generates clearer, less electro-statically distorted pictures with spatial resolution as low as one, which is three to six times better than the conventional microscope. With the little electrical charge of the samples, excellent quality, low-voltage pictures are generated. FE-SEM requires a high chamber vacuum mode (10⁻¹⁰ to 10⁻¹¹ torr) during operation.

2.3.2.2 TEM (Transmission electron microscopy)

TEM analyses were performed with an FEI-Technai G2 S-Twin TEM instrument (acceleration voltage of 200 kV). Carbon-coated copper grids have been used for the sample preparation. IPA, distilled water, and methanol were the main solvent used for the disperse Preparation of carbon dots, and mesoporous carbon nanocapsules.Based on the dispensability, synthesized solvents were used to disperse a pinch of powder sample was dispersed in 1 mL of propanol and then drop-cast on carbon-coated Cu grids (200 Mesh) followed by drying at 25 °C. Further, a drop of PTA stains (2% of phosphotungstic acid) was added to the Cu grid and kept for 15 s.TEM is a microscopic method in which an electron beam is delivered through an ultra-thin specimen, reacting with it as it goes through, and a picture is created as a result of the interaction of the electrons transmitted through the material. Imaging equipment is used to magnify and concentrate the image.In comparison to light microscopes, TEM is capable of imaging at very high resolution.

It produces images that are tens thousands of times smaller than that of the smallest resolvable object in a light microscope. TEM characterization provides information about the sample's micro and nanostructure upon imaging, as well as crystal structure, de-spacing, and pattern of the nanostructure. The absorption of electrons on the surface of the specimen sample or substance causes contrast. The brightness and contrast of a substance are determined by its thickness and composition.

2.3.2.3 AFM (Atomic force microscope)

The surface topography was investigated using an atomic force microscopy INTEGRA Aura model (NT-MDT, Russia). In general, atomic force microscopy is classified as SPM, which uses a mechanical probe to scan the surface of a material. Monitoring the scanning probe scans the surface topography. AFM is made up of a cantilever with a nanometre-sized tip (size 10nm). When the tip is brought closer to the sample surface, the forces between the tip and the sample create cantilever deflection. The laser shined on the cantilever surface measures the deflection in the cantilever. The photodiode records the laser's deflection, and the differential amplifier collects the output signal. Feedback control is used to regulate the tip's height above the surface, resulting in a topographic map of the surface.

Sample separation: A carbon samples solution was diluted and drop-casted onto mica sheets, and the surface topography was scanned. The sample was scanned in non-contact mode.

2.3.2.4 BET (Brunauer-Emmett-Teller)

The micromeritics Tristar-II 3020 model equipment was used to determine the BET surface area, Langmuir surface area, capsule/particle thickness, and porosity of the sample (Version 2. 00 unit). All of the above parameters, including specific surface area, were determined using nitrogen (N₂) gas adsorption-desorption isotherms. Well-dried and measured (amount of sample) samples were

put into sample tubes and linked to a heat chamber to remove moisture from the samples under evacuation circumstances, followed by the samples' optimal temperatures. The dried samples were fed into the BET device to get sample data.

2.3.2.5 DSC (Differential scanning calorimetry)

The TAQ200 model (Waters, Milan, Italy) DSC instrument was used to determine the heat flow of (mW) studies such as endothermic (heat require) and exothermic (heat release) from samples to observe the melting temperature (Tm) or glass transition temperature (Tg) of a material, particularly polymeric samples. DSC studies on polymeric materials were carried out in an N₂ gas environment from 30 to 600 °C at heating and cooling speeds of 10 °C min ⁻¹. The DSC is a Thermo analytical method that measures differences as a function of temperature. During the experiment, both the specimen samples and the reference samples are kept at about the same temperature. In general, the temperature program for a DSC study is constructed so that the temperature of the sample holder increases linearly as a function of time. The reference sample should have a well-defined heat capacity over the temperature range being scanned. The DSC instrument, most crucially, may be used to determine the following properties: (a) glass transition (Tg), (b) melting temperature (Tm), (c) heat of fusion (H_f), (d) percentage of crystallinity, and (e) crystallization kinetics and phase transitions. DSC instruments are made up of four main components that are used to examine the thermal characteristics of samples such as (1) furnace, which is the main assembly where the specimen sample and reference are heated according to the temperature program, and (2) auto sampler unit, which works to load and unload the pans as needed. (3) A cooling system or unit that allows the sample to be cooled and assists in archiving the desired temperature program and (4) A computer that serves as an interface between the user and the instruments and enables automated control of the instrument based on the program parameters.

2.3.2.6 TGA (Thermo gravimetric analysis)

Mesoporous carbon nanostructure samples were studied using a Thermo ONIX Gaslab 300 TGA equipment to determine the thermal stability (degradation and breakdown temperature) of carbon dots. The temperature scanning range for carbon samples is adjusted at 30 to 800°C in N₂ atmosphere with a heating rate of 10 °C/min. TGA measures the quantity and rate of change in a material's weight as a function of temperature or time in a controlled environment. Measurements are typically used to identify material composition and forecast thermal stability at temperatures up to 1000 °C. This method can describe materials that lose or increase weight owing to breakdown, oxidation, or dehydration. TGA accurately determines endotherms and exotherms in terms of weight lost during the heating and cooling processes. The procedures involved in sample preparation for TGA as well as its benefits are, sample preparation has a major influence on acquiring excellent quality data, it is proposed that increasing the surface area of the sample in a TGA pan enhances resolution and repeatability of weight loss temperature, samples weight affects the accuracy of weight loss data, normally 10 to 20 mg of sample is considered.

2.3.2.7 XRD (X-Ray Diffraction)

Bruker D8 Advance powder X-ray diffractometer was used to analyze the crystal structure and solid state (amorphous, crystalline, and semi-crystalline nature) of the mesoporous carbon nanocapsules samples (XRD). XRD is mostly used to determine the phases of samples in unit cell dimensions. The crystalline sample contains information at the unit cell level, including significant parameters such as the crystal's lattice, space group, and point group. The XRD apparatus was designed mostly on Bragg's equation

$$n\lambda = 2d \sin\theta$$
.....(eq no 1)

A crystal is defined by the periodic organization of a unit cell into a lattice for the formation of crystal. Crystalline materials are layered at different atomic planes to forma crystalline structure.

2.3.2.8 DLS and Zeta Potential

The hydrodynamic particle size of the samples was measured using the DLS method and the Mastersizer 3000 equipment (Malvern Instruments). The rate of particle diffusion in Brownian motion is size dependent. The instrumentation section deals with the laser illumination of suspended particles. At a scattering angle, the change in the scattering of the incident laser is calculated. The Stoke-Einstein relation describes the relationship between the diffusion coefficient recorded by the instrument and particle size Stoke-Einstein relation.

Where $D_h=K_BT/3\Pi\eta D_t$(eq no 2)

D_h is the hydrodynamic diameter,

D_t is the translational diffusion coefficient,

K_B is Boltzmann's constant,

T is thermodynamic temperature, and

η is Dynamic viscosity

The velocity of the particles owing to electrophoresis determines the zeta potential of the sample. Under applied force, a particle with zeta potential tends to move toward an electrode. The particle speed is evaluated using laser Doppler electrophoresis, and the theoretical zeta potential of the samples is obtained.

2.3.2.9 Multimode plate reader

A multimode reader is sometimes known as a plate reader or a multimode reader. Cell inhibition using our created nano formulations (anticancer medicines inserted inside the pores of the micro and nanoporous capsules) was examined using the MTT test on a Bio Teck Synergy H4 model multimode reader to determine the percentage of cell survival (viability). The anticancer medicines doxorubicin hydrochloride (DOX) was loaded into 96-well plates and utilized to test cell viability and cell inhibition in triplicate. For cell-based research, four distinct cell lines (MCF-7, MDA-MB-231) were employed. A photoluminescence (PL) study was performed on the microplate reader.

2.3.2.10 Fluorescence Spectroscopy (FL)

HITACHI F-4600 fluorescence spectrophotometer was used to record the fluorescence spectrum of a hierarchical self-assembled zinc phosphate nanostructure.

Fluorescence spectroscopy examines the sample's fluorescence. UV light is typically employed for these experiments, which entail the lighting of light on the material. Fluorescence spectroscopy is concerned largely with electronic and vibration states. By absorbing photons during illumination, the fluorescence species are stimulated to a higher energy level from the ground state. This excited molecule then returns to its ground electronic state, causing pictures to be emitted. In fluorescence spectroscopy, the energy and frequency of the emitted pictures change depending on the sort of excited molecules. The fluorescence spectroscopy apparatus comprises a light source (Xenon arc and mercury-vapour lamp) as an excitation source. A monochromatic control the wavelength of light, while the detector detects the wavelength of light emitted by the sample. The excitation light is kept constant during the collection of emission spectra, and the spectrum is canned for emission.

2.3.3. Biological studies

2.3.3.1. UV-Visible: (Drug loading and release)

The absorbance of released drug molecules was determined using a Perkin Elmer ((lambda-750) type UV-Vis-NIR spectrometer. The medication (anticancer) loading is mostly determined by the surface area of the particle or capsules and pore size (pore width and depth). Along with porosity, several aspects must be considered while calculating the number of drug molecules loaded, such as interactions between drug molecules and capsules such as Vander Waals, electrostatic, dipole-dipole, and forces induced by everlasting techniques. Most notably, bigger pores have higher loading efficiency than smaller pores. The amount of drug loaded and released was determined using the excitation and emission values of the drug. UV (ultraviolet) wavelengths range from 180 to 400 nm, visible scanning wavelengths range from 400 to 600 nm, and NIR (near infrared) wavelengths range from 600 to 3000 nm, with medication molecule (DOX) showing excitation (max) at 530 nm. At 530nm, an absorbance calibration curve against varied concentrations of pure DOX was obtained. There are three detection modalities for UV-VIS-NIR: transmittance, absorbance, and reflectance. Based on our needs, we must select one of the modes listed above for the UV-VIS-NIR examination.

The amount of drug loaded and released was determined using the excitation and emission values of the drug. For example, UV (ultraviolet) wavelengths range from 180 to 400 nm, visible scanning wavelengths range from 400 to 600 nm, and NIR (near infrared) wavelengths range from 600 to 3000 nm, with medication molecule (DOX) showing excitation (max) at 530 nm. At 530 nm, an absorbance calibration curve against varied concentrations of pure DOX was obtained. There are three detection modalities for UV-VIS-NIR: transmittance, absorbance, and reflectance. We must select one of the above-mentioned modes for UV-VIS-NIR analysis based on our needs.

2.3.3.2 Confocal laser scanning microscope (CLSM)

Using a Zeiss LSM 700 model laser scanning confocal microscope, we performed fluorescence microscopy imaging for capsules filled with live cell imaging after the treatment. To examine the cellular interaction with anticancer drug molecules, a medium (5uL) was dispersed on a glass slide and covered with a cover slop to prevent sample leakage.

The entire specimen is drenched uniformly with a light source in a normal wide-field fluorescence microscope. The microscopes or cameras detect the ensuing fluorescence from all areas of the specimen in the optical path, including a huge unfocused background region. In contrast, a confocal microscope eliminates out-of-focus signals by using point illumination and a pinhole in an optically conjugate plane in front of the detector; the term "confocal" comes from this design.

Sample preparation:

MCF-7 and MDA-MB-231 cells were seeded on glass culture dishes (35 mm diameter) for 24 h. Then culture medium was replaced with fresh media (2. 5 mL) containing (800 μ g mL⁻¹) and then incubated for another 24 h at 37 °C under 5% CO2. Then the treated cells were washed three times with PBS (pH = 7. 4) and examined through the confocal laser scanning microscope (CLSM) at a fixed excitation wavelength of λ = 405, 488, and 514 nm.

2.3.3.3 MTT: Toxicity and cell viability studies

The MTT test was used to assess the biocompatibility of nanocapsules and drug-loaded nanocapsules. The cell lines utilized in the MTT experiment for biocompatibility are as follows:

Study the Cytotoxicity by MTT Assay: Cytotoxicity effect of the synthesized carbon nanocapsules the MTT assay was performed separately on normal splenocytes, MCF-7 and MDA-MB-231. Isolated splenocytes were seeded in 96-well culture plates and kept in a CO₂ incubator for 24 h at 37°C in 5% CO₂. Similarly, MCF-7 and MDA-MB-231 cells were seeded separately in another

96-well plate and incubated for 24 h. The treatment with mCNCs with different concentrations such as 1,0. 5, 0.25, 0. 125, and 0 mg. ·mL⁻¹ (control) was performed for 48 h. Then, the freshly prepared 10 μ L of MTT solution in PBS was added to each well of the 96-well plates and incubated for 6–7 h at 37 °C with 5% CO2. To collect the prepared formazan crystals by viable cells, plates were centrifuged at 1200 rpm for 8 min and the supernatant was removed, and then DMSO was added to each well to dissolve formazan crystals. Then the absorbance was acquired by ELISA reader 595 nm.

2.3.3.4 Flow cytometry (FC) cell cycle and apoptosis

Cell sorting and counting are important tasks in biotechnology, biomedical, biophysical, and other medicinal domains. Flow cytometry from BD Biosciences has been used to investigate cell-based topics such as cell cycle and apoptosis. Flow cytometry uses FACS (fluorescence-activated cell sorting) to identify cells suspended in a stream of fluids and going through an electron detection device. The FACS method is commonly used to examine proteins, intracellular proteins, membranes, and nucleic acids like DNA. To analyze and collect data, the FC BD-FACS Diva program was utilized, which is a very adaptable package, designed for cell cycle and apoptosis.

Sample preparation: MCF-7 and MD-MB-231 cells were treated with carbon nanocapsules separately and then analyzed the percentage of apoptotic/dead cells. Before treatment, 1×10^6 breast cancer cells were cultured into a 6- well culture plate for 24 h. After that, the samples were added and incubated for 48 h, and then analyzed the percentage of apoptosis and necrotic cell death. Cells were taken after trypsinization and washed with cold PBS (pH 7. 4) and removed the supernatant. Subsequently, cells were resuspended in 100 μ L per sample with 1× binding buffer. Further, cells were incubated with 5 μ L of each annexin-V and PI solution and gently swirled to mix in dark conditions at room temperature. To measure the mitochondrial membrane potential (MMP, $\Delta \psi m$) through flow cytometry, rhodamine 123 dye was used. Rhodamine 123 (Rh-123) is

a green-fluorescent cationic dye that permeates cells and exclusively labels the respiring mitochondria without cytotoxic effects.Rh-123 is widely used to evaluate the magnitude of mitochondrial membrane potential to measure the population of apoptotic cells.²⁵² A total of 10,000 cells were acquired from each sample to analyze the apoptosis and MMP, $\Delta \psi m$ by BD FACS Caliber flow cytometry.

2. 3.3.5 Cell culture

Isolation of Splenocytes. Pathogen-free BALB/c (8–10 weeks old) was used for the isolation of the spleen. Mice were sacrificed after the treatment of anesthesia (diethyl ether). Spleens were removed and collected into the chilled PBS (pH 7. 4). Then spleens were minced using a hand homogenizer and single cells preparation was done with PBS buffer (pH 7) containing 2% FBS. After that, splenocytes were washed three times and cells were counted using a hemocytometer. **Cell Culture and Maintenance:** MCF-7 and MDA-MB-231 cells were cultured in DMEM medium supplemented with 10% fetal bovine serum (FBS) solution, 100 I. U. mL^{-1} penicillin, and 100 μ g/mL streptomycin. The culture was performed in a CO₂ incubator with humidified air at 37. 4 °C with 5% CO₂ supply according to our standard method. ²⁵³

Bacterial culture & Disc diffusion Method: Antibacterial activity checked through MIC and inhibition zone technique. To estimate the bactericidal impact of Neem bark harmful bacteria, disk diffusion and MIC test were carry out using *E.coli*¹¹⁰(*ATCC-25922*), *Candida*Albicans²⁵⁴(*ATCC-24433*), *Staphylococcus Aureus*⁹⁹(*ATCC-25923*), and *Klebsiella*pneumoniae²⁵⁵ (*ATCC-700603*) strain. In this study, MIC was obtained using the broth dilution technique where multiple concentrations of nanofiber were added in a 1OD of grown microbes. It should be mentioned that seven various doses were investigated after combining the nutritional broth and incubated for 24 hours at 37 °C to determine the Minimum inhibitory concentration: 2.5 mg/ml, 1.25 g mg/ml, 0.625 mg/ml, 0.312 mg/ ml, 0.156 mg/ml, 0.07 mg/ml, 0.03 mg/ml. The MIC value was determined to be the lowest concentration that precluded significant growth. The

nanofiber MIC result was compared to the outcomes obtained by utilizing nanofiber individually.

Continuing the MIC value was determined to be the lowest concentration that precluded significant growth. Ultrasonication was used to distribute these nanoparticles in distilled water.

The aqueous dispersion of the necessary concentration of neem bark nanofibers was created.

Results and Discussion Chapter-3

CHAPTER-3

RESULTS AND DISCUSSION

3. 1 Results and Discussion: Part-I

Synthesis of seed derived carbon nanocapsules cell imaging, depolarization of mitochondrial membrane potential, and dose-dependent control death of breast Cancer.

3. 2 Results and Discussion: Part -II

Synthesize of carbon dots for kernal part of seed: Photoluminescence mechanisms and applications in detection of biological relevant metal ions.

3. 3 Results and Discussion: Part -III

High temperature synthesized carbon dots and its absorption of heavy metal ions.

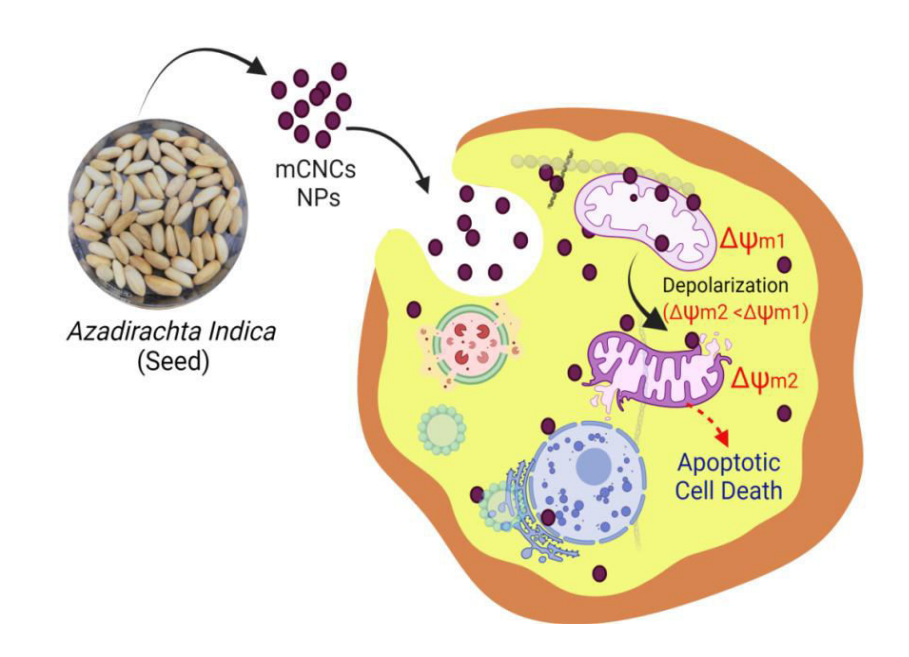
3. 4 Results and Discussion: Part –IV

Attempt to reveal the structures of cellulose from bark Neem antimicrobial activity and Their Application: An in vitro study.

Chapter: 3

RESULTS AND DISCUSSION: PART -I

Synthesis of Seed Derived Carbon Nanocapsules Cell Imaging, Depolarization of
Mitochondrial Membrane Potential, and Dose-Dependent Control Death of
Breast Cancer.



The outcome from part I: The results discussed in Part-I, have been published as "Azadirachta indica Seed Derived Carbon Nanocapsules: Cell Imaging, Depolarization of Mitochondrial Membrane Potential, and Dose-Dependent Control Death of Breast Cancer" ACS Biomater. Sci. Eng. 2022, 8, 8, 3608–3622.

Chapter: 3

RESULTS AND DISCUSSION: PART –I

Synthesis of Seed Derived Carbon Nanocapsules Cell Imaging, Depolarization of Mitochondrial Membrane Potential, and Dose-Dependent Control Death of Breast Cancer.

3.1.1 Introduction & Motivation

A special type of nanoparticles exhibited fascinating properties for their usages in theranostic applications. ^{256–258} These nanoparticles possess the potential for molecular imaging and are effective in the treatment of the infected cells together with better molecular understanding. ²⁵⁹ Further the advantage of these NPs are: (1) they can monitor the response of the treatment very precisely, (2) can avoid the unnecessary side effects to the patients, and (3) they are potential for the cost effective treatment and ease the treatment procedures. ²⁵⁸ Another advantage of these NPs to use in theranostic applications, especially for cancer therapy, is that the cancer growth can be controlled even in the diagnostic steps and in the subsequent steps it becomes easier to treat cancer. ^{258–263} Apart from the nanoparticles, the biologically engineered cells can also be used for theranostic applications. ²⁶⁴ However, every material proposed to use in theranostic applications faces various challenges that must be overcome for safer clinical usages. ²⁶⁵ For instance, cancer cells grow faster and create leaky vascular systems in the surrounding tissues, and for the effective treatment with conventional

chemotherapy drugs, the highly efficient drug delivery vehicles with enhanced permeability and retention (EPR) are required. 266-267 Developing such suitable material is always a challenging task. In the early stage of the concept 'theranostics', the fluorophore (or fluorescent component) was usually attached with the drug delivery vehicles loaded with therapeutic components for the diagnostic purposes and it was found the progress was very slow. We should also note that the cancer cells can efficiently interact with the surrounding immune cells, endothelial cells, neovasculature and fibroblast. Further, they develop dangerous survival strategies with eight hallmarks, such as, (1) self-sufficiency with growing signal, (2) evasion of apoptosis, (3) inactivate the antigrowth signal, (4) sustained angiogenesis, (5) metastasis, (6) rapid replication, (7) deregulation of cellular energetics and finally (8) escape from immune regulation. 256,154,157,268 The cancer cells can also develop severe genome instability and tumour promoting inflammation. 269 Therefore, in such a situation a better understanding of theranostics is required and it demands suitable materials to be developed for these purposes.

Various nanomaterials have been developed to address the therapeutic problems, especially for the cancer diagnosis, monitoring and for the treatment. These nanomaterials along with drugs and photosensitive materials (all together make formulation) enable to enhance the treatment with safety to an extent. Such as, super paramagnetic nanoparticles can enhance the MRI contrast, ²⁷⁰⁻²⁷¹ CNTs ¹⁷⁴ enhance the quality of photo acquoustic image, ²⁷² inorganic (Ag NPs) ²⁷³ and other carbon-based materials ²⁷⁴⁻²⁷⁵ including graphene increase the photo thermal effects, ²⁷⁶and photo thermal properties of polymers ^{177,277} enhance the effective gene delivery to the target for multiple therapies including suppression of tumours. ²⁷⁸⁻²⁷⁹ However, all these materials have their own advantages and disadvantages with respect to the cytotoxicity and photoluminescence/emission properties and suffer many challenges for effective treatment. In this line, the present work is focused on the designing of carbon-based mesoporous nanocapsules from biological response/naturally occurring component with high biocompatibility and for the theranostic applications.

Herein, we report on the easy synthesis of mesoporous carbon nanocapsules (mCNCs) that from

Azadirachta indica seeds. The process reported here is cost-effective with excellent viability towards normal healthy cells and it is useful for theranostic applications such as for the cancer diagnosis is and treatment. Azadirachta indica belongs to mahogany Meliaceae family, known as Neem and is famous for medicinal purpose and Ayurveda. ²⁸⁰⁻²⁸¹ In the last few years, different plant extracts are also used for different medicinal purposes such as antifungal, ²⁵⁴ antibacterial, ²⁸² antiviral, ²⁸³ insecticidal ²⁸⁴ antimicrobial ²⁸⁵ activity, bio-imaging, and apoptotic activity. To perform our work, a series of mesoporous carbon nanocapsules have been prepared from "Azadirachta Indica" seeds and their cytotoxicity against the cancer cells has been tested.

The theranostic efficiencies, especially the imaging and treatment of cancer cells, such as normal breast cancer and TNBC have been investigated. To study this, the MTT assay, mitochondrial membrane potential, and Annexin V apoptosis assay were performed and the biological significance for the treatment has been demonstrated. It can be noted that the change in the mitochondrial membrane potential (MMP, $\Delta\psi$ m) is the primary symbol to determine the change in physiological parameters and cellular metabolic energy of the cancer cells. ²⁸⁶ Through the interaction of mCNCs with MCF-7 and MDA-MB-231 (TNBC cells), how the mitochondrial membrane potential takes role that has also been investigated using different doses of mCNCs. It can also be noted that the $\Delta\psi$ m has a vital role in monitoring the mitochondrial actions, since it demonstrates the control of electron transportation and oxidative phosphorylation to create the driving force behind ATP generation, ²¹² which has also been investigated thoroughly in this work.

To perform a routine activity of the cell, the level of ($\Delta\psi$ m) and ATP should be relatively stable, albeit the controlled fluctuation of $\Delta\psi$ ms and ATP also results in regular physiological activity. Nevertheless, the steady alter in both these factors may be detrimental to the cell viability against the MCF-7 and TNBC (MDA-MB-231) that have also been explored through this work. Further, how the $\Delta\psi$ m is inevitable for the upkeep of cellular health and viability for both MCF-7 and MDA-MB-231, once the mCNCs have interacted, has also been studied. The reduction of MMP ($\Delta\psi$ ms) occurs before the chromatin condensation, and DNA break (characteristics of nuclear apoptosis) is regarded as the earliest

incident in the apoptotic cascade, which also has been explored through this work. Interestingly, in this work, the cancer cell killing efficiency of mCNCs have been studied without using/loading any conventional chemotherapy drugs.

3.1.2 Results and discussions

3.1.2.1. Morphological characterization

The mesoporous carbon nanocapsules (mCNCs) were synthesized from *Azadirachta Indica* seeds as the carbon source as described in the experimental section. The morphology and structure of the mCNCs were scrutinized through HRTEM. From TEM macrographs (Fig. 3.1.1) it is evident that the mCNCs are uniform in size and they are mono-dispersed with an average size of 6 nm in diameter (Fig 3.1.1A-C). The Energy–dispersive X-ray spectroscopy (EDAX) band acquired from TEM instruments also confirmed the presence of carbon as an element for the mCNCs (Figure 3.1.1D). From the HRTEM, it is obvious that the mCNCs are porous, which is again evident through the BET study (see in the subsequent section). To compare the nanostructure for other samples, the TEM results have been provided in Fig. 3.1.2. The particle size obtained for SN-4 is the smallest in size compared to the other samples. It is found that the SN-1, (b) SN-2, and (c) SN-3 sizes of capsules range from ~ 7-12 nm with an average capsule size of 10 nm.

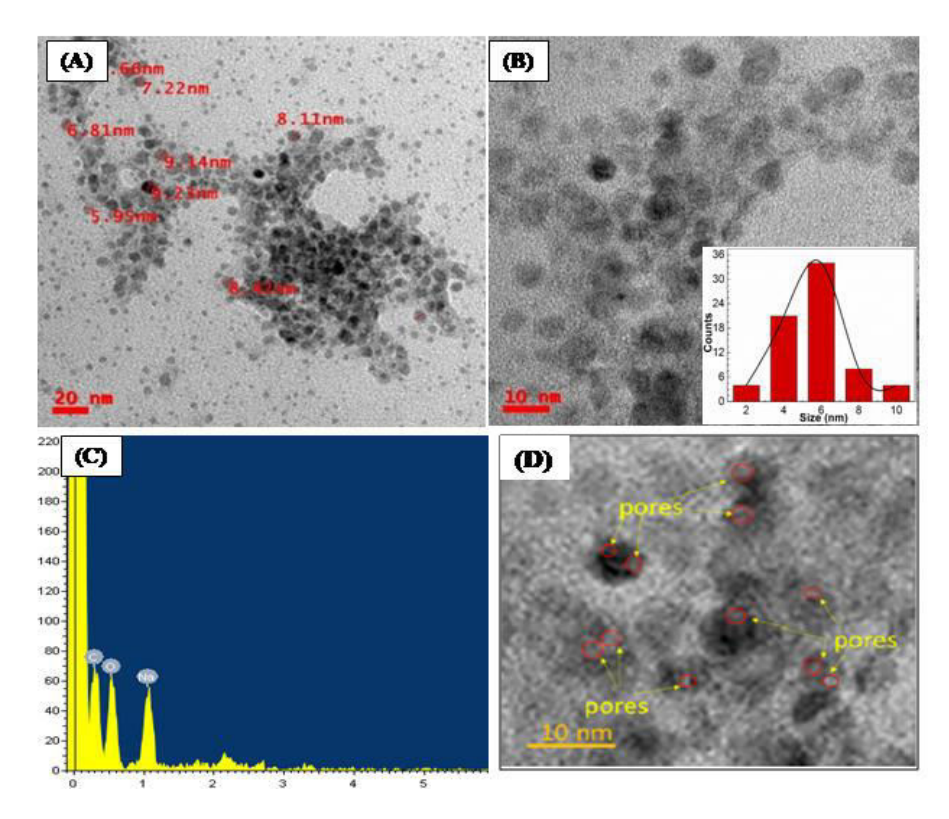


Figure 3.1.1 (A)-(B) TEM micrographs of the mCNCs (SN4), (C) particle size distribution of the mCNCs , and (D) EDAX spectrum of mCNCs.

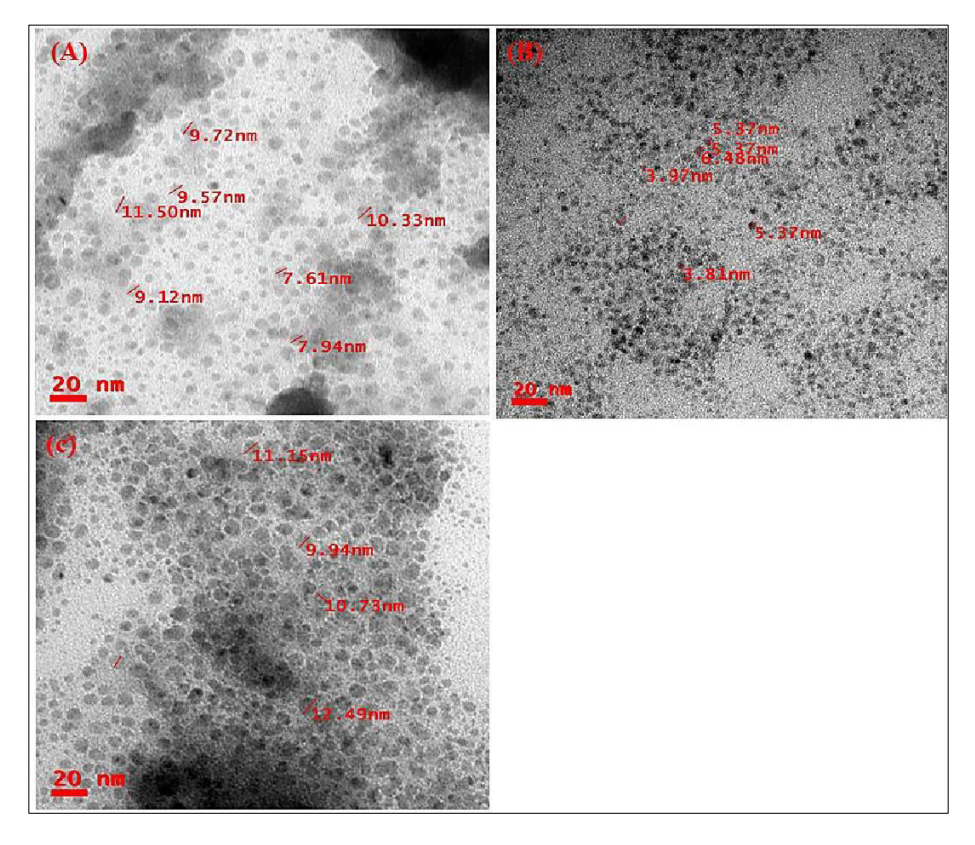


Figure 3.1.2 Particle size and morphology studied through the TEM for the samples: (A) SN-1, (B) SN-2, and (C) SN-3

3.1.2.2. Study the Chemical Functionality and Thermal stability

The surface chemical properties of the synthesized mCNCs and the presence of functional groups were examined through FTIR spectroscopy. As observed from the FTIR spectrum, the stretching bands that appeared at 3311, 1735, 1653, 1440, 1125, 881, and 844 cm⁻¹ are specified for the existence of –NH, - CH, -C=O, -C=C-, -N=O, -CN and epoxy ring, ²⁸⁸ respectively (see Fig 3.1.3 A). The strong absorption band at 3200-3600 cm⁻¹ could be assigned to the presence of O-H (stretching) and N-H (stretching) vibrations. Further, the band that appeared at 1653 cm⁻¹ is due to the -NH- group present in the mCNCs. The occurrence of these functional groups on mCNCs possesses excellent dispersity of mCNCs in water. The thermal stability of mCNCs samples was studied through TGA in an N₂ atmosphere. From (Fig 3.1.3 B), the weight loss of the sample between 30°C to 800°C has been identified.

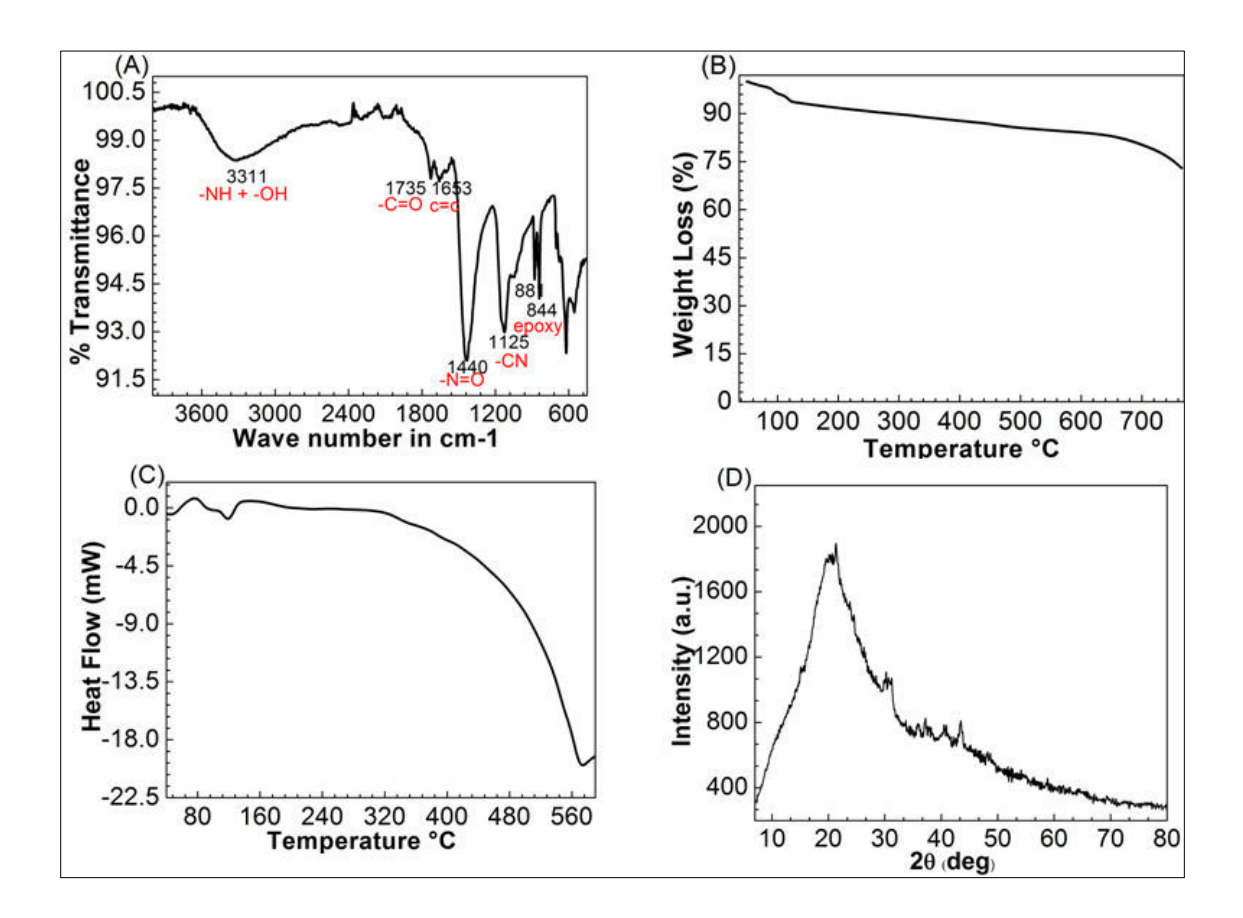


Figure 3.1.3 (A) FT-IR spectrum for mCNCs (SN4), (B) TGA thermogram for mCNCs(SN4), (C) DSC thermogram of mCNCs (SN4) and (D) XRD pattern of the mCNCs (SN4).

The first stage of weight loss (~9 wt.%) occurred between 30°C to 111°C, is due to the evaporation of unbound moisture followed by a second stage of weight loss (~5wt. %) from 112 °C to 127°C due to the entrapped moisture inside the pores of the mCNCs. Further,~56 wt. % loss occurred till 762°C which is due to the thermal decomposition of the organic component/functional groups present in mCNCs. Thermal properties of mCNCs further were evaluated using DSC. It measures the heat flow between the samples as it undergoes phase transformation. DSC study also supports the change in the thermal properties of the mCNCs (see Fig 3.1.3C). The solid-state crystal structure of the mCNCs has been studied through the XRD (see Fig 3.1.3D) and shows a broad diffraction peak at $2\theta = 20.3^{\circ}$ along with a few additional peaks (minor). 289 An inter layer spacing of ~0. 3 nm is identified, which is attributed to the (002) diffraction plan for the carbon-based component. However, from XRD it is obvious that the mCNCs (SN4) are majorly amorphous in nature.

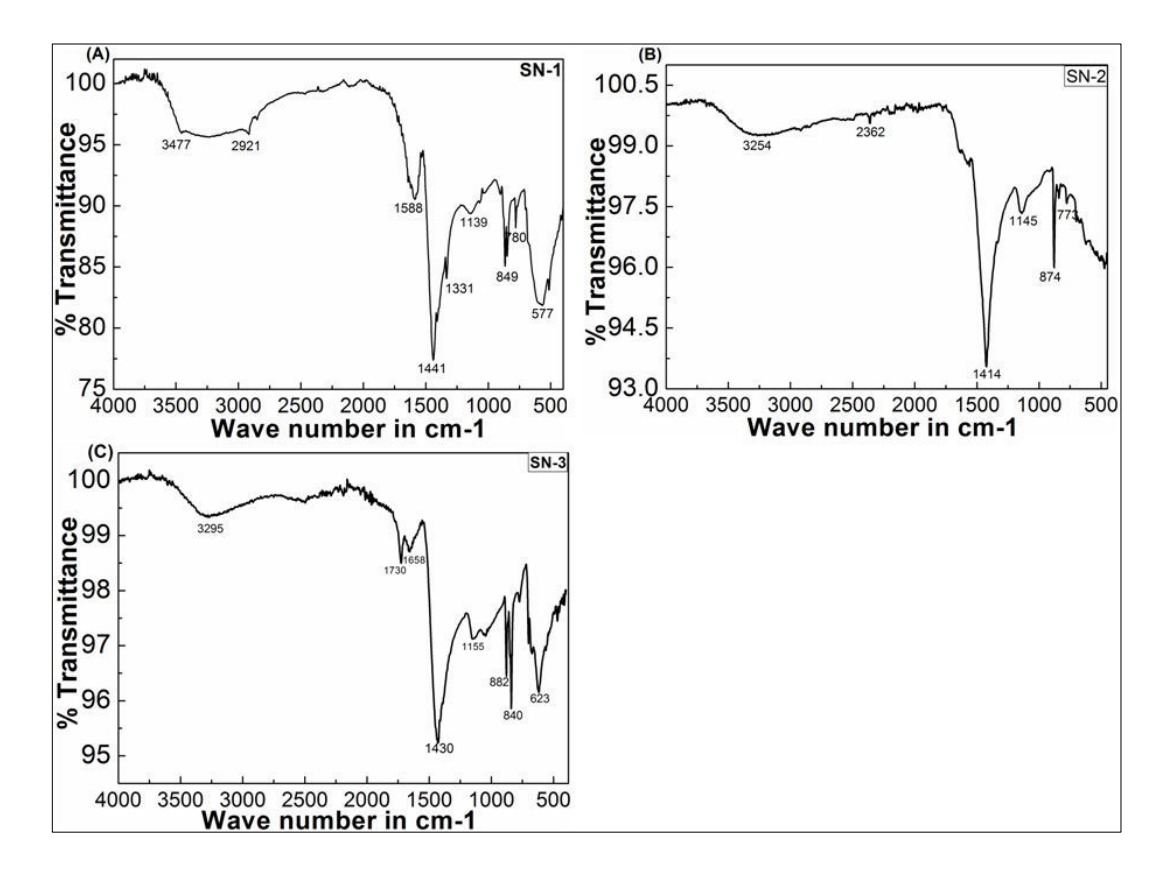


Figure 3.1.4 Schematic shows the FTIR spectrum of the samples: (A) SN-1, (B) SN-2, and (C) SN-3.

FTIR spectra of all other samples have been provided in Fig.3.1.4 for SN1, SN2, and SN3. SN-1 shows stretched 3477 OH stretch, 2921 -C-H stretch, 1588C=C, and 1441 CH₂ bend, respectively. FTIR spectra of SN-2 are 3254 OH stretch, 2362 O-H stretching, 1414 O-H bending, and 1145 C-O stretching. FTIR results of SN-3 3295 N-H stretching, 1730 strong C=O stretching, 1658 C=C medium stretching, 1430 O-H bending, 1155 C-O stretching, 882 C-H bendings.

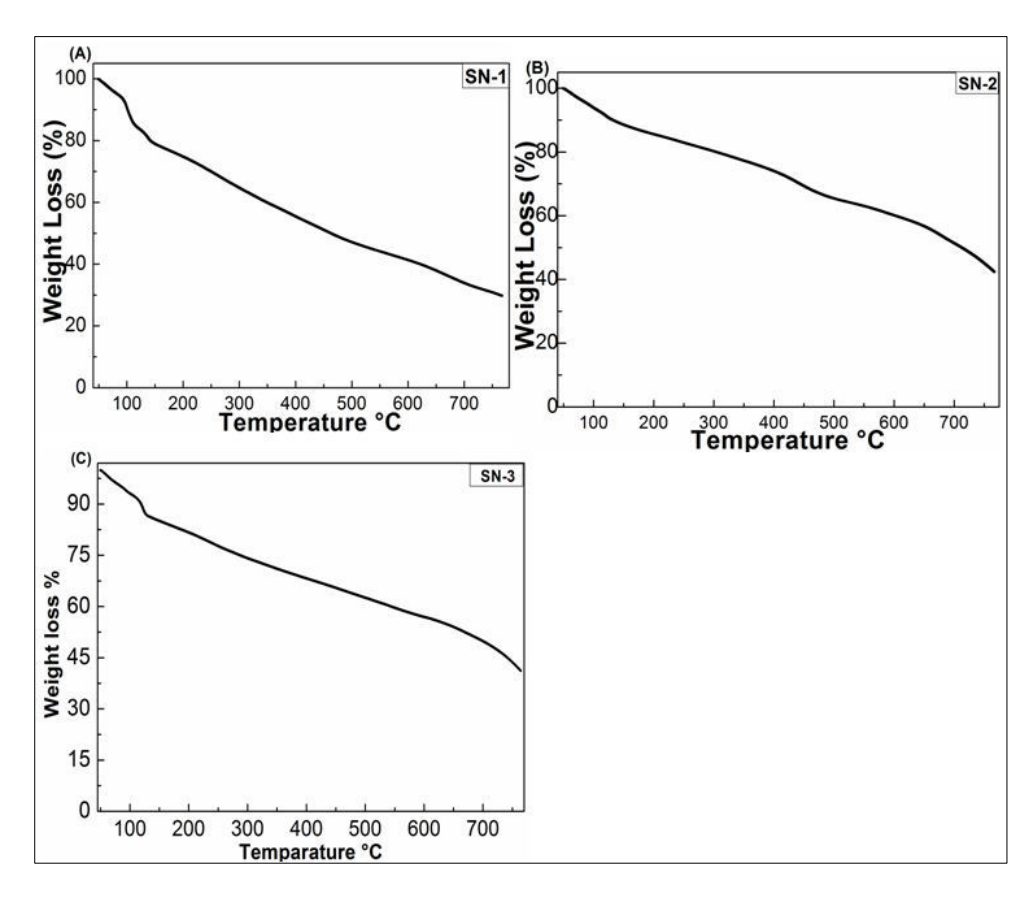


Figure 3.1.5 Thermal stability studied through TGA for the samples:(A) SN-1, (B) SN-2, and for sample (C) SN-3.

From Fig. 3.1.5 (A-C), TGA measurements it has been evidence that SN-1, SN-2, SN-3 degradation at changes with temperature. The first stage of weight loss starts from the ~40°C - 110 °C continuing with second stage SN-1 at 150°C SN-2 at 162 °C and SN-3 at 143°C due to the entrapped moisture inside the pores continuing complete degradation of SN-1 happened at 70% at 760 °C, SN-2 54% and SN-3 65% thermal decomposition of the functional group.

The heat flow (endothermic which means absorbing heat and exothermic which releases heat was

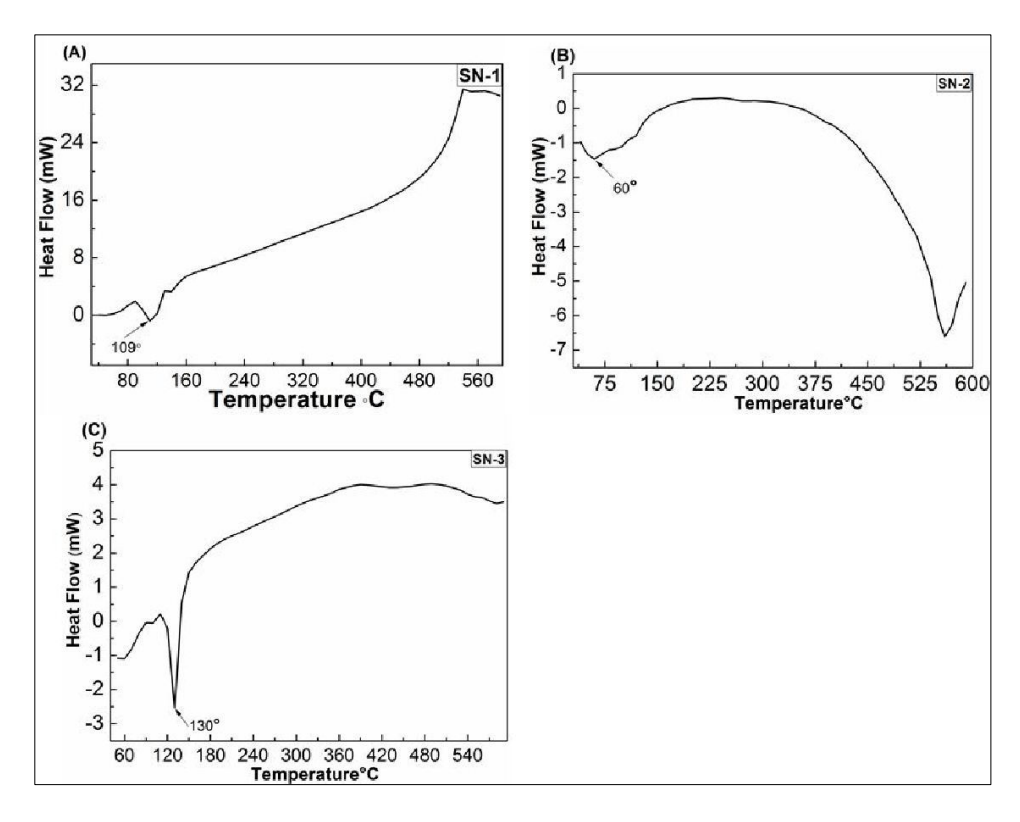


Figure 3.1.6 DSC thermo grams for the samples: (A) SN-1, (B) SN-2 and (C) SN-3.

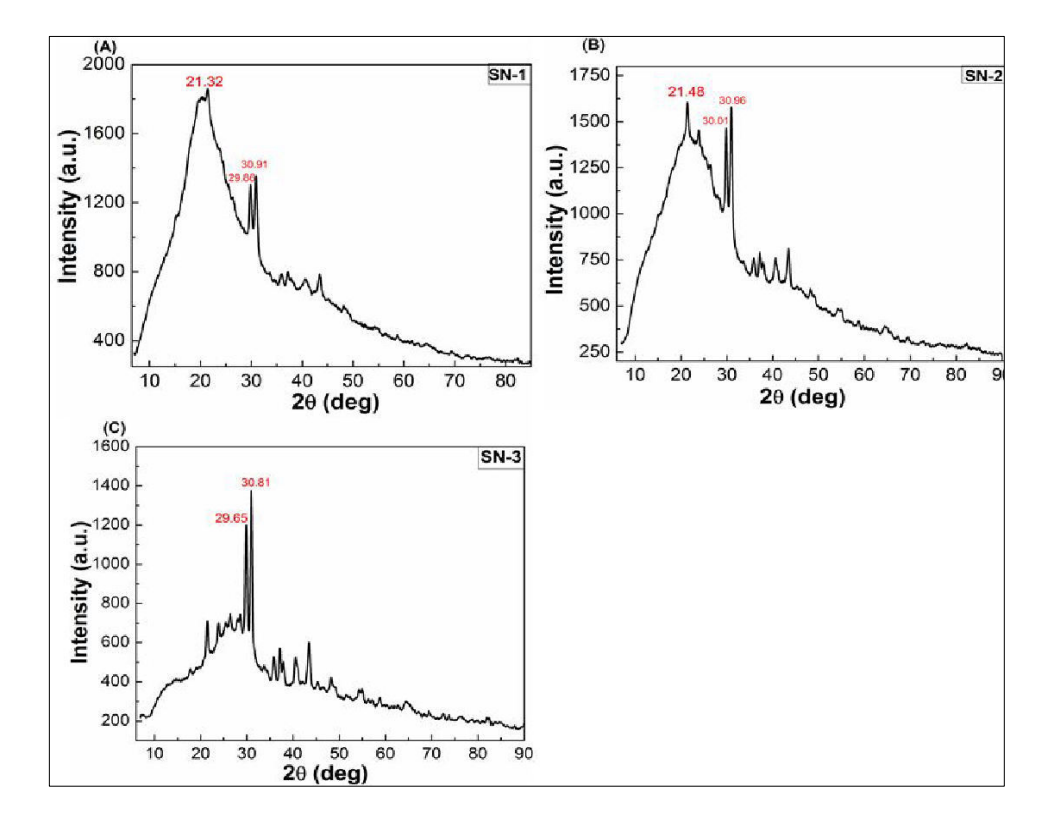


Figure 3. 1.7 XRD pattern for the samples: (A) SN-1, (B) SN-2, and (C) SN-3.

Performed for SN-1, SN-2, and SN-3 (Fig. 3.1.6). From the above-mentioned graph, it isvisible that all three samples' heat flow is exothermic (109°C, 60°C,130°C). The temperature scanning range is ~50 °C to 600 °C with a heating rate of 10 °C/min measurements. The physical properties of synthesized SN-1, SN-2, and SN-3 compounds such as solid state by XRD. In order to XRD results, it is found that they are semi-crystalline in nature.

3.1.2.3. BET Surface Area Analysis and Surface Zeta Potential

To find out the surface area and pore size distribution of the mCNCs, BET analysis was performed. The N₂ adsorption-desorption isotherm (BJH) for them CNCs exhibited a type IV isotherm with a clear hysteresis (Fig. 3.1.8A), which proves the porous structure of the mCNCs. The pore size and their distribution have been calculated (see Fig. 3.1.8 B) and found to be of average size, 2.5 nm in diameter which supports to the HRTEM results for the porous structure of mCNCs. The surface area for the mCNCs (SN4) is calculated to be 203. 0 m²/g. The surface zeta potential is very crucial for the nanoparticles for its utility in various biomedical applications. ²⁹⁰ Therefore, the zeta potential of the synthesized mCNCs (SN4) has been measured and found to be -34. 95 mV (Fig. 3.1.8 C), and this value is quite high compared to the reported carbon nanomaterials or C-dot synthesized from red chilli, turmeric, cinnamon, and black pepper Cdots. 291-293 This high value of zeta potential of the mCNCs is obtained due to the functional groups present in the sample (see FTIR results, Fig. 3.1.8A). Such a high zeta potential value further confirms the colloidal stability of mCNCs, and it is suitable for theranostic applications. In the present scenario, pH sensing in aqueous media has been emphasized by considering the significant role of pH in a broad range of applications that demands high colloidal stability.²⁹⁴ such as for biomedical, industrial, environmental, analytical chemistry, cellular biology, and molecular biology. Therefore, the zeta potential for the synthesized materials was measured at different pH and showed the highest zeta potential at pH 5 for SN4 (Fig. 3.1.8D). However, in all the pH ranging from pH 3 to pH 8, the mCNCs (SN-4) are very colloidal stable, DLS measurements showed that the average diameter of mCNCs (SN-4) was 6 nm (Fig. 3.1.8 E), which is matching well with the TEM results and is further evidence for the colloidal stability of the mCMCs. The Raman spectra for the mCNCs (SN-4) have been acquired, and the presence of D band at 1320 cm⁻¹ was found for the presence of sp² hybridization (in-plane vibration) and G bands appeared at 1180 cm⁻¹ for out-of-plane vibration which represented to the associated structural defects(Fig. 3.1.8 F).

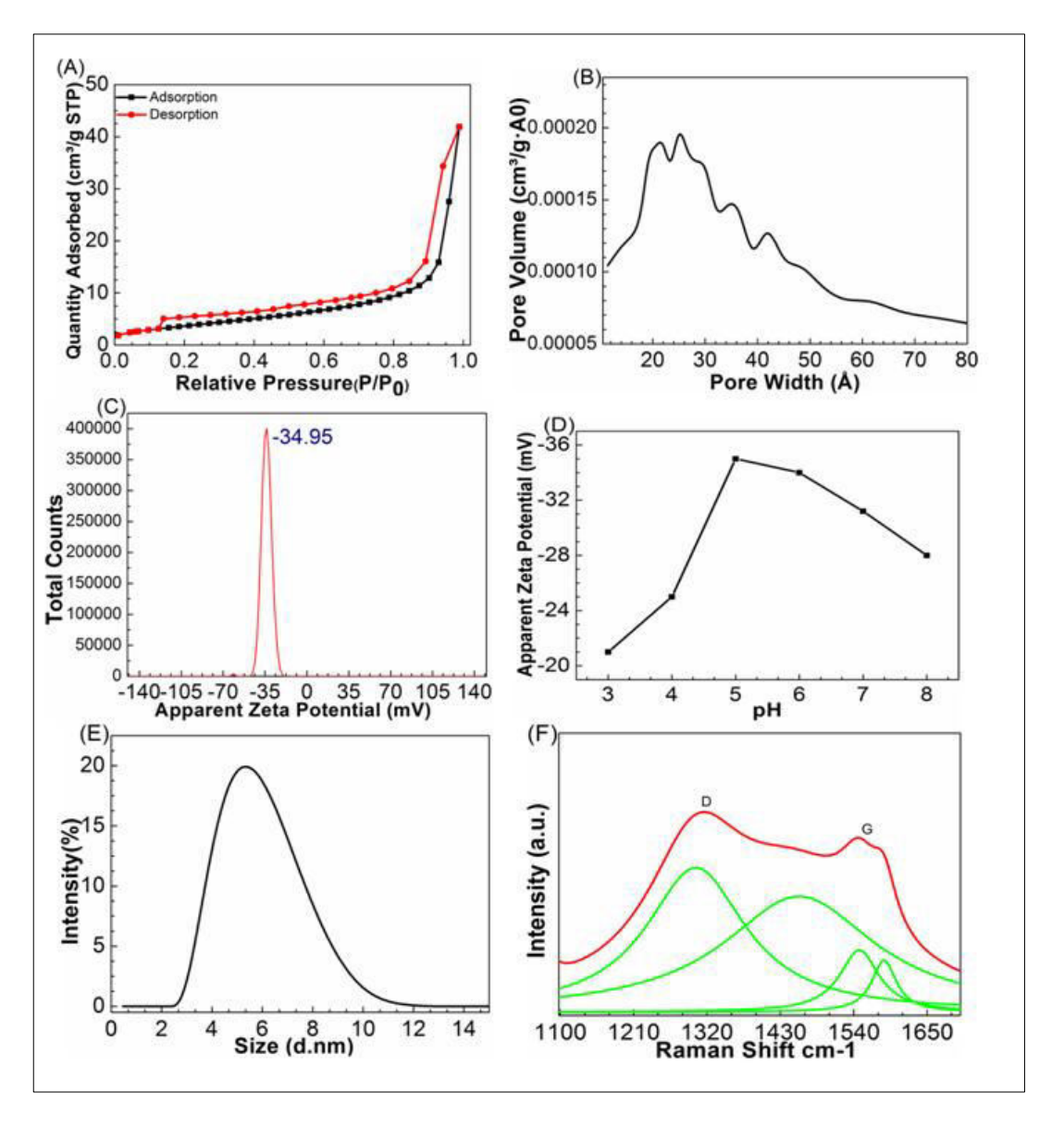


Figure 3.1.8 (A) BJH adsorption—desorption isotherm and (B) pore size distribution profile calculated from desorption isotherm, (C) zeta potential profile acquired in a water medium, (D) effect of pH on zeta potential (for sample SN-4), (E) particle size obtained from DLS in a water medium, and (F) Raman spectra of mCNCs, respectively.

BJH adsorption—desorption isotherm (Figure 4.1.9) and BET surface area results of the other samples have been provided in SN-1 is 29.9 m²/g,SN-2 26.32 m²/g,SN-3 is 29.56 m²/g respectively.

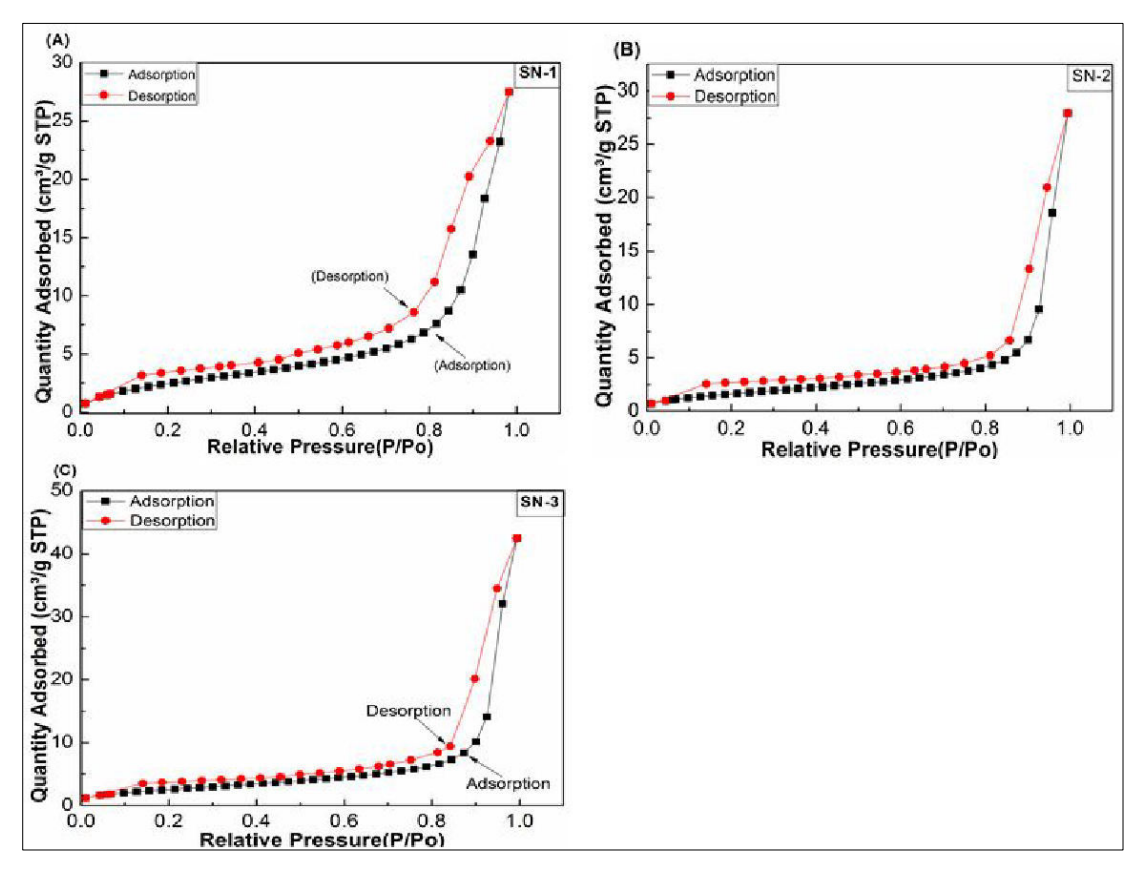


Figure 3.1.9 BET experiments: BJH adsorption–desorption isotherm for the samples: (A) SN-1, (B) SN-2, and (C) SN-3.

The pore size distribution for SN-1, SN-2, and SN-3 proves that they are less porous in nature as well as their surface area is also less compared to the SN-4 sample Figure 4.1.10. The pore size distribution as follows for SN-1 is ~2. 3nm to 3.6nm, SN-2 is ~2. 3 nm- 3.0 nm, and SN-3 is ~2. 4 nm.

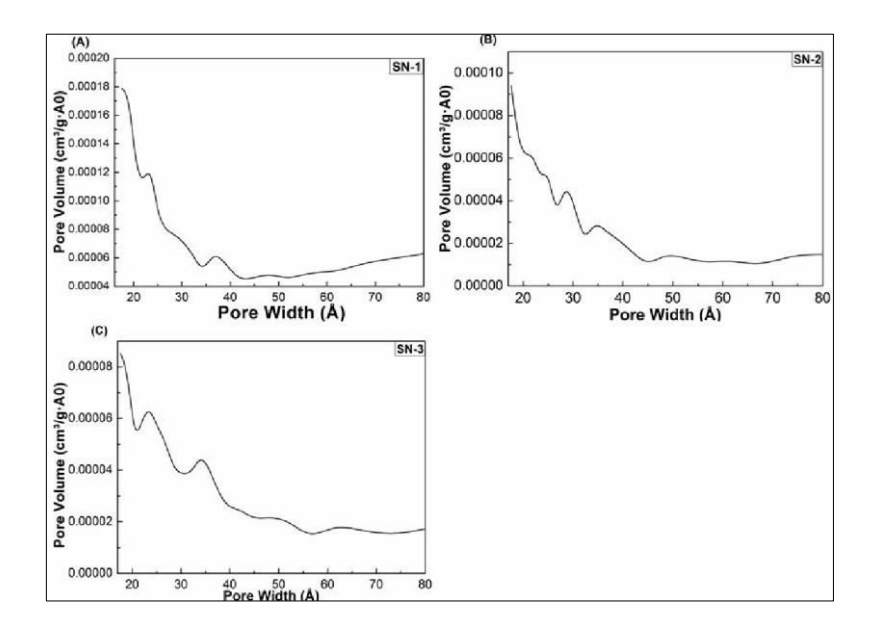


Figure 3.1.10 Pore size distribution profile for the samples. Pore size was calculated from BET for (A) SN-1, (B) SN-2, and (C) SN-3.

Zeta potential for the other samples i.e.SN-1, SN-2, SN-3 is also comparable to the mCNCs (SN4). The values are the following for SN-1-23.59 mV, SN-2 -30.05 mV, and SN-3 -33.27 mV (Figure 3.1.11).

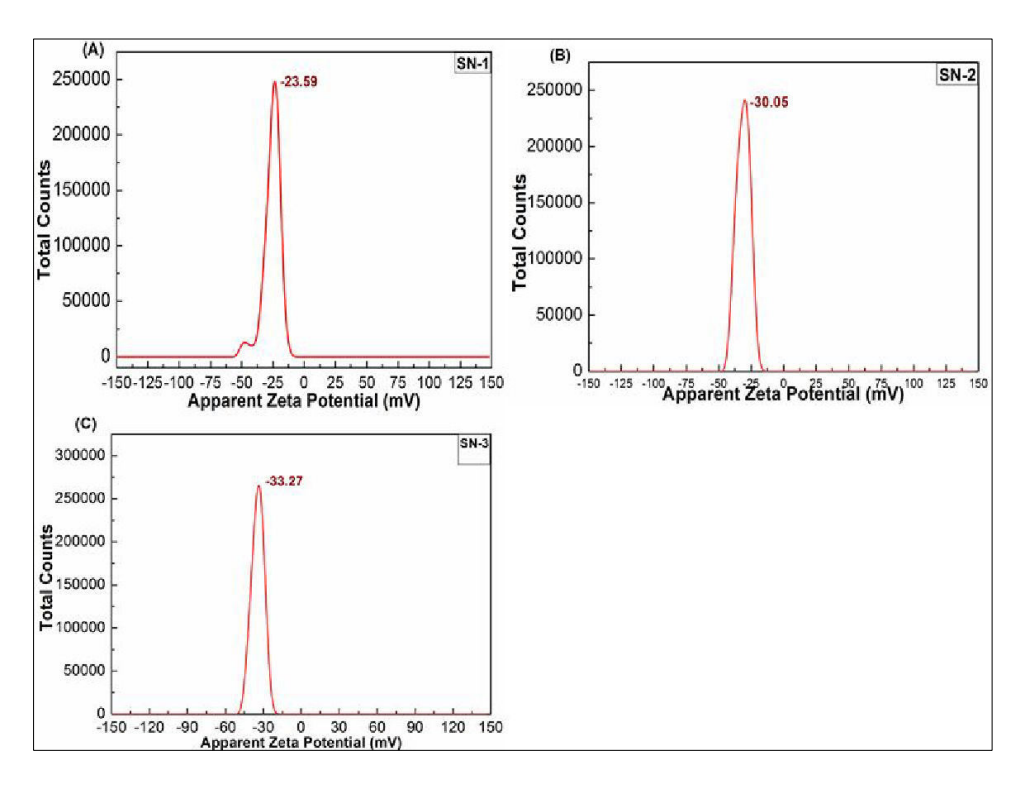


Figure 3.1.11 Zeta potential profile for the samples: (A) SN-1, (B) SN-2, and (C) SN-3.

However, different samples such as SN1, SN2, and SN3 have different colloidal stability and that also varied with a change in the pH (Figure 3.1.12). It is visible that with different pH zeta potential changes for SN-1 at pH 5 it has the highest zeta potential which is -24 mV followed by SN-2 -30mV and SN-3 -33 mV.

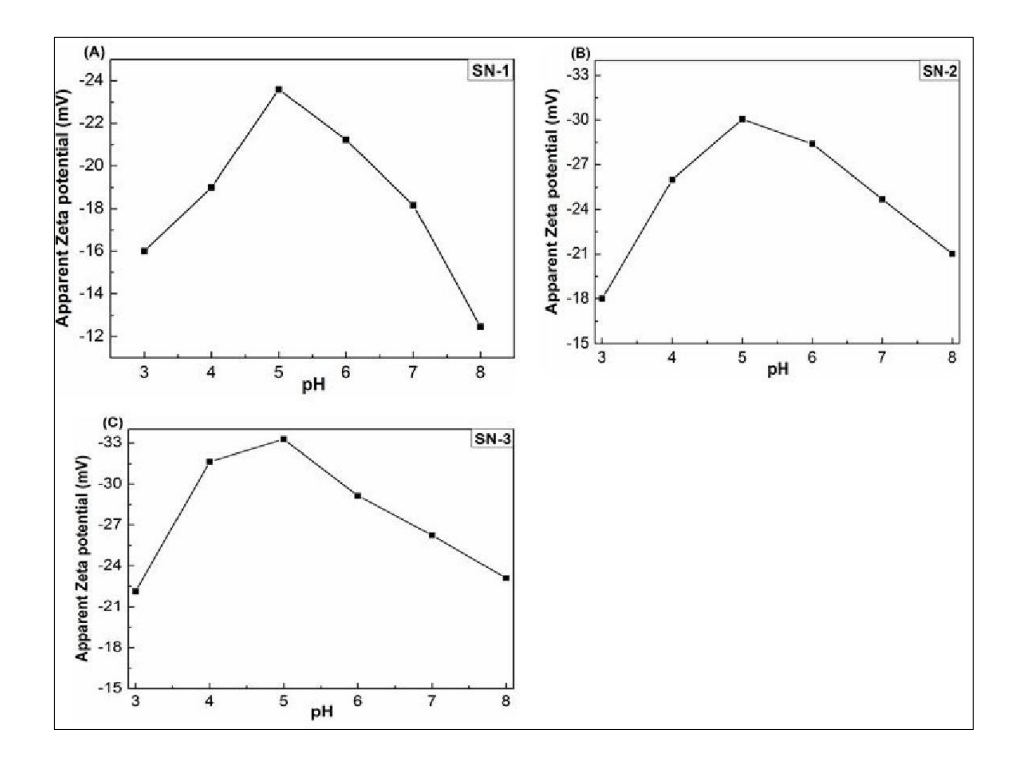


Figure 3.1.12 Effect of pH on zeta potential for the sample (A) SN-1, (B) SN-2, and (C) SN-3. DLS measurements showed that the average diameter of mCNCs as follows SN-1,SN-2,SN-3 is 14nm,18nm, and 22nm (Figure 3.1.13), which is matching well with the TEM results (Figure 3.1.2) and the further evidence for the colloidal stability of the mCNCs.

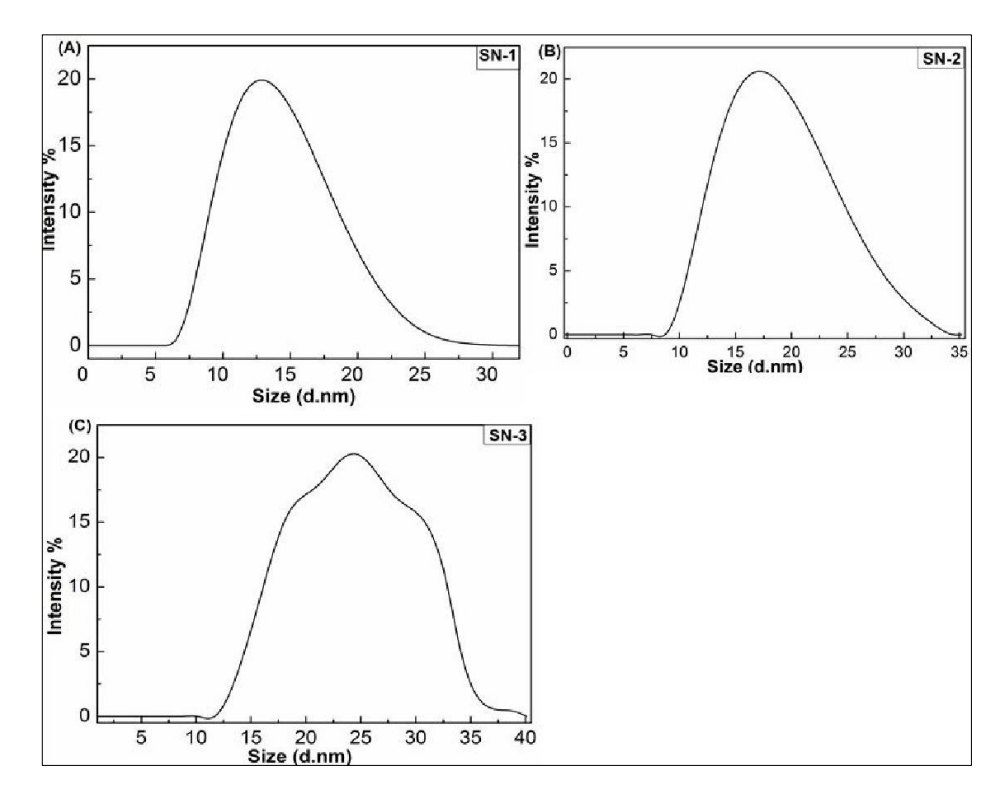


Figure 3.1.13 Particle size obtained from DLS for (A) SN-1, (B) SN-2, (C) SN-3.

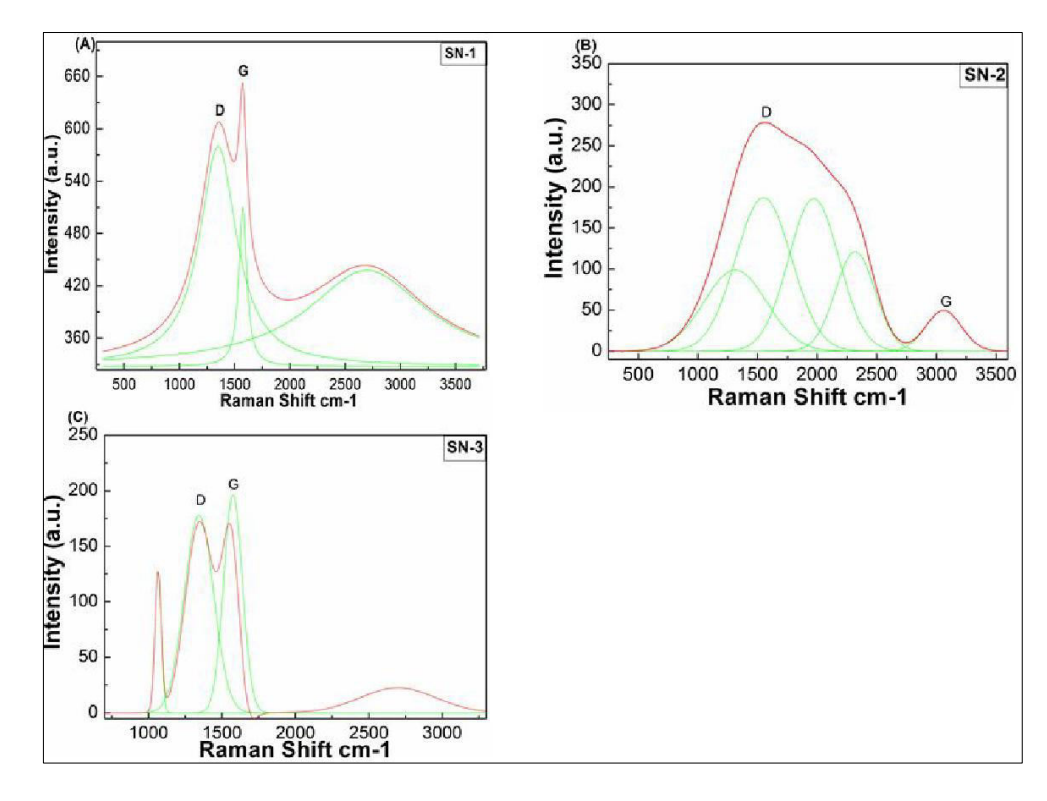


Figure 3.1.14 Raman spectra for the samples, (A) SN-1, (B) SN-2, (C) SN-3

The Raman spectra for the reaming samples i.e.SN-1, SN-2 ,SN-3 have been acquired as the presence of D & G bands respectively. D band was found for the presence of sp² hybridization

(in-plane vibration) and G bands appeared for out-of-plane vibration which represented the associated structural defects (Figure 3.1.14).

3.1.2.4 Absorbance and Optical characterization:

The UV- vis absorption of mCNCs was acquired (Figure 3.1.15A). An absorption band that appeared in between 200 and 250 nm is due to the $n-\pi^*$ transition of the C-O band and $\pi-\pi^*$ transition occurred due to the conjugated C=C conjugated bond present in mCNCs (Figure 3.1. 15A). One of the unique characteristics of the carbon dots is photoluminescence, and the luminescence properties can be varied with varying the particle size²⁹⁵ and excitation wavelength. However, from the application point of view, the synthesized mCNCs in an aqueous solution show luminescence with UV light irradiation.

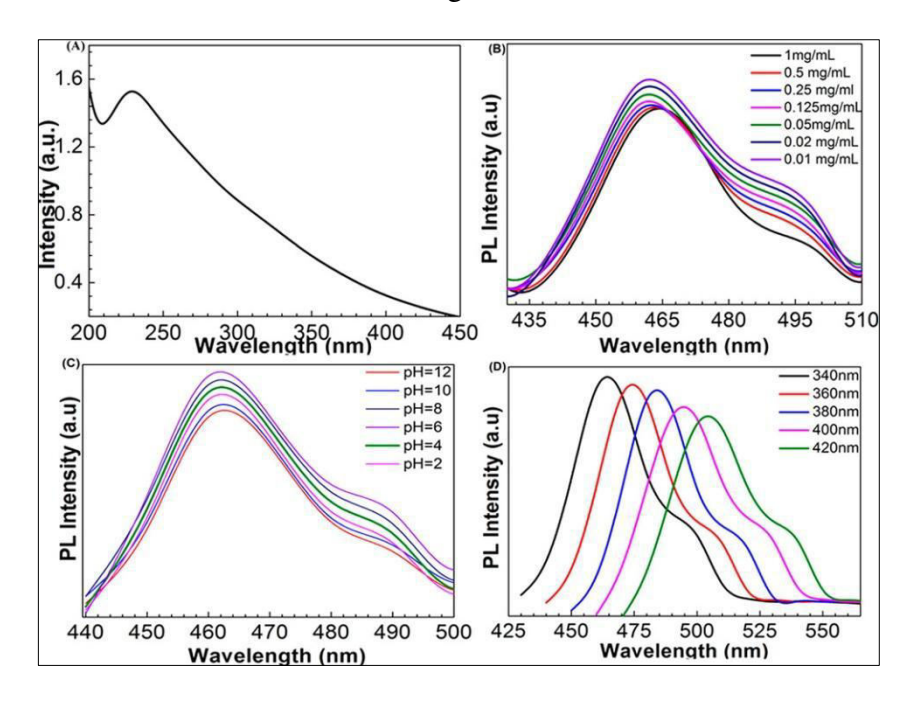


Figure 3.1.15 (A) UV-vis spectra, (B) PL variation with concentration, (C) effect of pH in luminescent, of the mCNCs (SN4). (D) Fluorescence behavior of the mCNCs (SN4) obtained with an excitation wavelength of 340–420 nm.

The luminescent properties strongly depended on the concentration of mCNCs. The intensity of the luminescent spectra depends on the amount of material used (say for SN-4), see

(Figure 3.1.15 B) and due to the decrease in the electrostatic interactions played between the polar groups exist on the surface of the mesoporous materials (see Figure 3. 1. 15 B) for SN4).²⁹⁷

The occurrence of a high amount of polar functional groups assistances in procedure agglomeration at high concentrations and the size of the agglomeration likewise controls the luminescence properties of the sample.²⁹⁸ The PL intensity also differs with the different excitation wavelengths. The intensity of luminescent of mCNCs also depends on the pH of the colloidal solution as shown in Figure 3.1.15C. Here we have noticed the variation of PL intensity with a change in the concentration of mCNCs within the pH 2–12 (Figure 3.1.15C). High intensity of PL is observed in pH 4 to 8 where the π - π * and n- π * transition occurred by refilling or depleting of valence band electrons. The fluorescence spectra of mCNCs with the variation of excitation wavelength (340–420 nm) are shown in Figure 3.1.15D, and it is obvious that the band shifted with varying excitation wavelength.

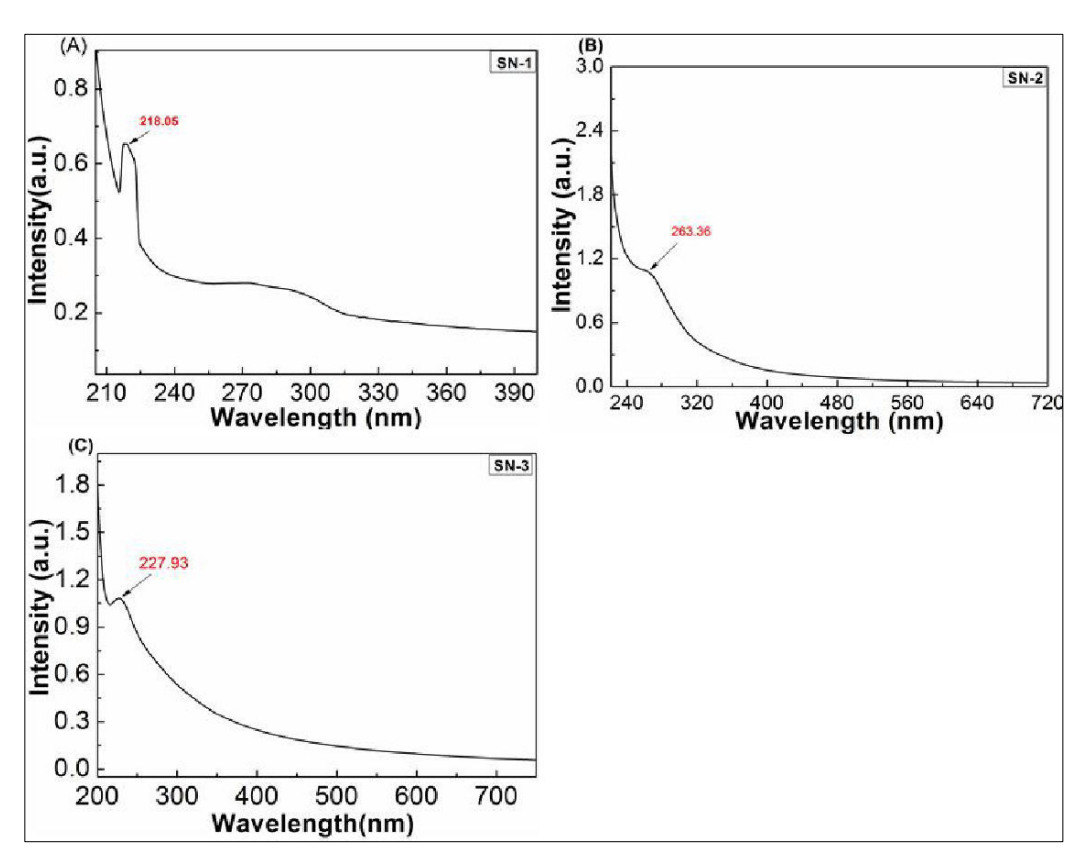


Figure 3.1.16 UV-Vis spectra for the samples, (A) SN-1, (B) SN-2, (C) SN-3

The peak of SN-1 was observed at 218 nm for SN-2 at 263 nm and SN-3 227 nm. Because of the difference in the chemical functionality, the intensity of UV-Vis absorption varied as shown in Figure 3.1.16.

3.1.2.5 Cytotoxicity and living cell imaging:

In vivo imaging of cells is very important for the diagnosis of diseases. Photo luminescent mCNCs are necessary units for determining their applicability as an imaging probe. It is reported that C-dots are good candidates for diagnosis and imaging. To find out the utility of mCNCs for theranostic applications, the imaging and biocompatibility studies were performed using normal splenocytes, MCF-7 and MDA-MB-231 (see Fig 3.1.17a-b and Fig.3.1.18). The cytotoxic study was carried out with various concentrations of mCNCs. The mCNCs showed an excellent distinct characteristic by responding in multicolor imaging profile (Fig 3.1.17). As we can see when the mCNCs were incubated with cells, they emitted fluoresce in different ranges. In the presence of light, we can easily detect the existence of mCNCs which are ultimately present in the cytoplasm, cell membrane, and specifically near the nucleus. Many research groups have reported the potential uses of C-dots in cell imaging with photon luminescence microscopy. ²⁹⁹⁻³⁰⁰ For extraction of C-dots, it has been reported that after giving the treatment of intravenous injection, it was accumulated in the reticulo endothelial system (RES)³⁰¹ as well as in the kidneys ³⁰²⁻³⁰³ which can be gradually extracted from the faecal and renal pathway.

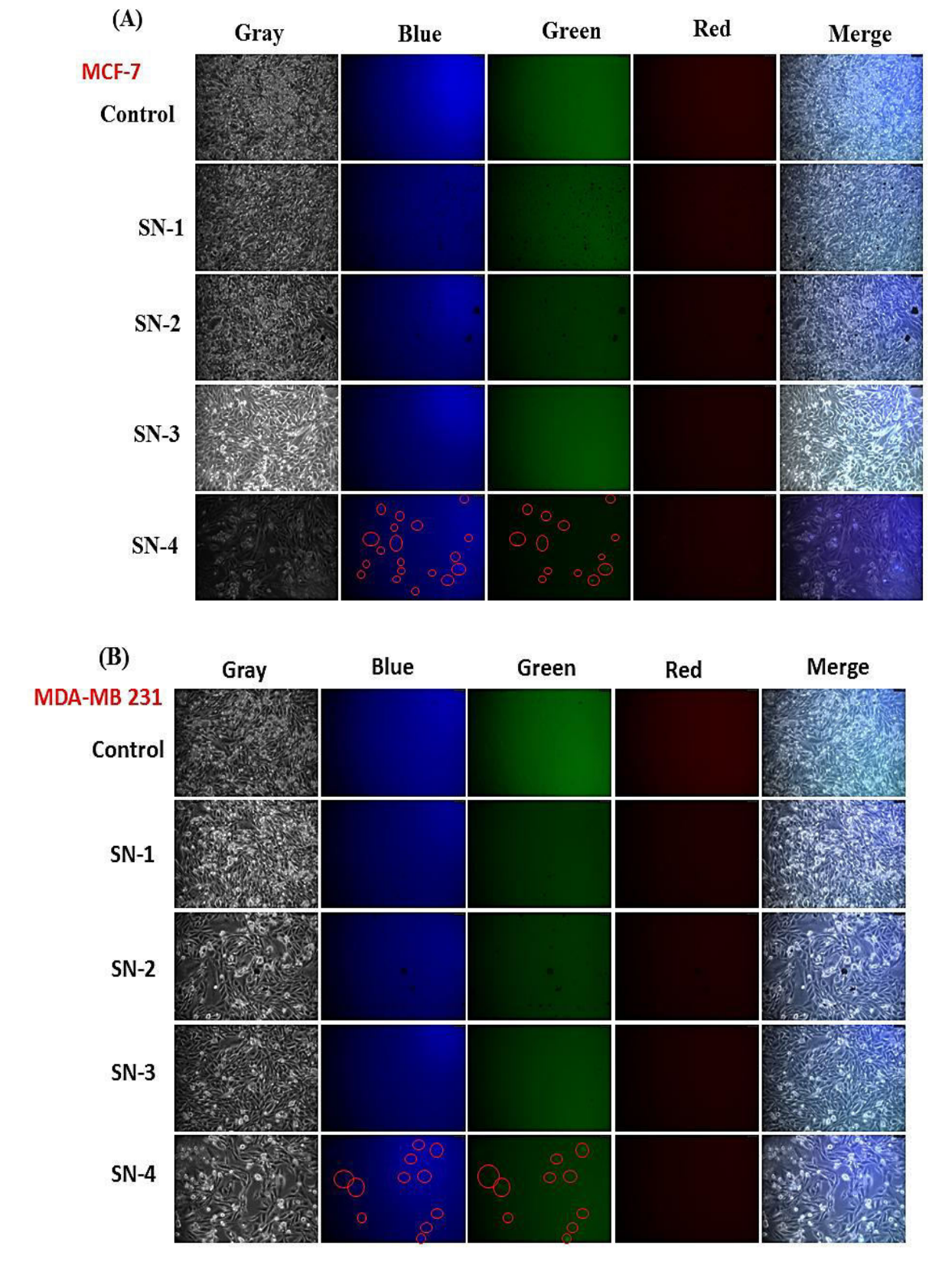


Figure: 3.1.17: Showing the interaction Nano formulated SN-1, SN-2, SN-3 and SN-4 samples on (A) MCF-7 cells and (B) MDA-MB-231 cells. The red arrows represent the capsules, under fluorescent microscopy.

To explore the potential effect of our mCNCs, cyto compatibility has been studied on normal healthy cells and cancer cells. We have used normal splenocytes extracted from mice and normal breast cancer cells (MCF-7) and TNBC cells (MDA-MB-231). In vitro studies have been performed through MTT assay. From Figure 3.1.18A-B, it is evident that the SN-4 (mCNCs) shows excellent cell inhibition on MCF-7 and TNBC cells (MDA-MB-231) as compared to the SN-1, SN-2, and SN-3 in the concentration range of 0–1 mg mL⁻¹. Henceforth, SN-4 has exhibited more than 90% cell viability with mouse splenocytes (Figure 3.1.18A). Similarly, we checked the cytotoxicity of all other samples, and it is found that the SN-4 sample showed 80% and 82% cell viability on MDA-MB-231 and MCF-7 breast cancer cells, respectively. Thus, our results further indicated that the mCNCs (SN-4) are inhibiting the cancer cells, although it is quite biocompatible with normal splenocytes. In conclusion, mCNCs can be used as a safe probe for imaging and the treatment of normal breast cancer (MCF-7) as well as TNBC (MDA-MB-231) (Figure 3.1.18A-B).

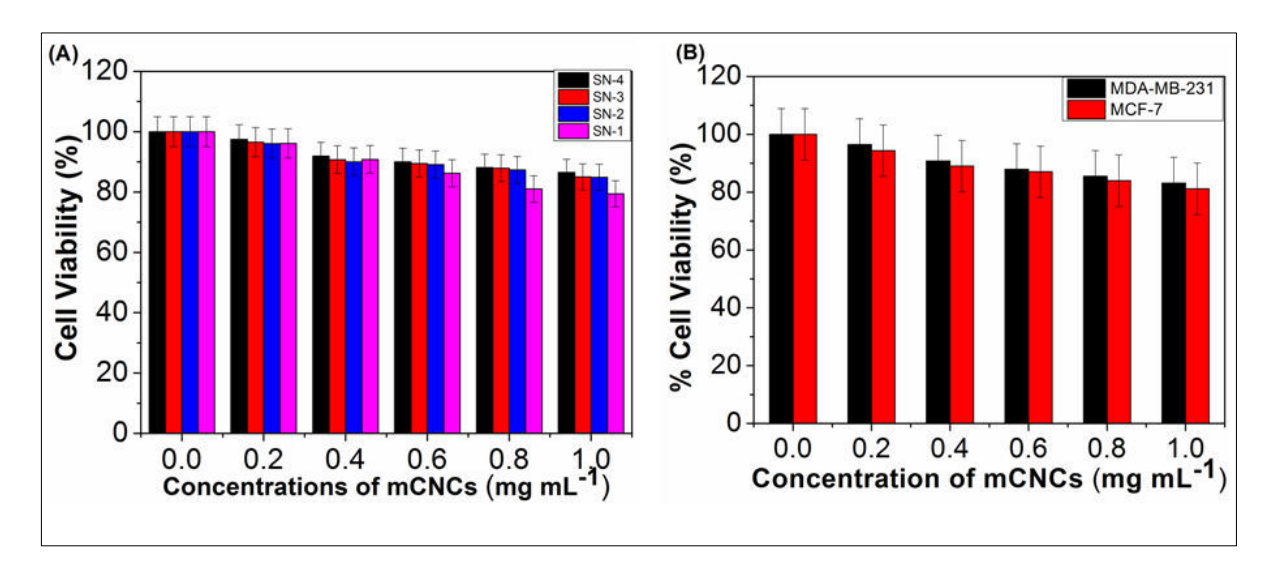


Figure 3.1.18 (A) Cell viability of normal splenocytes at different concentrations of nanocapsules (SN-1, SN-2, SN-3, and SN-4) and (B) cytotoxicity of the mCNCs (SN-4) against the MDA-MB-231 and MCF-7 (statistical value considered as p < 0.05)

3.1.2.6 Mitochondrial apoptosis analysis

To investigate the tumor targeting mechanism, it can be noted that apoptosis is primarily associated with the change in mitochondria membrane potential and mitochondrial damage. It is illustrated that apoptosis is induced in MCF-7 and MDA-MB-231 on treatment with mCNCs. It is a quite recognized fact that the mitochondria play an important role in the apoptotic cascade by serving as convergent signals of apoptotic cells for both the pathway, i.e., intrinsic and extrinsic pathways. The mitochondrial potential charges show determinant to carrying out the cell death. Henceforth, to know the process of apoptosis in different cancer cell lines, the change in the mitochondrial membrane potential on the different treatments of synthesized carbon nanocapsules was examined. Rhodamine 123 (Rh123) has been used to estimate the mitochondrial membrane potential.

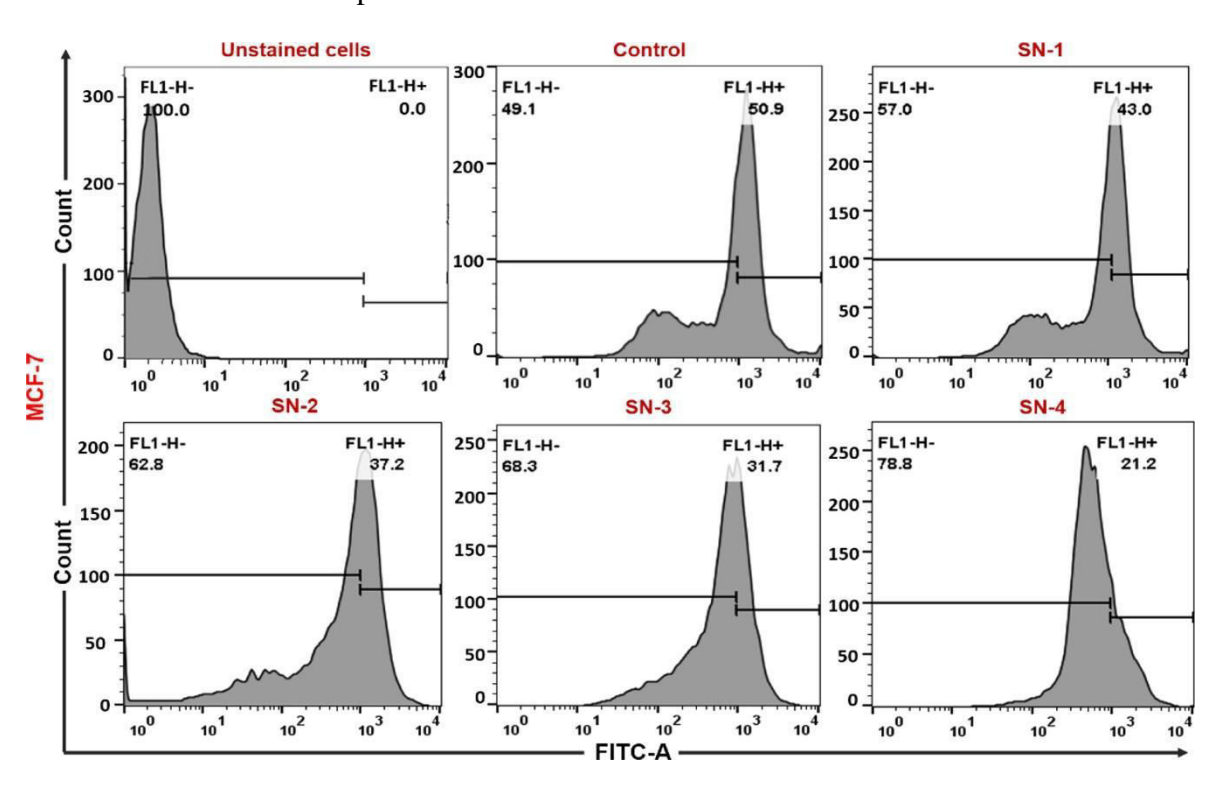


Figure 3.1.19 FACS study for quantifying the depletion of mitochondrial membrane potential by using Rh123. For MCF-7 cells were treated with various porous carbon nanocapsules (SN-1, SN-2, SN-3, and SN-4). After 24 h incubation, cells were stained with Rh 123 and analyzed through a flow cytometer. Figures show the percentage of mitochondrial depolarization calculated in MCF-7 cell lines against different carbon capsules.

Rh123 enters into the mitochondria with intact membrane potential. When mitochondria lost their potential, extra Rh123 leaches out from the mitochondria and henceforth detectable reduction of fluorescence occurred which is directly interrelated with the mitochondrial potential. The reported data showed that the mitochondrial membrane potential of MDA-MB-231 and MCF-7 cells were reduced after the treatment with different carbon nanocapsules (Figure 3.1.19, Figure 3.1.20, and Figure 3.1.21). The average depletion of mitochondrial membrane potential in MCF-7 was more as compared to the TNBC cell lines (MDA-MB-231). We also observed that the mesoporous carbon nanocapsule (sample SN-4) is potent to change in the membrane potential more compared to the other carbon nanocapsules (SN-1, SN- 2, or SN-3). The percentage change in mitochondria membrane potential (MMP) was calculated systematically and is shown in Figure 3.1.21(each value represents the mean \pm SD, *p < 0.05 compared with the control).

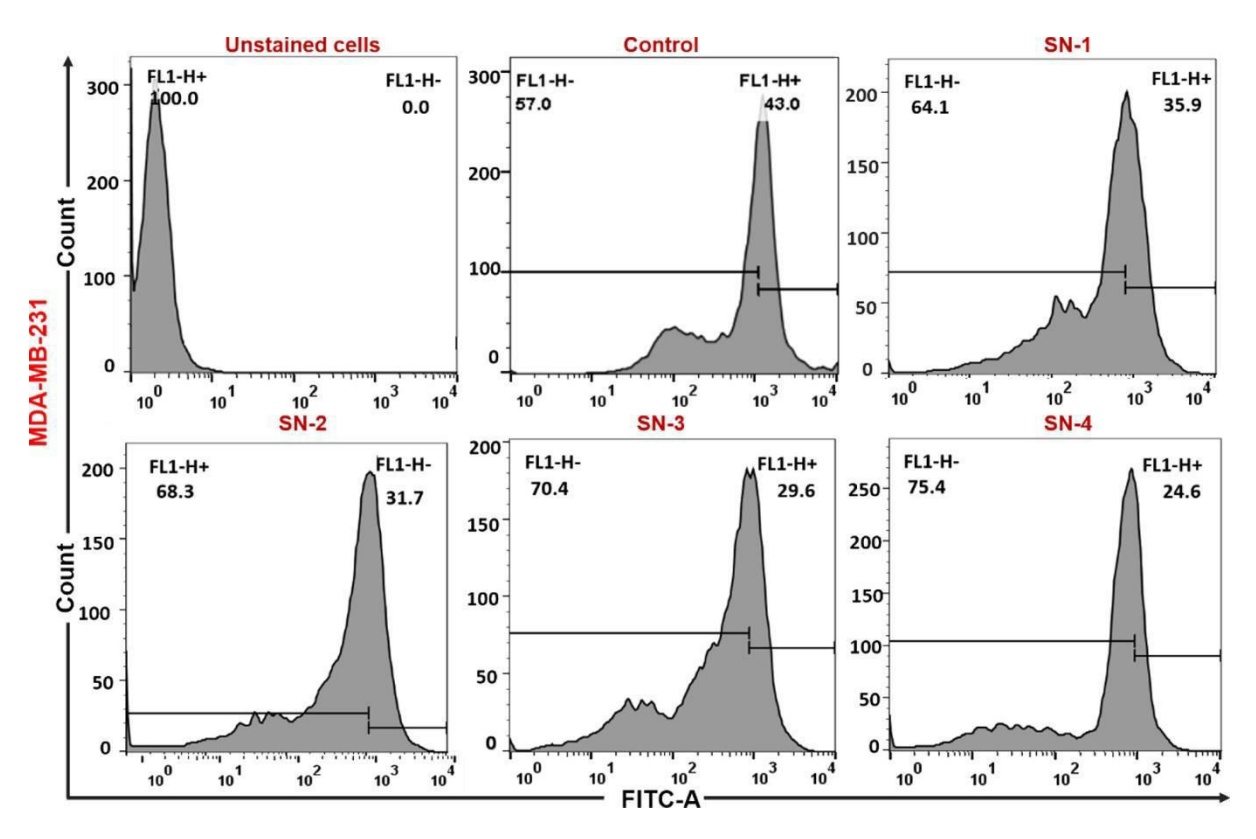


Figure 3.1.20 FACS study for quantifying the depletion of mitochondrial membrane potential by using Rh123. MDA-MB-231 cells were treated with various porous carbon nanocapsules (SN-1, SN-2, SN-3, and SN-4). After 24 h incubation, cells were stained with Rh 123 and analyzed through a flow cytometer. Figures show the percentage of mitochondrial depolarization in MDA-MB-231 cell lines obtained for different carbon nanocapsules.

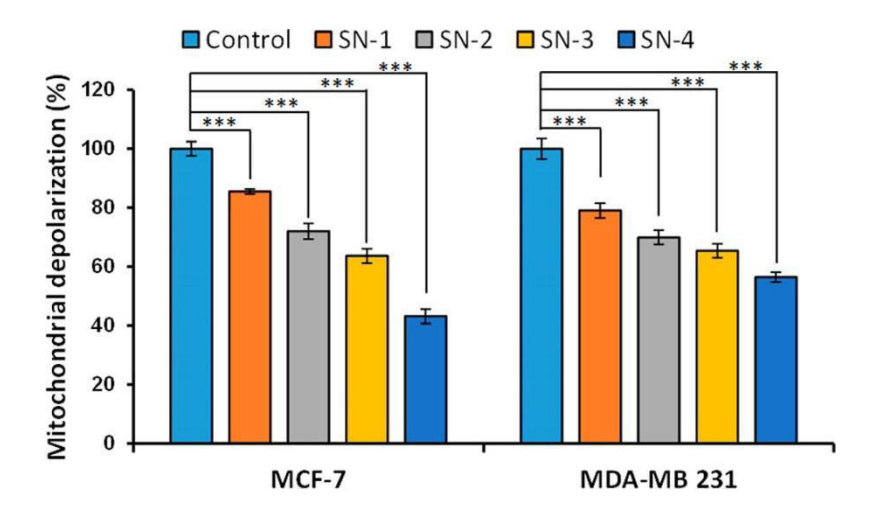


Figure 3.1.21Quantitative estimation of mitochondrial membrane potential by using Rh123. MDA-MB-231 and MCF-7 cells were treated with various porous carbon nano capsules(SN-1, SN-2, SN-3, and SN-4). After 24 h incubation, cells were stained with Rh 123 and analyzed through a flow cytometer. The percentage of mitochondrial depolarization in different cell lines calculated from Figures 3. 1. 19 and 3. 1. 20 for MCF-7 and MDA-MB-231 cells, respectively (n = 3, * denotes the level of significant difference as compared to control at p < 0.05).

3. 1. 2.7 Effect of Carbon Nanocapsules on Apoptotic Cell Death through Flow Cytometry.

Primarily, to check the apoptotic effect of carbon nanocapsules, we initiate treatment from the lower doses of SN-1, SN-2, SN-3, and SN-4 samples against MCF-7 cells (Figure 3.1.22) and MDA-MB-231 (Figure 3.1.23). We have taken untreated cells as a control.

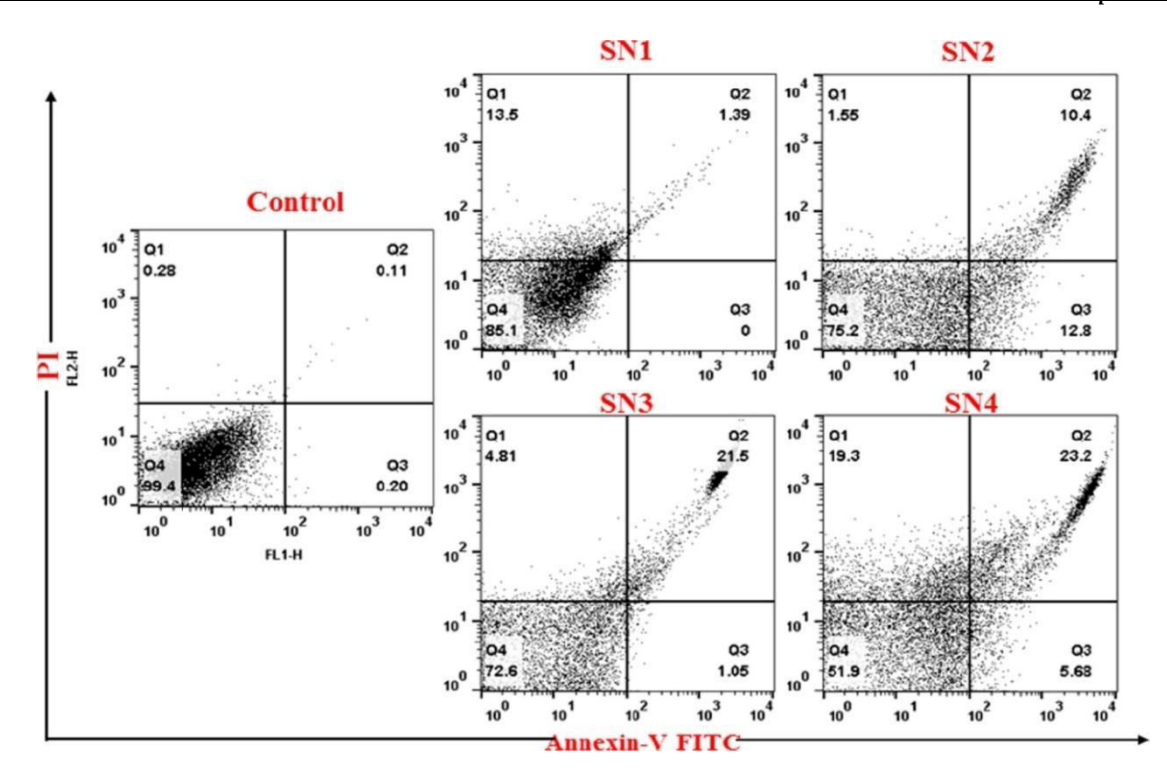


Figure 3.1.22 Cancer cells were treated with carbon nanocapsules (SN1, SN2, SN3, and SN4). Cells were stained with PI and annexin-V FITC antibodies to determine the apoptotic and necrotic cell death effect of synthesized compounds. Total 10 000 cells were acquired by flow cytometry and quadrants were set according to unstained control. Quadrants represent Q1, necrotic cells; Q2, late apoptotic cells; Q3, early apoptotic cells; Q4, healthy cells for MCF-7 human breast cancer cells after carbon nanoparticle treatment (comparison of apoptosis index of SN-1, SN-2, SN-3, and SN-4 with the MCF-7 breast cancer cells).

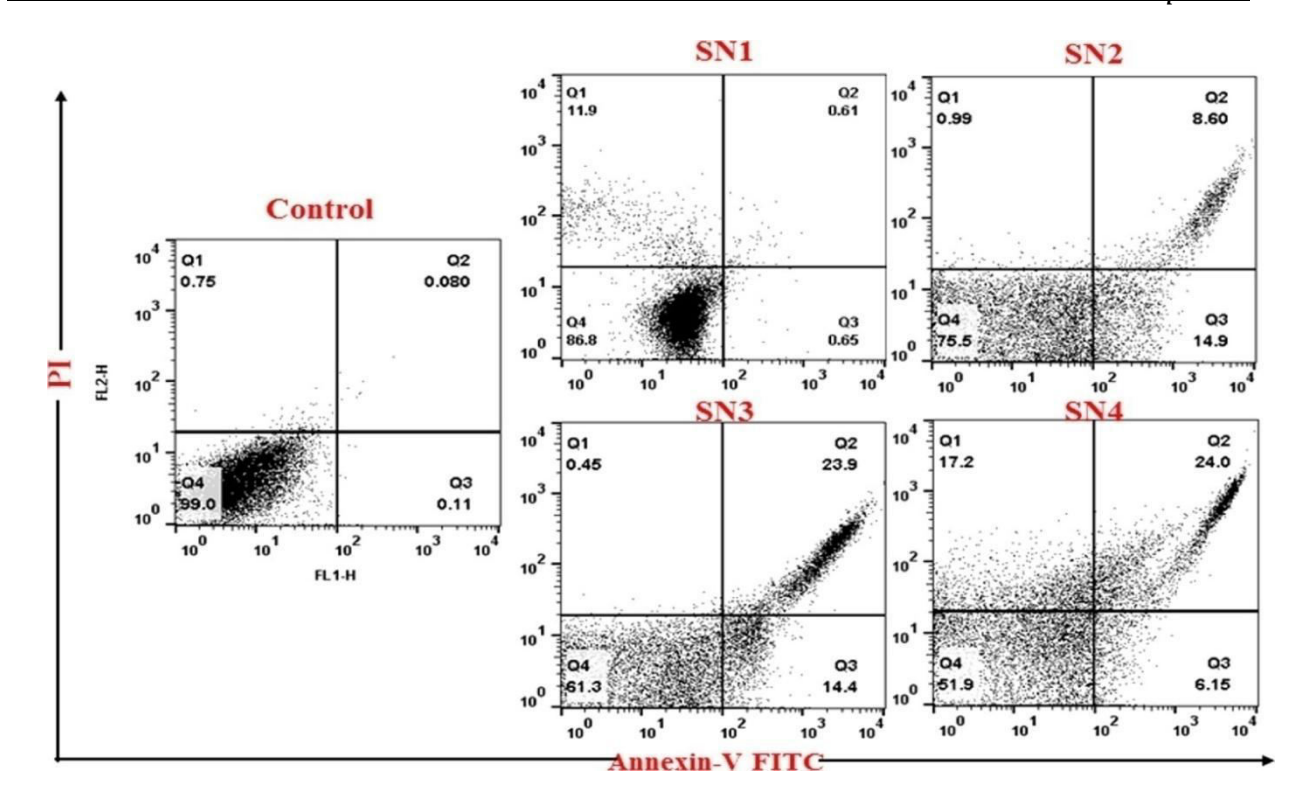


Figure 3.1.23 Cancer cells were treated with carbon nanocapsules (SN-1, SN-2, SN-3, and SN-4). Cells were stained with PI and annexin-V FITC antibodies to determine the apoptotic and necrotic cell death effect of synthesized compounds. Total 10 000 cells were acquired by flow cytometry and quadrants were set according to unstained control. Quadrants represent Q1, necrotic cells; Q2, late apoptotic cells; Q3, early apoptotic cells; Q4, healthy cells, for MDA-MB-231 triplenegative human breast cancer cells after the treatment of carbon nanocapsules.

Then we acquired 10,000 cells from each sample with BD FACS Calibur. To analyze the apoptotic cell death through flow cytometry, we have plotted the four quadrants Q1, Q2, Q3, and Q4, which denote necrotically, late apoptotic, early apoptotic, and live cells, respectively. We have performed the study for each sample and compared it to the control. Results showed that the percentage of the live cell (Q4) of breast cancer cells in response to the treatment of SN-1, SN-2, SN-3, and SN-4 samples mostly entered the late apoptotic (Q2) and necrotic cells (Q1) quadrants as compared to the untreated controlled cells. The comparison of the apoptosis index of SN-1, SN-2, SN-3, and SN-4 with the MCF-7 and MDA-MB-231 breast cancer cells (see Tables 3.1and 3.2) has been shown.

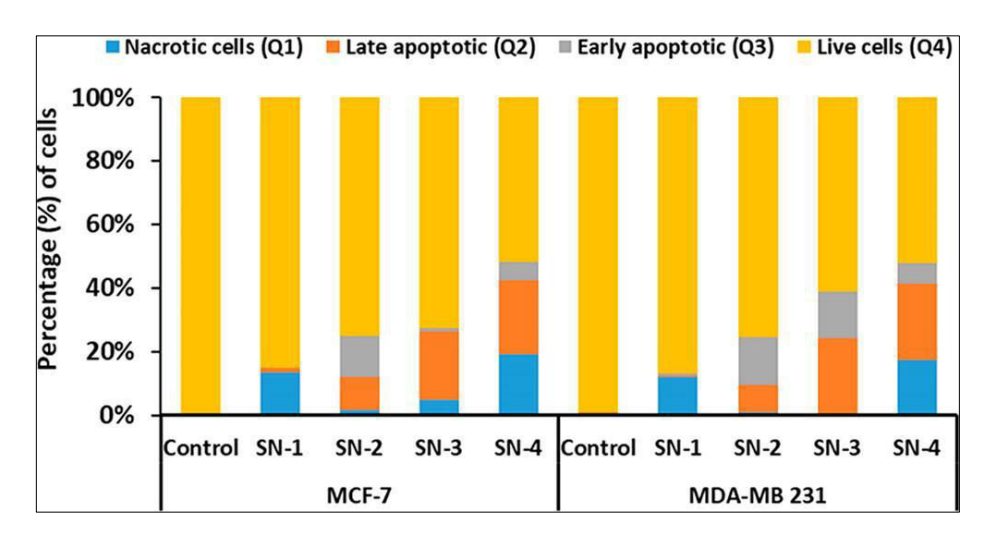


Figure 3.1.24 MCF-7 and MDA-MB-231 breast cancer cells were treated with carbon nanocapsules (SN-1, SN-2, SN-3, and SN-4). Cells were stained with PI and annexin-V FITC antibodies to determine apoptotic and necrotic cell death due to the effect of synthesized compounds. A total of 10 000 cells were acquired by flow cytometry, and quadrants were set according to unstained control. The percentage change in different stages of cell death: Q1, necrotic cells; Q2, late apoptotic cells; Q3, early apoptotic cells; Q4, healthy cells pattern of MCF-7 (left) and MDA-MB-231 (right) (comparison of apoptosis index of SN-1, SN-2, SN-3, and SN-4 with the MDAMB- 231 breast cancer cells).

Remarkably, SN-1 showed 13. 5% and 11.9% necrotic cells (Q1) in MCF-7 and MDA-MB-231 cells, respectively, without entering the early or late apoptotic cell.Interestingly, we observed that sample SN-4 showed more potent killing as compared to the SN-1, SN-2, and SN-3 toward breast cancer cell death for both of the cell lines. We also found that sample SN-4 demonstrated 19.3% necrotic cells (Q1) in MCF-7 which is slightly higher as compared to 17. 2% necrotic (Q1) cell death in MDA-MB-231 cell lines (Figure 4.1.22, Figure 4.1.23, Figure 4.1.24). The Comparison of the apoptosis index of SN-1, SN-2, SN-3, and SN-4 with the MCF-7 and MDA-MB-231 breast cancer cells have been provided in Tables 3.1 and 3.2.

Table 3. 1 Comparison of Apoptosis Index SN-1, SN-2, SN-3

Table 3. 2 Comparison of Apoptosis Index SN-1, SN-2, SN-3

and SN-4 with MCF-7 breast cancer cells

and SN-4 with MDA-MB-231 breast cancer cells

MCF-7	p values	significant level	MDA-MB-231	p values	significant lev
	Control vs SN-1			Control vs SN-1	
live cells	p < 0.001	***	live cells	p < 0.001	***
early apoptotic cells	p > 0.05	ns	early apoptotic cells	p > 0.05	ns
late apoptotic cells	p > 0.05	ns	late apoptotic cells	p > 0.05	ns
necrotic cells	p < 0.001	***	necrotic cells	p < 0.001	***
	Control vs SN-2			Control vs SN-2	
live cells	p < 0.001	***	live cells	p < 0.001	***
early apoptotic cells	p < 0.001	***	early apoptotic cells	p < 0.001	***
late apoptotic cells	p < 0.001	***	late apoptotic cells	p < 0.001	***
necrotic cells	p > 0.05	ns	necrotic cells	p > 0.05	ns
	Control vs SN-3			Control vs SN-3	
live cells	p < 0.001	***	live cells	p < 0.001	***
early apoptotic cells	p > 0.05	ns	early apoptotic cells	p > 0.05	•••
late apoptotic cells	p < 0.001	***	late apoptotic cells	p < 0.001	***
necrotic cells	p < 0.001	***	necrotic cells	p > 0.05	ns
	Control vs SN-4			Control vs SN-4	
live cells	p < 0.001	***	live cells	p < 0.001	***
early apoptotic cells	p < 0.001	***	early apoptotic cells	p < 0.001	***
late apoptotic cells	p < 0.001	***	late apoptotic cells	p < 0.001	***
necrotic cells	p < 0.001	***	necrotic cells	p < 0.001	***
	SN-1 vs SN-2			SN-1 vs SN-2	
live cells	p < 0.001	***	live cells	p < 0.001	***
early apoptotic cells	p < 0.001	***	early apoptotic cells	p < 0.001	***
late apoptotic cells	p < 0.001	***	late apoptotic cells	p < 0.001	***
necrotic cells	p < 0.001	***	necrotic cells	p < 0.001	***
	SN-1 vs SN-3			SN-1 vs SN-3	
live cells	p < 0.001	***	live cells	p < 0.001	***
early apoptotic cells	p > 0.05	ns	early apoptotic cells	p > 0.05	***
late apoptotic cells	p < 0.001	***	late apoptotic cells	p < 0.001	***
necrotic cells	p < 0.001	***	necrotic cells	p < 0.001	***
neerode cens	SN-1 vs SN-4		neerode cens	SN-1 vs SN-4	
live cells	p < 0.001	***	live cells	p < 0.001	***
early apoptotic cells	p < 0.001	***	early apoptotic cells	p < 0.001	***
late apoptotic cells	p < 0.001	***	late apoptotic cells	p < 0.001	***
necrotic cells	p < 0.001	***	necrotic cells	p < 0.001	***
necrotic cens	SN-2 vs SN-3		necrotic cens	SN-2 vs SN-3	
live cells	p > 0.05	ns	live cells	p < 0.001	***
early apoptotic cells	p < 0.001	***	early apoptotic cells	p > 0.05	ns
late apoptotic cells	p < 0.001 p < 0.001	***	late apoptotic cells	p > 0.05 p < 0.001	ns ***
necrotic cells	p < 0.001 p < 0.05	*	necrotic cells	p < 0.001 p > 0.05	ns
necrotic cells	p < 0.05 SN-2 vs SN-4		necrotic cens	p > 0.05 SN-2 vs SN-4	ns
livo colle		***	live cell-		***
live cells	p < 0.001	***	live cells	p < 0.001	***
early apoptotic cells	p < 0.001	***	early apoptotic cells	p < 0.001	***
late apoptotic cells	p < 0.001	***	late apoptotic cells	p < 0.001	***
necrotic cells	p < 0.001	ጥ ጥ ጥ	necrotic cells	p < 0.001	***
1: 11	SN-3 vs SN-4	***	1: 1:	SN-3 vs SN-4	***
live cells	p < 0.001	***	live cells	p < 0.001	***
early apoptotic cells	p < 0.001	***	early apoptotic cells	p < 0.001	
late apoptotic cells	p < 0.05	****	late apoptotic cells	p > 0.05	ns
necrotic cells	p < 0.001		necrotic cells	p < 0.001	

N. B. Statistical analysis of Neem seed derived compounds SN-1, SN- 2, SN3, and SN4 with their control for MCF-7 (A) and MDA-MB-231 (B) by applying 2-way ANOVA. The tabular results represent the significant values by *, **, ***, and **** at p < 0.05. "ns" represent for non significant value.

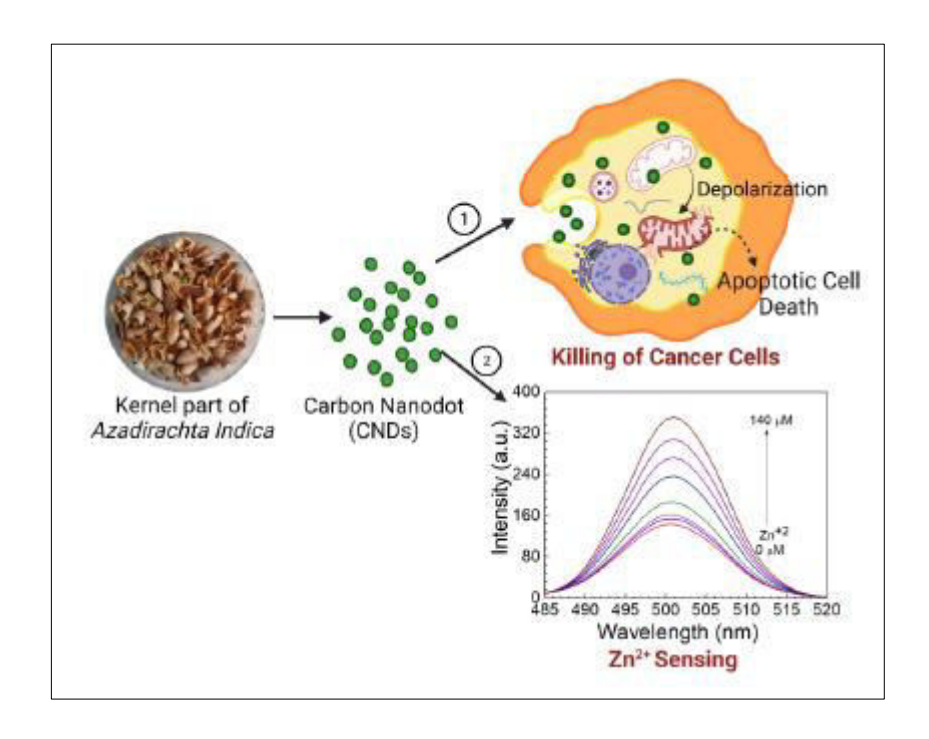
3.1.3. Summary

In this work, we reported a green one-step synthesis approach of mesoporous carbon nanocapsules from Azadirachta indica seeds and their uses for theranostic applications. The synthesis method of carbon nanocapsules is economical for large-scale production. The mesoporous carbon nanocapsules are highly water-soluble, emit strong fluorescence light, and are highly stable. The mesoporous carbon nanocapsules are highly biocompatible with normal healthy cells and are good candidates for absorption in the cytoplasm. These mCNCs substantially affect breast cancer cells more than normal cells and are further useful for multicolor living cell imaging. Thus, the prepared mesoporous carbon nanocapsules can be used as an eco-friendly material for theranostic applications. The change in mitochondrial membrane potential and the increasing number of apoptotic cells corroborated a smart mitochondrial-targeted delivery of these carbon nanocapsules. In the future, we can easily modify the properties of these samples and enhance the capability of drug loading to check its anticancer activities against various cancers and other diseases. Finally, Azadirachta indica seeds derived from carbon nanocapsules potential may hold huge for cell imaging and therapeutic applications.

Chapter: 3

RESULTS AND DISCUSSION: PART -II

Synthesize Of carbon dots for kernel part of seed: Photoluminescence mechanisms and applications in detection of biologically relevant metal ions.



The outcome from part II: The results discussed in Part-II, have been communicated as "Green synthesis of Carbon Nano dots from Kernel part of Azadirachta Indica seeds: selective detection of biologically relevant metal ions and drug delivery applications".

Chapter: 3

RESULTS AND DISCUSSION:

PART -II

Synthesize of carbon dots from Kernel part of Neem seed: Photoluminescence mechanisms and applications in detection of biologically relevant metal ions.

3.2.1 Introduction and Motivation

Carbon nanomaterials such as carbon quantum dots (CQDs),³¹⁰ graphene quantum dots (GQDs),³¹¹etc. have shown huge attention in recent years due to their unique properties and applications in medical biotechnology.³¹² CQDs are also known as carbon dots (CDs), precisely their size below 10 nm in diameter has attracted researchers due to their high chemical stability, optical and optoelectronic properties, luminescence, and for unique optical absorption (broadband). These properties of CDs are unique concerning other carbon nanomaterials due to their smaller dimension (d, <10 nm), defect-induced properties, functionality, and because of quantum confinement.³¹³ On the other hand, the usages of CDs in biomedical applications such as for therapeutic detection and imaging, drug delivery, and designing biosensors are much more than the inorganic/metallic/semiconductor quantum dots (e. g., CdS, CdS, CdTe, PbSe, etc.)¹⁰¹ due to their more photostability, blinking stability, and biocompatibility.³¹⁴ CD possesses defects and oxygen-containing functional groups on their surface caused to hydrophilicity and hence much more dispersible in water.³¹⁵ Further, the properties of the CDs depend on the size, shape, crystallinity and the extent of sp² hybridized carbon present in the structure.³¹⁶ Further, the

biocompatibility is also a concern for CDs for their use in biomedical applications, which is strongly influenced by the presence of oxygen and nitrogen-containing functional groups (e. g., -COOH, -OH, NH-, -CO-, -NH₂, etc.) and the confined size.³¹⁷ Such as ultra-small size CDs attributed to the low toxicity and high *in vivo* bio distribution in mammalian systems for the CDs of relatively bigger size.³¹⁸ In line of the properties developed in CDs, they can also be used as a probe for sensors to detect different analytes using their intrinsic defects and functional group-induced fluorescent properties.³¹⁹ However, all other properties including analyte sensing properties of CDs can be induced by following a suitable synthesis approach.²²⁸ However, different synthesis approaches, carbon precursors of CDs, size, morphology, defects, and chemical functionality can yield the effectiveness of the sensing efficiency.³²⁰ Therefore, there is a huge scope for designing low-cost materials with better detection capacity.

In this work, biocompatible CDs were synthesized through a green synthesis approach, and the fluorescent-based sensing activity ²²⁹ of the metallic ions such as Ca²⁺, K⁺, Na⁺, Fe³⁺, Fe²⁺, and Zn²⁺ have been explored since these are very essential ions in body to control the biological processes in the body. Further, the CDs synthesized in this work have been used to explore the drug delivery efficiency such as for killing the cancer cells. The CDs were synthesized from the kernel part of the *Azadirachta indica* seeds. CDs-based sensor detection selectivity towards the specific metallic ions specifically Zn²⁺ and Fe³⁺are very important. The detection of these two ions is important for the Amyloid-β stability, oligomerization, and aggregation. ³²¹ In the present study, further, we established that the functional groups present on the surface of the synthesized CDs play important role in the detection of these metal ions. This study has been performed with as-received CDs, i. e. ,without any additional surface modifications. Further, from the metallic ions sensing outcomes, we establish CD-based molecular logic gates mechanism of detection. Herein, implication of logic gates, e. g., YES and NOT gate were constructed using different Zn²⁺, and Fe³⁺ions as inputs. ³²² Overall, the characteristics of the synthesized CDs have been

exposed up with a new prototype for constructing the chemical logic gates through fluorescent chemo sensors for the detection of metallic ions.³²³ It can also be noted that through the construction of the chemical depended molecular logic gates, how it can be significantly attractive for the fabrication of the molecular scale electronic devices that also has been found out through this work. Herein, we have concentrated our study more on Zn²⁺ and Fe³⁺, because iron is one of the most abundant elements on the earth and both Zn²⁺and Fe³⁺ take part in several vital biological processes³²⁴, e. g., oxygen transportation³²⁵, transcriptional regulation³²⁶, replication of DNA and electron transfer.³²⁷ As an example, insufficient iron intake caused many health issues, and even it can be life threatening.³²⁸ An adequate amount of Fe⁺³ is connected to the diseases like Alzheimer's and other neuron-generative disorders. On the other hand excess, Fe⁺³ ingestions can lead to the formation of free radicals and tissue damage. 328,329 Thus, finding out the Fe⁺³concentrations is very important in clinical research. Further, Zn⁺² takes part in many enzymatic reactions of the body, such as the creation of DNA, maintaining the growth of cells, building different proteins, healing and regeneration of damaged tissues, and one of the most desired elements that retained immunity and having anti-inflammatory properties. 330 Further, based on the sensing of the ions, several research groups explained the mechanism through the constitution of molecular logic gates using various biomolecules such as nucleic acids, ³³¹ proteins, and other organic molecules. 199 Such as, CDs can affect the DNA structure by inducing DNA B-Z transition and the mechanism of operation can be accomplished by constituting a DNA logic operation. Other than the DNA molecule, using another biomedical logic gate can also be constituted to explain the biological process mechanism and their electronic transformation. ³³² To note, several methods have been reported for the synthesis of CDs, such as chemical carbonization, sono chemical synthesis³³³, microwave synthesis³³⁴, thermal decomposition of different carbon sources³³⁵, etc. from the various source of carbon precursors.³³⁶ Many of the reported methods required toxic chemicals and hence produce toxic CDs. Furthermore, the source of carbon also greatly influences the quality of CDs as well as their characteristic properties varied due to the content of hydrogen, oxygen, and nitrogen-containing functional groups. In the above line, herein, we report the new synthesis of CDs to form *Azadirachta Indica* seeds and illustrate their application in ion sensing output through the logic functions of OR, XOR, and IMP. Some of the CDs reported show remarkable characteristics such as relatively low toxicity and biocompatible and directed their use in the delivery of anticancer drugs, and good photo stability, with excellent luminescence properties. Moreover, how the CDs are found to reveal an attractive "ON-OFF" switching mood with the stepwise addition of Fe⁺³ has also been studied. The sensing mechanism has been established based on adding Fe⁺³ ions followed by the formation of a CDs-Fe⁺³ complexes. Finally, how the rational for executing several logic operations rely on the association of metal ions and their corresponding fluorescence intensity varies with our CDs that have also been studied.

In the next objective, we evaluated the efficiency of CD for breast cancer therapy. Doxorubicin (DOX) is a well-known anticancer drug and widely used chemotherapy agent to cure early and advanced breast cancer. Although, tumour resistance has constrained the implications of the agent in single-drug treatment regimes. Therefore, to enhance the effectiveness of DOX, we loaded it with CDs and designed different complex formulations of CDs. We tested the different complex formulations of CDs against the MCF-7 breast cancer cell line. The synergic effect of CDs with doxorubicin has been examined in detail regarding biocompatibility, therapeutic effectiveness, and cytotoxicity. To investigate this, the MTT assay, mitochondrial membrane potential (MMP, $\Delta\psi$ m), apoptosis assay, and cell imaging were performed to evaluate the therapeutic roles of CDs, and the biological relevance of the treatment was demonstrated. It could also be mentioned that $\Delta\psi$ m has a significant role in controlling the mitochondrial movements as it shows the control of electron transportation and oxidative phosphorylation to generate force behind the ATP generation. Executing a regular biological activity of the cells, the level of MMP and ATP generation ought to be quite stable, albeit the regulated fluctuation of $\Delta\psi$ ms and ATP also leads to

ordinary physiological activity. These CDs are biocompatible with normal healthy cells; however, it has a potential synergic cytotoxic effect with DOX towards the MCF-7 breast cancer cell line (a human breast cancer cell with estrogen, progesterone, and glucocorticoid receptors). Thus, from this work, a clear direction for our CDs in designing various molecular devices for sensing and detection of biological analytes has been found along with a huge possibility of their uses in drug delivery and cancer therapy applications.

3.2.2. Results and Discussion

3.2.2.1. Structural confirmation

CDs were synthesized as it has been described in the experimental section. The morphology and size of the as-synthesized CDs were characterized by HRTEM and shown for different magnifications (Fig.3.2.1 a-c). The lattice fringes within the particles indicate that the assynthesized CDs were crystalline and the lattice fringes of the CD nanoparticles were calculated to be 4 nm. The crystalline nature of the CDs is also further confirmed through the SAED spectra (Fig.3.2.1d). It is obvious from TEM images that the synthesized CDs are mono dispersed spherical with an average diameter of ~4 nm (Fig.3.2.1e). The elemental composition of CDs was calculated from EDAX spectra acquired from the TEM experiment (Fig.3.2.1f) and confirmed the presence of elemental oxygen and carbon. It is noticed that the average size of the particles for CDs is not more than 10 nm in diameter.

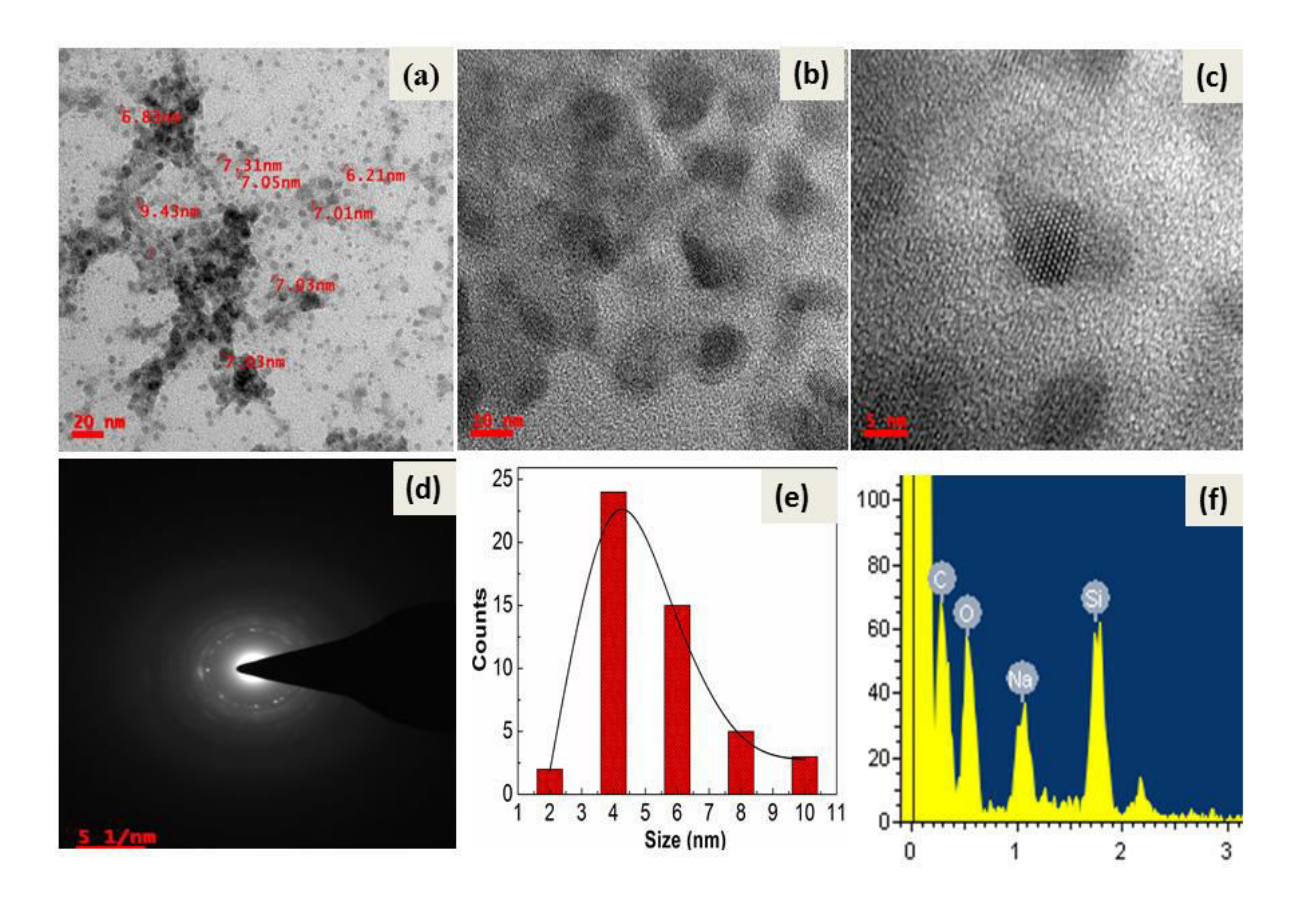


Figure 3.2.1 TEM results of CDs (KS-1),(a)-(c) TEM micrographs at different magnifications, (d) SAED pattern, (e) particle size distribution, and (f) EDAX spectrum of CDs.

3.2.2.2. Chemical functionality and thermal stability

To find out the chemical functionality, FT-IR spectra were acquired for synthesized CDs and the results are shown in (Fig.3.2.2a). From the FT-IR spectrum, the bands appeared at 2958, 2474, 1768, 1612, 1432, and 862 cm⁻¹ specified for the presence of stretching bands due to - CH, -C=O, C=C, -N=O, -CN, and epoxy ring, respectively. Due to the presence of these functional groups, the synthesized CDs are well dispersed in water.From TGA, the thermal stability of the CDs has been studied, and found that 10.3% mass loss over the temperature range of 0 °C to 800°C occurred (Fig.3.2.2b).Further, the thermal properties of CDs were evaluated using DSC (Fig.3.2.2c). The study was conducted up to 600 °C under N₂-gas with a heating rate of 10°C/min (Fig.3.2.2c).DSC plots exhibit the heat flow behaviors of the samples to check whether it undergoes any phase transformation or not. However, an endothermic

peak is observed around 95-100 °C due to the evaporation of any volatile component that is confirmed from TGA. XRD patterns for CDs (KS-1) are shown (Fig.3.2.2d). There is a diffraction peak at $2 \sim 20$. 47° , which corresponds to the carbon (100) plane. A broad diffraction peak is observed at $2 \sim 20^{\circ}$, due to the smaller size of the CDs. However, (Fig.3.2.2d), it is noticed that the synthesized CDs are crystalline which is further confirmed by the TEM results (Fig.3.2.1c-d).

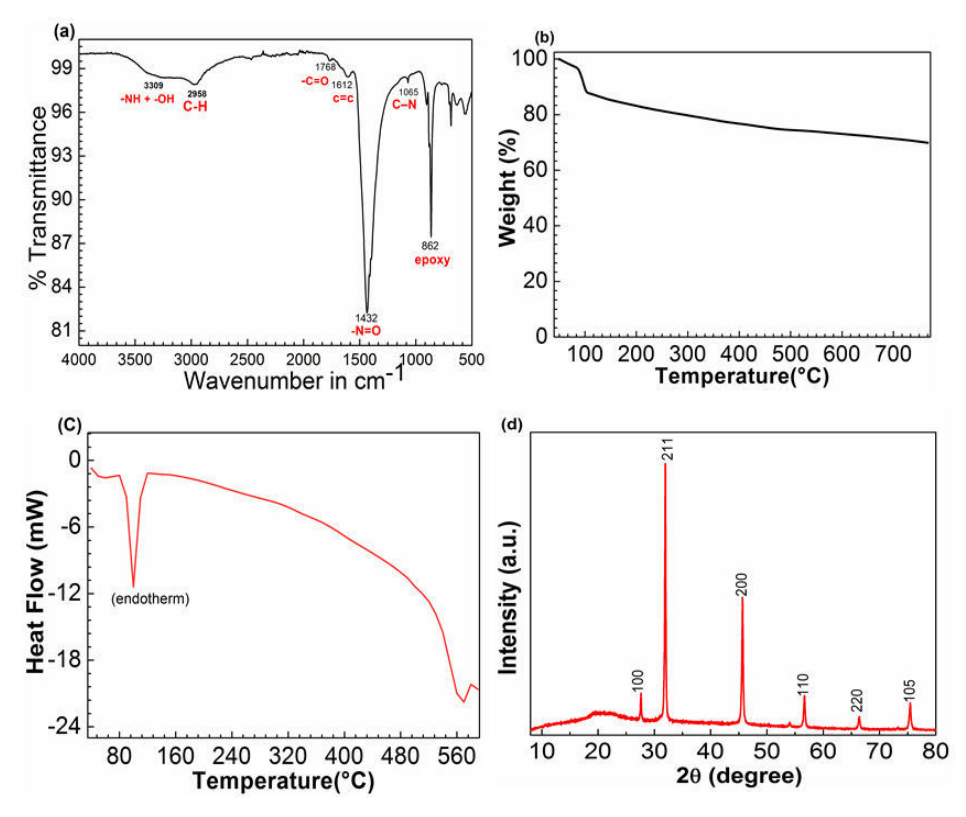


Figure 3.2.2(a) FT-IR spectrum, (b) TGA thermogram, (c) DSC, and (d) XRD pattern of the CDs.

3.2.2.3 Surface properties:

To confirm the surface area and pore size, BET experiments were performed. From (Fig 3.2.3a), it is confirmed that CDs showed a type-IV adsorption-desorption isotherm with a clear hysteresis. The surface area and pore size of as-prepared CDs were found to be 82.1 m² g⁻¹ and 2-3 nm in diameter, respectively (Fig.3.2.3a and 3.2.3b). Furthermore, the hydrodynamic diameter (DLS) of the CDs was found to be 12.74 nm, which can be correlated with the TEM results for particle size

(Fig. 3.2.3c). The hydrodynamic diameter of CDs is found to be 13.72 nm. Raman spectra for the synthesized CDs were acquired and results confirmed the presence of the 'D' band (at 1341cm^{-1}) and 'G' band (at 1559cm^{-1}), which are two signature bands for the carbon (CDs). The intensity ratio of D and G bands i. e I_D/I_G designates the ratio of sp^3 and sp^2 hybridized carbon present in the CDs. The intended I_D/I_G value was obtained to be 0. 83, implying that CDs is having a similar assembly to graphitic structure (Fig.3.2.3d).It is known that the surface zeta potential is very important for various biomedical applications of nanoparticles. Therefore, the zeta potential for the sample was calculated to be -37 mV (Fig. 3.2.3e). This is a quite high value as compared to the results for CDs, 293 due to the different extent of the functional groups present on the surface. This high zeta value is responsible for the electronic transport of the CDs. Mainly due to the presence of surface amino groups present on CDs, it resulted from very high zeta potential. Further, the 1 H-NMR spectroscopic analysis revealed distinct regions such as at 1-3 ppm, 3-6 ppm, 6-8 ppm, and 8-10 ppm due to the sp^3 C–H protons, protons attached with the hydroxyl and ether or carbonyl groups, and for the aromatic or sp^2 protons and the aldehydic protons, respectively (see Fig.3.2.3f).

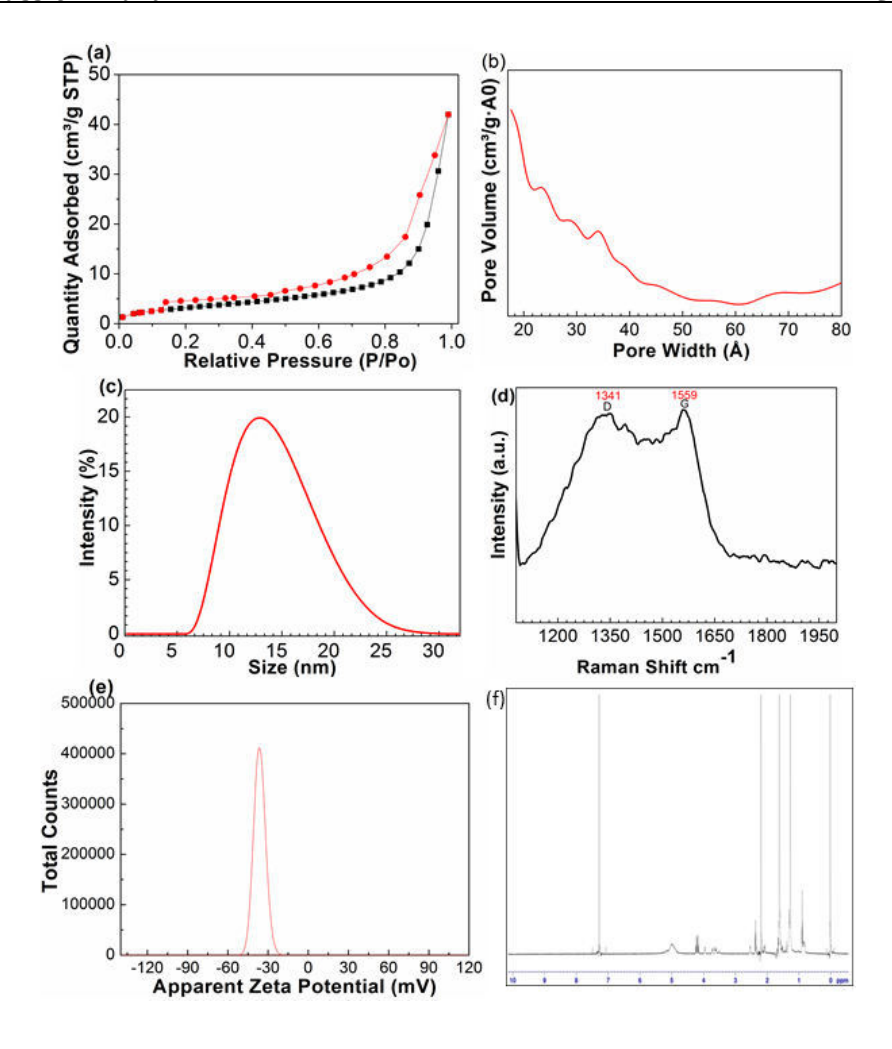


Figure 3.2.3. Shows the (a) BJH adsorption–desorption isotherm acquired in N_2 gas, Fig. (b) Pore size distribution of CDs obtained from desorption isotherm, Fig. (c) Particle size results obtained from DLS, Fig. (d) Raman spectra of solid CDs sample and Fig. (e) Zeta Potential results for the CDs in water medium and Fig. (f) 1 H-NMR spectrum for CDs acquired in CDCl₃, 400Hz (KS-1), respectively.

3.2.2.4 Optical and photoluminescence properties of CDs

The optical properties of the CDs are very important to decide their uses in various purposes such as for therapeutic detection and imaging, drug delivery, and designing biosensors. ^{101,322,325,338} In this direction, the UV-Vis and fluorescence spectroscopy analysis were performed and the bands were identified to explore reasons for the fluorescence properties of synthesized CDs. From the UV-Vis absorption spectrum for CDs, a strong absorption band at 275 nm is identified and

assigned to the π - π * transition of C = C (Fig3.2.4a). Due to the various chemical functional groups present, the intensity of fluorescence varies in different solvents and temperature as shown in Fig.3.2.4, Table-3.3 and Table-3.4 represent more detailed information about the optical properties of synthesized CDs in presence of the various solvent and shows that optical properties of CDs also depend on the solvents, which may be due to the different type of interactions played between solvent molecules and CDs.

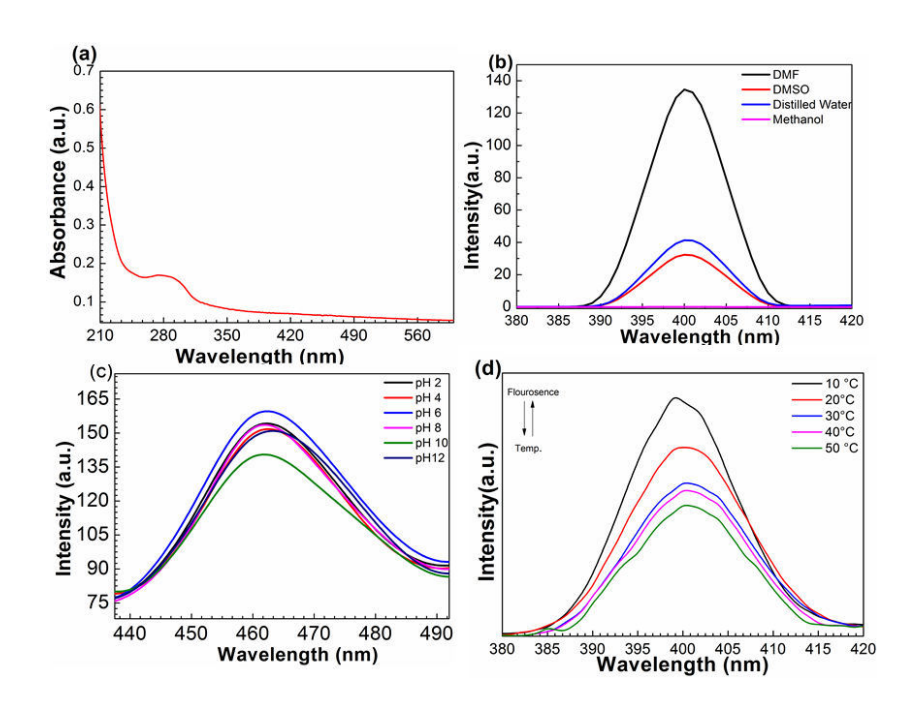


Fig 3.2.4 Figure shows (a) UV-Vis absorption spectrum in water, (b) Fluorescence spectra in different solvents, (c) Photoluminescence variation with differences in pH from 2 to 12, and (d) Fluorescence intensity dependency on temperature variance for synthesized CDs.

Table 3.3: Shows the effects of pH on photo luminance on synthesized CDs.

Sl	p	Intensity (a.u.)
No	Н	
1	2	168. 2
2	4	169. 5
3	6	173. 2
4	8	165. 6
5	10	161. 2
6	12	151. 4

Table 3.4: Effect of temperature on the fluorescence intensity of synthesized CDs.

Sl	Temp.	Wavelength	Intensity (a.u.)
No	(°C)	(nm)	
1	10	399. 8	31. 7
2	20	399. 8	24. 9
3	30	400. 9	20. 1
4	40	400. 9	19. 2
5	50	401. 9	17. 2

To explore the optical properties of our CDs, detailed fluorescence spectra of CDs were also acquired in various solvents, i. e. (distilled water, methanol, DMF, and DMSO) (Fig 3.2.4b) and the effect of solvent on the fluorescence intensity was studied. The synthesized CDs are highly dispersible and visible and in DMF, it has maximum fluorescence intensity. The possible reason behind the high fluorescent intensity is due to the presence of amide groups on the surface of the CDs, which further has confirmed through the FT-IR. The effect of pH is one of the essential parameters that affect fluorescence intensity. A series of experiments were conducted with different pHs to get an appropriate pH with the highest fluorescent intensity. It is also noticed that the fluorescence intensity varied with the change in the concentration of CDs as well as it varied with a change in the pH (pH 2 to pH 12) (Fig.3.2.4c). From figure 3.2.4c, fluorescence emission is observed (pH 4 to pH 8) due to the π - π * and n- π * favourable transitions of free electrons. To gain detailed insight into the underlying decay process, we acquired the fluorescence spectra of the CDs as a function of temperature from 10 °C to 50 °C, as shown in (Fig 3.2.4 d). It is obvious that with an increase in temperature the intensity of fluorescence displays a weakening tendency due to the thermal/lattice vibration of the functional groups present or due to the change in the electronic and transition states.³³⁹

3.2.2.5 Fluorescence quenching and enhancement of CDs and detection of metal ions

It has been reported by many researchers that the activity of CDs can be influenced by several factors, i. e., pH, concentration of carbon dots, metal ions concentration, reaction time, experimental conditions ^{228,320,340}, etc. Therefore, among the parameters illustrated in the sensing mechanism, we evaluate the selectivity of the detection system by acquiring the fluorescence spectra in presence of different metal ions. Here we considered fluorescent properties as one of the important output parameters. Thus, we have investigated the fluorescence quenching or enhancement effects of various metal ions on CDs (KS-1) in deionized water (Fig.3.2.5). Accordingly, the impact of different metal ions (e. g., Ca²⁺, K⁺, Na⁺, Zn²⁺, and Fe³⁺) are important for various biological process, and thus each one at a concentration of 1 µM was used during the experiment. The difference in fluorescence intensity of the CDs solutions in presence of various metal ions was acquired. The fluorescence response of our CDs in presence of different concentrations of Fe³⁺ (from top to bottom 0, 10, 20, 40, 60, 80 and 120 µM) was measured (Fig 3.2.5). As shown in (Fig3.2.5 a), the change in the fluorescent spectra has been shown for Fe³⁺. The fluorescent intensity decreases with an increase in the concentration of Fe³⁺. Further, a two steps fluorescent quenching is observed; one is between 1-20 µM with a sharp slope and the second is 20-140 µM with an inclined slope of quenching (Fig. 3.2.5). Further, the fluorescence quenching effect of the Fe³⁺ ions is much stronger than that of the other ions such as Ca²⁺, Na⁺, K^+ (Fig. 3.2.6).

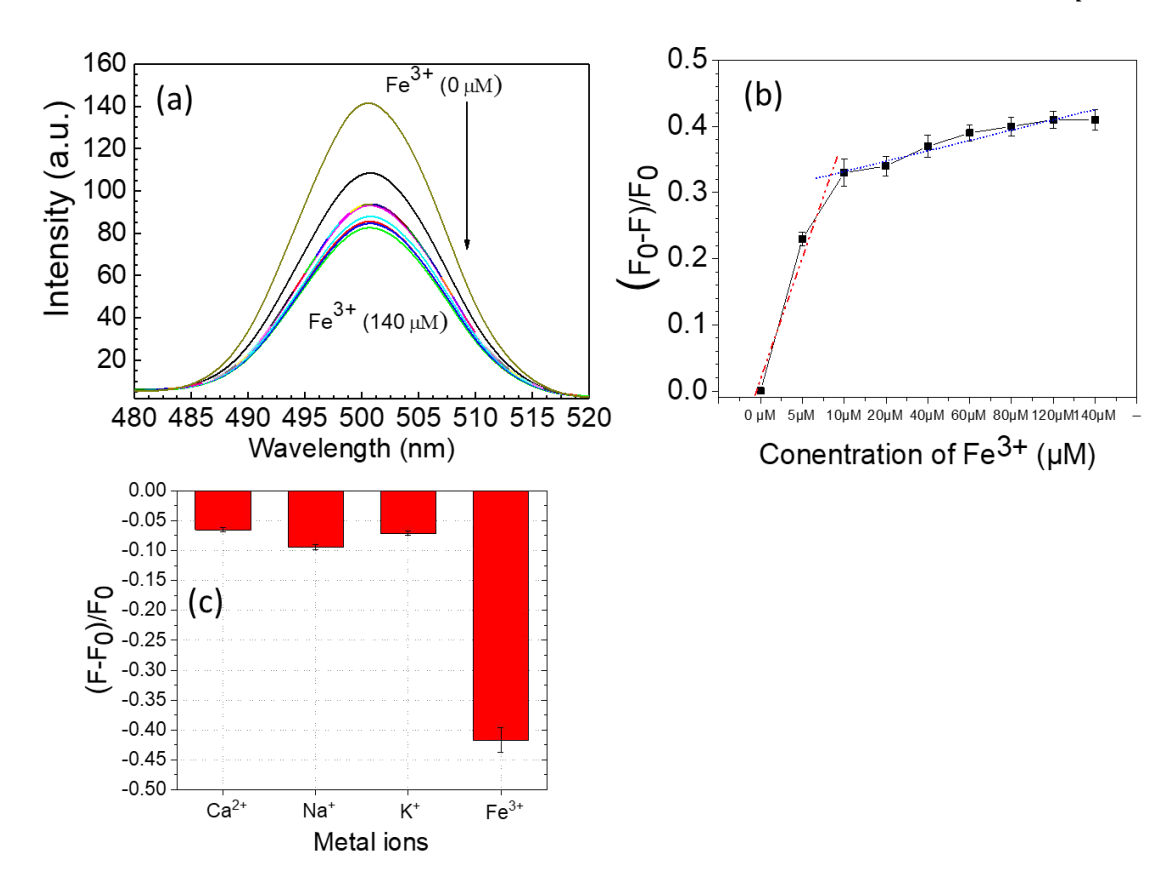


Figure 3.2.5 (a) Fluorescence spectra of CDs of (100 μg. mL^{-1}) with different concentrations of Fe⁺³.(b) Shows the dependence of fluorescence intensity on the CDs at 0-140 μM solution of Fe⁺³, shows a linear relationship between the fluorescence intensity and Fe⁺³ concentrations. so a two steps linear relationship between the fluorescence intensity and concentration of Fe³⁺ in between 0-10 μM and 0-140 μM concentrations, respectively,(c) Shows the fluorescence intensity ratios (F-F₀)/F₀ of the CDs solution in presence of various metal ions and observed the quenching of fluorescent.

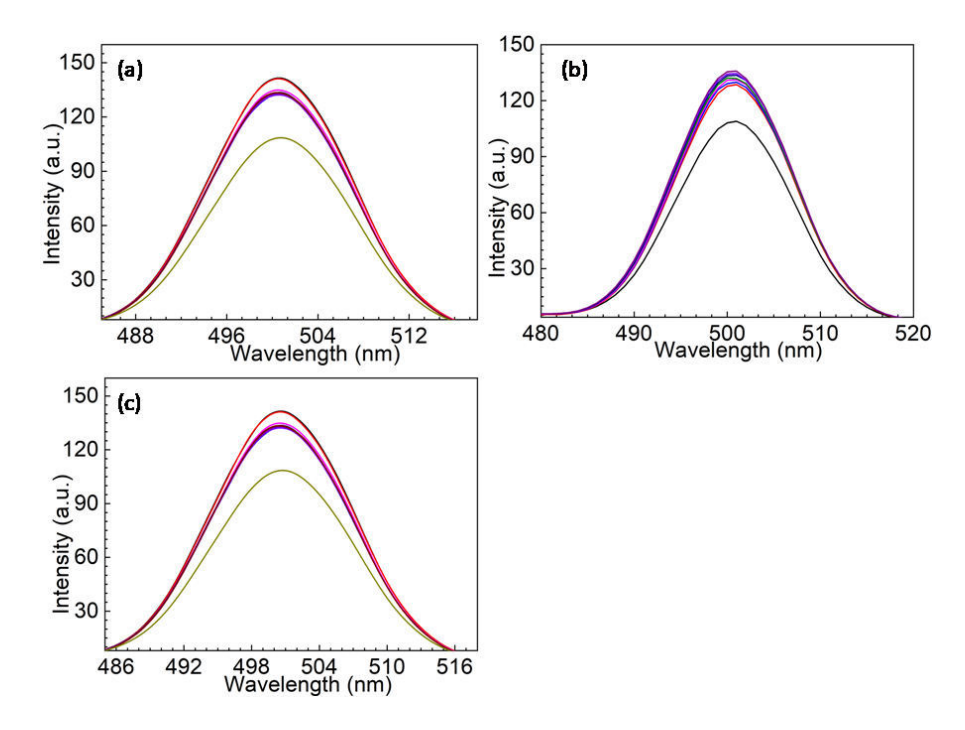


Figure 3.2.6: Fluorescence spectra of CDs of at 0-140 μM solution with different concentrations of a) Ca²⁺ b) Na⁺ c) K⁺

The dependence of fluorescence quenching for Fe⁺³ found is concentration dependent (Fig.3.2.5 a-c). This phenomenon was observed typically due to the oxygen and nitrogen-containing groups present on the surfaces of the CDs, which contribute to excellent water solubility and exhibited their strong affinity towards metal ions. The external electronic environment of synthesized CDs and their fluorescent properties are the keys in interaction with Fe⁺³ and CDs rolled as an electron or charge (energy) donor. Thus, the utility of the proposed CD-based sensor displays a turn-on sensing podium for the Ca²⁺, K⁺, Na⁺, and Fe³⁺ that are essential in the living body for various biological reactions. It can also be noted that the sensitivity of metal ions was studied under an optimized state to estimate the change in fluorescence intensity of CDs with metal ions at different concentrations.

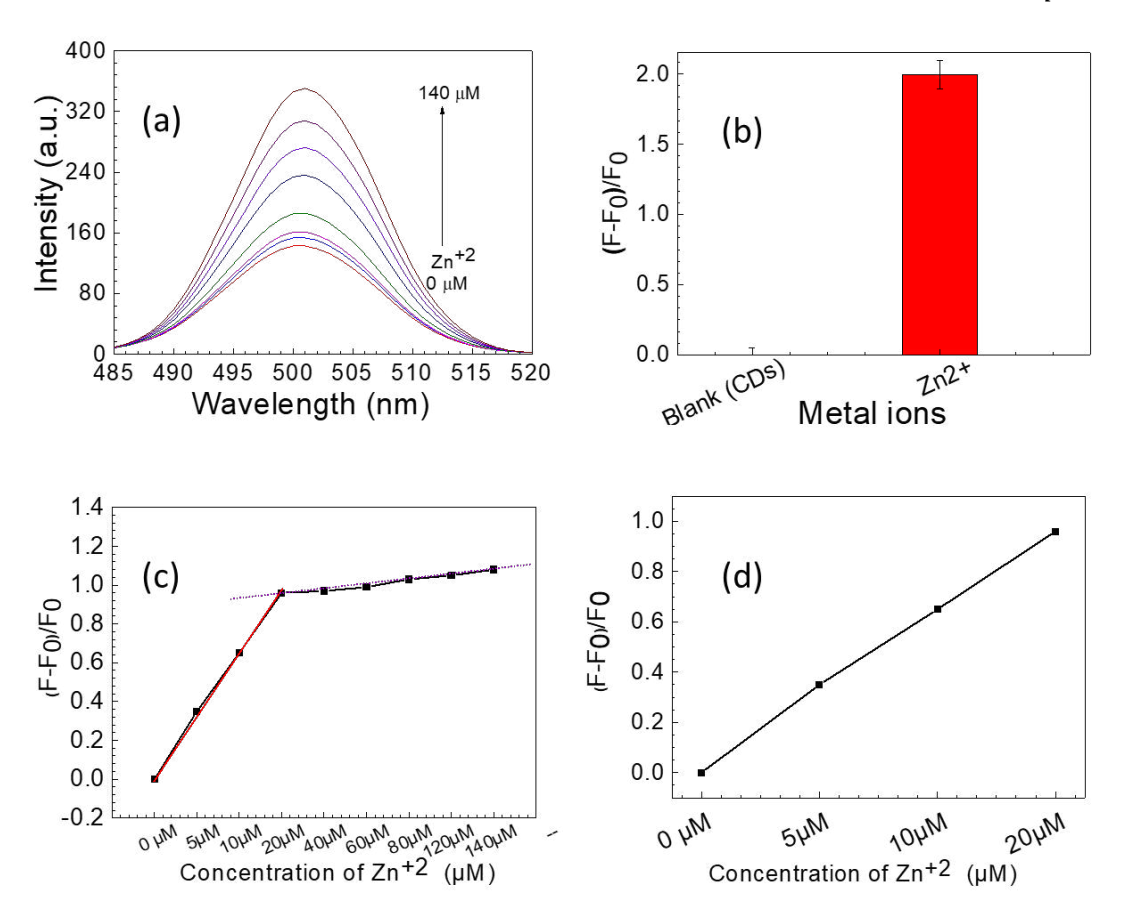


Figure 3.2.7.(a) Fluorescence spectra of carbon dots of (100 μg/mL) with different concentrations of Zn²⁺ (0-140 μM), (b) The enhanced in fluorescence intensity ratios (F-F₀)/F₀ of the CDs solution in the presence of metal ions Zn²⁺ and the CDs (as Blank).Fig.(c) Shows the dependence of fluorescence intensity on the concentrations of Zn⁺² (0-140 μM) and two steps linear relation of (F-F₀)/F₀ and Zn²⁺ concentration and Fig. (d) Shows a clear linear relationship between the fluorescence intensity ratio (F-F₀)/F₀ vs. concentrations of Zn⁺² (0-20 μM) and relatively an inclined linear response in between 20 to 140 μM.

Further, we have extended our study to check the detection ability of Zn^{+2} by CDs, since it is an essential metallic ion that is part of various biological processes in the body. It is evident that our CDs show an enhancement in fluorescence emission as the Zn^{+2} was added to the CDs solution (Fig.3.2.7a). The fluorescence intensity increases with an increase in the concentration of Zn^{+2} ions. This fluorescence enhancement occurred due to the higher affinity of the amine groups of CDs to the Zn^{2+} as it is shown in Fig.3.2.7 (b). From Fig.3.2.7 (c) it is obvious that the

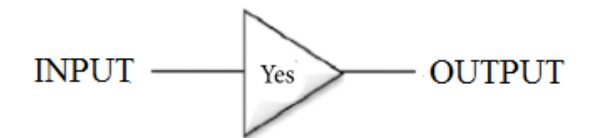
fluorescence emission of CDs in presence of Zn^{2+} with varying concentrations such as from top to bottom: 0, 10, 20, 40, 60, 80, 120, and 140 μ M revealed a two-steps linear enhancement; step-1 observed in 0-20 μ M and step-2 observed in between 20 to 140 μ M. The enhancement in the emission intensity attributes that the Zn^{2+} exhibit a stronger electrostatic interaction with the surface of CDs. It can be noted that Zn^{2+} was incubated with CDs for 15 min for all the concentration of Zn^{2+} ions and the increase in the fluorescence intensity denotes that Zn^{2+} exhibit a strong coordination affinity with CDs due to the presence of -NH₂ groups. Thus, the Zn^{2+} ions can be successfully analyzed with the fluorescence intensity of CDs. Further, from Fig 3.2.7 (c), it can be concluded that the linear relationship for Zn^{2+} ions in a range of 0 to 20 μ m (Fig.3.2.7 (c)) could be useful in designing biological sensors.In conclusion, our CDs are a better sensing platform for the biologically important metal ions, since the achieved detection limit using our CDs is excellent compared to the reported results. 35,344

3.2.2.6 Biological relevant metal ion sensing activity

The fluorescent property of the nano materials is important for sensing and potential for constituting molecular logic gate.³⁴¹ Further, designing logic gates and developing electronic circuits in nano regimes based on multi-target sensing is important in molecular computation, chemical detection, and fluorescent imaging.³⁴² Multi-target sensing activity of the CDs to metal ions can be correlated with a logic gate as it is shown in Fig.3.2.8.Using the synthesized CDs, the fluorescence intensity was kept fixed at 500 nm. The chemical detection signal activity of CDs has been realized in the logic gate with the basic types as YES or NOT. Here, the output signal is assumed as 'ON' state with a Boolean arithmetic value of '1' with the original fluorescent intensity. Whereas, the "OFF" state assumed with Boolean -arithmetic value of '0' for the low signal or no signal. Further, it can be noted that the main of the molecular logic gate is the signal output that was produced by molecular physical or chemical interactions between CDs and metallic ions. Therefore, the physicochemical and biological changes that occurred by interaction

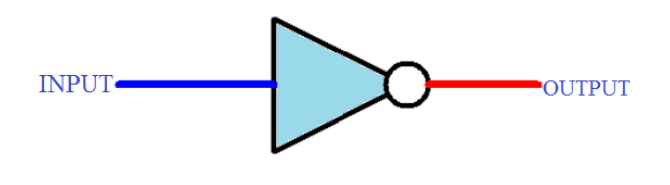
of CDs and metallic ions are their inputs for molecular logic gates. On the basis of the electronic changes of CDs as output, we have designed individual elementary logic operations. Herein, our CDs were used as a probe and Fe⁺³ and Zn⁺² as chemical inputs. Therefore, '1' and '0' term the presence and absence of signals, respectively and deliver the inputs and outputs, respectively to the logic gates. The CDs interact with the metal ion Fe³⁺ ions and form a simple biochemical circuit that is represented as a YES gate and represented a single input signal as shown in Fig.3.2.8a. The NOT gate 'inverts' the input signal and hence can be termed as an inverter gate (Fig.3.2.8b) for the Zn²⁺.CDs have a specific fluorescent intensity and on the addition of Zn²⁺, enhancement of fluorescent emission occurred as considered as response output (Fig.3.2.8b). These gates can be operational and insignificantly can be used in the intracellular state of a complex contact of diverse forms of neurological processes occurring in the living cells.³⁴³ Further, this process can be useful to describe the small regulatory circuits to repair the happened disorder.³⁴⁴ Likewise, this fluorescent-based logic gate concept to sense the oxidized or reduced form of the neurotransmitter can be used.³⁴⁵

Thus, in a two-input logic operation system, our CDs operate as a gate for the two chemical inputs such as Fe^{3+} and Zn^{2+} (see Fig.3.2.8 (a)-(b)) although the signal outputs are different. For Fe^{3+} , the output signal diminished (quenching in fluorescence) with a continuous increase in the concentration, whereas reversed phenomenon (enhancement of fluorescence) is observed with an increase in the Zn^{2+} concentration. Thus, difference in the emission of CDs with the addition of ions was considered as the output signal for analyzing 'ON' and 'OFF' states in the system. Ion inputs with varying concentrations resulted in four possible input string combinations such as $\underline{0}$, $\underline{0}$; $\underline{1}$, $\underline{0}$; and $\underline{0}$, $\underline{1}$; $\underline{1}$, $\underline{1}$. It can be noted that the metal ion such as Fe^{+3} used as input in absence of the Zn^{+2} as the 'YES' gate and vice versa process has been followed for our study as the 'NOT' gate.



Input	Output
0	0
1	1

Figure 3.2.8.a: Scheme of a simple 'YES' logic gate based on optical responses received at 500 nm considering as a device with input (Fe³⁺) and corresponding truth table for the schematic logic presentation.



Input	Output
0	1(0)
1	0(1)

Figure 3.2.8.b: Scheme of a simple 'NOT' logic gate based on optical responses received at 500 nm considering as a device with input Zn²⁺ ions and corresponding truth table, for the schematic logic presentation.

3.2.2.7 Drug loading and release study:

As discussed in the experimental section, 1000 µg of CDs were taken in free DOX (water-based solution with 1:1 ratio, w/w) and then incubated for 24 h in dark with 50 RPM stirring. Then the DOX-loaded CDs were separated through high-speed centrifugation and then dried in a vacuum and stored at 4°C.With the supernatant, we analyzed the loading efficiency of DOX and calculated it to be 527 ng per 1 µg of CDs in 24 h of incubation, which is quite a high loading. In this work, CDs were synthesized from a naturally occurring carbon source (a waste product) and the process of preparation is easy and cost-effective.

The release of DOX from CDs-DOX is important to decide the doses for the treatment of cancer cells (MCF-7). A set of experiments were conducted to check the amount of release of DOX

from the CDs-DOX formulation as it is explained in the experimental section. The release amount was calculated with a certain time interval in PBS, (pH=7. 2) at physiological temperature (37 °C) and found a sustained release up to 12 h. Further, it is calculated that the extent of release is time-dependent (see Fig. 3. 2. 9). As an example, let's say for 1, 2, 5, 10, and 12 h, the extent of DOX released (out of the loaded amount of DOX) from CDs-DOX calculated to be 54. 86±6. 32 ng, 141. 39±14. 22 ng, 254. 86±14. 49 ng, 322. 31±11. 85 ng, and 333.33 ±11. 33 ng, respectively. However, obtained release behaviour is very important for the treatment for a longer time, since frequent doges are not required to apply to the patients to achieve effective treatment efficiency.

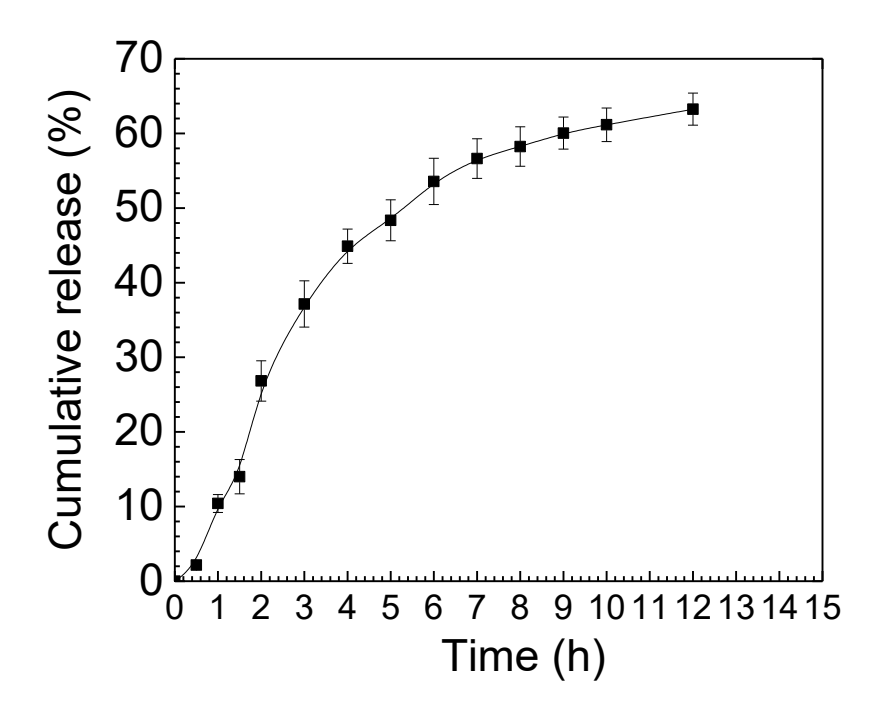


Fig.3.2.9 Cumulative DOX released from the CDs-DOX formulation. A released study was performed in PBS (pH=7. 2) at 37°C.

3.2.2.8 Biocompatibility studies of CDs

To study the toxicity assessment of synthesized CDs, we have conducted *in vitro* cytotoxicity of the CDs and the results are shown in Fig. 3.2.10a and in Fig. 3.2.10b for CDs with and without loading with DOX, respectively. Cell viability study was conducted through a standard MTT

assay with different concentrations of the samples. We chose the incubation time of 24 h to check the cell viability of CD concentrations using different concentrations such as 0, 15. 62, 31. 25, 62. 5, 125, 250, 500, and 1000 µg mL⁻¹ on normal splenocyte cells. As shown, CDs exhibited viability of over 90 ± 3 . 5 % up to a concentration of $500 \mu g \text{ mL}^{-1}$. Above this concentration, such as for 1000 μ g mL⁻¹, the cell viability was found to be less than 83. 0 ± 10 %. Thus, no significant amount of cytotoxicity was observed as compared to the pure CDs (Fig. 11a). Then to check the therapeutic efficiency of CDs, it was loaded with DOX (a chemotherapeutic drug). Then the formulation (CDs-DOX) was tested against MCF-7, which is an adenocarcinoma breast cancer cell, which has estrogen (ER), progesterone (PR), and glucocorticoid receptors. The toxicity against MCF-7 cells after 24 h incubation with free DOX of different concentrations such as 0. 15,0. 3,0.625, 1.25,2.5, 5.0, and 10. 0 µg mL⁻¹. DOX-loaded CDs (CDs-DOX) were taken with the equivalent weight of DOX loaded in CDs-DOX and the experiments were performed at 37°C and pH 6. 5. Results showed that the cytotoxicity of DOX encapsulated in CDs (CDs-DOX) was higher than free DOX in direct contact with the cells. For example, with free DOX, with equivalent concentrations of DOX 0. 15,0. 3, 0. 625, 1. 25, 2. 5, 5. 0, and 10. 0 µg. mL⁻¹ the toxicity found to be 0. 52 ± 5.54 %, 6. 75 ± 4.49 %, 10. 76 ± 4.52 %, 18. 90 ± 4.27 %, 32. 63 ± 3.54 %, 38.24± 3.492 % and 49.58± 2.92 %, respectively. Whereas, for CDs-DOX with equivalent concentrations of DOX e. g. 0. 15, 0.3, 0.625, 1.25, 2.5, 5.0, and 10.0 µg/mL the toxicity was found to be 11. $96 \pm 5.54 \%$, $37.62 \pm 3.49 \%$, $50.30 \pm 4.92 \%$, $56.11 \pm 4.73 \%$, $67.00 \pm 2.92 \%$, $65.12 \pm 4.73 \%$ 3.27 %, and 71. 40± 4.27 %, respectively. Thus, the lower values of loaded DOX in CDs revealed that CDs significantly promoted the efficacy of DOX in killing the MCF-7 cells concerning the free DOX. Further, the IC50 for the free DOX has been calculated to be 9. 85±0. 15 µg mL⁻¹, whereas IC50 of DOX loaded in CDs is found to be 0. 615±0. 15 µg mL⁻¹, which is almost 16 times lower in value. This lower IC50 of DOX of CDs-DOX formulation suggests that MCF-7 can be killed in lower doses of DOX as well a lower dose can reduce the associated side effects. Therefore, it suggests that the CDs synthesized in this work can be a potential delivery system for anticancer drugs (Fig 3.2.10b), which further can be used for the loading and delivery of other bio molecules/medicines too.

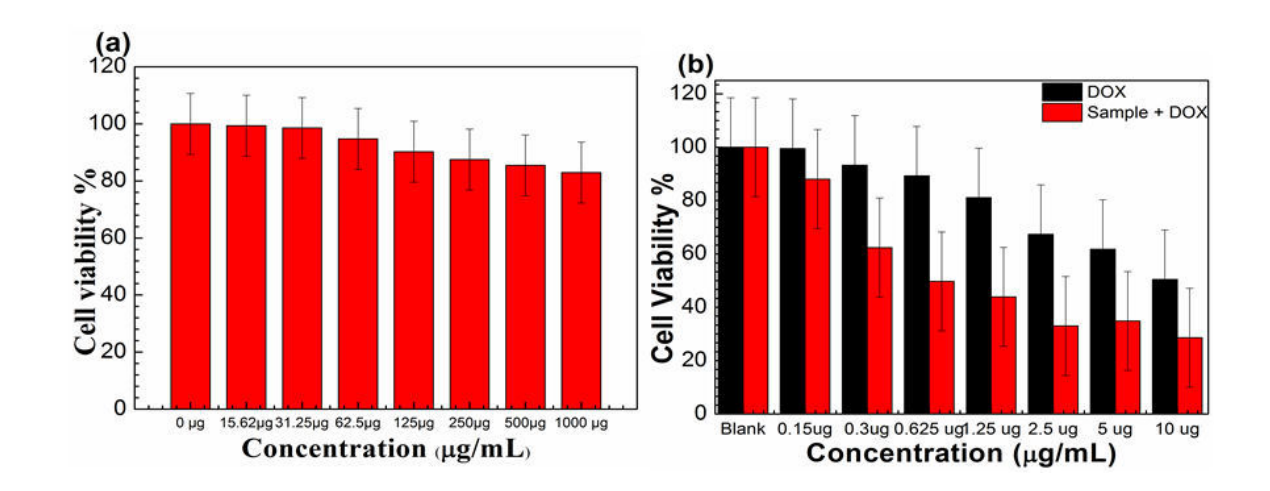


Figure 3.2.10: Cell viability values (%) estimated by MTT assay for different concentrations of CDs. (a) Cell viability for CDs alone and (b) Cell viability of the DOX loaded CDs (CDs-DOX) and DOX alone. DOX loaded in CDs exhibited more toxicity towards the breast cancer cells MCF-7.

3.2.2.9 The synergic effect of CDs with DOX decreases the mitochondrial membrane potential (MMP) ($\Delta \psi m$)

The alteration in mitochondria membrane potential and mitochondrial damage is largely linked to the underlying mechanism of apoptosis. It is performed that apoptosis is induced in the MCF-7 after treatment with CDs and the different loads of DOX with CDs. The loss of MMP during the induction of apoptosis has been implied. Mitochondria play a crucial role in programmed cell death and can be visualized by the loss of MMP. Flow cytometry is used to measure the change in MMP and linked with the apoptosis of cells. To examine mitochondrial functions, fluorescent potentio metric probes are available to measure the change in MMP. The fluctuation in mitochondrial depolarization can vary according to the stimulus, cell types, and the approach of observation. The decline in $\Delta \Psi m$ indicates a decrease in fluorescence owing to the diminished capacity of mitochondria to hold the probe. Rhodamine 123 (Rh123) is well established staining

dye to measure the change in mitochondrial membrane potential. Rh123 enters mitochondria and is retained in the mitochondria. It leaches out from mitochondria whenever the mitochondria lose their potential and here after the detectable reduction of fluorescence is observed which is directly interconnected to the change in mitochondrial potential.

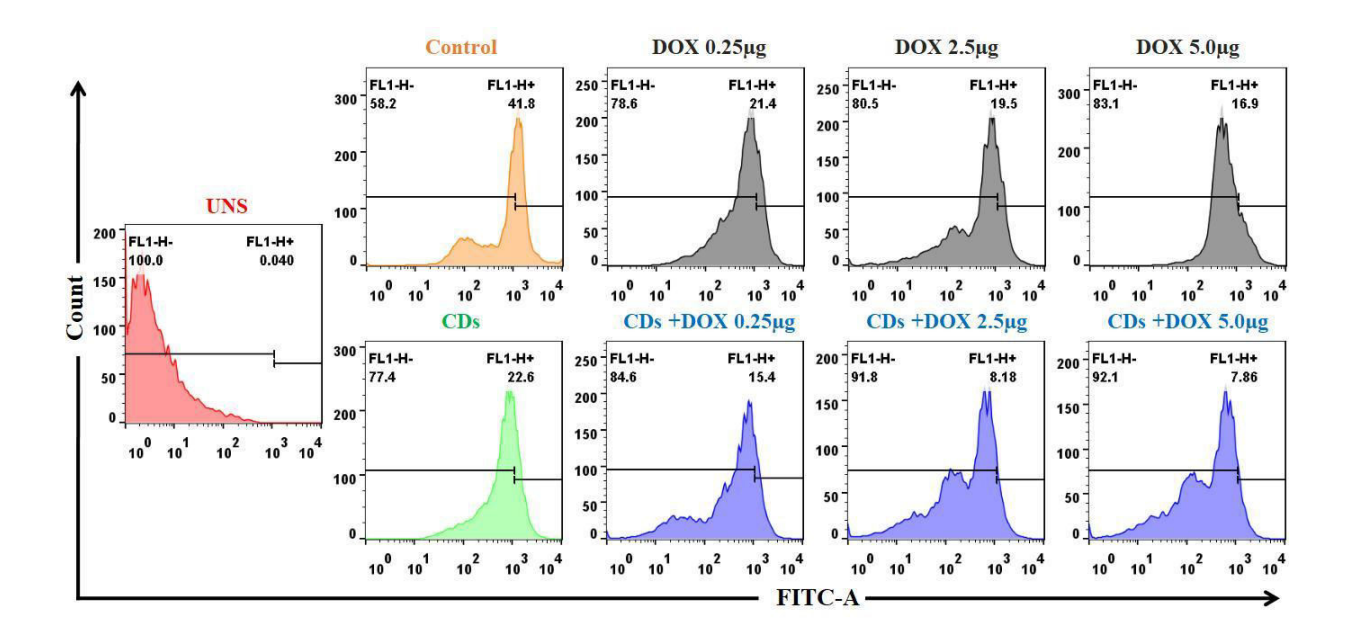


Figure: 3.2.11. Flow cytometry study to calculate the diminution of mitochondrial membrane potential by using fluorescent potentiometric probes Rh123. MCF-7 breast cancer cells were treated with different concentrations of Dox (0. 25, 2. 5, and 5μg. mL⁻¹) and different complex formulations of CDs+DOX. After 24 h of treatment, cells were stained with Rh 123 and analyzed through a flow cytometer. Figures show the percentage of mitochondrial depolarization in the MCF-7 cell line attained for different carbon dots. (Here KS-1 is the CDs).

Initially, we observed a change in the MMP of CDs as compared to the control sample (Fig.3.2. 11). Further, we found the increased doses of DOX (0.25, 2.5, and 5µg. mL⁻¹) enhanced the change in MMP in the MCF-7 breast cancer line. The interesting results observed after loading DOX with CDs significantly decreased the MMP. The synergic effect of CDs with DOX was observed in the manner of an altered MMP in the MCF-7 breast cancer cell line. All the data were statistically evaluated by comparing them with the control sample.

3.2.2.10 The synergic effect of CDs with DOX enhances the apoptotic cell death of MCF-7 breast cancer cells:

The apoptotic assay is one of the most commonly used assays to detect and quantify the cellular events associated with programmed cell death. To determine the synergic effect of CDs with DOX on the MCF-7 cell line the apoptotic cell death was quantified in different quadrants (Q1, Q2, Q3, and Q4) (Fig. 3.2.12). We acquired 10,000 cells per sample to analyze the cell apoptotic cell death. Cells were stained with Annexin-V and PI to detect apoptotic cell death. The quadrants were set up according to the control cell result. Further, we noticed increased apoptotic cell death as per the increasing concentration of DOX. Likewise, the combined effect of CDs with DOX enhanced additional apoptotic cell death of MCF-7 breast cancer cells.

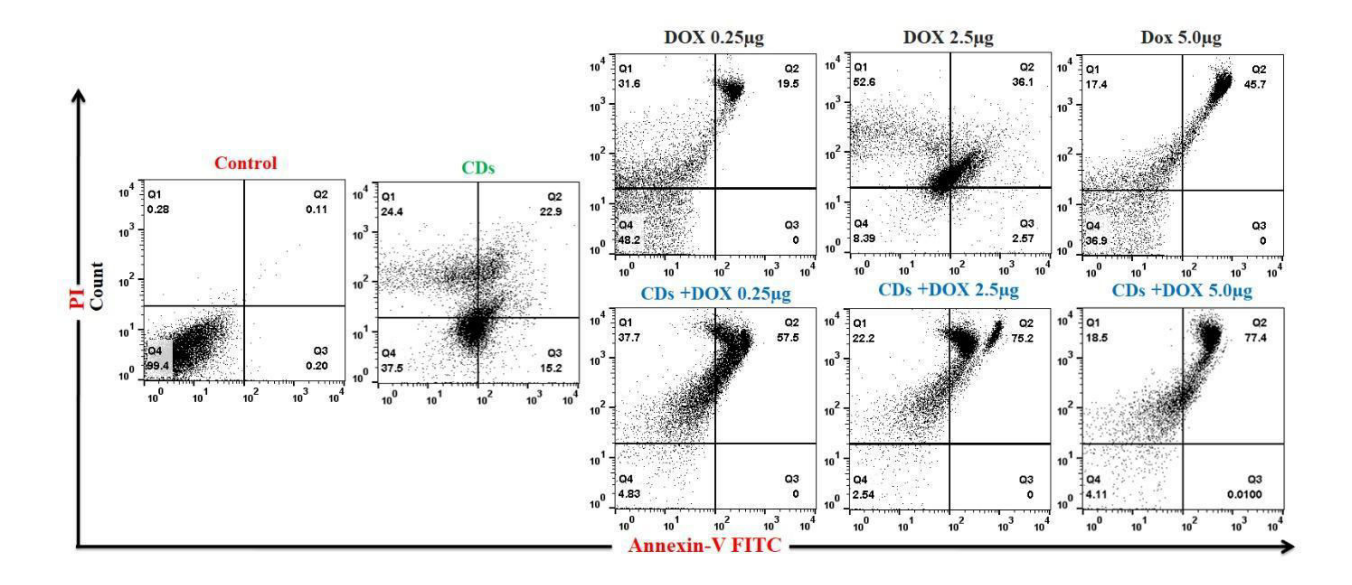


Figure 3.2.12. MCF-7 cells were treated with CDs. After 24hr treatments with different complex formulations of CDs+DOX, cells were stained with PI and Annexin-V FITC antibodies to explore the apoptotic and necrotic cell death effect. Flow cytometry was used to acquire a total of 10,000 cells and quadrants were set according to control. Quadrants represent Q1, necrotic cells; Q2, late apoptotic cells; Q3, early apoptotic cells; Q4, healthy cells for MCF-7 human breast cancer cells after CDs (KS-1) treatment.

3.2.2.11 Cell Imaging and study the cell morphology:

The imaging of cells is one of the essential factors to analyse cell morphology and easy to identify the state of cells (Fig. 3.2.13). The representative photomicrographs of MCF-7 breast cancer cells were displayed as typical 2D morphology with different dose conditions of CDs-DOX. The images were taken with the help of light microscopy. In the image of MCF-7 cells in the control (without treatment) condition, cells looked similar to polygonal-shaped sized. While after the treatment with CDs-DOX (0.5µg), the cell size of MCF-7 cells was reduced, and the number of live cells was also reduced. As we noticed that the auto fluorescence of the live cells was found to be reduced with the higher dose of DOX. We also observed a lower number of cells alive as the dose of CDs-DOX increased. The morphology of MCF-7 cells was observed to be round with a higher concentration of CDs-DOX.

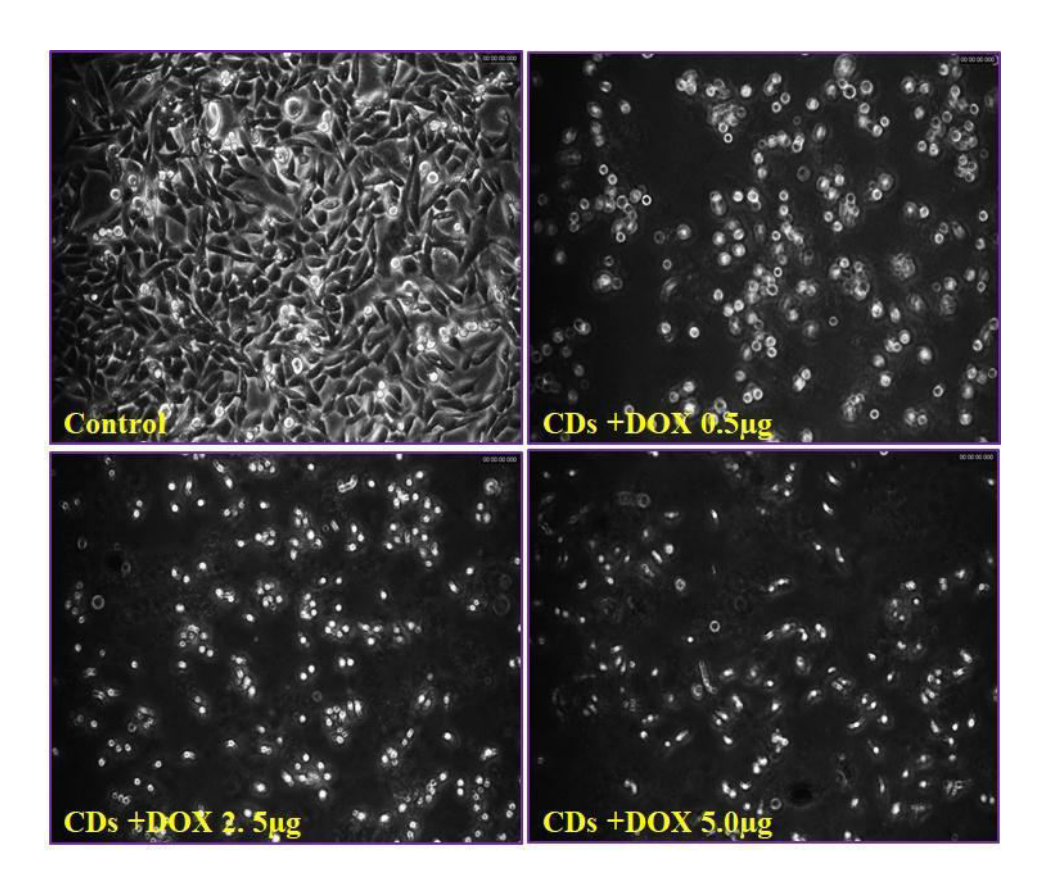


Figure **3.2.13.** The representative photomicrographs of MCF-7 cells were shown as typical 2D morphology. The upper left: MCF-7 cells without treatment, upper right KS-1 (CDs) +DOX 0.

5ug, lower left KS-1(CDs)+DOX 2.5 μ g, and lower right KS-1(CDs)+DOX 5 μ g (10× magnification). In normal conditions, the most established cell masses with a polygonal morphology. Images were taken by light microscopy and shown with fluorescence at phase contrast.

3.2.3. Summary

In this work, CDs were synthesized through a green synthesis method. The prepared CDs are spherical and a distinct green fluorescent emission was obtained from the CDs. These CDs exhibited an efficient metal ion detection ability, predominantly Fe³⁺, and Zn²⁺. Further, a comprehensive study was made on the advancement of CDs-based logic gates based on the metal ion sensing properties. The sensing properties of metallic ions have been explained mechanistically by two types of possible logic operations based on the nature of CDs. Further, the results can help researchers to develop more biocompatible and cost-effective CD-based chemo sensors with logic gate applications and can provide a huge impact in the clinical area. Finally, our CDs can be loaded with anticancer drugs and are useful for the treatment of breast cancer with low doses of drugs.

Chapter: 3

RESULTS AND DISCUSSION:PART –III

High temperature synthesized carbon dots and its absorption of heavy metal ions.

3.3.1. Introduction & Motivation

In the present days, heavy metal ion pollution has become a serious issue in rapidly developing economy causing around the world.³⁴⁶ The environment and ecological balance are diversely threatened by the heavy metal ions and non-biodegradability²⁸⁷ in nature. Henceforth, the identification of ions of heavy metals becomes a focus for researchers.³⁴⁷ The basic definition of heavy metal is it has an atomic weight greater than 20 and a density³⁴⁸ greater than 5.0g/cm³. It is usually believed that the heavy metal ions present naturally do not threaten the human body and ecology.³⁴⁹ However, day after day revolution in the industry the standard limit has been increased in rivers, lakes, and soils. Once heavy metal accumulated in water sources or animals and plants, it entered the food chain and which leads to its presence inside the human body.²²⁵As soon as heavy metal ions entered the body it interacts with enzymes and protein but it never metabolized by the human body³⁵⁰,so they lose biological activity. In continuation with this heavy metal ions can accumulate inside the body acute kidney failure (AKD)³⁵¹, memory loss²⁴³, breathing difficulties³⁵², and possibly even cancer.²⁵⁴ It has been stipulated by The United States Environmental Protection Agency (USEPA) thehighest concentration in drinking water for heavymetals, such as 1.3 ppm Cu, 2 ppb Hg, 15 ppb Pb, 10 ppb As, 5 ppb Cd and 100 ppb Cr,

respectively.²⁵⁵ Keeping this in mind the detection and removal of heavy metal ions have been studied by scientists.

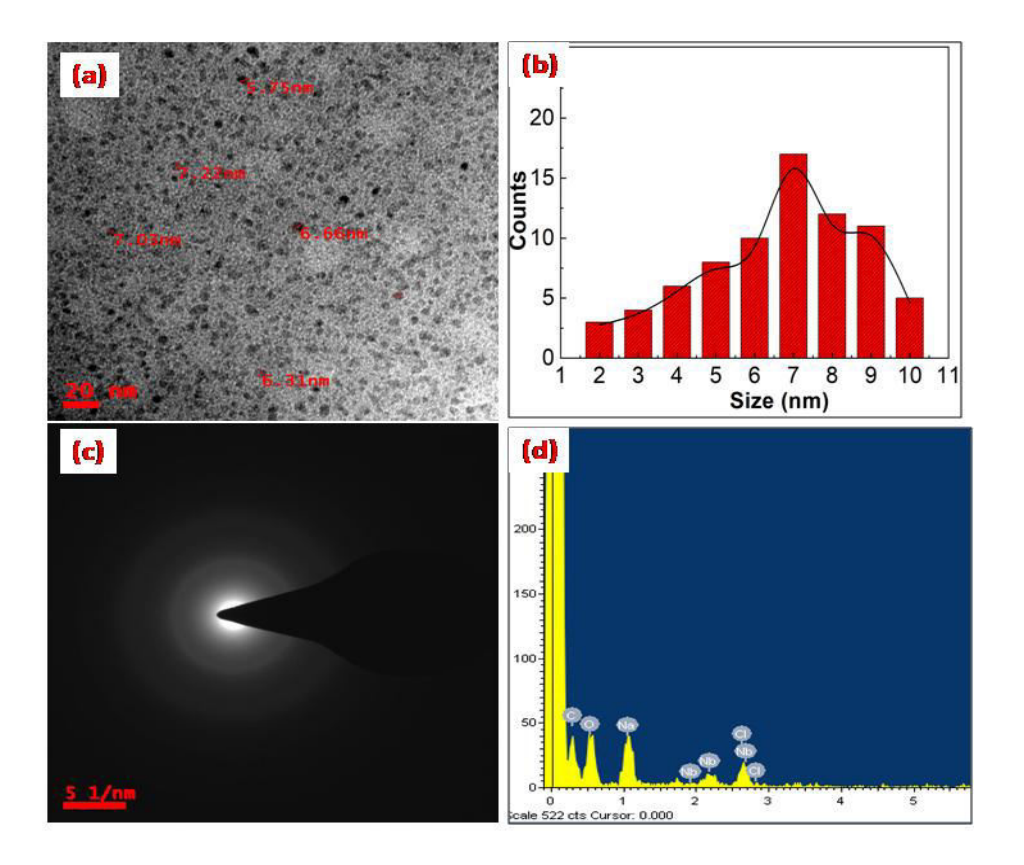
In the last few years, the identification and detection of the process of fluorescence quenching is the process where quantum yield decrease in the form of fluorescence induced by a variety of molecular interactions with a quencher molecule. There are various methods that we can use for the detection of heavy metal ions among them ICP emission spectroscopy, fluorescence spectroscopy, UV-Visible spectroscopy, atomic absorption, etc.²⁵⁶ Among them, few are previously mentioned, and fluorescence spectroscopy is one of the ways a more appealing techniques due to its great sensitivity, facile operation, and wide range availability. One of the problems associated with the detection of heavy metal ions that flour sense is the ability among some metal ions to reduce emissions resulting in intense quenching in flour sense. We all know that quenching refers to the process where the fluorescence intensity decreases in a given substance. The process involved in this process is excited-state reactions.

3.3.2. Results and discussions

3.3.2.1 Morphology Structural characterization

CDs were created in the manner specified in the experimental section. HRTEM was used to describe the shape and size of the as-synthesized CDs, which were then shown at various magnifications (Fig.3.3.1a). The TEM pictures clearly show that the CDs are synthesized monodispersed spherical, with a mean size of 7 nm (Fig.3.3.1.b). The crystalline character of the CDs is likewise corroborated by the SAED spectra (Fig. 3.3.1c). The elemental composition of CDs was determined using EDAX spectra obtained from a TEM experiment (Fig 3.3.1d), and the existence of elemental oxygen and carbon was confirmed for KN-1 and KN-2 CDs is shown in the (Fig.3.3.1e) and particle size distribution in shown Fig.3.3.1f. To know crystalline nature the SAED pattern of KN-2 has been shown (Fig.3.3.1g). From EDAX spectra obtained from TEM

elemental analysis has been shown in Fig. 3.3.1 h. To assess the morphology TEM images of the carbon dots shown in Figure 3.3.1 for KN-1(a-d) and KN-2 (e-h), and shows them spherical, approximately 6-7 nm in diameter. From the TEM data, it is clear that the Carbon dots are eventually self-assembled on the copper grid with a long-range order.



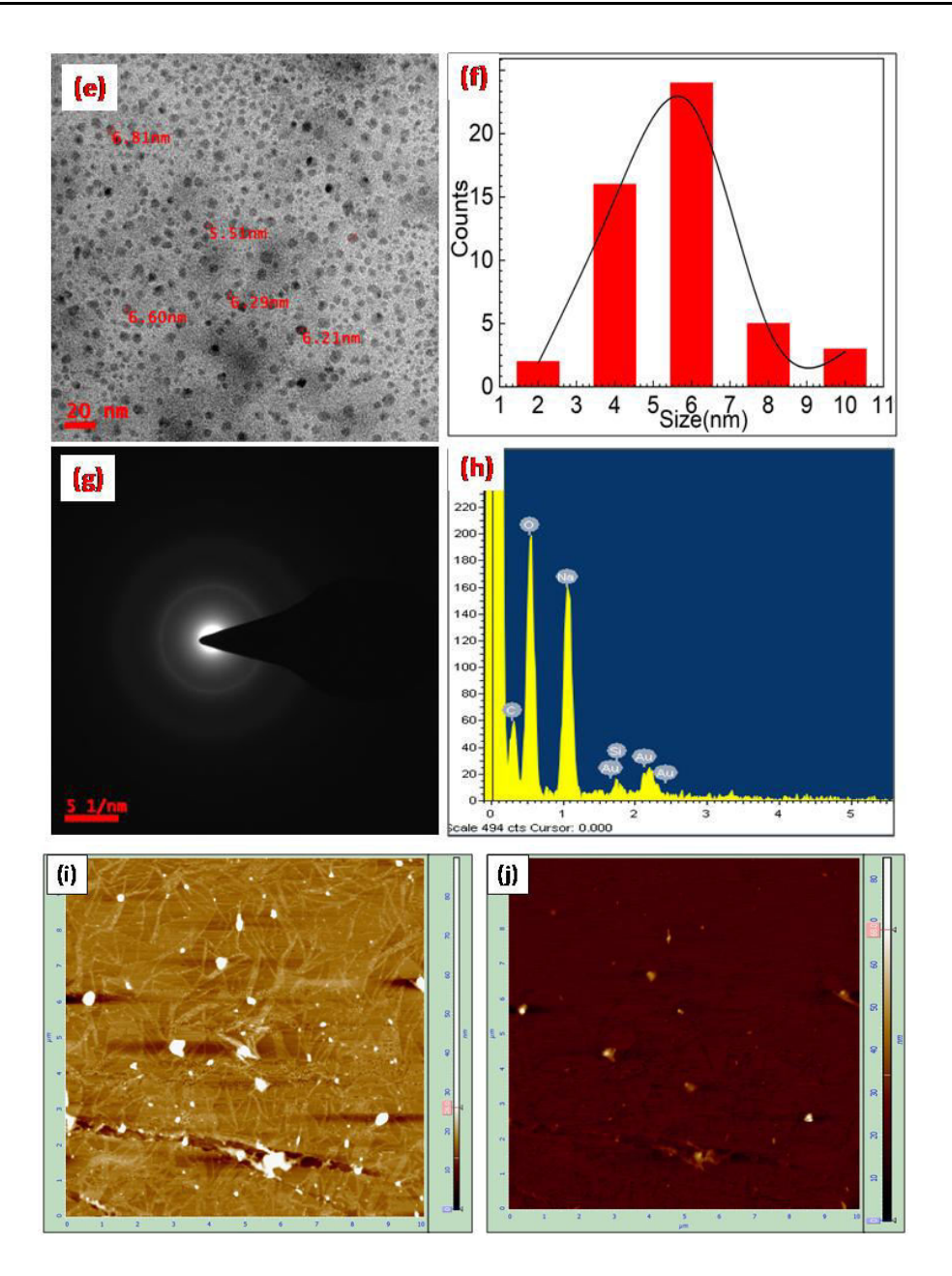


Figure 3.3.1 Particle size and morphology studied through the TEM for the samples: (a) typical image of KN-1, (b) Particle size distribution of KN-1,(c) SAED generated by TEM for KN-1 (d) EDAX of KN-1 (e) TEM images of KN-2, (f) Particle size distribution of KN-2, (g) corresponding SAED patterns of the specimens processedKN-2, (h) EDAX elemental analysis of synthesized CDs, (i-j) AFM images of synthesized CDs for KN-1 and KN-2.

3.3.2.2 Chemical Functionality

The synthesized carbon dots composition of the surface functional groups was determined with FT-IR spectroscopy. Figure 3.3.2(a-b) shows the FT-IR absorption spectra of CDs evaporate from an aqueous suspension. It can be seen from Figure 3.3.2(a-b), on the surface of both types of CDs, $cm^{-1}(N-H)$ that there many functional presents 3305 are groups stretch,1729cm⁻¹(C=O)stretch,1434cm⁻¹(H-O) bending,1063cm⁻¹(O-C) stretch,871-837cm⁻¹(C-H) bending for KN-1 and 3021cm⁻¹(C-H), 2933 (C-H) stretching, $2848 \text{ cm}^{-1}(\text{N-H})$ $cm^{-1}(N-O),$ stretching,1422cm⁻¹(O-H) bending,1218cm⁻¹(Ostretching,1557 H)stretching,750cm⁻¹(C-H) bending, 669 cm⁻¹(C=C) bending for KN-2. From the FT-IR analysis of both the samples, it is very clear that the surface composition of the surface of KN-1, and KN-2 are different as obtained from the FT-IR spectra of the samples. . NMR spectroscopic techniques are performed Fig. 3.3.2(c-d). Signals are found at roughly at 1.3 and 1.8-1.95 ppm in the C-dots ¹H NMR spectra, before and after dialysis, perhaps due to the presence of hydrogen (H) from non-cyclic alkenes. Signals ranging from 3.5 to 4.3 ppm observed might be caused by the presence of oxygen-containing groups (alcohols, esters, or carboxylic acids). The most noticeable changes in C-dots in NMR spectra observed between 3.5 and 4.3 ppm, which is caused by the presence of oxygen-containing compounds, and small molecules, according to the NMR finding. Henceforth, NMR can categorize the chemical modifications, which can be occurred during carbonization due to the surface modifiers. Furthermore, CDs' characterization is quite easy using NMR, because of its non-destructive nature. Although these advantages, NMR also considerable demerits such as lower sensitivity, greater time-consumption, and higher costs, as compared to the mass spectrometric methods.

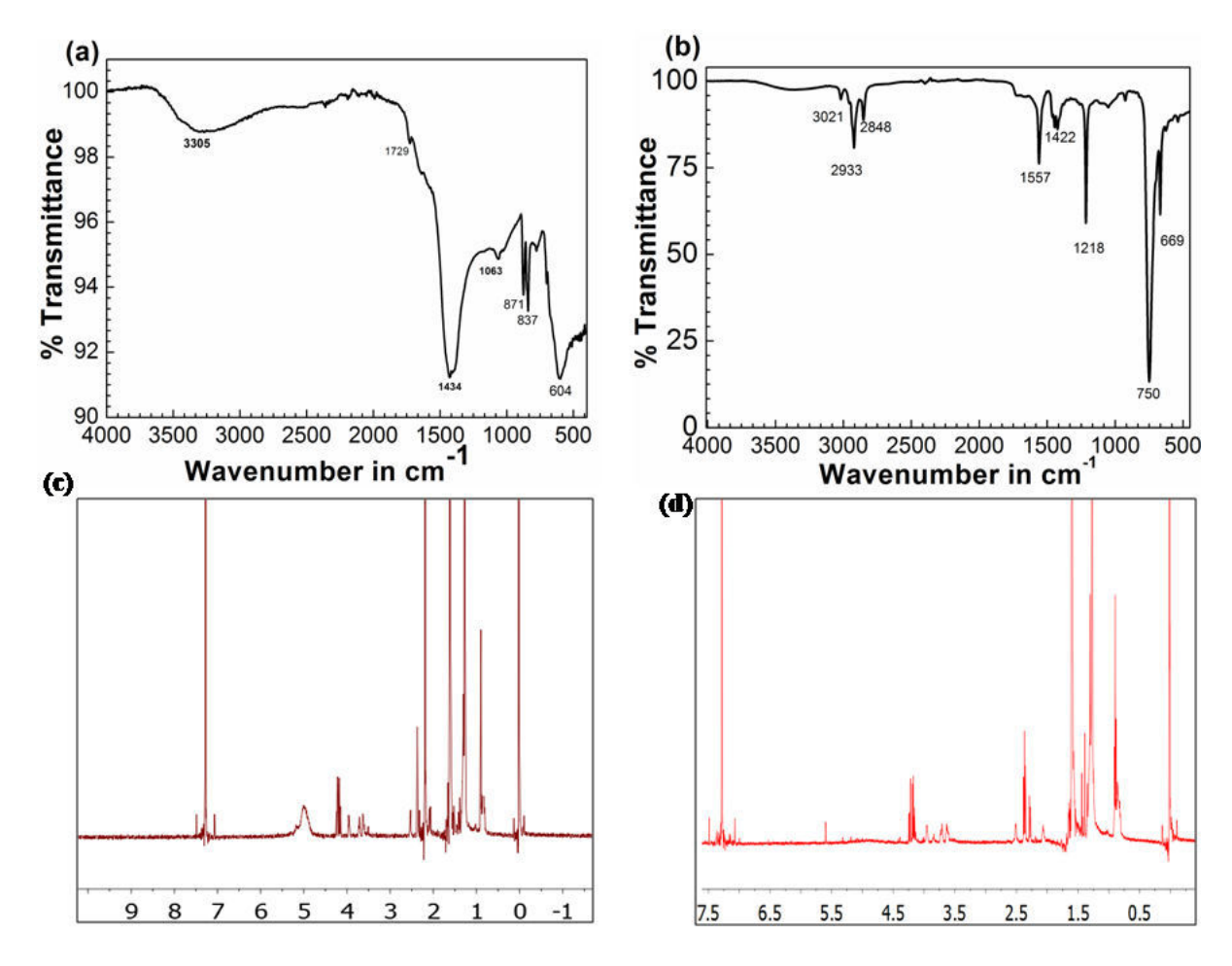


Figure 3.3.2 FT-IR spectrum of the samples: (a) KN-1 and (b) KN-2 and NMR data for (c) KN-1 and (d) KN-2.

3.3.2.3 Thermal stability of Carbon dots

Carbon Dots (CDs) in the most up-to-date years are thermally stable. The thermal stability of CDs has already been discovered to have significant benefits with numerous factors, paving the way for further research and development in the area. In the continuation of TGA data in Fig 3.3.3(a-b),the carbon dot weight loss curve shows mass loss of ~20 %at 40–150 °C, because of moisture depletion in carbon dots. In the temperature interval at 151–620 °C, the mass loss was attributed to the decomposition of organic components in carbon dots. While there was no visible weight loss at temperatures greater than 720°C, the final weight loss that nearly began at about 620 °C might represent the breakdown of remaining carbon for KN-1 and KN-2 showing 20% loss around 40-130 °C followed by 130-390 °C mass loss and 580 °C decompositions of all carbon residuals. Differential scanning calorimetric (DSC) for KN-1 shows exothermic peaks at about

100, 124 °C (Figure 3.3.3c) and for KN-2 at around 73 °C (Figure 3.3.3d). The DSC for KN-1 displays a sharp exothermic peak between 100–130 °C. Furthermore; the differential scanning calorimetric data shows precursor KN-1 has strong exothermic decomposition as compared to KN-2.

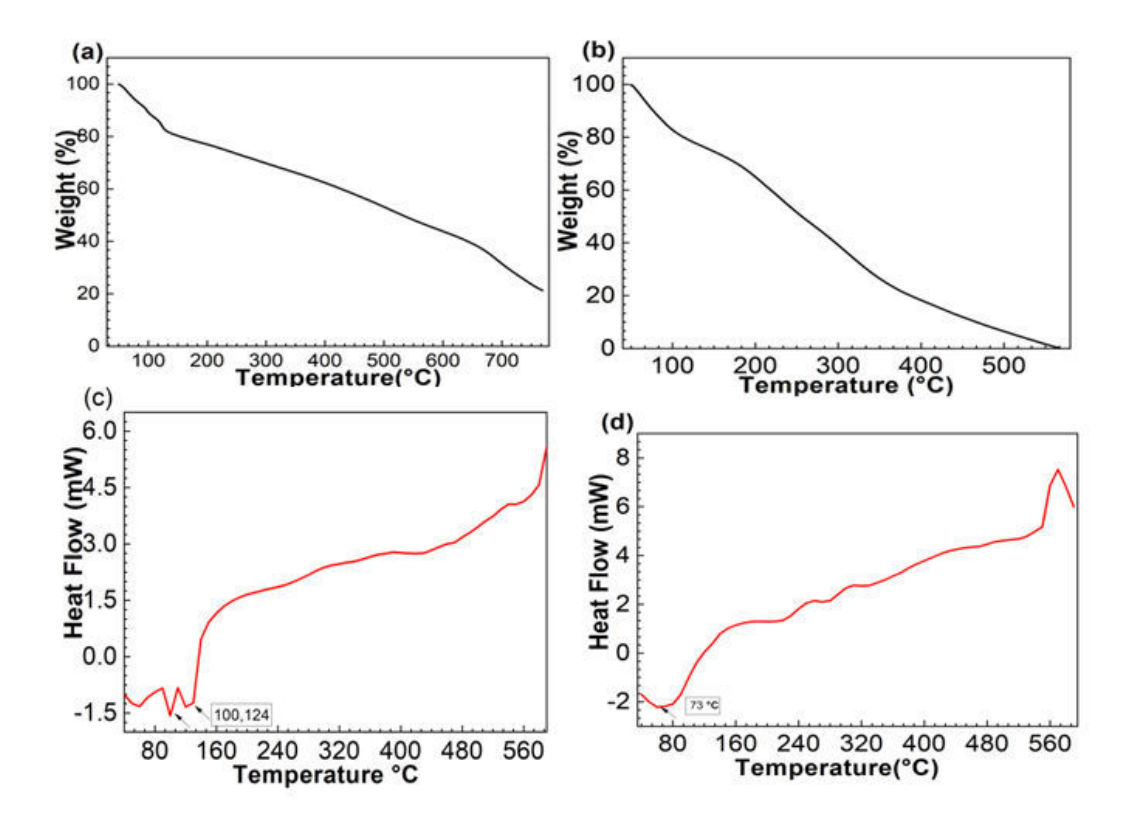


Figure 3.3.3: Thermal stability studied through TGA for the samples: (a) KN-1, (b) KN-2, DSC thermal graph for the samples: (c) KN-1, (d) KN-2.

3.3.2.4 Structural properties

Figure 3.3.4 a-b indicates the powder XRD pattern of carbon dots of KN-1 and KN-2. The XRD pattern shows a mixture of crystalline and amorphous materials. The XRD will show both sharp and wide characteristics, if the material is a combination of both amorphous and crystalline materials. The pointed peaks are caused by the crystalline component as well as the wide or blunt characteristics of the amorphous part which also support the data SAED pattern of the TEM image.

The synthesized CDs' Raman spectrum (Figure 3.3.4c-d) demonstrates two wide ranges of peaks at concerning 1573 and 1333 cm⁻¹ for KN-1 and 1578 and 1335 cm⁻¹ and KN-2, respectively, which might be allocated to G (graphitic, sp³ carbon) and D (defect, sp² carbon) bands accordingly. The existence of another band can be stated by the amorphous characteristic of prepared CDs. We know that the D band derives from the carbon molecule vibrations and with dangling bonds within the termination plane of disordered graphite or glassy carbon, whereas the G band is associated with the graphite E_{2g} mode and the sp²-bonded carbon atoms vibration in a two-dimensional hexagonal lattice³⁵³. Henceforth, we can conclude that during the plasma process, functional groups like C=O, C-O, and O-H are effectively linked to graphitic-structure carbon dots. The presence of hydroxyl and carboxyl groups in CDs results in excellent solubility in water. Whereas, Carbon dot oxidation state affects emission properties.

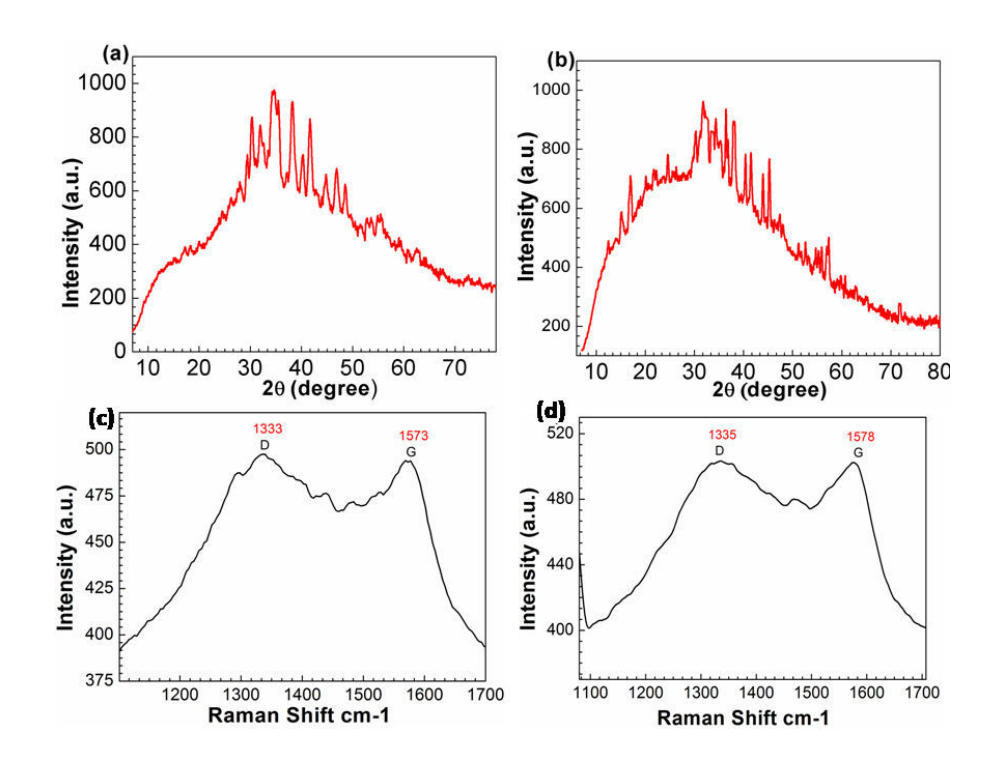


Figure 3.3.4: XRD pattern for the samples: (a) KN-1 and (b) KN-2 Raman spectroscopy (c) KN-1 and (d) KN-2

3.3.2.5 BET (Adsorption-desorption) surface area analysis, pore size analysis

The synthesized isotherms of nitrogen adsorption/desorption of CDs are shown in Figure 33.5 a-b for KN-1 and KN-2, respectively. The degassing process has been done at 150 °C for 4 hr. Thus, the results of KN-1 and KN-2 are compared to discover changes in porosity produced by annealing. The isotherms, as depicted in Fig 6a-b revealed a type IV isotherm with a clear hysteresis. The BET surface area of KN-1 is calculated to be 9.6862 m²/g, whereas 8.7338 m²/g obtained for KN-2.

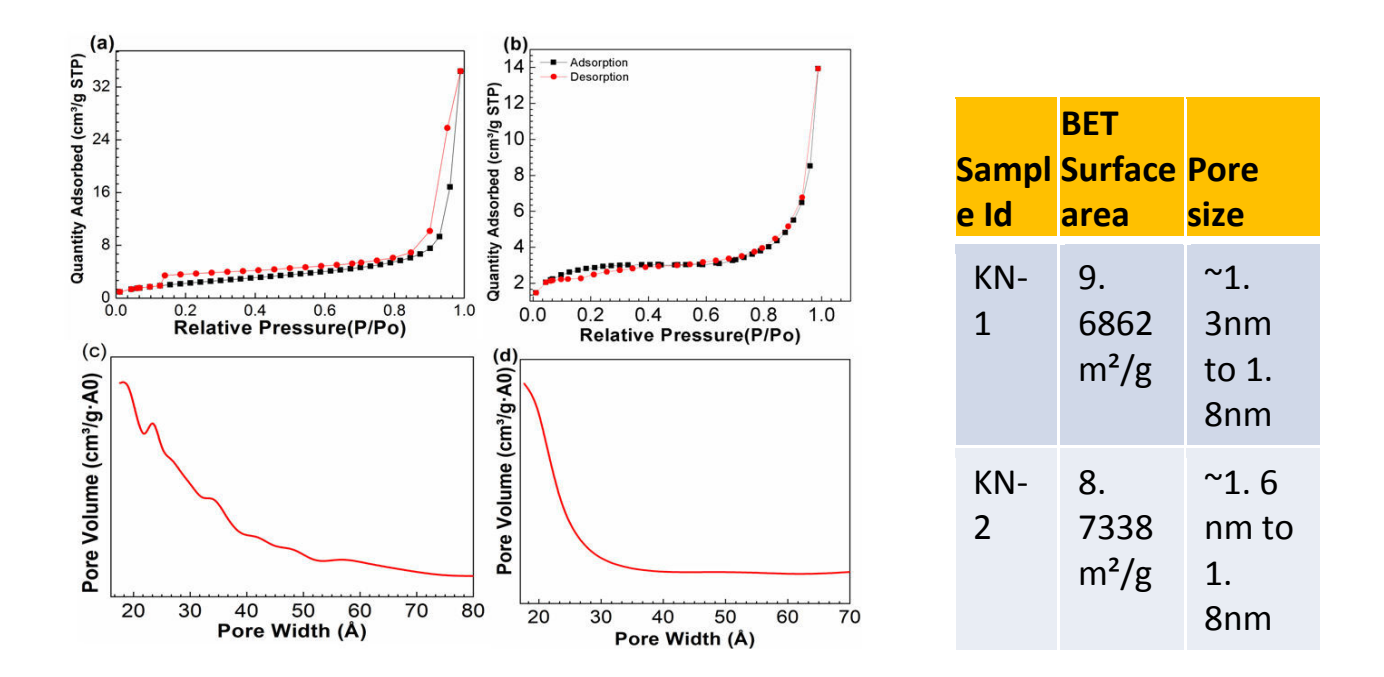


Figure 3.3.5: BET experiments: BJH adsorption-desorption isotherm for the samples: (a) KN-1 and (b) KN-2. Pore size distribution profile for the samples. Pore size calculated from BET for (c) KN-1 and (d) KN-2.

3.3.2.6 Zeta potential and Zeta size

As one of the divisions of the characterization of an aqueous suspension of CDs at the first stage, the value of size and zeta potentials in aqueous suspensions were determined. When we investigated the armed with liquid phase measurements positive detection methods, the photon correlation spectroscopy technique is useful for more of the hydrodynamic element dimension

purpose for CDs' characterization. Although this process, the radius of CDs is able to be analysed via which depends on the diffusion rate of CDs in liquid media. In addition, zeta-potential dimensions can find out the surface charge of CDs, which can be generally engaged for the chemical functionalization and characterization on the surface of CDs.³⁵⁴

The sample zeta potential informed the degree to which the equally charged and neighbouring molecules in dispersion, resulting in adapting the stability of CDs. In addition to this, the zeta potential technique gives information regarding CD's qualities such as double-layer properties with different hydrophilic groups (hydroxyl, carboxyl, and carbonyl). It follows from the obtained results that the KN-2 samples are more prone to aggregation in water as compared to the KN-1, which also be explained by the lesser value of the zeta potential of the suspension.

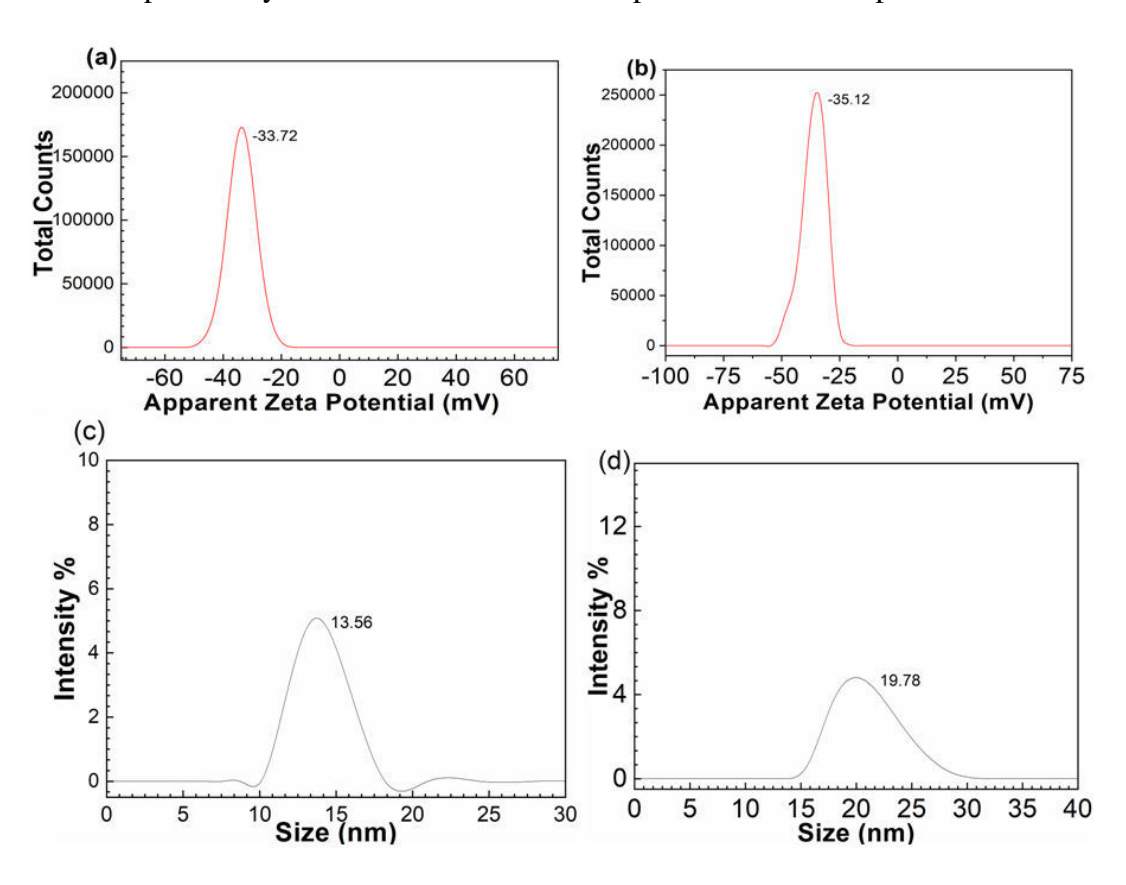


Figure 3.3.6: Zeta potential profile for the samples: (a) KN-1 and (b) KN-2. Particle size obtained from DLS for (c) KN-1 and (d) KN-2.

3.3.2.7 UV-Vis absorption

The ocular image of CDs dispersed into water and absorbance measured in presence of UV light is shown in Fig.3.3.7 (a-b), correspondingly for KN-1 and KN-2. The synthesized CDs suspended in water exhibit UV radiation causing a significant emission (at 273 nm and 268nm). The ultraviolet absorption spectrum of the as-synthesized CDs is revealed in Fig.3.3.7, related to the C=C bonds and the $n-\pi^*$ transition of C=O bonds.

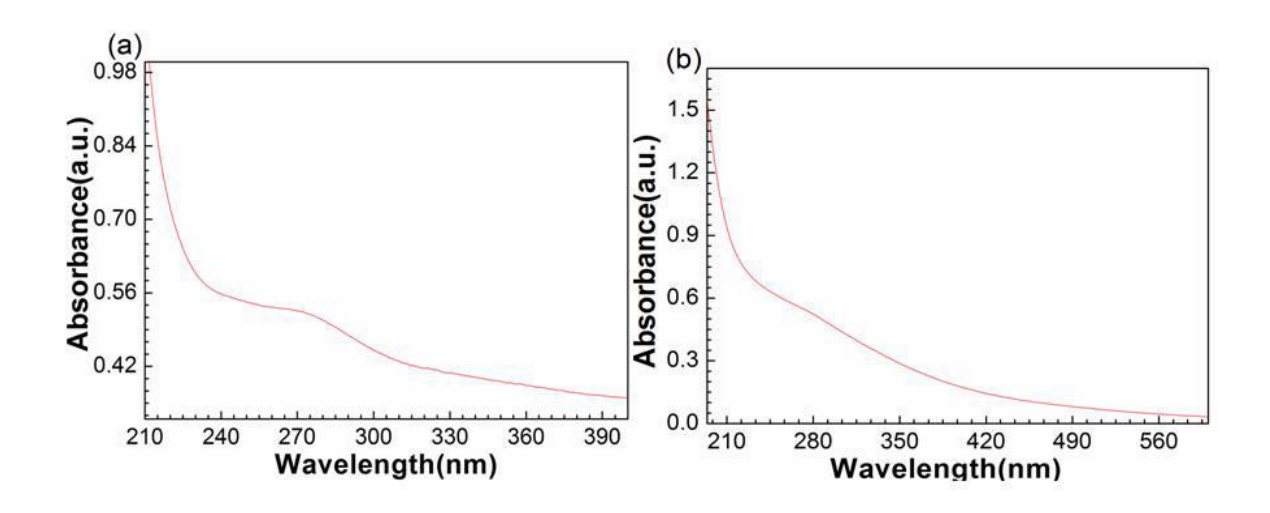


Figure 3.3.7: UV-Vis spectra for the samples (a) KN-1 and (b) KN-2.

3. 3.2.8 Fluorescence spectra of heavy metal quenching of carbon dots

The previously published carbon dots have made footprints for their non-toxic and hydrophilicity characteristic of fluorescence sensing, and have become environment friendly. As a result, the newly designed facile synthetic way with attractive sustainable carbon sources has caused the researchers to focus on Carbon Dots. Considerably, CDS can reduce production costs and make a possible large-scale synthesis. The fluorescence quenching characteristic of the CDs is changed when it reacts with the metal ions in presence of surface functional groups of the CDs. Usually, the suitable plan of a Carbon Dots sensor can optically detect heavy metal analytes (metal ions). The selection of a carbon source is necessary for this and synthesis of the CDs is the primary criteria. In the same way, in optical sensing, the existence of carbon dots with metal ions can

change the dot's optical signal, which causes a turndown or change in the strength of emission spectra or the absorption spectrum. 172

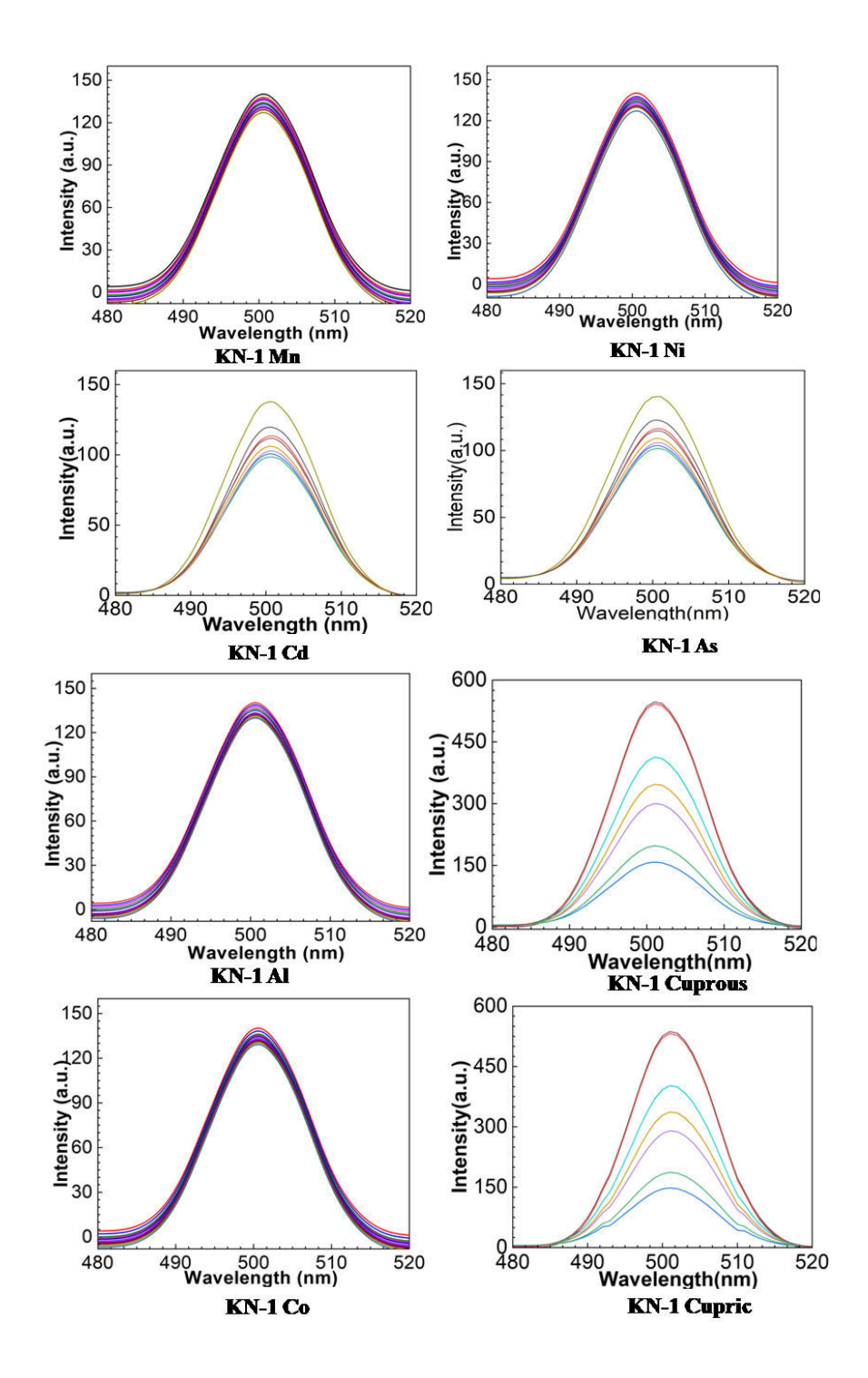


Figure 3.3.8: a) Fluorescence spectra of KN-1 carbon dots of (100 μ g/mL) with different concentrations of different metal ions (Al³⁺,Cd²⁺, Mn²⁺, Ni²⁺, Co⁺², Cu²⁺, Cu⁺, and As⁺³) concentrations (0-140 μ M).

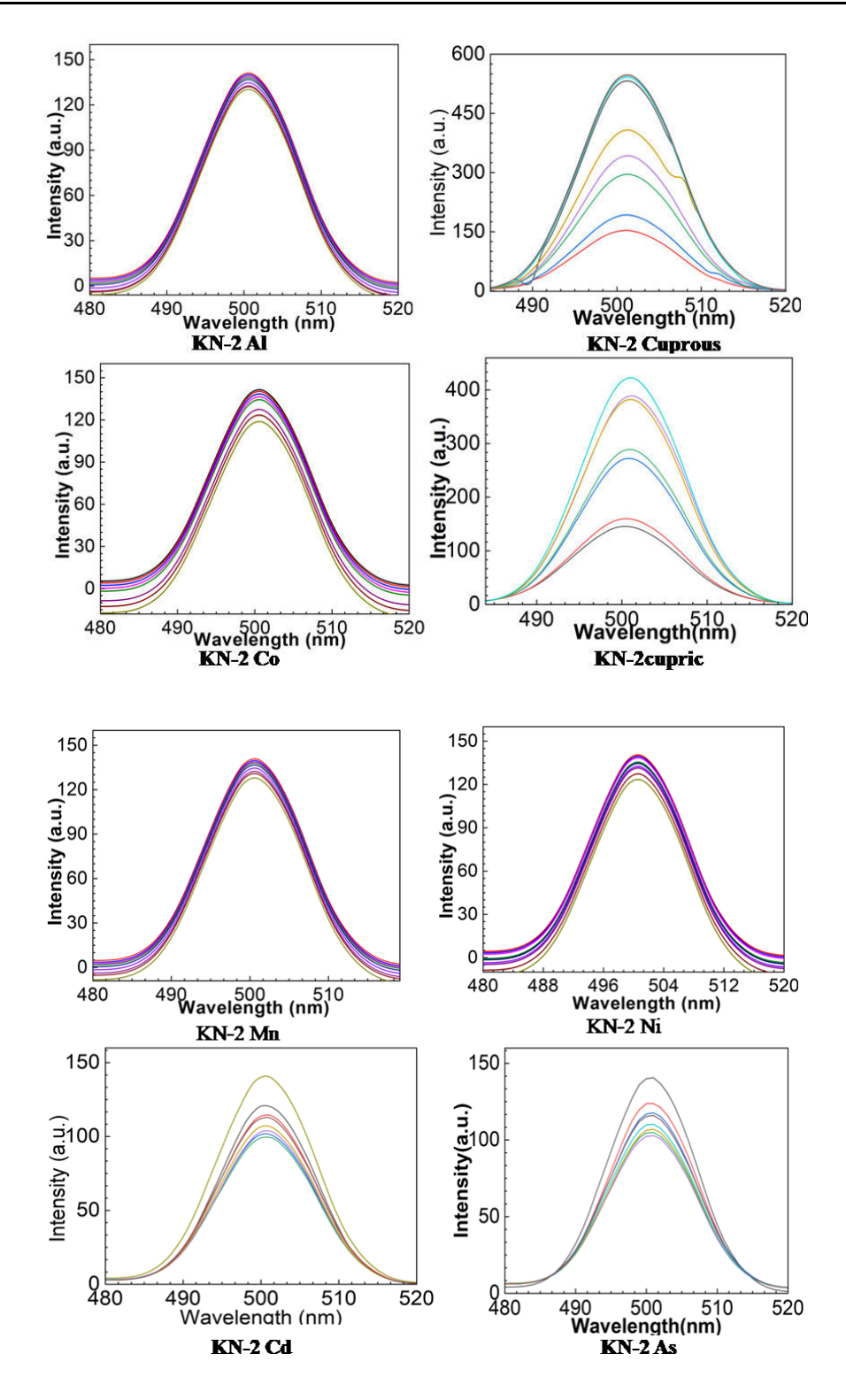


Figure 3.3.8: b) Fluorescence spectra of KN-2 carbon dots of (100 μ g/ mL) with different concentrations of different metal ions (Al³⁺, Cd²⁺, Mn²⁺, Ni²⁺, Co⁺², Cu²⁺, Cu⁺, and As⁺³) concentrations (0-140 μ M).

This signal indicates how the specific metal ions are interacting. It cannot be utilized as a fluorescence sensor, if the metal ion does not affect the CDs signal. As a result, among the criteria depicted in the sensing mechanism, we test the detection system's selectivity by capturing fluorescence spectra, when several metal ions are present. One of the key output characteristics here was fluorescence properties. As a result, we evaluated the quenching or enhancing effects of several metal ions on CDs (KN-1) and (KN-2) in deionised water (Fig.3.3.8a-b).As a result, the influence of several metal ions (e. g., Al³⁺,Cd²⁺, Mn²⁺, Ni²⁺, Co⁺², Cu²⁺, Cu⁺, and As⁺³) is significant for water pollution or related to heavy metal ions related hazards, and each one was employed at a concentration of 1 μM during the experiment. CD solvent fluorescence intensity is measured in the existence of various metals. Next, metal-induced fluorescence was investigated using Al³⁺, Cd²⁺, Mn²⁺, Ni²⁺, Co⁺², Cu²⁺, C

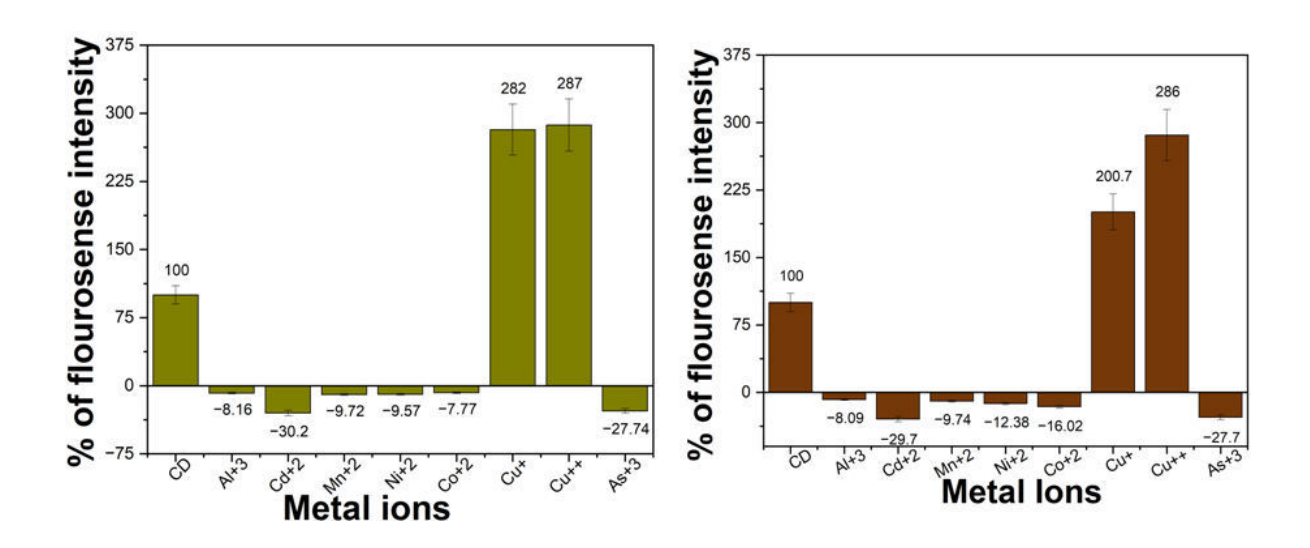


Figure 3.3.9: Fluorescence spectra with different concentrations of metallic ions (a) KN1 and (b) KN2, The fluorescence intensity percentage ratios (F-F₀)/F₀ with different ions (Al³⁺, Cd²⁺, Mn²⁺, Ni²⁺, Co⁺², Cu²⁺, Cu⁺, and As⁺³).

Notably, the fluorescence response of our CDs in the presence of various metal ions such as Al³⁺,Cd²⁺, Mn²⁺, Ni²⁺, Co⁺², Cu²⁺, Cu⁺ and As⁺³ in different concentrations (from top to bottom 0, 10, 20, 40, 60, 80, and 120 M) was measured. The decrease in intensity of fluorescence spectra for Al³⁺, Cd²⁺, Mn²⁺, Ni²⁺, Co⁺², and As⁺³ is illustrated with a percentage of decrease. The fluorescence intensity diminishes as the concentration of Al³⁺,Cd²⁺, Mn²⁺, Ni²⁺, Co⁺², and As⁺³ increases. Furthermore, the fluorescence quenching impact of cadmium (-30%) KN-1 and arsenic (27%) KN-1 ions in manufactured CDs are significantly higher than that of other ions such as Al³⁺, Mn²⁺, Ni²⁺, Co⁺², etc. Furthermore, we have expanded our research to examine the detection capabilities of Cu²⁺, and Cu⁺ by CDs. Our CDs exhibits an increase in fluorescence emission Cu²⁺ and Cu⁺ as added to the CDs solution. The intensity of the fluorescence increases as the concentration of Cu²⁺, and Cu⁺ ions increase. This fluorescence amplification is caused by the greater affinity of CD functional groups for Cu²⁺ and Cu⁺ ions. The fluorescence emission of CDs in the presence of copper with different concentrations, such as from top to bottom: 0, 10, 20, 40, 60, 80, 120, and 140 M, is seen (Figure 3.3. 9 a-b).

3.3.2.9 Biocompatibility

The biocompatibility of carbon dots *in vitro* conditions on normal splenocytes cells was investigated how it influences the effect of carbon dots on cell proliferation assay by the MTT. To study whether carbon dots affect cell proliferation or not, the MTT assay (Figure 3.3.10a-b) was performed for KN-1 and KN-2. Untreated cells were treated with (0, 15. 62, 31. 25, 62. 5, 125,250, 500, and 1000 μg/ mL various concentrations of carbon dots for 24 hrs were followed to the MTT assay for biocompatibility determination, whereas after 24 hrs of carbon dots treatment, normal cells showed more than 90% viability up to 125μM and 250 μM concentrations of carbon dots (Figure 3.3.2.10a-b). These results directed that carbon dots do not show detectable cytotoxicity up to 125μM and 250μM concentrations of CDs until 24 hrs of incubation.

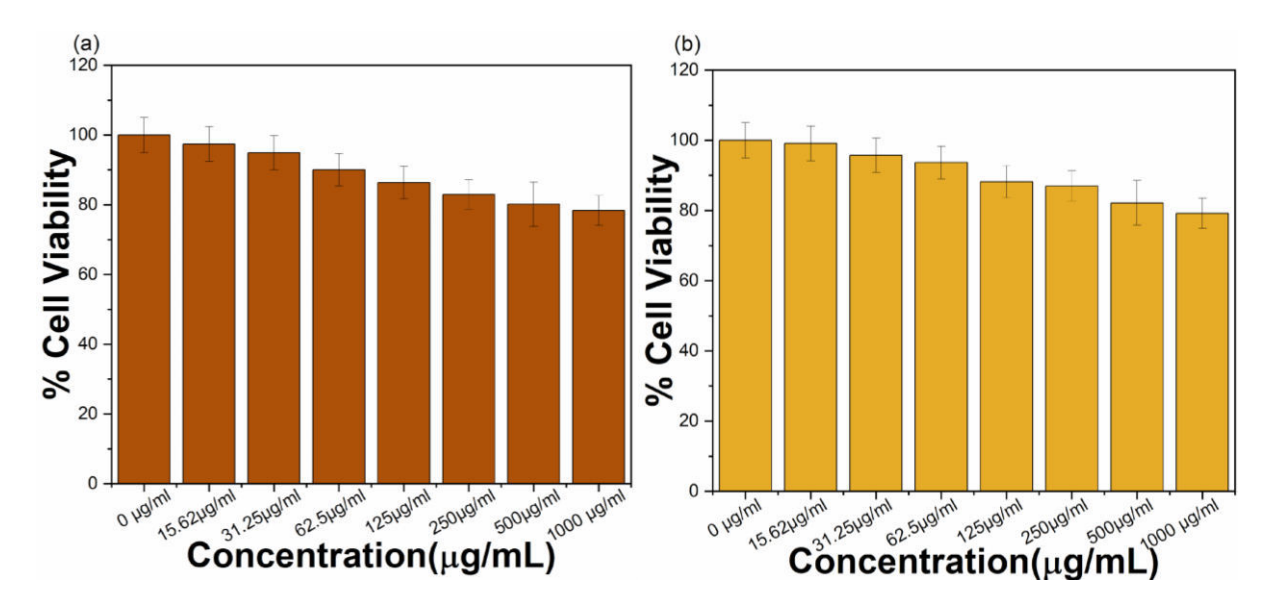


Figure 3.3.10 Illustrate the Cell viability values (%) estimated by MTT assay versus incubation concentration of CDs at different concentrations (0, 15. 62, 31. 25, 62. 5, 125,250, 500, 1000 μg/mL) at 37°C for 24 hrs. for two different samples i.e (a) KN-1 and (b) KN-2 in normal splenocytes without any drug molecule.

3. 3.3 Summary

In the summary, we successfully synthesized heavy metal quencher carbon dots from the neem seed kernel part at a higher temperature calcinations process. Our study demonstrates that CDS sensitivity on heavy metal ions is as low as a low detection limit. CDs were produced using a green synthesis process in this work. The synthesized CDs are spherical, and CDs with sizes of 7 nm and 6 nm emit a unique green light. These CDs were capable of detecting metal ions such as Al³⁺,Cd²⁺, Mn²⁺,Ni²⁺, Co⁺², Cu²⁺, Cu⁺, and As³⁺ with cadmium fluorescence quenching and Cu²⁺ fluorescence intensity increasing. This method offers advantages of selectivity, economics, and simplicity and it is a green approach for the environment. The prepared sensing system possesses specific binding and selectivity toward heavy metal ions and has been successfully used for the analysis of samples. This article also demonstrates the green methodology of fluorescence and biocompatible capability on the small-size carbon sample.

Chapter: 3

RESULTS AND DISCUSSION: PART –IV

Attempt to reveal the structures of cellulose from bark Neem antimicrobial activity and Their Application: An in vitro study.

Chapter: 3

RESULTS AND DISCUSSION:

PART -IV

Revealing the structures of nano cellulose from Neem bark antimicrobial activity and their application: an *in vitro* study.

Introduction & Motivation:

Agricultural waste products are increasingly being used to create value-added bio composites³⁵⁵ for a variety of industrial uses. 356 Among them, neem barks are intriguing. These agro residues are primarily constituted of three constituents: cellulose³⁵⁷, hemicelluloses³⁵⁸, and lignin.³⁵⁹ Among them, cellulose and hemicelluloses are carbohydrate compounds that can be easily degraded via biological enzymes and/or chemicals and fermented product useful in production of bio fuels⁵, bioelectricity³⁶⁰ and biomass derived chemicals etc., Because of the demand for renewable³⁶¹ resources and ecological sustainability, both the academic and industrial sectors have recently focused heavily on the creation of bio products in a more cost-effective and timeefficient manner. Certain cellulose¹⁰ compounds have already been used in medicines and scaffolds, as well as food additives, building materials, and textiles. According to a numerous recent investigation, nanocellulose (NC) may be isolated from the Neem bark (scientific name: Azadirachta Indica). 362 Because of its great porous ness and magnificent water absorbing qualities, in addition to its flexibility to mould into any shape and experiment with different bio agents. Nanocomposite¹¹¹ is incredibly clever nano biomaterials towards biological applications⁶. Extract of neem bark (NM) is employed within this study because of its antibacterial 126, antiviral³⁶³, and antifungal³⁶ capabilities. However, there has been little study observed on the application of bio-extracts, particularly neem bark extract, to illustrate the antibacterial 24 characteristics of Nano cellulose. Cultivation of herbal agents are quite easy and herbal medicine shows low mammalian cytotoxic effects, mortify quickly in the surroundings, eco-friendly and

alternatives to synthetic antibiotics that cause side effects and increase the resistance. Nanocellulose is appealing for applications in many industries due to its exceptional characteristics and biodegradability; including Surface modified material, nanocomposite materials, or permeable paper with specific functionalities. Agricultural wastes are becoming increasingly appealing as a resource for nanocellulose manufacturing. It is not only prolific, but the use of agricultural left overs may increase the value of nanocellulose from non-valuable waste to significant profits. Furthermore, effective agricultural waste management is essential to the environment. As previously indicated, lignocelluloses biomass contains both cellulose and noncellulosic material components such as hemicelluloses, lignin, and other natural fibers chemicals. Pre-treatment of biomass is critical for eliminating components that are not cellulosic and leaving only cellulosic materials to be extracted later from nanocellulose.

Various components of the Neem plant (leaf, bark, and seeds) have been demonstrated to offer a wide range of pharmacological actions like anti-oxidant, anti-malarial, anti-mutagenic, anti-carcinogenic, anti-inflammatory²⁵⁵, anti-hyperglycemic, anti-bacterial²⁸¹, antiulcer, and anti-diabetic properties. With this background knowledge, we have developed cellulosic nanofiber and assessed for their physicochemical parameters and anti-bacterial activity.

3. 4. 2 Results and Discussion

3. 4. 2. 1 Morphology confirmation

TEM assisted image the shows the hairy form of nanofiber structure 3.4.1(a-d) with mean diameter of 160 nm and the hydrodynamic diameter of 240 nm. The TEM images show spherical droplets or elongated, segregated regions along the fiber's long axis. TEM images also elucidated the nanocellulose fibers are semicrystalline in nature which further conformed through XRD. Nanofiber shows the crystalline nature (fig 3.4.1d). FESEM images elucidated the surface of the fibers are smooth and arrangement create the Nano pores Fig 3.4.1e. These nanopores could give the highest surface area and could be beneficial for the loading and

releasing of drug. From the AFM surface topography and height profile, it is estimated that the nanofiber has an average depth of 30 nm (AFM images Fig 3.4.2.(a-b)). Channel can be seen even at lower magnifications.

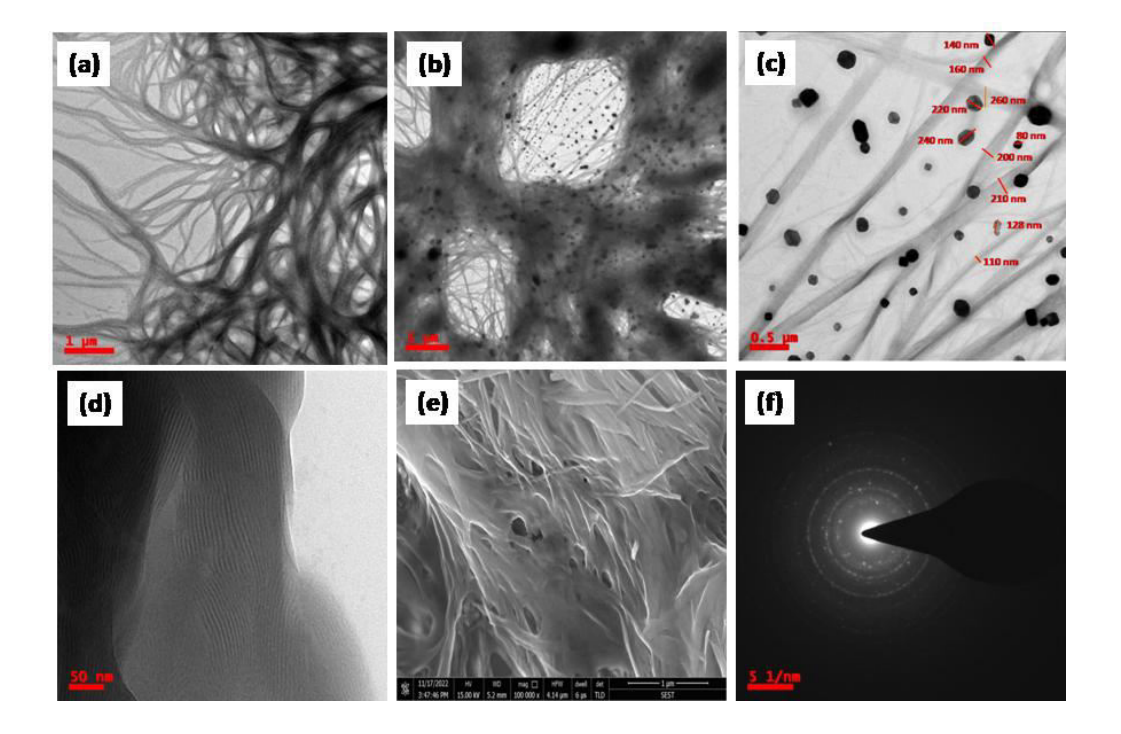


Figure 3.4.1 Transmission electron microscope (TEM) micrographs of nanofibers shown from lower to higher magnification. Fig. (a-d) and (e) FESEM micrographs of a synthesized NC of nanofiber, scale bar is ~1 μm; (f) SAED pattern of neem bark Nano cellulose synthesized in the acid hydrolysis process.

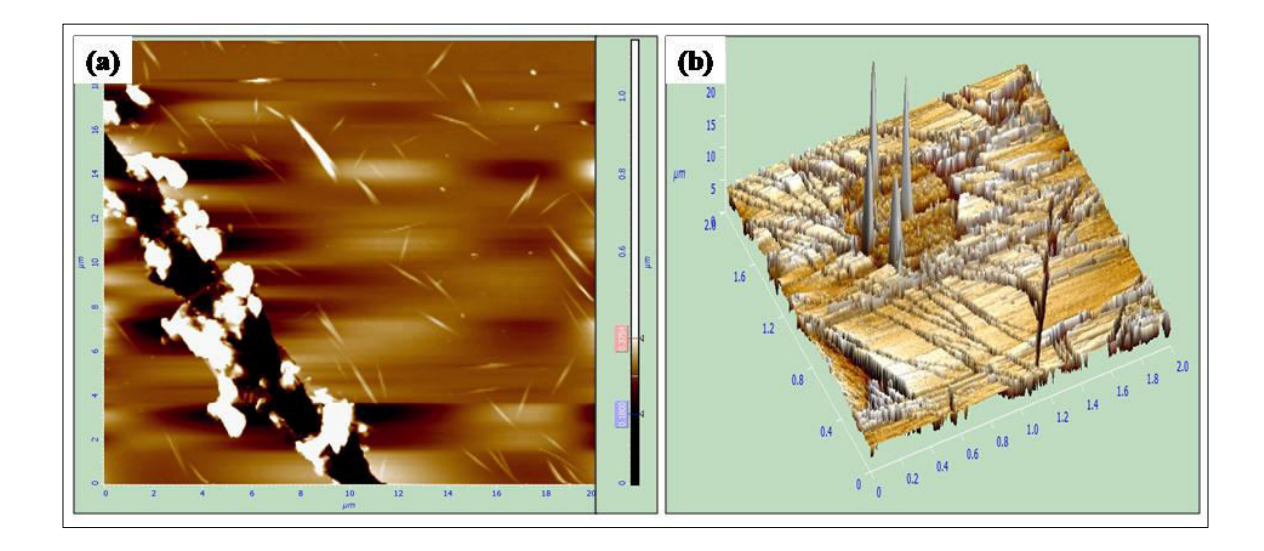


Figure 3.4.2 (a) AFM images of nanofiber, and (b) Corresponds to 3D image of NC.

AFM results shows the surface roughness, depth profile and increased surface area provided by void space, which could be an advantage to load with the assistance of its branch structure and it can used medicines.

3.4.2.2 Chemical functionality and thermal stability

The differential scanning calorimetry (DSC) methodology is utilized to examine the thermal characteristics of the materials (Fig 3a). The thermal behaviour of neem nanofibers (TGA) is depicted in Figure 3.4.3 b.It was observed that nanofiber has three stages of thermal degradation. The very first stage upto 150°C, due to moisture evaporation along with solvent has been shown. Further degradation of fibers observed from 212 °C to 354°C. The third step decomposition observed from 355°C to 625°C shows the degradation of functional groups. Furthermore, the nanofiber decomposes completed at temperatures ranging from 625°C to 761°C. In continuation to identify those functional groups specific to the extract, FT-IR spectra were acquired.

FTIR analysis was carried out on raw materials and cellulosic nanofibers. And further change in chemical structure were studies by total attenuated reflection (ATR) analysis. The interactions between the active component and the nanofiber, as well as their functional qualities, were investigated using FT-IR spectroscopy. Fig.3.4.3c shows the FTIR spectra of nanofiber compositions. The nanofiber spectra showed the characteristic peaks appeared at 3292 cm⁻¹ induced by N-H stretching, 2925 cm⁻¹ for C-H stretching in alkenes, 2839cm⁻¹ for C-H, as well as 1557 cm⁻¹ for N-O and 1410 cm⁻¹ for O-H, 1043 cm⁻¹ for S=O. (Fig.3.4.3c). The UV-Vis absorption spectra was recorded (Figure 3D). And absorption band appeared at 258 nm, for the $n\rightarrow \sigma^*$ changed the bond present in NC (see Figure 3.4.3 d).

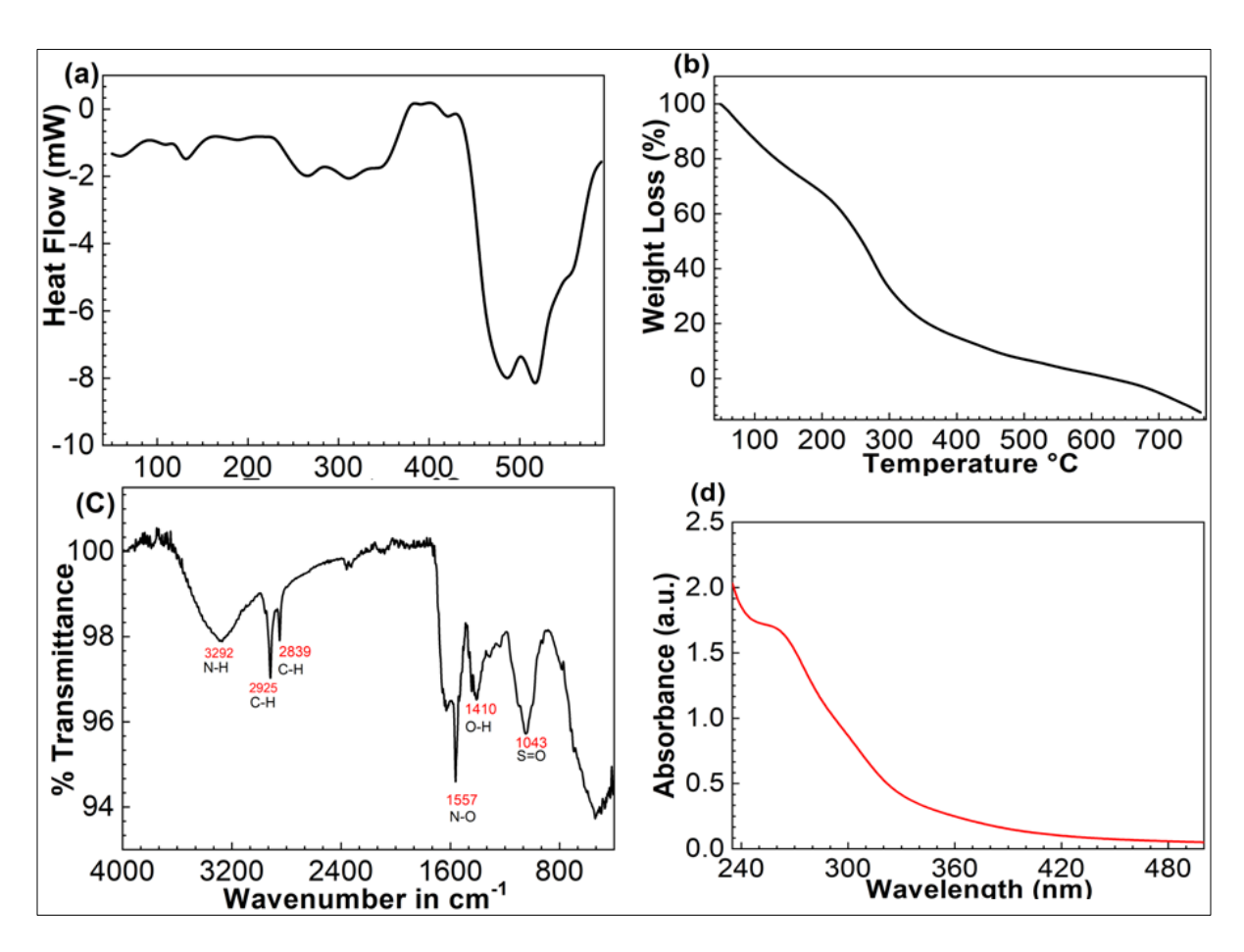


Figure 3.4.3 (a) Differential scanning calorimetry (DSC) illustrates the difference phase of change at different temperature. (b) TGA thermogram of nanofiber @ heating rate of 10 °C/min, (c) FT-IR spectrum and (d) UV-VIS spectrum with a maximal absorbance peak appeared at 259 nm.

3. 4. 2. 3 Structural and surface zeta potential

The Raman shift for the Nanofiber has been obtained and also decongratulated spectra has been shown in Figure 3.4.4 a. The Raman shift for the NC has been obtained, and the existence of the D band at 1335 cm⁻¹ has been confirmed for the presence of sp2 combination (in-plane vibration) with a G band emerged at 1564 cm⁻¹ for out-of-plane vibration, signifying structural defects. The cellulose nanofibres obtained from neem bark get a negative charge zeta potential. Cellulose nanofibres is having negative zeta potential, -43 mV (Figure 3.4.4 b), indicating that these nanofibres are stable. (Figure 3.4.4 c) depicts the results of DLS determinations in continuation of Z-average diameter. The particle sizes of the cellulose nanofibres processed by

acid hydrolysis, are greater in size than those are found in the other products. The typical width of cellulose nanofibres particle was 411.1nm and 68.2 nm. The XRD analysis demonstrated the understanding of the synthesized NC crystalline structure. The much broadened and less intense XRD peaks in Figure 3.4.4 (d) indicated the semi crystalline state of the product.

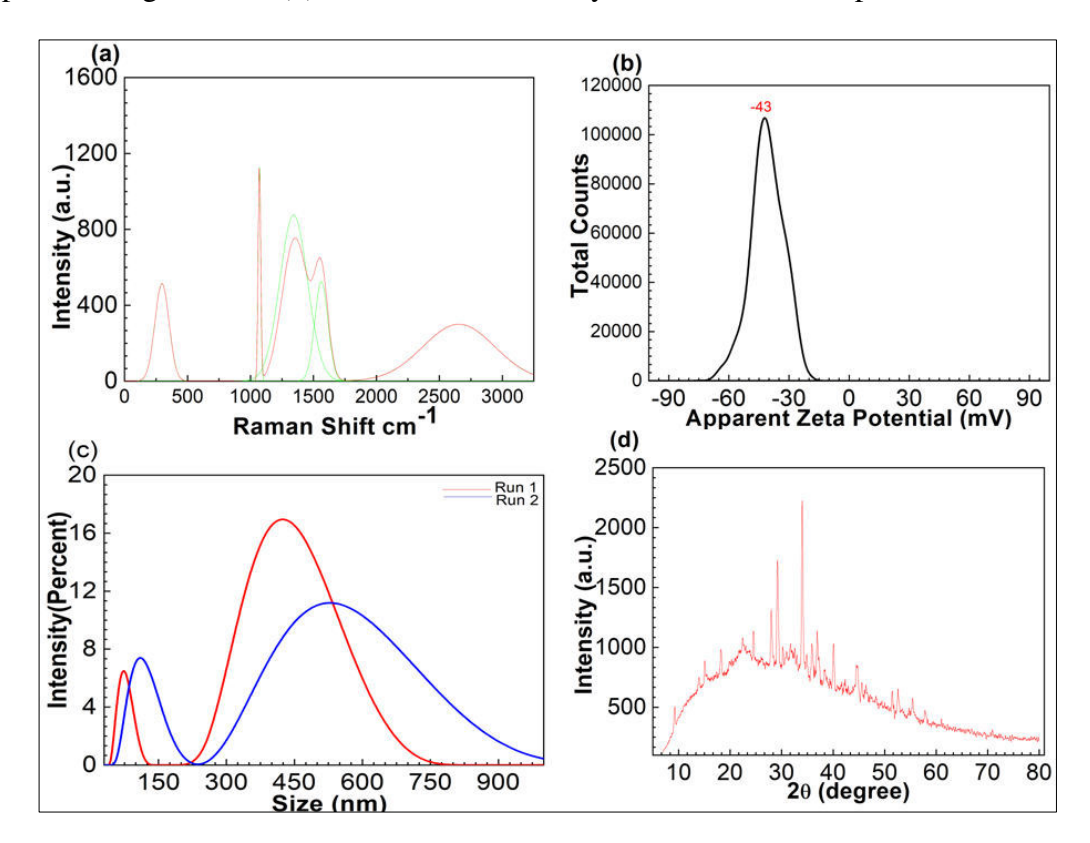


Figure 3.4.4 (a) Carbon nanofibers with Raman defects reported from regenerated cellulose nanofibers,b) The zeta potential values of cellulose nanofibres derived from neem bark. (c) The diameter, size distribution of Neem bark nanofibres, and (d) XRD patterns of the Neem bark nanofibers.

3. 4. 2. 4 Surface area analysis and pore size

Nitrogen adsorption/desorption isotherms of CDs produced are shown in Figure 3.4.5 a-b for the nanofiber sample. The degassing procedure took 4 hours at 150 °C. As a result, nanofibers are compared to identify the changes in porosity produced by annealing. The isotherms revealed a type IV isotherm with obvious hysteresis, as shown in (Fig 3.4.5a). The estimated BET surface

area is 12.7338 m²/g. The dynamic viscosity of the liquid against temperature is depicted in Figure 3.4.5(c-d). Because of the higher velocities of individual molecules, the period of contact between surrounding molecules of a liquid reduces as the temperature rises. The macroscopic result appears to be a reduction in intermolecular force and viscosity.

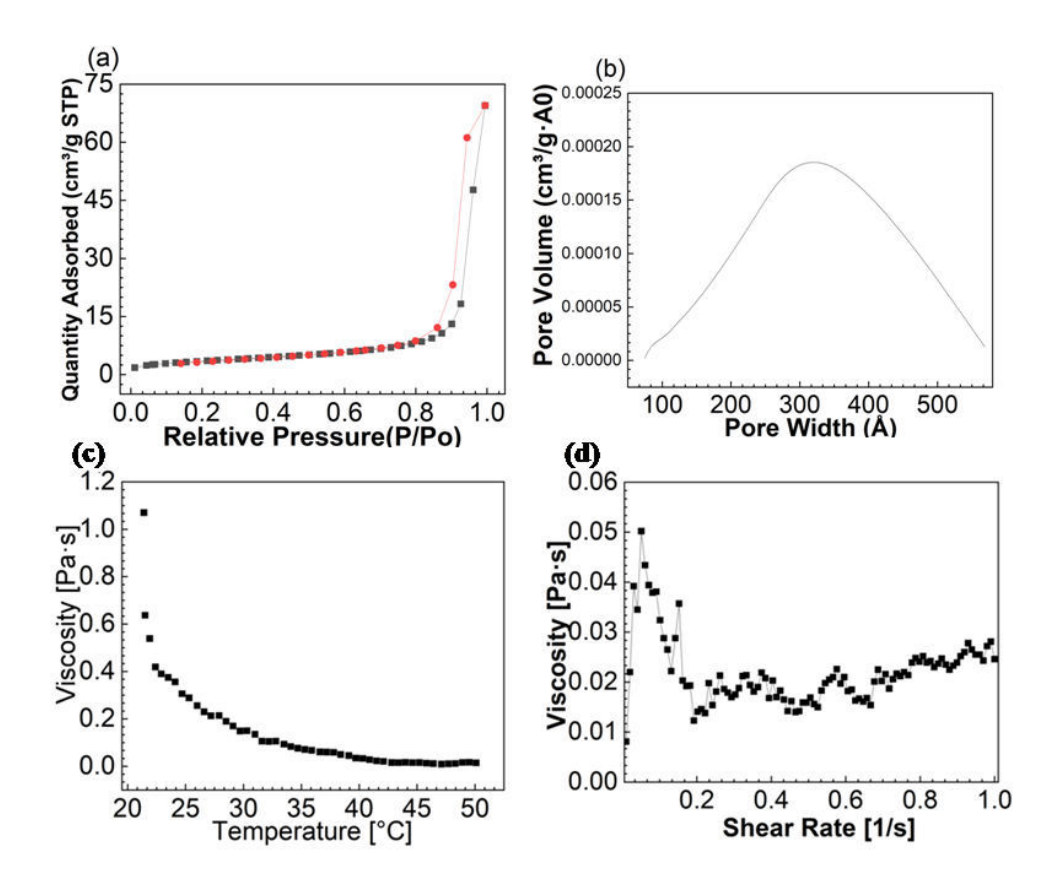


Figure 3.4.5 (a) BET-adsorption-desorption isotherm of the investigated carbon nanofibers, (b) Pore size distribution, (c) Graph of Dynamic Viscosity Vs Temperature of nanofiber. It is evident from the graph, as temperature increases, the density decreases. (d) The plot of viscosity vs. Shear rate of nanofiber

3.4.2.5 In vitro antibacterial activity of cellulose nanofibers

The disk diffusion results depicted in (Fig. 3.4.6) indicated 4 th number sample was used to investigate the antibacterial response of nanofiber. In case of *Staphylococcus aureus* has shown MIC 0.281mg/mL and followed by 16 mm inhibition zone). *Candida albican and E.coli* also shown less than 5 mm and 7 mm inhibition zones, with MIC 2.25 mg/mL for both. *Klebsiella*

pneumonia is not showed any inhibition zone. Further our results conclude that nano cellulose fibers shows the antibacterial property against *Staphylococcus aureus*, *Candida albican and E.coli*.

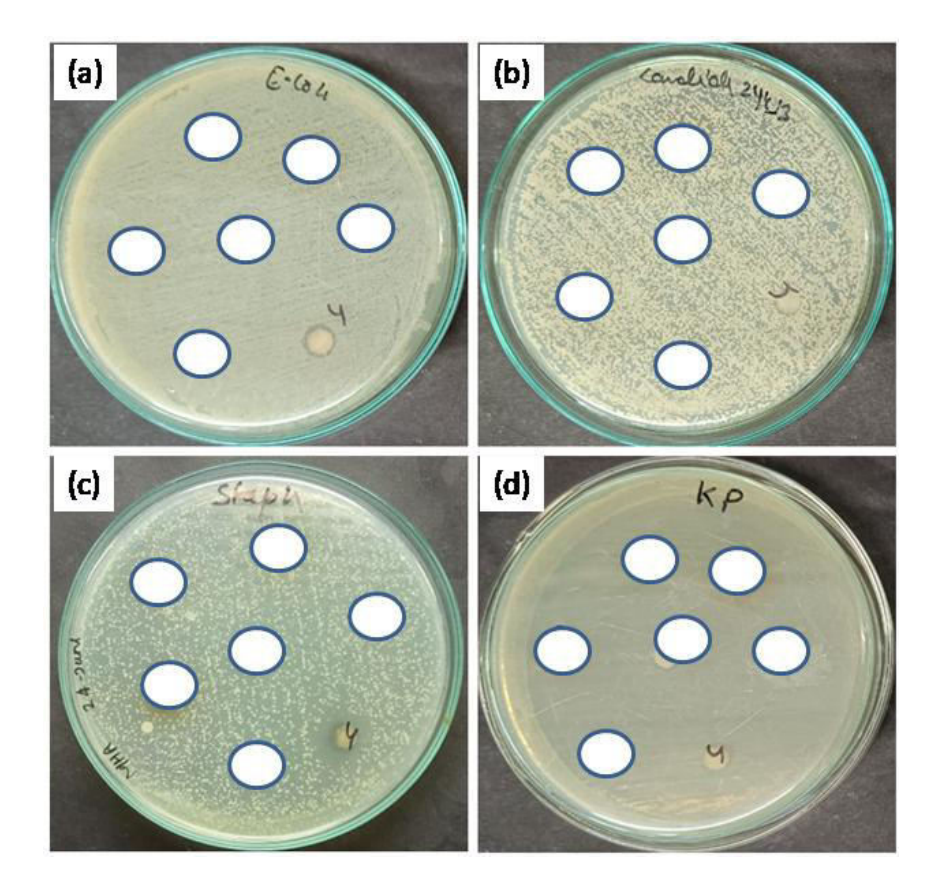


Figure 3.4.6. Antibacterial activity images of several discs concentrations of Neem bark nanofiber antibiotics on (A) Escherichia coli, (B) *Candida albicans*, (C) *Staphylococcus aureus* and (D) *Klebsiella pneumoniae*

3. 4. 3 **Summary**

The synthesized nano cellulose fiber was quantitatively and qualitatively tested for antibacterial activity. Nanofiber was synthesized successfully by chemical process respectively. Spectra, photon correlation spectroscopy, Scanning Electron Microscopy (FESEM), and X-Ray Diffraction (XRD) analysis were used to characterize the nanocellulose fibers in detail. The mean particle size was determined using photon correlation spectroscopy and FESEM image analysis. The antibacterial activity ¹²⁶ of neem bark cellulosic nanofiber as a factor of

nanoparticle concentration was evaluated against four different bacteria, especially E.coli., Candida albicans, Staphylococcus aureus, and Klebsiella pneumoniae. Staphylococcus aureus 364 is a Gram-positive spherically shaped bacterium that belongs to the Bacillota and is commonly found in the upper respiratory tract and on the skin. It is a facultative anaerobe that can grow without oxygen and is typically positive for catalase and nitrate reduction. When germs enter the circulation, it causes sepsis. Pneumonia is a disease that mostly affects persons with underlying lung illness, especially those on mechanical ventilation. Endocarditis³⁶⁵ is an infection of the heart valves that can cause heart failure or stroke. Osteomyelitis³⁶⁴ (bone infection) can be caused by staph bacteria in the bloodstream or by direct contacts, such as after a foot puncture wound or intravenous (IV) drug miss use. Some E. Coli 285 bacteria produce a toxin (a harmful chemical) that can harm the small intestinal lining. This might result in severe stomach pains, vomiting, and diarrhea (often with blood in it). People can become dehydrated as a result of this. Therefore, the test was performed by the disc diffusion assay estimation method. From the study, synthesized nanofibers were observed to have strong antimicrobial potential. The MIC and inhibition zone study of four different microorganisms was carried out in presence of a different concentration of nanofiber to observe the effect on the growth of the bacteria in liquid media. It was observed that both E.coli and Staphylococcus aureus strongly affected by Nanocellulose fibers. It was also observed that the growth rate was strongly inhibited by the presence of a small concentration of nanofiber. We investigated A. Indica (Neem), for their antimicrobial effectiveness against target endodontic pathogens such as Escherichia coli, Candida albicans, Staphylococcus aureus, and but it is not effective on Klebsiella pneumonia.

CHAPTER -4 SUMMARY AND CONCLUSIONS

CHAPTER -4

SUMMARY AND CONCLUSIONS

4.1 Summary and Conclusions

The brief of this thesis has been discussed in this chapter; The study's goal was to investigate the synthesis of Carbon Nanodots (CDs) and the notion of applications in lighting, sensing, and cancer cell death. The scientists also needed to determine if the CDs were hazardous or not, as this may impact their applicability.

The literature on CD toxicity is fairly sparse, including inconsistent cell-based in-vitro investigations. Three of these questions were addressed in the study: 1) Is it possible to limit the emission of CDs? 2) Are the CDs non-toxic, despite the fact that the majority of the literature claims that they are? 3) Can the CDs be used for illumination, sensing, or biological applications?etc. However, the chapter wise summery of this dissertation is appended below.

Chapter -1 Covers the introduction to biomaterials and nanotechnology, and then discusses the application of nanotechnology in biomedical domains. Furthermore, a thorough literature analysis on biomaterials and nanomaterial production for cancer applications has been presented. Finally, the first chapter elaborates on the dissertation's motivation and aims.

Chapter -2 Provides information on the preliminary materials utilized in this thesis. More information on the process used to create mesophorous carbon material, carbon dots. In addition, the fundamental principles of the experiment procedures employed for the characterisation of produced nanocapsules/nanoparticles have been thoroughly described.

Chapter-3 is the results and discussion part of these dissertations. Which is further divided into three parts. They are as below:

In Part I of **chapter-3**: Synthesis of seed derived carbon nanocapsules cell imaging, depolarization of mitochondrial membrane potential, and dose-dependent control death of breast Cancer.

The main findings of this part have been summarized below point wise.

- ❖ We reported a green one-step synthesis approach of mesoporous carbon nanocapsules from *Azadirachta indica* seeds and their uses for theranostic applications.
- ❖ Carbon nanocapsules is economical for the large-scale production also highly water-soluble, emit strong fluorescence light, and are highly stable.
- However highly biocompatible to the normal healthy cells and are good candidates for the absorption in the cytoplasm and affects the breast cancer cells more than normal cells and multicolor living cell imaging.
- Finally, Azadirachta indica seeds derived carbon nanocapsules may hold a huge potential for the cell imaging and therapeutic applications.

In Part II of **chapter-3:** Synthesize of carbon dots for Kernal part of seed: Photoluminescence mechanisms and applications in detection of biological relevant metal ions.

The main findings of this part have been summarized below point wise.

- CDs was synthesized through a green synthesis method.
- The prepared CDs are spherical in shape and a distinct green fluorescent emission was obtained from the CDs.
- ❖ These CDs exhibited efficient metal ion detection ability, predominantly Fe³⁺, and Zn^{2+.}
- ❖ Finally, our CDs can be loaded with anticancer drugs and useful for the treatment ofbreast cancer with low doses of drugs.

In this direction, more study in in vivo can be accomplished as a future scope of this work.

In Part III of **chapter-3:** High temperature synthesized carbon dots and its absorption of heavy metal ions.

The main findings of this part have been summarized below point wise.

We successfully synthesized heavy metal quencher carbon dots from neem seed kernel Part at higher temperature calcinations process.

- ♦ Our study demonstrates that CDS sensitivity on heavy metal ions is as low as a low detection limit i. e Al ³⁺, Cd ²⁺, Mn ²⁺, Ni ²⁺, Co ⁺², Cu ²⁺, Cu + and As ⁺³.
- This method offers advantages of selectivity, economics, and simplicity and it is a green approach for the environment.
- ❖ The prepared sensing system possesses specific binding and selectivity toward heavy metal ions and has been successfully used for the analysis of samples.
 - This part also demonstrates the green methodology of fluorescence and biocompatible capability on the small-size carbon sample.

Part IV of **chapter-3:** Revealing the structures of nano cellulose from Neem bark antimicrobial activity and their application: an *in vitro* study.

The main findings of this part have been summarized below point wise.

In this part of the work nano cellulose from Neem bark was extracted and the antimicrobial activity and their application have been performed *in vitro*.

- We reported that can be stated A. *indica* has antibacterial properties.
- ❖ The endodontic pathogens such as *E.coli*, *Candida albicans*, *Staphylococcus aureus*, and *Klebsiella pneumonia*.

However, more preclinical and clinical trials are needed to assess the Cytotoxicity and safety of these plant extracts before they may be suggested.

<u>References</u> <u>Chapter-5</u>

5. References

(1) Giannouli, M.; Karagkiozaki, V.; F.Pappa; Moutsios, I.; C.Gravalidis; Logothetidis, S. Fabrication of Quercetin-Loaded PLGA Nanoparticles via Electrohydrodynamic Atomization for Cardiovascular Disease. *Mater. Today Proc.* 2018, 5 (8, Part 2), 15998–16005. https://doi.org/https://doi.org/10.1016/j.matpr.2018.05.044.

- (2) Elmowafy, E. M.; Tiboni, M.; Soliman, M. E. Biocompatibility, Biodegradation and Biomedical Applications of Poly(Lactic Acid)/Poly(Lactic-Co-Glycolic Acid) Micro and Nanoparticles. *J. Pharm. Investig.* **2019**, *49* (4), 347–380. https://doi.org/10.1007/s40005-019-00439-x.
- Titirici, M.-M.; White, R. J.; Brun, N.; Budarin, V. L.; Su, D. S.; del Monte, F.; Clark, J. H.; MacLachlan, M. J. Sustainable Carbon Materials. *Chem. Soc. Rev.* 2015, 44 (1), 250–290. https://doi.org/10.1039/C4CS00232F.
- (4) Hoa, L. Q.; Vestergaard, M. C.; Tamiya, E. Carbon-Based Nanomaterials in Biomass-Based Fuel-Fed Fuel Cells. *Sensors (Basel)*. 2017, 17 (11). https://doi.org/10.3390/s17112587.
- (5) Abbas, A.; Mariana, L. T.; Phan, A. N. Biomass-Waste Derived Graphene Quantum Dots and Their Applications. *Carbon N. Y.* 2018, 140, 77–99. https://doi.org/https://doi.org/10.1016/j.carbon.2018.08.016.
- (6) Shen, P.; Gao, J.; Cong, J.; Liu, Z.; Li, C.; Yao, J. Synthesis of Cellulose-Based Carbon Dots for Bioimaging. *ChemistrySelect* 2016, 1 (7), 1314–1317. https://doi.org/https://doi.org/10.1002/slct.201600216.
- (7) Lu, W.; Qin, X.; Liu, S.; Chang, G.; Zhang, Y.; Luo, Y.; Asiri, A. M.; Al-Youbi, A. O.; Sun, X. Economical, Green Synthesis of Fluorescent Carbon Nanoparticles and Their Use

<u>References</u> <u>Chapter-5</u>

as Probes for Sensitive and Selective Detection of Mercury(II) Ions. *Anal. Chem.* **2012**, *84* (12), 5351–5357. https://doi.org/10.1021/ac3007939.

- (8) Yan, Y.; Miao, J.; Yang, Z.; Xiao, F.-X.; Yang, H. Bin; Liu, B.; Yang, Y. Carbon Nanotube Catalysts: Recent Advances in Synthesis, Characterization and Applications. *Chem. Soc. Rev.* 2015, 44 (10), 3295–3346. https://doi.org/10.1039/C4CS00492B.
- (9) Li, H.; Kang, Z.; Liu, Y.; Lee, S.-T. Carbon Nanodots: Synthesis, Properties and Applications. J. Mater. Chem. 2012, 22 (46), 24230–24253. https://doi.org/10.1039/C2JM34690G.
- (10) Wang, J.; Liu, G.; Leung, K. C.-F.; Loffroy, R.; Lu, P.-X.; Wang, Y. X. J. Opportunities and Challenges of Fluorescent Carbon Dots in Translational Optical Imaging. *Curr. Pharm. Des.* 2015, 21 (37), 5401–5416.
 https://doi.org/10.2174/1381612821666150917093232.
- (11) Yan, Y.; Chen, J.; Li, N.; Tian, J.; Li, K.; Jiang, J.; Liu, J.; Tian, Q.; Chen, P. Systematic Bandgap Engineering of Graphene Quantum Dots and Applications for Photocatalytic Water Splitting and CO2 Reduction. ACS Nano 2018, 12 (4), 3523–3532. https://doi.org/10.1021/acsnano.8b00498.
- (12) Szczęch, M.; Szczepanowicz, K. Polymeric Core-Shell Nanoparticles Prepared by Spontaneous Emulsification Solvent Evaporation and Functionalized by the Layer-by-Layer Method. *Nanomaterials*. 2020. https://doi.org/10.3390/nano10030496.
- (13) Escalona-Rayo, O.; Fuentes-Vázquez, P.; Jardon-Xicotencatl, S.; García-Tovar, C. G.; Mendoza-Elvira, S.; Quintanar-Guerrero, D. Rapamycin-Loaded Polysorbate 80-Coated PLGA Nanoparticles: Optimization of Formulation Variables and in Vitro Anti-Glioma Assessment. J. Drug Deliv. Sci. Technol. 2019, 52, 488–499.

<u>References</u> <u>Chapter-5</u>

- https://doi.org/https://doi.org/10.1016/j.jddst.2019.05.026.
- (14) Traeger, A.; Voelker, S.; Shkodra-Pula, B.; Kretzer, C.; Schubert, S.; Gottschaldt, M.; Schubert, U. S.; Werz, O. Improved Bioactivity of the Natural Product 5-Lipoxygenase Inhibitor Hyperforin by Encapsulation into Polymeric Nanoparticles. *Mol. Pharm.* 2020, 17 (3), 810–816. https://doi.org/10.1021/acs.molpharmaceut.9b01051.
- (15) Saqib, M.; Ali Bhatti, A. S.; Ahmad, N. M.; Ahmed, N.; Shahnaz, G.; Lebaz, N.; Elaissari,
 A. Amphotericin B Loaded Polymeric Nanoparticles for Treatment of Leishmania
 Infections. *Nanomater. (Basel, Switzerland)* 2020, 10 (6).
 https://doi.org/10.3390/nano10061152.
- (16) Zielińska, A.; Carreiró, F.; Oliveira, A. M.; Neves, A.; Pires, B.; Venkatesh, D. N.; Durazzo, A.; Lucarini, M.; Eder, P.; Silva, A. M.; Santini, A.; Souto, E. B. Polymeric Nanoparticles: Production, Characterization, Toxicology and Ecotoxicology. *Molecules* 2020, 25 (16). https://doi.org/10.3390/molecules25163731.
- (17) Sachdev, A.; Gopinath, P. Green Synthesis of Multifunctional Carbon Dots from Coriander Leaves and Their Potential Application as Antioxidants, Sensors and Bioimaging Agents. *Analyst* 2015, 140 (12), 4260–4269. https://doi.org/10.1039/C5AN00454C.
- (18) Rooj, B.; Dutta, A.; Islam, S.; Mandal, U. Green Synthesized Carbon Quantum Dots from Polianthes Tuberose L. Petals for Copper (II) and Iron (II) Detection. *J. Fluoresc.* **2018**, 28 (5), 1261–1267. https://doi.org/10.1007/s10895-018-2292-6.
- (19) Wu, Z. L.; Zhang, P.; Gao, M. X.; Liu, C. F.; Wang, W.; Leng, F.; Huang, C. Z. One-Pot Hydrothermal Synthesis of Highly Luminescent Nitrogen-Doped Amphoteric Carbon Dots for Bioimaging from Bombyx Mori Silk – Natural Proteins. *J. Mater. Chem. B* 2013,

- 1 (22), 2868–2873. https://doi.org/10.1039/C3TB20418A.
- (20) Gehrke, H.; Pelka, J.; Hartinger, C. G.; Blank, H.; Bleimund, F.; Schneider, R.; Gerthsen,
 D.; Bräse, S.; Crone, M.; Türk, M.; Marko, D. Platinum Nanoparticles and Their Cellular
 Uptake and DNA Platination at Non-Cytotoxic Concentrations. *Arch. Toxicol.* 2011, 85
 (7), 799–812. https://doi.org/10.1007/s00204-010-0636-3.
- (21) Dykman, L. A.; Khlebtsov, N. G. Gold Nanoparticles in Biology and Medicine: Recent Advances and Prospects. *Acta Naturae* **2011**, *3* (2), 34–55. https://doi.org/10.32607/20758251-2011-3-2-34-56.
- (22) Gupta, R.; Rai, B. Penetration of Gold Nanoparticles through Human Skin: Unraveling Its Mechanisms at the Molecular Scale. *J. Phys. Chem. B* **2016**, *120* (29), 7133–7142. https://doi.org/10.1021/acs.jpcb.6b03212.
- (23) Fonseca-Gomes, J.; Loureiro, J. A.; Tanqueiro, S. R.; Mouro, F. M.; Ruivo, P.; Carvalho, T.; Sebastião, A. M.; Diógenes, M. J.; Pereira, M. C. In Vivo Bio-Distribution and Toxicity Evaluation of Polymeric and Lipid-Based Nanoparticles: A Potential Approach for Chronic Diseases Treatment. *Int. J. Nanomedicine* 2020, *15*, 8609–8621. https://doi.org/10.2147/IJN.S267007.
- (24) Kalwar, K.; Shan, D. Antimicrobial Effect of Silver Nanoparticles (AgNPs) and Their Mechanism a Mini Review. *Micro Nano Lett.* 2018, 13 (3), 277–280. https://doi.org/https://doi.org/10.1049/mnl.2017.0648.
- (25) Paladini, F.; Pollini, M. Antimicrobial Silver Nanoparticles for Wound Healing Application: Progress and Future Trends. *Mater. (Basel, Switzerland)* **2019**, *12* (16). https://doi.org/10.3390/ma12162540.
- (26) Dreaden, E. C.; Austin, L. A.; Mackey, M. A.; El-Sayed, M. A. Size Matters: Gold

- Nanoparticles in Targeted Cancer Drug Delivery. *Ther. Deliv.* **2012**, *3* (4), 457–478. https://doi.org/10.4155/tde.12.21.
- (27) Farzin, A.; Etesami, S. A.; Quint, J.; Memic, A.; Tamayol, A. Magnetic Nanoparticles in Cancer Therapy and Diagnosis. *Adv. Healthc. Mater.* **2020**, *9* (9), e1901058. https://doi.org/10.1002/adhm.201901058.
- (28) Spanos, A.; Athanasiou, K.; Ioannou, A.; Fotopoulos, V.; Krasia-Christoforou, T. Functionalized Magnetic Nanomaterials in Agricultural Applications. *Nanomater. (Basel, Switzerland)* **2021**, *11* (11). https://doi.org/10.3390/nano11113106.
- (29) Shishir, M. R. I.; Xie, L.; Sun, C.; Zheng, X.; Chen, W. Advances in Micro and Nano-Encapsulation of Bioactive Compounds Using Biopolymer and Lipid-Based Transporters. *Trends Food Sci. Technol.* **2018**, 78, 34–60.
- (30) Yasmin, R.; Shah, M.; Khan, S. A.; Ali, R. Gelatin Nanoparticles: A Potential Candidate for Medical Applications. *Nanotechnol. Rev.* **2017**, *6* (2), 191–207.
- (31) George, B.; Suchithra, T. V. Plant-Derived Bioadhesives for Wound Dressing and Drug Delivery System. *Fitoterapia* **2019**, *137*, 104241.
- (32) Iravani, S.; Varma, R. S. Plants and Plant-Based Polymers as Scaffolds for Tissue Engineering. *Green Chem.* **2019**, *21* (18), 4839–4867.
- (33) Ravindran, R. S. E.; Subha, V.; Ilangovan, R. Silver Nanoparticles Blended PEG/PVA Nanocomposites Synthesis and Characterization for Food Packaging. *Arab. J. Chem.*2020, 13 (7), 6056–6060.
- (34) Kumaravel, V.; Nair, K. M.; Mathew, S.; Bartlett, J.; Kennedy, J. E.; Manning, H. G.; Whelan, B. J.; Leyland, N. S.; Pillai, S. C. Antimicrobial TiO2 Nanocomposite Coatings for Surfaces, Dental and Orthopaedic Implants. *Chem. Eng. J.* 2021, 416, 129071.

- https://doi.org/https://doi.org/10.1016/j.cej.2021.129071.
- (35) Li, J.; Zhu, B.; Yao, X.; Zhang, Y.; Zhu, Z.; Tu, S.; Jia, S.; Liu, R.; Kang, H.; Yang, C. J. Synergetic Approach for Simple and Rapid Conjugation of Gold Nanoparticles with Oligonucleotides. ACS Appl. Mater. Interfaces 2014, 6 (19), 16800–16807. https://doi.org/10.1021/am504139d.
- (36) Qamar, H.; Rehman, S.; Chauhan, D. K.; Tiwari, A. K.; Upmanyu, V. Green Synthesis, Characterization and Antimicrobial Activity of Copper Oxide Nanomaterial Derived from Momordica Charantia. *Int. J. Nanomedicine* 2020, *15*, 2541–2553. https://doi.org/10.2147/IJN.S240232.
- (37) Larese Filon, F.; Mauro, M.; Adami, G.; Bovenzi, M.; Crosera, M. Nanoparticles Skin Absorption: New Aspects for a Safety Profile Evaluation. *Regul. Toxicol. Pharmacol.*2015, 72 (2), 310–322. https://doi.org/10.1016/j.yrtph.2015.05.005.
- (38) Nogueira, D. J.; Vaz, V. P.; Neto, O. S.; Silva, M. L. N. da; Simioni, C.; Ouriques, L. C.; Vicentini, D. S.; Matias, W. G. Crystalline Phase-Dependent Toxicity of Aluminum Oxide Nanoparticles toward Daphnia Magna and Ecological Risk Assessment. *Environ. Res.*2020, 182, 108987. https://doi.org/https://doi.org/10.1016/j.envres.2019.108987.
- (39) Sun, C.; Chen, S.; Li, Z. Controllable Synthesis of Fe2O3-Carbon Fiber Composites via a Facile Sol-Gel Route as Anode Materials for Lithium Ion Batteries. *Appl. Surf. Sci.* **2018**, 427, 476–484. https://doi.org/https://doi.org/10.1016/j.apsusc.2017.08.070.
- (40) Habte, L.; Shiferaw, N.; Mulatu, D.; Thenepalli, T.; Chilakala, R.; Ahn, J. W. Synthesis of Nano-Calcium Oxide from Waste Eggshell by Sol-Gel Method. *Sustainability* 2019, *11* (11). https://doi.org/10.3390/su11113196.
- (41) Lei, M.; Chen, L.; Huang, B.; Chen, K. Determination of Magnesium Oxide Content in

Mineral Medicine Talcum Using Near-Infrared Spectroscopy Integrated with Support Vector Machine. *Appl. Spectrosc.* **2017**, *71* (11), 2427–2436. https://doi.org/10.1177/0003702817727016.

- (42) Mohapatra, M.; Anand, S. Synthesis and Applications of Nano-Structured Iron Oxides/Hydroxides a Review. *Int. J. Eng. Sci. Technol.* **2011**, 2.
- (43) Srivastava, P.; Sharma, P. K.; Muheem, A.; Warsi, M. H. Magnetic Nanoparticles: A Review on Stratagems of Fabrication and Its Biomedical Applications. *Recent Pat. Drug Deliv. Formul.* 2017, 11 (2), 101–113. https://doi.org/10.2174/1872211311666170328150747.
- (44) Wahajuddin; Arora, S. Superparamagnetic Iron Oxide Nanoparticles: Magnetic Nanoplatforms as Drug Carriers. *Int. J. Nanomedicine* 2012, 7, 3445–3471. https://doi.org/10.2147/IJN.S30320.
- (45) Huang, Q.; Lin, X.; Lin, C.; Zhang, Y.; Hu, S.; Wei, C. A High Performance Electrochemical Biosensor Based on Cu2O–Carbon Dots for Selective and Sensitive Determination of Dopamine in Human Serum. *RSC Adv.* 2015, 5 (67), 54102–54108. https://doi.org/10.1039/C5RA05433H.
- (46) Jeung, D.-G.; Lee, M.; Paek, S.-M.; Oh, J.-M. Controlled Growth of Silver Oxide Nanoparticles on the Surface of Citrate Anion Intercalated Layered Double Hydroxide. Nanomater. (Basel, Switzerland) 2021, 11 (2). https://doi.org/10.3390/nano11020455.
- (47) Asati, A.; Santra, S.; Kaittanis, C.; Perez, J. M. Surface-Charge-Dependent Cell Localization and Cytotoxicity of Cerium Oxide Nanoparticles. *ACS Nano* **2010**, *4* (9), 5321–5331. https://doi.org/10.1021/nn100816s.
- (48) Sivalingam, A.; Balusamy, T.; Krishnan, S. S. J.; Nagarajan, P. K. Evaluating the

Potential of Azadirachta Indica—Assisted Zinc Oxide Particles as Efficacious Nanofluids by Convective Experiments with Twisted Tape Annexed Circular Tube. *Biomass Convers. Biorefinery* **2021**. https://doi.org/10.1007/s13399-021-01344-w.

- (49) Hasegawa, G.; Tanaka, M.; Vequizo, J. J. M.; Yamakata, A.; Hojo, H.; Kobayashi, M.; Kakihana, M.; Inada, M.; Akamatsu, H.; Hayashi, K. Sodium Titanium Oxide Bronze Nanoparticles Synthesized via Concurrent Reduction and Na+-Doping into TiO2(B).
 Nanoscale 2019, 11 (3), 1442–1450. https://doi.org/10.1039/C8NR08372J.
- (50) Chung, I.-M.; Venkidasamy, B.; Thiruvengadam, M. Nickel Oxide Nanoparticles Cause Substantial Physiological, Phytochemical, and Molecular-Level Changes in Chinese Cabbage Seedlings. *Plant Physiol. Biochem.* 2019, *139*, 92–101. https://doi.org/https://doi.org/10.1016/j.plaphy.2019.03.010.
- (51) Burke, J. M.; Soli, F.; Miller, J. E.; Terrill, T. H.; Wildeus, S.; Shaik, S. A.; Getz, W. R.; Vanguru, M. Administration of Copper Oxide Wire Particles in a Capsule or Feed for Gastrointestinal Nematode Control in Goats. *Vet. Parasitol.* 2010, *168* (3–4), 346–350. https://doi.org/10.1016/j.vetpar.2009.10.027.
- (52) Lin, F.; Yang, J.; Lu, S.-H.; Niu, K.-Y.; Liu, Y.; Sun, J.; Du, X.-W. Laser Synthesis of Gold/Oxide Nanocomposites. *J. Mater. Chem.* 2010, 20 (6), 1103–1106. https://doi.org/10.1039/B918945A.
- (53) Zhi, B.; Cui, Y.; Wang, S.; Frank, B. P.; Williams, D. N.; Brown, R. P.; Melby, E. S.; Hamers, R. J.; Rosenzweig, Z.; Fairbrother, D. H.; Orr, G.; Haynes, C. L. Malic Acid Carbon Dots: From Super-Resolution Live-Cell Imaging to Highly Efficient Separation. ACS Nano 2018, 12 (6), 5741–5752. https://doi.org/10.1021/acsnano.8b01619.
- (54) Ansari, S. A. M. K.; Ficiarà, E.; Ruffinatti, F. A.; Stura, I.; Argenziano, M.; Abollino, O.;

References Chapter-5

- Cavalli, R.; Guiot, C.; D'Agata, F. Magnetic Iron Oxide Nanoparticles: Synthesis, Characterization and Functionalization for Biomedical Applications in the Central Nervous System. *Materials (Basel)*. **2019**, *12* (3). https://doi.org/10.3390/ma12030465.
- (55) Ding, H.; Yu, S.-B.; Wei, J.-S.; Xiong, H.-M. Full-Color Light-Emitting Carbon Dots with a Surface-State-Controlled Luminescence Mechanism. *ACS Nano* **2016**, *10* (1), 484–491. https://doi.org/10.1021/acsnano.5b05406.
- (56) Wang, L.; Yin, Y.; Jain, A.; Zhou, H. S. Aqueous Phase Synthesis of Highly Luminescent, Nitrogen-Doped Carbon Dots and Their Application as Bioimaging Agents. *Langmuir* 2014, 30 (47), 14270–14275. https://doi.org/10.1021/la5031813.
- (57) Wang, L.; Gu, D.; Su, Y.; Ji, D.; Yang, Y.; Chen, K.; Pan, H.; Pan, W. Easy Synthesis and Characterization of Novel Carbon Dots Using the One-Pot Green Method for Cancer Therapy. *Pharmaceutics* **2022**, *14* (11). https://doi.org/10.3390/pharmaceutics14112423.
- (58) Das, P.; Ganguly, S.; Maity, P. P.; Srivastava, H. K.; Bose, M.; Dhara, S.;
 Bandyopadhyay, S.; Das, A. K.; Banerjee, S.; Das, N. C. Converting Waste Allium
 Sativum Peel to Nitrogen and Sulphur Co-Doped Photoluminescence Carbon Dots for
 Solar Conversion, Cell Labeling, and Photobleaching Diligences: A Path from Discarded
 Waste to Value-Added Products. J. Photochem. Photobiol. B. 2019, 197, 111545.
 https://doi.org/10.1016/j.jphotobiol.2019.111545.
- (59) Chandra, A.; Singh, N. Cell Microenvironment PH Sensing in 3D Microgels Using Fluorescent Carbon Dots. ACS Biomater. Sci. Eng. 2017, 3 (12), 3620–3627. https://doi.org/10.1021/acsbiomaterials.7b00740.
- (60) Wang, L.; Zhou, H. S. Green Synthesis of Luminescent Nitrogen-Doped Carbon Dots from Milk and Its Imaging Application. *Anal. Chem.* 2014, 86 (18), 8902–8905.

- https://doi.org/10.1021/ac502646x.
- (61) El-Ansary, A.; Faddah, L. M. Nanoparticles as Biochemical Sensors. *Nanotechnol. Sci. Appl.* **2010**, *3* (1), 65–76. https://doi.org/10.2147/NSA.S8199.
- (62) Hyun, B.-R.; Chen, H.; Rey, D. A.; Wise, F. W.; Batt, C. A. Near-Infrared Fluorescence Imaging with Water-Soluble Lead Salt Quantum Dots. *J. Phys. Chem. B* **2007**, *111* (20), 5726–5730.
- (63) Li, H.; Shih, W. Y.; Shih, W.-H. Synthesis and Characterization of Aqueous Carboxyl-Capped CdS Quantum Dots for Bioapplications. *Ind. Eng. Chem. Res.* 2007, 46 (7), 2013–2019.
- (64) Jaiswal, J. K.; Mattoussi, H.; Mauro, J. M.; Simon, S. M. Long-Term Multiple Color Imaging of Live Cells Using Quantum Dot Bioconjugates. *Nat. Biotechnol.* 2003, 21 (1), 47–51.
- (65) Olerile, L. D.; Liu, Y.; Zhang, B.; Wang, T.; Mu, S.; Zhang, J.; Selotlegeng, L.; Zhang, N. Near-Infrared Mediated Quantum Dots and Paclitaxel Co-Loaded Nanostructured Lipid Carriers for Cancer Theragnostic. *Colloids Surfaces B Biointerfaces* 2017, 150, 121–130.
- (66) Le Broc-Ryckewaert, D.; Carpentier, R.; Lipka, E.; Daher, S.; Vaccher, C.; Betbeder, D.; Furman, C. Development of Innovative Paclitaxel-Loaded Small PLGA Nanoparticles: Study of Their Antiproliferative Activity and Their Molecular Interactions on Prostatic Cancer Cells. *Int. J. Pharm.* 2013, 454 (2), 712–719. https://doi.org/10.1016/j.ijpharm.2013.05.018.
- (67) Kunzmann, A.; Andersson, B.; Thurnherr, T.; Krug, H.; Scheynius, A.; Fadeel, B.
 Toxicology of Engineered Nanomaterials: Focus on Biocompatibility, Biodistribution and Biodegradation. *Biochim. Biophys. Acta Gen. Subj.* 2011, 1810 (3), 361–373.

- https://doi.org/https://doi.org/10.1016/j.bbagen.2010.04.007.
- (68) Chen, K.; Mitra, S. Incorporation of Functionalized Carbon Nanotubes into Hydrophobic Drug Crystals for Enhancing Aqueous Dissolution. *Colloids Surf. B. Biointerfaces* 2019, 173, 386–391. https://doi.org/10.1016/j.colsurfb.2018.09.080.
- (69) Lotfi, M.; Morsali, A.; Bozorgmehr, M. R. Comprehensive Quantum Chemical Insight into the Mechanistic Understanding of the Surface Functionalization of Carbon Nanotube as a Nanocarrier with Cladribine Anticancer Drug. *Appl. Surf. Sci.* 2018, 462, 720–729. https://doi.org/https://doi.org/10.1016/j.apsusc.2018.08.151.
- (70) Wei, C.; Dong, X.; Zhang, Y.; Liang, J.; Yang, A.; Zhu, D.; Liu, T.; Kong, D.; Lv, F. Simultaneous Fluorescence Imaging Monitoring of the Programmed Release of Dual Drugs from a Hydrogel-Carbon Nanotube Delivery System. *Sensors Actuators B Chem.*2018, 273, 264–275. https://doi.org/https://doi.org/10.1016/j.snb.2018.06.064.
- (71) Li, H.; Sun, X.; Li, Y.; Li, B.; Liang, C.; Wang, H. Preparation and Properties of Carbon Nanotube (Fe)/Hydroxyapatite Composite as Magnetic Targeted Drug Delivery Carrier. Mater. Sci. & Eng. C, Mater. Biol. Appl. 2019, 97, 222–229. https://doi.org/10.1016/j.msec.2018.11.042.
- (72) Karthika, V.; Kaleeswarran, P.; Gopinath, K.; Arumugam, A.; Govindarajan, M.; Alharbi, N. S.; Khaled, J. M.; Al-Anbr, M. N.; Benelli, G. Biocompatible Properties of Nano-Drug Carriers Using TiO2-Au Embedded on Multiwall Carbon Nanotubes for Targeted Drug Delivery. *Mater. Sci. & C, Mater. Biol. Appl.* 2018, 90, 589–601. https://doi.org/10.1016/j.msec.2018.04.094.
- (73) Prencipe, G.; Tabakman, S. M.; Welsher, K.; Liu, Z.; Goodwin, A. P.; Zhang, L.; Henry, J.; Dai, H. PEG Branched Polymer for Functionalization of Nanomaterials with Ultralong

- Blood Circulation. *J. Am. Chem. Soc.* **2009**, *131* (13), 4783–4787. https://doi.org/10.1021/ja809086q.
- (74) Kavyani, S.; Dadvar, M.; Modarress, H.; Amjad-Iranagh, S. Molecular Perspective Mechanism for Drug Loading on Carbon Nanotube–Dendrimer: A Coarse-Grained Molecular Dynamics Study. J. Phys. Chem. B 2018, 122 (33), 7956–7969. https://doi.org/10.1021/acs.jpcb.8b04434.
- (75) Wahsner, J.; Gale, E. M.; Rodríguez-Rodríguez, A.; Caravan, P. Chemistry of MRI Contrast Agents: Current Challenges and New Frontiers. *Chem. Rev.* 2019, 119 (2), 957– 1057. https://doi.org/10.1021/acs.chemrev.8b00363.
- (76) Smith, A. M.; Duan, H.; Mohs, A. M.; Nie, S. Bioconjugated Quantum Dots for in Vivo Molecular and Cellular Imaging. *Adv. Drug Deliv. Rev.* 2008, 60 (11), 1226–1240. https://doi.org/10.1016/j.addr.2008.03.015.
- (77) Wunderbaldinger, P.; Josephson, L.; Bremer, C.; Moore, A.; Weissleder, R. Detection of Lymph Node Metastases by Contrast-Enhanced MRI in an Experimental Model. *Magn. Reson. Med.* 2002, 47 (2), 292–297. https://doi.org/10.1002/mrm.10068.
- (78) Thorek, D. L. J.; Tsourkas, A. Size, Charge and Concentration Dependent Uptake of Iron Oxide Particles by Non-Phagocytic Cells. *Biomaterials* 2008, 29 (26), 3583–3590. https://doi.org/10.1016/j.biomaterials.2008.05.015.
- (79) Daraee, H.; Eatemadi, A.; Abbasi, E.; Fekri Aval, S.; Kouhi, M.; Akbarzadeh, A. Application of Gold Nanoparticles in Biomedical and Drug Delivery. *Artif. cells, nanomedicine, Biotechnol.* 2016, 44 (1), 410–422.
 https://doi.org/10.3109/21691401.2014.955107.
- (80) Cole, L. E.; Ross, R. D.; Tilley, J. M. R.; Vargo-Gogola, T.; Roeder, R. K. Gold

- Nanoparticles as Contrast Agents in X-Ray Imaging and Computed Tomography. *Nanomedicine* **2015**, *10* (2), 321–341. https://doi.org/10.2217/nnm.14.171.
- (81) Bae, K. H.; Lee, K.; Kim, C.; Park, T. G. Surface Functionalized Hollow Manganese Oxide Nanoparticles for Cancer Targeted SiRNA Delivery and Magnetic Resonance Imaging. *Biomaterials* 2011, 32 (1), 176–184. https://doi.org/10.1016/j.biomaterials.2010.09.039.
- (82) Huang, P.; Bao, L.; Zhang, C.; Lin, J.; Luo, T.; Yang, D.; He, M.; Li, Z.; Gao, G.; Gao, B.; Fu, S.; Cui, D. Folic Acid-Conjugated Silica-Modified Gold Nanorods for X-Ray/CT Imaging-Guided Dual-Mode Radiation and Photo-Thermal Therapy. *Biomaterials* 2011, 32 (36), 9796–9809. https://doi.org/https://doi.org/10.1016/j.biomaterials.2011.08.086.
- (83) Prabaharan, M.; Grailer, J. J.; Pilla, S.; Steeber, D. A.; Gong, S. Gold Nanoparticles with a Monolayer of Doxorubicin-Conjugated Amphiphilic Block Copolymer for Tumor-Targeted Drug Delivery. *Biomaterials* 2009, 30 (30), 6065–6075. https://doi.org/10.1016/j.biomaterials.2009.07.048.
- (84) Lee, J.-H.; Lee, K.; Moon, S. H.; Lee, Y.; Park, T. G.; Cheon, J. All-in-One Target-Cell-Specific Magnetic Nanoparticles for Simultaneous Molecular Imaging and SiRNA Delivery. *Angew. Chem. Int. Ed. Engl.* 2009, 48 (23), 4174–4179. https://doi.org/10.1002/anie.200805998.
- (85) Ling, Y.; Wei, K.; Luo, Y.; Gao, X.; Zhong, S. Dual Docetaxel/Superparamagnetic Iron Oxide Loaded Nanoparticles for Both Targeting Magnetic Resonance Imaging and Cancer Therapy. *Biomaterials* 2011, 32 (29), 7139–7150. https://doi.org/10.1016/j.biomaterials.2011.05.089.
- (86) Roy, I.; Ohulchanskyy, T. Y.; Pudavar, H. E.; Bergey, E. J.; Oseroff, A. R.; Morgan, J.;

Dougherty, T. J.; Prasad, P. N. Ceramic-Based Nanoparticles Entrapping Water-Insoluble Photosensitizing Anticancer Drugs: A Novel Drug-Carrier System for Photodynamic Therapy. *J. Am. Chem. Soc.* **2003**, *125* (26), 7860–7865. https://doi.org/10.1021/ja0343095.

- (87) Park, J.-H.; Gu, L.; von Maltzahn, G.; Ruoslahti, E.; Bhatia, S. N.; Sailor, M. J. Biodegradable Luminescent Porous Silicon Nanoparticles for in Vivo Applications. *Nat. Mater.* **2009**, *8* (4), 331–336. https://doi.org/10.1038/nmat2398.
- (88) Pantarotto, D.; Singh, R.; McCarthy, D.; Erhardt, M.; Briand, J.-P.; Prato, M.; Kostarelos, K.; Bianco, A. Functionalized Carbon Nanotubes for Plasmid DNA Gene Delivery.
 Angew. Chem. Int. Ed. Engl. 2004, 43 (39), 5242–5246.
 https://doi.org/10.1002/anie.200460437.
- (89) Liu, Z.; Chen, K.; Davis, C.; Sherlock, S.; Cao, Q.; Chen, X.; Dai, H. Drug Delivery with Carbon Nanotubes for in Vivo Cancer Treatment. *Cancer Res.* **2008**, *68* (16), 6652–6660. https://doi.org/10.1158/0008-5472.CAN-08-1468.
- (90) Savla, R.; Taratula, O.; Garbuzenko, O.; Minko, T. Tumor Targeted Quantum Dot-Mucin 1 Aptamer-Doxorubicin Conjugate for Imaging and Treatment of Cancer. *J. Control.* release Off. J. Control. Release Soc. 2011, 153 (1), 16–22. https://doi.org/10.1016/j.jconrel.2011.02.015.
- (91) Yuan, J.; Guo, W.; Yang, X.; Wang, E. Anticancer Drug–DNA Interactions Measured Using a Photoinduced Electron-Transfer Mechanism Based on Luminescent Quantum Dots. Anal. Chem. 2009, 81 (1), 362–368. https://doi.org/10.1021/ac801533u.
- (92) Jain, K. K. Nanodiagnostics: Application of Nanotechnology in Molecular Diagnostics. *Expert Rev. Mol. Diagn.* **2003**, *3* (2), 153–161. https://doi.org/10.1586/14737159.3.2.153.

(93) Fortina, P.; Kricka, L. J.; Surrey, S.; Grodzinski, P. Nanobiotechnology: The Promise and Reality of New Approaches to Molecular Recognition. *Trends Biotechnol.* **2005**, *23* (4), 168–173. https://doi.org/10.1016/j.tibtech.2005.02.007.

- (94) Stupp, S. I.; Donners, J. J. J. M.; Li, L.; Mata, A. Expanding Frontiers in Biomaterials.
 MRS Bull. 2005, 30 (11), 864–873. https://doi.org/10.1557/mrs2005.276.
- (95) Wu, Z.; Bidlingmaier, M.; Liu, C.; De Souza, E. B.; Tschöp, M.; Morrison, K. M.; Strasburger, C. J. Quantification of the Soluble Leptin Receptor in Human Blood by Ligand-Mediated Immunofunctional Assay. *J. Clin. Endocrinol. Metab.* 2002, 87 (6), 2931–2939. https://doi.org/10.1210/jcem.87.6.8610.
- (96) Yang, A. S.; Estécio, M. R. H.; Doshi, K.; Kondo, Y.; Tajara, E. H.; Issa, J.-P. J. A Simple Method for Estimating Global DNA Methylation Using Bisulfite PCR of Repetitive DNA Elements. *Nucleic Acids Res.* 2004, 32 (3), e38. https://doi.org/10.1093/nar/gnh032.
- (97) Schultz, S.; Smith, D. R.; Mock, J. J.; Schultz, D. A. Single-Target Molecule Detection with Nonbleaching Multicolor Optical Immunolabels. *Proc. Natl. Acad. Sci.* **2000**, *97* (3), 996–1001. https://doi.org/10.1073/pnas.97.3.996.
- (98) Storhoff, J. J.; Lucas, A. D.; Garimella, V.; Bao, Y. P.; Müller, U. R. Homogeneous Detection of Unamplified Genomic DNA Sequences Based on Colorimetric Scatter of Gold Nanoparticle Probes. *Nat. Biotechnol.* 2004, 22 (7), 883–887. https://doi.org/10.1038/nbt977.
- (99) Storhoff, J. J.; Marla, S. S.; Bao, P.; Hagenow, S.; Mehta, H.; Lucas, A.; Garimella, V.; Patno, T.; Buckingham, W.; Cork, W.; Müller, U. R. Gold Nanoparticle-Based Detection of Genomic DNA Targets on Microarrays Using a Novel Optical Detection System.
 Biosens. Bioelectron. 2004, 19 (8), 875–883. https://doi.org/10.1016/j.bios.2003.08.014.

(100) Park, S.-J.; Taton, T. A.; Mirkin, C. A. Array-Based Electrical Detection of DNA with Nanoparticle Probes. *Science* 2002, 295 (5559), 1503–1506. https://doi.org/10.1126/science.1067003.

- (101) Chan, W. C.; Nie, S. Quantum Dot Bioconjugates for Ultrasensitive Nonisotopic Detection. *Science* 1998, 281 (5385), 2016–2018.
 https://doi.org/10.1126/science.281.5385.2016.
- (102) Bruchez, M. J.; Moronne, M.; Gin, P.; Weiss, S.; Alivisatos, A. P. Semiconductor Nanocrystals as Fluorescent Biological Labels. *Science* 1998, 281 (5385), 2013–2016. https://doi.org/10.1126/science.281.5385.2013.
- (103) Alivisatos, A. P. Semiconductor Clusters, Nanocrystals, and Quantum Dots. *Science* (80-.
). 1996, 271 (5251), 933–937. https://doi.org/10.1126/science.271.5251.933.
- (104) Nirmal, M.; Brus, L. Luminescence Photophysics in Semiconductor Nanocrystals. *Acc. Chem. Res.* **1999**, *32* (5), 407–414. https://doi.org/10.1021/ar9700320.
- (105) Chong, Y.; Ma, Y.; Shen, H.; Tu, X.; Zhou, X.; Xu, J.; Dai, J.; Fan, S.; Zhang, Z. The in Vitro and in Vivo Toxicity of Graphene Quantum Dots. *Biomaterials* **2014**, *35* (19), 5041–5048. https://doi.org/10.1016/j.biomaterials.2014.03.021.
- (106) Molkenova, A.; Amangeldinova, Y.; Aben, D.; Sayatova, S.; Atabaev, T. S. Quick Synthesis of Fluorescent Nitrogen-Doped Carbon Nanoparticles for Selective and Sensitive Fe(III) Detection in Water. Sens. Bio-Sensing Res. 2019, 23, 100271. https://doi.org/https://doi.org/10.1016/j.sbsr.2019.100271.
- (107) Huh, A. J.; Kwon, Y. J. "Nanoantibiotics": A New Paradigm for Treating Infectious

 Diseases Using Nanomaterials in the Antibiotics Resistant Era. J. Control. release Off. J.

 Control. Release Soc. 2011, 156 (2), 128–145.

- https://doi.org/10.1016/j.jconrel.2011.07.002.
- (108) Chatzimitakos, T. G.; Stalikas, C. D. Qualitative Alterations of Bacterial Metabolome after Exposure to Metal Nanoparticles with Bactericidal Properties: A Comprehensive Workflow Based on (1)H NMR, UHPLC-HRMS, and Metabolic Databases. *J. Proteome Res.* **2016**, *15* (9), 3322–3330. https://doi.org/10.1021/acs.jproteome.6b00489.
- (109) Zhao, L.; Ashraf, M. A. Influence of Silver-Hydroxyapatite Nanocomposite Coating on Biofilm Formation of Joint Prosthesis and Its Mechanism. West Indian Med. J. 2015, 64 (5), 506–513. https://doi.org/10.7727/wimj.2016.179.
- (110) Li, H.; Chen, Q.; Zhao, J.; Urmila, K. Enhancing the Antimicrobial Activity of Natural Extraction Using the Synthetic Ultrasmall Metal Nanoparticles. *Sci. Rep.* **2015**, *5* (1), 11033. https://doi.org/10.1038/srep11033.
- (111) Armentano, I.; Arciola, C. R.; Fortunati, E.; Ferrari, D.; Mattioli, S.; Amoroso, C. F.; Rizzo, J.; Kenny, J. M.; Imbriani, M.; Visai, L. The Interaction of Bacteria with Engineered Nanostructured Polymeric Materials: A Review. *Scientific World Journal*. 2014, 2014, 410423. https://doi.org/10.1155/2014/410423.
- (112) Luan, B.; Huynh, T.; Zhou, R. Complete Wetting of Graphene by Biological Lipids.

 Nanoscale 2016, 8 (10), 5750–5754. https://doi.org/10.1039/C6NR00202A.
- (113) Xu, Y.; Wei, M.-T.; Ou-Yang, H. D.; Walker, S. G.; Wang, H. Z.; Gordon, C. R.; Guterman, S.; Zawacki, E.; Applebaum, E.; Brink, P. R.; Rafailovich, M.; Mironava, T. Exposure to TiO2 Nanoparticles Increases Staphylococcus Aureus Infection of HeLa Cells. J. Nanobiotechnology 2016, 14, 34. https://doi.org/10.1186/s12951-016-0184-y.
- (114) Yang, W.; Shen, C.; Ji, Q.; An, H.; Wang, J.; Liu, Q.; Zhang, Z. Food Storage Material Silver Nanoparticles Interfere with DNA Replication Fidelity and Bind with DNA.

- Nanotechnology **2009**, 20 (8), 85102. https://doi.org/10.1088/0957-4484/20/8/085102.
- (115) Gurunathan, S.; Han, J. W.; Dayem, A. A.; Eppakayala, V.; Kim, J.-H. Oxidative Stress-Mediated Antibacterial Activity of Graphene Oxide and Reduced Graphene Oxide in Pseudomonas Aeruginosa. *Int. J. Nanomedicine* 2012, 7, 5901–5914. https://doi.org/10.2147/IJN.S37397.
- (116) Zakharova, O. V; Godymchuk, A. Y.; Gusev, A. A.; Gulchenko, S. I.; Vasyukova, I. A.; Kuznetsov, D. V. Considerable Variation of Antibacterial Activity of Cu Nanoparticles Suspensions Depending on the Storage Time, Dispersive Medium, and Particle Sizes. *Biomed Res. Int.* 2015, 2015, 412530. https://doi.org/10.1155/2015/412530.
- (117) Leung, Y. H.; Ng, A. M. C.; Xu, X.; Shen, Z.; Gethings, L. A.; Wong, M. T.; Chan, C. M. N.; Guo, M. Y.; Ng, Y. H.; Djurišić, A. B.; Lee, P. K. H.; Chan, W. K.; Yu, L. H.; Phillips, D. L.; Ma, A. P. Y.; Leung, F. C. C. Mechanisms of Antibacterial Activity of MgO: Non-ROS Mediated Toxicity of MgO Nanoparticles towards Escherichia Coli. Small 2014, 10 (6), 1171–1183. https://doi.org/10.1002/smll.201302434.
- (118) Qiao, Z. A.; Wang, Y.; Gao, Y.; Li, H.; Dai, T.; Liu, Y.; Huo, Q. Commercially Activated Carbon as the Source for Producing Multicolor Photoluminescent Carbon Dots by Chemical Oxidation. *Chem. Commun.* **2010**, *46* (46), 8812–8814. https://doi.org/10.1039/c0cc02724c.
- (119) Yang, Y.; Cui, J.; Zheng, M.; Hu, C.; Tan, S.; Xiao, Y.; Yang, Q.; Liu, Y. One-Step Synthesis of Amino-Functionalized Fluorescent Carbon Nanoparticles by Hydrothermal Carbonization of Chitosan. *Chem. Commun.* **2012**, *48* (3), 380–382. https://doi.org/10.1039/c1cc15678k.
- (120) Liu, H.; Li, Z.; Sun, Y.; Geng, X.; Hu, Y.; Meng, H.; Ge, J.; Qu, L. Synthesis of

Luminescent Carbon Dots with Ultrahigh Quantum Yield and Inherent Folate Receptor-Positive Cancer Cell Targetability. *Sci. Rep.* **2018**, 8 (1), 1086. https://doi.org/10.1038/s41598-018-19373-3.

- (121) Zhang, Y.; Ye, A.; Yao, Y.; Yao, C. A Sensitive Near-Infrared Fluorescent Probe for Detecting Heavy Metal Ag⁺ in Water Samples. *Sensors (Basel)*. **2019**, *19* (2). https://doi.org/10.3390/s19020247.
- (122) Cao, W.; Wu, Y.; Li, X.; Jiang, X.; Zhang, Y.; Zhan, Y.; Sun, Z. One-Pot Synthesis of Double Silane-Functionalized Carbon Dots with Tunable Emission and Excellent Coating Properties for WLEDs Application. *Nanotechnology* 2022, 33 (11), 115703. https://doi.org/10.1088/1361-6528/ac4067.
- (123) Gong, N.; Wang, H.; Li, S.; Deng, Y.; Chen, X.; Ye, L.; Gu, W. Microwave-Assisted Polyol Synthesis of Gadolinium-Doped Green Luminescent Carbon Dots as a Bimodal Nanoprobe. *Langmuir* **2014**, *30* (36), 10933–10939. https://doi.org/10.1021/la502705g.
- (124) Du, F.; Zeng, F.; Ming, Y.; Wu, S. Carbon Dots-Based Fluorescent Probes for Sensitive and Selective Detection of Iodide. *Microchim. Acta* **2013**, *180* (5–6), 453–460. https://doi.org/DOI:101007/s00604-013-0954-2.
- (125) Wang, X.; Qu, K.; Xu, B.; Ren, J.; Qu, X. Microwave Assisted One-Step Green Synthesis of Cell-Permeable Multicolor Photoluminescent Carbon Dots without Surface Passivation Reagents. J. Mater. Chem. 2011, 21 (8), 2445–2450.
 https://doi.org/10.1039/C0JM02963G.
- (126) Liu, J.; Lu, S.; Tang, Q.; Zhang, K.; Yu, W.; Sun, H.; Yang, B. One-Step Hydrothermal Synthesis of Photoluminescent Carbon Nanodots with Selective Antibacterial Activity against Porphyromonas Gingivalis. *Nanoscale* **2017**, *9* (21), 7135–7142.

- https://doi.org/10.1039/C7NR02128C.
- (127) Li, P.; Liu, S.; Cao, W.; Zhang, G.; Yang, X.; Gong, X.; Xing, X. Low-Toxicity Carbon Quantum Dots Derived from Gentamicin Sulfate to Combat Antibiotic Resistance and Eradicate Mature Biofilms. *Chem. Commun.* **2020**, *56* (15), 2316–2319. https://doi.org/10.1039/C9CC09223D.
- (128) Lu, S.; Liu, L.; Wang, H.; Zhao, W.; Li, Z.; Qu, Z.; Li, J.; Sun, T.; Wang, T.; Sui, G. Synthesis of Dual Functional Gallic-Acid-Based Carbon Dots for Bioimaging and Antitumor Therapy. *Biomater. Sci.* 2019, 7 (8), 3258–3265.
 https://doi.org/10.1039/C9BM00570F.
- (129) Zhang, F.; Zhang, M.; Zheng, X.; Tao, S.; Zhang, Z.; Sun, M.; Song, Y.; Zhang, J.; Shao, D.; He, K.; Li, J.; Yang, B.; Chen, L. Berberine-Based Carbon Dots for Selective and Safe Cancer Theranostics. *RSC Adv.* 2018, 8 (3), 1168–1173.
 https://doi.org/10.1039/C7RA12069A.
- (130) Lin, C.-J.; Chang, L.; Chu, H.-W.; Lin, H.-J.; Chang, P.-C.; Wang, R. Y. L.; Unnikrishnan, B.; Mao, J.-Y.; Chen, S.-Y.; Huang, C.-C. High Amplification of the Antiviral Activity of Curcumin through Transformation into Carbon Quantum Dots. *Small* **2019**, *15* (41), e1902641. https://doi.org/10.1002/smll.201902641.
- (131) Tong, T.; Hu, H.; Zhou, J.; Deng, S.; Zhang, X.; Tang, W.; Fang, L.; Xiao, S.; Liang, J. Glycyrrhizic-Acid-Based Carbon Dots with High Antiviral Activity by Multisite Inhibition Mechanisms. *Small* 2020, *16* (13), e1906206.
 https://doi.org/10.1002/smll.201906206.
- (132) Chen, R.; Liu, G.; Sun, X.; Cao, X.; He, W.; Lin, X.; Liu, Q.; Zhao, J.; Pang, Y.; Li, B.; Qin, A. Chitosan Derived Nitrogen-Doped Carbon Dots Suppress Osteoclastic Osteolysis

- via Downregulating ROS. *Nanoscale* **2020**, *12* (30), 16229–16244. https://doi.org/10.1039/D0NR02848G.
- (133) Tripathi, S. K.; Kaur, G.; Khurana, R. K.; Kapoor, S.; Singh, B. Quantum Dots and Their Potential Role in Cancer Theranostics. *Crit. Rev. Ther. Drug Carrier Syst.* **2015**, *32* (6), 461–502. https://doi.org/10.1615/critrevtherdrugcarriersyst.2015012360.
- (134) Luo, G.; Long, J.; Zhang, B.; Liu, C.; Ji, S.; Xu, J.; Yu, X.; Ni, Q. Quantum Dots in Cancer Therapy. *Expert Opin. Drug Deliv.* **2012**, *9* (1), 47–58. https://doi.org/10.1517/17425247.2012.638624.
- (135) Jain, M. P.; Vaisheva, F.; Maysinger, D. Metalloestrogenic Effects of Quantum Dots.

 Nanomedicine (Lond). 2012, 7 (1), 23–37. https://doi.org/10.2217/nnm.11.102.
- (136) Qu, M.; Qiu, Y.; Lv, R.; Yue, Y.; Liu, R.; Yang, F.; Wang, D.; Li, Y. Exposure to MPA-Capped CdTe Quantum Dots Causes Reproductive Toxicity Effects by Affecting Oogenesis in Nematode Caenorhabditis Elegans. *Ecotoxicol. Environ. Saf.* **2019**, *173*, 54–62. https://doi.org/10.1016/j.ecoenv.2019.02.018.
- (137) Bosi, S.; Da Ros, T.; Spalluto, G.; Prato, M. Fullerene Derivatives: An Attractive Tool for Biological Applications. *Eur. J. Med. Chem.* 2003, 38 (11–12), 913–923. https://doi.org/10.1016/j.ejmech.2003.09.005.
- (138) Pagona, G.; Tagmatarchis, N. Carbon Nanotubes: Materials for Medicinal Chemistry and Biotechnological Applications. *Curr. Med. Chem.* **2006**, *13* (15), 1789–1798. https://doi.org/10.2174/092986706777452524.
- (139) Talamini, L.; Violatto, M. B.; Cai, Q.; Monopoli, M. P.; Kantner, K.; Krpetić, Ž.; Perez-Potti, A.; Cookman, J.; Garry, D.; Silveira, C. P.; Boselli, L.; Pelaz, B.; Serchi, T.; Cambier, S.; Gutleb, A. C.; Feliu, N.; Yan, Y.; Salmona, M.; Parak, W. J.; Dawson, K. A.;

- Bigini, P. Influence of Size and Shape on the Anatomical Distribution of Endotoxin-Free Gold Nanoparticles. *ACS Nano* **2017**, *11* (6), 5519–5529. https://doi.org/10.1021/acsnano.7b00497.
- (140) Zhao, Y.; Sun, X.; Zhang, G.; Trewyn, B. G.; Slowing, I. I.; Lin, V. S. Y. Interaction of Mesoporous Silica Nanoparticles with Human Red Blood Cell Membranes: Size and Surface Effects. ACS Nano 2011, 5 (2), 1366–1375. https://doi.org/10.1021/nn103077k.
- (141) Kong, B.; Seog, J. H.; Graham, L. M.; Lee, S. B. Experimental Considerations on the Cytotoxicity of Nanoparticles. *Nanomedicine* 2011, 6 (5), 929–941. https://doi.org/10.2217/nnm.11.77.
- (142) Hamilton, R. F.; Wu, N.; Porter, D.; Buford, M.; Wolfarth, M.; Holian, A. Particle Length-Dependent Titanium Dioxide Nanomaterials Toxicity and Bioactivity. *Part. Fibre Toxicol.* 2009, 6 (1), 35. https://doi.org/10.1186/1743-8977-6-35.
- (143) Champion, J. A.; Mitragotri, S. Role of Target Geometry in Phagocytosis. *Proc. Natl.* Acad. Sci. U. S. A. 2006, 103 (13), 4930–4934. https://doi.org/10.1073/pnas.0600997103.
- (144) Park, K. H.; Chhowalla, M.; Iqbal, Z.; Sesti, F. Single-Walled Carbon Nanotubes Are a New Class of Ion Channel Blockers. *J. Biol. Chem.* **2003**, 278 (50), 50212–50216. https://doi.org/10.1074/jbc.M310216200.
- (145) Schaeublin, N. M.; Braydich-Stolle, L. K.; Schrand, A. M.; Miller, J. M.; Hutchison, J.; Schlager, J. J.; Hussain, S. M. Surface Charge of Gold Nanoparticles Mediates Mechanism of Toxicity. *Nanoscale* 2011, 3 (2), 410–420. https://doi.org/10.1039/c0nr00478b.
- (146) El Badawy, A. M.; Silva, R. G.; Morris, B.; Scheckel, K. G.; Suidan, M. T.; Tolaymat, T.M. Surface Charge-Dependent Toxicity of Silver Nanoparticles. *Environ. Sci. Technol.*

- **2011**, 45 (1), 283–287. https://doi.org/10.1021/es1034188.
- (147) Arami, H.; Khandhar, A.; Liggitt, D.; Krishnan, K. M. In Vivo Delivery, Pharmacokinetics, Biodistribution and Toxicity of Iron Oxide Nanoparticles. *Chem. Soc. Rev.* 2015, 44 (23), 8576–8607. https://doi.org/10.1039/c5cs00541h.
- (148) Kim, A. L.; Athar, M.; Bickers, D. R.; Gautier, J. Stage-Specific Alterations of Cyclin Expression During UVB-Induced Murine Skin Tumor Development¶. *Photochem.*Photobiol. 2002, 75 (1), 58. https://doi.org/10.1562/0031-8655(2002)075<0058:ssaoce>2.0.co;2.
- (149) Chaudhary, G.; Saini, M. R.; Goyal, P. K. Chemopreventive Potential of Aloe Vera against 7,12-Dimethylbenz(a) Anthracene- Induced Skin Papillomagenesis in Mice. *Integr. Cancer Ther.* **2007**, *6* (4), 405–412. https://doi.org/10.1177/1534735407309079.
- (150) Azuine, M. A.; Amonkar, A. J.; Bhide, S. V. Chemopreventive Efficacy of Betel Leaf Extract and Its Constituents on 7,12-Dimethylbenz(a)Anthracene Induced Carcinogenesis and Their Effect on Drug Detoxification System in Mouse Skin. *Indian J. Exp. Biol.* 1991, 29 (4), 346–351.
- (151) Fahmy, H.; Zjawiony, J. K.; Konoshima, T.; Tokuda, H.; Khan, S.; Khalifa, S. Potent Skin Cancer Chemopreventing Activity of Some Novel Semi-Synthetic Cembranoids from Marine Sources. *Marine Drugs*. 2006, pp 28–36. https://doi.org/10.3390/md402028.
- (152) Brennan, K.; Offiah, G.; McSherry, E. A.; Hopkins, A. M. Tight Junctions: A Barrier to the Initiation and Progression of Breast Cancer? *J. Biomed. Biotechnol.* 2010, 2010, 460607. https://doi.org/10.1155/2010/460607.
- (153) Zhang, B.; Pan, X.; Cobb, G. P.; Anderson, T. A. MicroRNAs as Oncogenes and Tumor Suppressors. *Dev. Biol.* **2007**, *302* (1), 1–12. https://doi.org/10.1016/j.ydbio.2006.08.028.

(154) Hanahan, D.; Weinberg, R. A. Hallmarks of Cancer: The next Generation. *Cell* 2011, 144(5), 646–674. https://doi.org/10.1016/j.cell.2011.02.013.

- (155) Kreeger, P. K.; Lauffenburger, D. A. Cancer Systems Biology: A Network Modeling Perspective. *Carcinogenesis* **2010**, *31* (1), 2–8. https://doi.org/10.1093/carcin/bgp261.
- (156) Tran, P. T.; Fan, A. C.; Bendapudi, P. K.; Koh, S.; Komatsubara, K.; Chen, J.; Horng, G.; Bellovin, D. I.; Giuriato, S.; Wang, C. S.; Whitsett, J. A.; Felsher, D. W. Combined Inactivation of MYC and K-Ras Oncogenes Reverses Tumorigenesis in Lung Adenocarcinomas and Lymphomas. *PLoS One* 2008, *3* (5), e2125. https://doi.org/10.1371/journal.pone.0002125.
- (157) Hanahan, D.; Weinberg, R. A. The Hallmarks of Cancer. *Cell* **2000**, *100* (1), 57–70. https://doi.org/10.1016/s0092-8674(00)81683-9.
- (158) DeBerardinis, R. J.; Cheng, T. Q's next: The Diverse Functions of Glutamine in Metabolism, Cell Biology and Cancer. *Oncogene* **2010**, 29 (3), 313–324. https://doi.org/10.1038/onc.2009.358.
- (159) Blagosklonny, M. V. Cell Immortality and Hallmarks of Cancer. *Cell Cycle* **2003**, *2* (4), 296–299.
- (160) Anand, P.; Kunnumakkara, A. B.; Sundaram, C.; Harikumar, K. B.; Tharakan, S. T.; Lai,
 O. S.; Sung, B.; Aggarwal, B. B. Cancer Is a Preventable Disease That Requires Major
 Lifestyle Changes. *Pharm. Res.* 2008, 25 (9), 2097–2116. https://doi.org/10.1007/s11095-008-9661-9.
- (161) Pomerantz, M. M.; Freedman, M. L. The Genetics of Cancer Risk. *Cancer J.* 2011, 17 (6), 416–422. https://doi.org/10.1097/PPO.0b013e31823e5387.
- (162) Liao, J. B. Viruses and Human Cancer. *Yale J. Biol. Med.* **2006**, 79 (3–4), 115–122.

(163) Dich, J.; Zahm, S. H.; Hanberg, A.; Adami, H. O. Pesticides and Cancer. *Cancer Causes Control* **1997**, *8* (3), 420–443. https://doi.org/10.1023/a:1018413522959.

- (164) Breast Cancer India. Breast Cancer Statistics: India versus The World. 2018, 1–9.
- (165) Yang, Y.; Zhang, M.; Song, H.; Yu, C. Silica-Based Nanoparticles for Biomedical Applications: From Nanocarriers to Biomodulators. *Acc. Chem. Res.* **2020**, *53* (8), 1545–1556. https://doi.org/10.1021/acs.accounts.0c00280.
- (166) Ali, Y. F.; Cucinotta, F. A.; Ning-Ang, L.; Zhou, G. Cancer Risk of Low Dose Ionizing Radiation. *Front. Phys.* **2020**, 8. https://doi.org/10.3389/fphy.2020.00234.
- (167) Liu, H.; Ye, T.; Mao, C. Fluorescent Carbon Nanoparticles Derived from Candle Soot.
 Angew. Chemie Int. Ed. 2007, 46 (34), 6473–6475.
 https://doi.org/10.1002/anie.200701271.
- (168) Sun, Y. P.; Zhou, B.; Lin, Y.; Wang, W.; Fernando, K. A. S.; Pathak, P.; Meziani, M. J.; Harruff, B. A.; Wang, X.; Wang, H.; Luo, P. G.; Yang, H.; Kose, M. E.; Chen, B.; Veca, L. M.; Xie, S. Y. Quantum-Sized Carbon Dots for Bright and Colorful Photoluminescence. *J. Am. Chem. Soc.* 2006, 128 (24), 7756–7757.
 https://doi.org/10.1021/ja062677d.
- (169) Zhao, Q. L.; Zhang, Z. L.; Huang, B. H.; Peng, J.; Zhang, M.; Pang, D. W. Facile Preparation of Low Cytotoxicity Fluorescent Carbon Nanocrystals by Electrooxidation of Graphite. *Chem. Commun.* 2008, No. 41, 5116–5118. https://doi.org/10.1039/b812420e.
- (170) Xu, X.; Ray, R.; Gu, Y.; Ploehn, H. J.; Gearheart, L.; Raker, K.; Scrivens, W. A.
 Electrophoretic Analysis and Purification of Fluorescent Single-Walled Carbon Nanotube
 Fragments. J. Am. Chem. Soc. 2004, 126 (40), 12736–12737.
 https://doi.org/10.1021/ja040082h.

(171) Bourlinos, A. B.; Stassinopoulos, A.; Anglos, D.; Zboril, R.; Karakassides, M.; Giannelis,
 E. P. Surface Functionalized Carbogenic Quantum Dots. *Small* 2008, 4 (4), 455–458.
 https://doi.org/10.1002/smll.200700578.

- (172) Krysmann, M. J.; Kelarakis, A.; Dallas, P.; Giannelis, E. P. Formation Mechanism of Carbogenic Nanoparticles with Dual Photoluminescence Emission. *J. Am. Chem. Soc.*2012, 134 (2), 747–750. https://doi.org/10.1021/ja204661r.
- (173) Zhu, H.; Wang, X.; Li, Y.; Wang, Z.; Yang, F.; Yang, X. Microwave Synthesis of Fluorescent Carbon Nanoparticles with Electrochemiluminescence Properties. *Chem. Commun.* **2009**, No. 34, 5118–5120. https://doi.org/10.1039/b907612c.
- (174) Alagarsamy, K. N.; Mathan, S.; Yan, W.; Rafieerad, A.; Sekaran, S.; Manego, H.; Dhingra, S. Carbon Nanomaterials for Cardiovascular Theranostics: Promises and Challenges. *Bioactive Materials*. 2021, pp 2261–2280. https://doi.org/10.1016/j.bioactmat.2020.12.030.
- (175) Sun, X.; Lei, Y. Fluorescent Carbon Dots and Their Sensing Applications. *TrAC Trends Anal. Chem.* **2017**, 89 (C), 163–180. https://doi.org/10.1016/j.trac.2017.02.001.
- (176) Zhang, J.; Yu, S. H. Carbon Dots: Large-Scale Synthesis, Sensing and Bioimaging. *Mater. Today* **2016**, *19* (7), 382–393. https://doi.org/10.1016/j.mattod.2015.11.008.
- (177) Chen, P.; Ma, Y.; Zheng, Z.; Wu, C.; Wang, Y.; Liang, G. Facile Syntheses of Conjugated Polymers for Photothermal Tumour Therapy. *Nat. Commun.* **2019**, *10* (1), 1192. https://doi.org/10.1038/s41467-019-09226-6.
- (178) Bondeson, D.; Mathew, A.; Oksman, K. Optimization of the Isolation of Nanocrystals from Microcrystalline Celluloseby Acid Hydrolysis. *Cellulose* **2006**, *13* (2), 171–180. https://doi.org/10.1007/s10570-006-9061-4.

(179) Xing, Y.; Rao, J. Quantum Dot Bioconjugates for in Vitro Diagnostics & in Vivo Imaging. *Cancer Biomark.* **2008**, *4* (6), 307–319. https://doi.org/10.3233/cbm-2008-4603.

- (180) Baker, S. N.; Baker, G. A. Luminescent Carbon Nanodots: Emergent Nanolights. *Angew*. *Chemie Int. Ed.* **2010**, *49* (38), 6726–6744. https://doi.org/10.1002/anie.200906623.
- (181) Hong, G.; Diao, S.; Antaris, A. L.; Dai, H. Carbon Nanomaterials for Biological Imaging and Nanomedicinal Therapy. *Chem. Rev.* **2015**, *115* (19), 10816–10906. https://doi.org/10.1021/acs.chemrev.5b00008.
- (182) Yang, Z.; Li, Z.; Xu, M.; Ma, Y.; Zhang, J.; Su, Y.; Gao, F.; Wei, H.; Zhang, L.
 Controllable Synthesis of Fluorescent Carbon Dots and Their Detection Application as
 Nanoprobes. Nano-Micro Lett. 2013, 5 (4), 247–259. https://doi.org/10.1007/bf03353756.
- (183) Basu, N.; Mandal, D. Time-Resolved Photoluminescence of PH-Sensitive Carbon Dots. *Carbon N. Y.* **2019**, *144*, 500–508. https://doi.org/10.1016/j.carbon.2018.12.056.
- (184) Sciortino, A.; Cannizzo, A.; Messina, F. Carbon Nanodots: A Review—From the Current Understanding of the Fundamental Photophysics to the Full Control of the Optical Response. *C* **2018**, *4* (4), 67. https://doi.org/10.3390/c4040067.
- (185) Kozák, O.; Sudolská, M.; Pramanik, G.; Cígler, P.; Otyepka, M.; Zbořil, R.
 Photoluminescent Carbon Nanostructures. *Chem. Mater.* 2016, 28 (12), 4085–4128.
 https://doi.org/10.1021/acs.chemmater.6b01372.
- (186) Wei, J.; Shen, J.; Zhang, X.; Guo, S.; Pan, J.; Hou, X.; Zhang, H.; Wang, L.; Feng, B. Simple One-Step Synthesis of Water-Soluble Fluorescent Carbon Dots Derived from Paper Ash. *RSC Adv.* **2013**, *3* (32), 13119–13122. https://doi.org/10.1039/C3RA41751D.
- (187) Yuan, F.; Li, S.; Fan, Z.; Meng, X.; Fan, L.; Yang, S. Shining Carbon Dots: Synthesis and Biomedical and Optoelectronic Applications. *Nano Today* **2016**, *11* (5), 565–586.

- https://doi.org/10.1016/j.nantod.2016.08.006.
- (188) Namdari, P.; Negahdari, B.; Eatemadi, A. Synthesis, Properties and Biomedical Applications of Carbon-Based Quantum Dots: An Updated Review. *Biomed. Pharmacother.* **2017**, *87*, 209–222. https://doi.org/10.1016/j.biopha.2016.12.108.
- (189) Liu, Q.; Guo, B.; Rao, Z.; Zhang, B.; Gong, J. R. Strong Two-Photon-Induced Fluorescence from Photostable, Biocompatible Nitrogen-Doped Graphene Quantum Dots for Cellular and Deep-Tissue Imaging. *Nano Lett.* **2013**, *13* (6), 2436–2441. https://doi.org/10.1021/nl400368v.
- (190) Du, J.; Xu, N.; Fan, J.; Sun, W.; Peng, X. Carbon Dots for In Vivo Bioimaging and Theranostics. *Small* 2019, *15* (32), 1805087.
 https://doi.org/https://doi.org/10.1002/smll.201805087.
- (191) Carbonaro, C. M.; Corpino, R.; Salis, M.; Mocci, F.; Thakkar, S. V.; Olla, C.; Ricci, P. C.
 On the Emission Properties of Carbon Dots: Reviewing Data and Discussing Models. *C*2019, 5 (4). https://doi.org/10.3390/c5040060.
- (192) Hamd-Ghadareh, S.; Salimi, A.; Fathi, F.; Bahrami, S. An Amplified Comparative Fluorescence Resonance Energy Transfer Immunosensing of CA125 Tumor Marker and Ovarian Cancer Cells Using Green and Economic Carbon Dots for Bio-Applications in Labeling, Imaging and Sensing. *Biosens. Bioelectron.* 2017, 96, 308–316. https://doi.org/10.1016/j.bios.2017.05.003.
- (193) Ramanan, V.; Thiyagarajan, S. K.; Raji, K.; Suresh, R.; Sekar, R.; Ramamurthy, P.
 Outright Green Synthesis of Fluorescent Carbon Dots from Eutrophic Algal Blooms for In
 Vitro Imaging. ACS Sustain. Chem. Eng. 2016, 4 (9), 4724–4731.
 https://doi.org/10.1021/acssuschemeng.6b00935.

(194) Koutsogiannis, P.; Thomou, E.; Stamatis, H.; Gournis, D.; Rudolf, P. Advances in Fluorescent Carbon Dots for Biomedical Applications. *Adv. Phys. X* **2020**, *5* (1). https://doi.org/10.1080/23746149.2020.1758592.

- (195) Datta, K. K. R.; Kozák, O.; Ranc, V.; Havrdová, M.; Bourlinos, A. B.; Šafářová, K.; Holá, K.; Tománková, K.; Zoppellaro, G.; Otyepka, M.; Zbořil, R. Quaternized Carbon Dot-Modified Graphene Oxide for Selective Cell Labelling Controlled Nucleus and Cytoplasm Imaging. *Chem. Commun.* 2014, 50 (74), 10782–10785. https://doi.org/10.1039/C4CC02637C.
- (196) Kang, Y.-F.; Fang, Y.-W.; Li, Y.-H.; Li, W.; Yin, X.-B. Nucleus-Staining with Biomolecule-Mimicking Nitrogen-Doped Carbon Dots Prepared by a Fast Neutralization Heat Strategy. *Chem. Commun.* 2015, 51 (95), 16956–16959. https://doi.org/10.1039/C5CC06304C.
- (197) Hua, X.-W.; Bao, Y.-W.; Chen, Z.; Wu, F.-G. Carbon Quantum Dots with Intrinsic Mitochondrial Targeting Ability for Mitochondria-Based Theranostics. *Nanoscale* 2017, 9 (30), 10948–10960. https://doi.org/10.1039/C7NR03658B.
- (198) Alagarsamy, K. N.; Mathan, S.; Yan, W.; Rafieerad, A.; Sekaran, S.; Manego, H.; Dhingra, S. Carbon Nanomaterials for Cardiovascular Theranostics: Promises and Challenges. *Bioact. Mater.* 2021, 6 (8), 2261–2280. https://doi.org/10.1016/j.bioactmat.2020.12.030.
- (199) Sharma, A.; Das, J. Small Molecules Derived Carbon Dots: Synthesis and Applications in Sensing, Catalysis, Imaging, and Biomedicine. *J. Nanobiotechnology* **2019**, *17* (1), 92. https://doi.org/10.1186/s12951-019-0525-8.
- (200) Zare, H.; Ahmadi, S.; Ghasemi, A.; Ghanbari, M.; Rabiee, N.; Bagherzadeh, M.; Karimi,

- M.; Webster, T. J.; Hamblin, M. R.; Mostafavi, E. Carbon Nanotubes: Smart Drug/Gene Delivery Carriers. *Int. J. Nanomedicine* **2021**, *16*, 1681–1706. https://doi.org/10.2147/IJN.S299448.
- (201) Li, H.; Zhang, Y.; Wang, L.; Tian, J.; Sun, X. Nucleic Acid Detection Using Carbon Nanoparticles as a Fluorescent Sensing Platform. *Chem. Commun.* **2011**, *47* (3), 961–963. https://doi.org/10.1039/C0CC04326E.
- (202) Liu, J.; Li, J.; Jiang, Y.; Yang, S.; Tan, W.; Yang, R. Combination of π–π Stacking and Electrostatic Repulsion between Carboxylic Carbon Nanoparticles and Fluorescent Oligonucleotides for Rapid and Sensitive Detection of Thrombin. *Chem. Commun.* 2011, 47 (40), 11321–11323. https://doi.org/10.1039/C1CC14445F.
- (203) Lin, Z.; Xue, W.; Chen, H.; Lin, J.-M. Peroxynitrous-Acid-Induced Chemiluminescence of Fluorescent Carbon Dots for Nitrite Sensing. *Anal. Chem.* **2011**, *83* (21), 8245–8251. https://doi.org/10.1021/ac202039h.
- (204) Shi, W.; Wang, Q.; Long, Y.; Cheng, Z.; Chen, S.; Zheng, H.; Huang, Y. Carbon Nanodots as Peroxidase Mimetics and Their Applications to Glucose Detection. *Chem. Commun.* **2011**, *47* (23), 6695–6697. https://doi.org/10.1039/C1CC11943E.
- (205) Zhou, L.; Lin, Y.; Huang, Z.; Ren, J.; Qu, X. Carbon Nanodots as Fluorescence Probes for Rapid{,} Sensitive{,} and Label-Free Detection of Hg2+ and Biothiols in Complex Matrices. *Chem. Commun.* 2012, 48 (8), 1147–1149. https://doi.org/10.1039/C2CC16791C.
- (206) Kong, B.; Zhu, A.; Ding, C.; Zhao, X.; Li, B.; Tian, Y. Carbon Dot-Based Inorganic-Organic Nanosystem for Two-Photon Imaging and Biosensing of PH Variation in Living Cells and Tissues. *Adv. Mater.* **2012**, *24* (43), 5844–5848.

- https://doi.org/10.1002/adma.201202599.
- (207) Qu, K.; Wang, J.; Ren, J.; Qu, X. Carbon Dots Prepared by Hydrothermal Treatment of Dopamine as an Effective Fluorescent Sensing Platform for the Label-Free Detection of Iron(III) Ions and Dopamine. *Chem. A Eur. J.* **2013**, *19* (22), 7243–7249. https://doi.org/https://doi.org/10.1002/chem.201300042.
- (208) Monte-Filho, S. S.; Andrade, S. I. E.; Lima, M. B.; Araujo, M. C. U. Synthesis of Highly Fluorescent Carbon Dots from Lemon and Onion Juices for Determination of Riboflavin in Multivitamin/Mineral Supplements. *J. Pharm. Anal.* **2019**, *9* (3), 209–216. https://doi.org/https://doi.org/10.1016/j.jpha.2019.02.003.
- (209) Carter, K. P.; Young, A. M.; Palmer, A. E. Fluorescent Sensors for Measuring Metal Ions in Living Systems. *Chem. Rev.* 2014, 114 (8), 4564–4601.
 https://doi.org/10.1021/cr400546e.
- (210) Tan, X. W.; Romainor, A. N. B.; Chin, S. F.; Ng, S. M. Carbon Dots Production via Pyrolysis of Sago Waste as Potential Probe for Metal Ions Sensing. *J. Anal. Appl. Pyrolysis* **2014**, *105*, 157–165. https://doi.org/10.1016/j.jaap.2013.11.001.
- (211) Choi, D.-H.; Cho, J.-Y.; Koo, J.-H.; Kim, T.-K. Effects of Electrolyte Supplements on Body Water Homeostasis and Exercise Performance during Exhaustive Exercise. *Appl. Sci.* **2021**, *11* (19). https://doi.org/10.3390/app11199093.
- (212) Zorova, L. D.; Popkov, V. A.; Plotnikov, E. Y.; Silachev, D. N.; Pevzner, I. B.;
 Jankauskas, S. S.; Babenko, V. A.; Zorov, S. D.; Balakireva, A. V; Juhaszova, M.; Sollott,
 S. J.; Zorov, D. B. Mitochondrial Membrane Potential. *Anal. Biochem.* 2018, 552, 50–59.
 https://doi.org/10.1016/j.ab.2017.07.009.
- (213) Ding, Y.; Tang, Y.; Zhu, W.; Xie, Y. Fluorescent and Colorimetric Ion Probes Based on

- Conjugated Oligopyrroles. *Chem. Soc. Rev.* **2015**, *44* (5), 1101–1112. https://doi.org/10.1039/c4cs00436a.
- (214) Lu, D.; He, L.; Wang, Y.; Xiong, M.; Hu, M.; Liang, H.; Huan, S.; Zhang, X. B.; Tan, W. Tetraphenylethene Derivative Modified DNA Oligonucleotide for in Situ Potassium Ion Detection and Imaging in Living Cells. *Talanta* 2017, *167*, 550–556.
 https://doi.org/10.1016/j.talanta.2017.02.064.
- (215) Brini, M.; Calì, T.; Ottolini, D.; Carafoli, E. Intracellular Calcium Homeostasis and Signaling. *Met. Ions Life Sci.* **2013**, *12*, 119–168. https://doi.org/10.1007/978-94-007-5561-1_5.
- (216) Brini, M.; Ottolini, D.; Calì, T.; Carafoli, E. Calcium in Health and Disease. *Met. Ions Life Sci.* **2013**, *13*, 81–137. https://doi.org/10.1007/978-94-007-7500-8_4.
- (217) Winter, W. E.; Bazydlo, L. A. L.; Harris, N. S. The Molecular Biology of Human Iron Metabolism. *Lab Med.* 2014, 45 (2), 92–102. https://doi.org/10.1309/LMF28S2GIMXNWHMM.
- (218) Xu, J.; Jia, Z.; Knutson, M. D.; Leeuwenburgh, C. Impaired Iron Status in Aging Research. *Int. J. Mol. Sci.* 2012, *13* (2), 2368–2386. https://doi.org/10.3390/ijms13022368.
- (219) Maret, W. Zinc and Human Disease. Met. Ions Life Sci. 2013, 13, 389–414. https://doi.org/10.1007/978-94-007-7500-8_12.
- (220) Vallee, B. L.; Falchuk, K. H. The Biochemical Basis of Zinc Physiology. *Physiol. Rev.* **1993**, *73* (1), 79–118. https://doi.org/10.1152/physrev.1993.73.1.79.
- (221) King, J. C. Zinc: An Essential but Elusive Nutrient. *Am. J. Clin. Nutr.* **2011**, *94* (2), 679S-84S. https://doi.org/10.3945/ajcn.110.005744.

(222) Ruz, M.; Carrasco, F.; Rojas, P.; Basfi-fer, K.; Hernández, M. C.; Pérez, A. Nutritional Effects of Zinc on Metabolic Syndrome and Type 2 Diabetes: Mechanisms and Main Findings in Human Studies. *Biol. Trace Elem. Res.* **2019**, *188* (1), 177–188. https://doi.org/10.1007/s12011-018-1611-8.

- (223) Takeda, A.; Tamano, H. The Impact of Synaptic Zn2+ Dynamics on Cognition and Its Decline. *Int. J. Mol. Sci.* **2017**, *18* (11). https://doi.org/10.3390/ijms18112411.
- (224) Gu, D.; Shang, S.; Yu, Q.; Shen, J. Green Synthesis of Nitrogen-Doped Carbon Dots from Lotus Root for Hg(II) Ions Detection and Cell Imaging. *Appl. Surf. Sci.* **2016**, *390*, 38–42. https://doi.org/https://doi.org/10.1016/j.apsusc.2016.08.012.
- (225) JAIN, J.; GAUBA, P. Heavy Metal Toxicity-Implications on Metabolism and Health. *Int. J. Pharma Bio Sci.* **2017**, 8 (4). https://doi.org/10.22376/ijpbs.2017.8.4.b452-460.
- (226) Batool, M.; Junaid, H. M.; Tabassum, S.; Kanwal, F.; Abid, K.; Fatima, Z.; Shah, A. T. Metal Ion Detection by Carbon Dots—A Review. *Crit. Rev. Anal. Chem.* 2022, 52 (4), 756–767. https://doi.org/10.1080/10408347.2020.1824117.
- (227) Zhou, X.; Zhang, Y.; Wang, C.; Wu, X.; Yang, Y.; Zheng, B.; Wu, H.; Guo, S.; Zhang, J. Photo-Fenton Reaction of Graphene Oxide: A New Strategy to Prepare Graphene Quantum Dots for DNA Cleavage. ACS Nano 2012, 6 (8), 6592–6599. https://doi.org/10.1021/nn301629v.
- (228) Ruiz-Palomero, C.; Benítez-Martínez, S.; Soriano, M. L.; Valcárcel, M. Fluorescent Nanocellulosic Hydrogels Based on Graphene Quantum Dots for Sensing Laccase. *Anal. Chim. Acta* **2017**, *974*, 93–99. https://doi.org/10.1016/j.aca.2017.04.018.
- (229) Batool, M.; Junaid, H. M.; Tabassum, S.; Kanwal, F.; Abid, K.; Fatima, Z.; Shah, A. T. Metal Ion Detection by Carbon Dots—A Review. *Crit. Rev. Anal. Chem.* **2020**, *0* (0), 1–

- 12. https://doi.org/10.1080/10408347.2020.1824117.
- (230) Abbasi, H.; Salimi, F.; Golmohammadi, F. Removal of Cadmium from Aqueous Solution by Nano Composites of Bentonite/TiO2 and Bentonite/ZnO Using Photocatalysis Adsorption Process. *Silicon* **2020**, *12* (11), 2721–2731. https://doi.org/10.1007/s12633-019-00372-6.
- (231) Agubra, V. A.; Zuniga, L.; Flores, D.; Villareal, J.; Alcoutlabi, M. Composite Nanofibers as Advanced Materials for Li-Ion, Li-O2 and Li-S Batteries. *Electrochim. Acta* **2016**, *192*, 529–550. https://doi.org/10.1016/j.electacta.2016.02.012.
- (232) Yao, Y.; Wu, H.; Ping, J. Simultaneous Determination of Cd(II) and Pb(II) Ions in Honey and Milk Samples Using a Single-Walled Carbon Nanohorns Modified Screen-Printed Electrochemical Sensor. *Food Chem.* 2019, 274, 8–15.
 https://doi.org/10.1016/j.foodchem.2018.08.110.
- (233) Zhou, W. Y.; Li, S. S.; Song, J. Y.; Jiang, M.; Jiang, T. J.; Liu, J. Y.; Liu, J. H.; Huang, X. J. High Electrochemical Sensitivity of TiO2- x Nanosheets and an Electron-Induced Mutual Interference Effect toward Heavy Metal Ions Demonstrated Using X-Ray Absorption Fine Structure Spectra. *Anal. Chem.* 2018, 90 (7), 4328–4337. https://doi.org/10.1021/acs.analchem.7b02315.
- (234) Zhou, W.; Li, C.; Sun, C.; Yang, X. Simultaneously Determination of Trace Cd2+ and Pb2+ Based on L-Cysteine/Graphene Modified Glassy Carbon Electrode. *Food Chem.* **2016**, *192*, 351–357. https://doi.org/10.1016/j.foodchem.2015.07.042.
- (235) Lu, L.; Zhou, L.; Chen, J.; Yan, F.; Liu, J.; Dong, X.; Xi, F.; Chen, P. Nanochannel-Confined Graphene Quantum Dots for Ultrasensitive Electrochemical Analysis of Complex Samples. *ACS Nano* **2018**, *12* (12), 12673–12681.

- https://doi.org/10.1021/acsnano.8b07564.
- (236) Zhang, B.; Zhang, F.; Zhang, P.; Shen, D.; Gao, X.; Zou, G. Ultrasensitive Electrochemiluminescent Sensor for MicroRNA with Multinary Zn-Ag-In-S/ZnS Nanocrystals as Tags. *Anal. Chem.* 2019, 91 (5), 3754–3758. https://doi.org/10.1021/acs.analchem.9b00199.
- (237) Sciuto, E. L.; Petralia, S.; van der Meer, J. R.; Conoci, S. Miniaturized Electrochemical Biosensor Based on Whole-Cell for Heavy Metal Ions Detection in Water. *Biotechnol. Bioeng.* **2021**, *118* (4), 1456–1465. https://doi.org/10.1002/bit.27646.
- (238) Shan, Q.; Tian, J.; Ding, Q.; Wu, W. Electrochemical Sensor Based on Metal-Free Materials Composed of Graphene and Graphene Oxide for Sensitive Detection of Cadmium Ions in Water. *Mater. Chem. Phys.* 2022, 284, 126064. https://doi.org/10.1016/j.matchemphys.2022.126064.
- (239) Stiboller, M.; Raber, G.; Gjengedal, E. L. F.; Eggesbø, M.; Francesconi, K. A. Quantifying Inorganic Arsenic and Other Water-Soluble Arsenic Species in Human Milk by HPLC/ICPMS. *Anal. Chem.* **2017**, *89* (11), 6265–6271. https://doi.org/10.1021/acs.analchem.7b01276.
- (240) Peres, T. V.; Schettinger, M. R. C.; Chen, P.; Carvalho, F.; Avila, D. S.; Bowman, A. B.; Aschner, M. "Manganese-Induced Neurotoxicity: A Review of Its Behavioral Consequences and Neuroprotective Strategies." *BMC Pharmacol. Toxicol.* 2016, 17 (1), 57. https://doi.org/10.1186/s40360-016-0099-0.
- (241) Stephenson, A. P.; Schneider, J. A.; Nelson, B. C.; Atha, D. H.; Jain, A.; Soliman, K. F. A.; Aschner, M.; Mazzio, E.; Renee Reams, R. Manganese-Induced Oxidative DNA Damage in Neuronal SH-SY5Y Cells: Attenuation of Thymine Base Lesions by

- Glutathione and N-Acetylcysteine. *Toxicol. Lett.* **2013**, *218* (3), 299–307. https://doi.org/10.1016/j.toxlet.2012.12.024.
- (242) Deng, Y.; Jiao, C.; Mi, C.; Xu, B.; Li, Y.; Wang, F.; Liu, W.; Xu, Z. Melatonin Inhibits

 Manganese-Induced Motor Dysfunction and Neuronal Loss in Mice: Involvement of

 Oxidative Stress and Dopaminergic Neurodegeneration. *Mol. Neurobiol.* **2015**, *51* (1), 68–

 88. https://doi.org/10.1007/s12035-014-8789-3.
- (243) Nemery, B. Metal Toxicity and the Respiratory Tract. Eur. Respir. J. 1990, 3 (2), 202–219.
- (244) Das, K. K.; Reddy, R. C.; Bagoji, I. B.; Das, S.; Bagali, S.; Mullur, L.; Khodnapur, J. P.; Biradar, M. S. Primary Concept of Nickel Toxicity An Overview. *J. Basic Clin. Physiol. Pharmacol.* **2019**, *30* (2), 141–152. https://doi.org/10.1515/jbcpp-2017-0171.
- (245) Linder, M. C. Ceruloplasmin and Other Copper Binding Components of Blood Plasma and Their Functions: An Update. *Metallomics* **2016**, 8 (9), 887–905. https://doi.org/10.1039/c6mt00103c.
- (246) Woimant, F.; Djebrani-Oussedik, N.; Poujois, A. New Tools for Wilson's Disease Diagnosis: Exchangeable Copper Fraction. *Ann. Transl. Med.* **2019**, *7* (S2), S70–S70. https://doi.org/10.21037/atm.2019.03.02.
- (247) Xia, T.; Kovochich, M.; Liong, M.; Mädler, L.; Gilbert, B.; Shi, H.; Yeh, J. I.; Zink, J. I.; Nel, A. E. Comparison of the Mechanism of Toxicity of Zinc Oxide and Cerium Oxide Nanoparticles Based on Dissolution and Oxidative Stress Properties. ACS Nano 2008, 2 (10), 2121–2134. https://doi.org/10.1021/nn800511k.
- (248) Lv, S.; Zhou, Y.; Xu, W.; Mao, W.; Wang, L.; Liu, Y.; He, C. Preparation of P-Type GaN-Doped SnO2 Thin Films by e-Beam Evaporation and Their Applications in p-n

- Junction. *Appl. Surf. Sci.* **2018**, *427*, 64–68. https://doi.org/https://doi.org/10.1016/j.apsusc.2017.07.297.
- (249) Svintsitskiy, D. A.; Kardash, T. Y.; Slavinskaya, E. M.; Stonkus, O. A.; Koscheev, S. V; Boronin, A. I. The Decomposition of Mixed Oxide Ag2Cu2O3: Structural Features and the Catalytic Properties in CO and C2H4 Oxidation. *Appl. Surf. Sci.* **2018**, *427*, 363–374. https://doi.org/https://doi.org/10.1016/j.apsusc.2017.08.010.
- (250) Amari, T.; Ghnaya, T.; Abdelly, C. Nickel, Cadmium and Lead Phytotoxicity and Potential of Halophytic Plants in Heavy Metal Extraction. *South African J. Bot.* **2017**, *111*, 99–110. https://doi.org/10.1016/j.sajb.2017.03.011.
- (251) Khan, I.; Saeed, K.; Khan, I. Nanoparticles: Properties, Applications and Toxicities. *Arab. J. Chem.* **2019**, *12* (7), 908–931. https://doi.org/10.1016/j.arabjc.2017.05.011.
- (252) Baracca, A.; Sgarbi, G.; Solaini, G.; Lenaz, G. Rhodamine 123 as a Probe of Mitochondrial Membrane Potential: Evaluation of Proton Flux through F0 during ATP Synthesis. *Biochim. Biophys. Acta - Bioenerg.* 2003, 1606 (1), 137–146. https://doi.org/https://doi.org/10.1016/S0005-2728(03)00110-5.
- (253) Zamzami, N.; Marchetti, P.; Castedo, M.; Decaudin, D.; Macho, A.; Hirsch, T.; Susin, S. A.; Petit, P. X.; Mignotte, B.; Kroemer, G. Sequential Reduction of Mitochondrial Transmembrane Potential and Generation of Reactive Oxygen Species in Early Programmed Cell Death. *J. Exp. Med.* 1995, 182 (2), 367–377. https://doi.org/10.1084/jem.182.2.367.
- (254) Mahmoud, D. A.; Hassanein, N. M.; Youssef, K. A.; Abou Zeid, M. A. Antifungal Activity of Different Neem Leaf Extracts and the Nimonol against Some Important Human Pathogens. *Brazilian J. Microbiol. [publication Brazilian Soc. Microbiol.* **2011**,

- 42 (3), 1007–1016. https://doi.org/10.1590/S1517-838220110003000021.
- (255) Tang, Y.; Wang,. Facile Synthesis of Monodisperse Superparamagnetic Fe3O4

 Core@hybrid@Au Shell Nanocomposite for Bimodal Imaging and Photothermal

 Therapy. *ACS Nano* **2021**, *5* (1), 2179–2195. https://doi.org/10.1021/nn301629v.
- (256) Lim, E.-K.; Kim, T.; Paik, S.; Haam, S.; Huh, Y.-M.; Lee, K. Nanomaterials for Theranostics: Recent Advances and Future Challenges. *Chem. Rev.* **2014**, *115* (1), 327–394. https://doi.org/10.1021/cr300213b.
- (257) Wong, X. Y.; Sena-Torralba, A.; Álvarez-Diduk, R.; Muthoosamy, K.; Merkoçi, A. Nanomaterials for Nanotheranostics: Tuning Their Properties According to Disease Needs. *ACS Nano* **2020**, *14* (3), 2585–2627. https://doi.org/10.1021/acsnano.9b08133.
- (258) Mitchell, M. J.; Billingsley, M. M.; Haley, R. M.; Wechsler, M. E.; Peppas, N. A.; Langer,
 R. Engineering Precision Nanoparticles for Drug Delivery. *Nat. Rev. Drug Discov.* 2021,
 20 (2), 101–124. https://doi.org/10.1038/s41573-020-0090-8.
- (259) Li, Y.; Zhuang, J.; Lu, Y.; Li, N.; Gu, M.; Xia, J.; Zhao, N.; Tang, B. Z. High-Performance Near-Infrared Aggregation-Induced Emission Luminogen with Mitophagy Regulating Capability for Multimodal Cancer Theranostics. ACS Nano 2021, 15 (12), 20453–20465. https://doi.org/10.1021/acsnano.1c08928.
- (260) Bardhan, R.; Lal, S.; Joshi, A.; J. Halas, N. Theranostic Nanoshells: From Probe Design to Imaging and Treatment of Cancer. *Acc. Chem. Res.* **2011**, *44* (10), 936–946. https://doi.org/10.1021/ar200023x.
- (261) Davis, M. E.; Chen, Z. (Georgia); Shin, D. M. Nanoparticle Therapeutics: An Emerging Treatment Modality for Cancer. *Nat. Rev. Drug Discov.* **2008**, *7* (9), 771–782. https://doi.org/10.1038/nrd2614.

(262) Riehemann, K.; Schneider, S. W.; Luger, T. A.; Godin, B.; Ferrari, M.; Fuchs, H. Nanomedicine--Challenge and Perspectives. *Angew. Chem. Int. Ed. Engl.* **2009**, *48* (5), 872–897. https://doi.org/10.1002/anie.200802585.

- (263) Simon, A. T.; Dutta, D.; Chattopadhyay, A.; Ghosh, S. S. Quercetin-Loaded Luminescent Hydroxyapatite Nanoparticles for Theranostic Application in Monolayer and Spheroid Cultures of Cervical Cancer Cell Line In Vitro. *ACS Appl. Bio Mater.* **2021**, *4* (5), 4495–4506. https://doi.org/10.1021/acsabm.1c00255.
- (264) McNerney, M. P.; Doiron, K. E.; Ng, T. L.; Chang, T. Z.; Silver, P. A. Theranostic Cells: Emerging Clinical Applications of Synthetic Biology. *Nat. Rev. Genet.* **2021**, 22 (11), 730–746. https://doi.org/10.1038/s41576-021-00383-3.
- (265) Shi, J.; Kantoff, P. W.; Wooster, R.; Farokhzad, O. C. Cancer Nanomedicine: Progress, Challenges and Opportunities. *Nat. Rev. Cancer* **2017**, *17* (1), 20–37. https://doi.org/10.1038/nrc.2016.108.
- (266) Ferrari, M. Cancer Nanotechnology: Opportunities and Challenges. *Nat. Rev. Cancer* **2005**, *5* (3), 161–171. https://doi.org/10.1038/nrc1566.
- (267) Torchilin, V. Tumor Delivery of Macromolecular Drugs Based on the EPR Effect. *Adv. Drug Deliv. Rev.* **2011**, *63* (3), 131–135. https://doi.org/10.1016/j.addr.2010.03.011.
- (268) Hsu, P. P.; Sabatini, D. M. Cancer Cell Metabolism: Warburg and Beyond. *Cell* 2008, *134*(5), 703–707. https://doi.org/10.1016/j.cell.2008.08.021.
- (269) Vogelstein, B.; Papadopoulos, N.; Velculescu, V. E.; Zhou, S.; Diaz, L. A. J.; Kinzler, K. W. Cancer Genome Landscapes. *Science* 2013, 339 (6127), 1546–1558. https://doi.org/10.1126/science.1235122.
- (270) Dong, W.; Li, Y.; Niu, D.; Ma, Z.; Gu, J.; Chen, Y.; Zhao, W.; Liu, X.; Liu, C.; Shi, J.

Facile Synthesis of Monodisperse Superparamagnetic Fe3O4 Core@hybrid@Au Shell Nanocomposite for Bimodal Imaging and Photothermal Therapy. *Adv. Mater.* **2011**, *23* (45), 5392–5397. https://doi.org/10.1002/adma.201103521.

- (271) Wang, S.; Wang, Z.; Hou, Y. Self-Assembled Magnetic Nanomaterials: Versatile Theranostics Nanoplatforms for Cancer. *Aggregate* **2021**, 2 (2), e18. https://doi.org/https://doi.org/10.1002/agt2.18.
- (272) Mantri, Y.; Jokerst, J. V. Engineering Plasmonic Nanoparticles for Enhanced Photoacoustic Imaging. *ACS Nano* **2020**, *14* (8), 9408–9422. https://doi.org/10.1021/acsnano.0c05215.
- (273) Lindley, S. A.; Zhang, J. Z. Bumpy Hollow Gold Nanospheres for Theranostic Applications: Effect of Surface Morphology on Photothermal Conversion Efficiency. *ACS Appl. Nano Mater.* **2019**, *2* (2), 1072–1081. https://doi.org/10.1021/acsanm.8b02331.
- (274) Zhang, Y.; Wu, M.; Wu, M.; Zhu, J.; Zhang, X. Multifunctional Carbon-Based Nanomaterials: Applications in Biomolecular Imaging and Therapy. ACS Omega 2018, 3 (8), 9126–9145. https://doi.org/10.1021/acsomega.8b01071.
- (275) Liu, J.; Li, R.; Yang, B. Carbon Dots: A New Type of Carbon-Based Nanomaterial with Wide Applications. *ACS Cent. Sci.* **2020**, *6* (12), 2179–2195. https://doi.org/10.1021/acscentsci.0c01306.
- (276) Cheng, L.; Wang, X.; Gong, F.; Liu, T.; Liu, Z. 2D Nanomaterials for Cancer Theranostic Applications. *Adv. Mater.* **2020**, *32* (13), 1902333. https://doi.org/https://doi.org/10.1002/adma.201902333.
- (277) Huang, H.; Firestone, G.; Fontecha, D.; Gorga, R. E.; Bochinski, J. R.; Clarke, L. I.

 Nanoparticle-Based Photothermal Heating to Drive Chemical Reactions within a Solid:

Using Inhomogeneous Polymer Degradation to Manipulate Mechanical Properties and Segregate Carbonaceous by-Products. *Nanoscale* **2020**, *12* (2), 904–923. https://doi.org/10.1039/C9NR07401E.

- (278) Zhang, H.; Wang, J.; Hu, M.; Li, B.; Li, H.; Chen, T.; Ren, K.-F.; Ji, J.; Jing, Q.; Fu, G. Photothermal-Assisted Surface-Mediated Gene Delivery for Enhancing Transfection Efficiency. *Biomater. Sci.* 2019, 7 (12), 5177–5186.
 https://doi.org/10.1039/C9BM01284B.
- (279) Oh, N.; Park, S.; Kim, J. W.; Park, J.-H. Photothermal Transfection for Effective Nonviral Genome Editing. *ACS Appl. Bio Mater.* **2021**, *4* (7), 5678–5685. https://doi.org/10.1021/acsabm.1c00465.
- (280) Giri, R. P.; Gangawane, D. A. K.; Giri, D. S. G. Neem the Wonder Herb: A Short Review.
 Int. J. Trend Sci. Res. Dev. 2019, Volume-3 (Issue-3), 962–967.
 https://doi.org/10.31142/ijtsrd23038.
- (281) Dubey, S.; Kashyap, P. Azadirachta Indica: A Plant With Versatile Potential. *Rajiv Gandhi Univ. Heal. Sci. J. Pharm. Sci.* **2014**, *4* (2), 39–46. https://doi.org/10.5530/rjps.2014.2.2.
- (282) Mohammed, H. A.; A. F. A. Omar. Antibacterial Activity of Azadirachta Indica (Neem)

 Leaf Extract against Bacterial Pathogens in Sudan. *Am. J. Res. Commun.* **2015**, *3* (5), 246–251.
- (283) Tiwari, V.; Darmani, N. A.; Yue, B. Y. J. T.; Shukla, D. In Vitro Antiviral Activity of Neem (Azardirachta Indica L.) Bark Extract against Herpes Simplex Virus Type-1 Infection. *Phyther. Res.* 2010, 24 (8), 1132–1140. https://doi.org/https://doi.org/10.1002/ptr.3085.

(284) Satti, A.; Ellaithy, M.; Mohamed, A. Insecticidal Activities of Neem (Azadirachta Indica A. Juss) Seeds under Laboratory and Field Conditions as Affected by Different Storage Durations. *Agric. Biol. J. North Am.* **2010**, *1* (5), 1001–1008. https://doi.org/10.5251/abjna.2010.1.5.1001.1008.

- (285) Muhammad, A.; I. M. Lawan; A. Abubakar; I. I. Dangora. Antimicrobial Activity of Azadirachta Indica (Neem) Leave Extract Against Some Clinical Isolates. *Dutse J. Pure Appl. Sci.* **2019**, *5* (1), 97–104.
- (286) Lu, J.; Wu, L.; Wang, X.; Zhu, J.; Du, J.; Shen, B. Detection of Mitochondria Membrane Potential to Study CLIC4 Knockdown-Induced HN4 Cell Apoptosis In Vitro. *J. Vis. Exp.* **2018**, No. 137. https://doi.org/10.3791/56317.
- (287) Medhi, H.; Khumukcham, S. S.; Manavathi, B.; Paik, P. Effective in Vitro Delivery of Paclitaxel by Nanocargo of Mesoporous Polycaprolactone against Triple Negative Breast Cancer Cells by Minimalizing Drug Dose. *RSC Adv.* **2020**, *10* (40), 24095–24107. https://doi.org/10.1039/D0RA04505E.
- (288) Enders, A. A.; North, N. M.; Fensore, C. M.; Velez-Alvarez, J.; Allen, H. C. Functional Group Identification for FTIR Spectra Using Image-Based Machine Learning Models. *Anal. Chem.* **2021**, *93* (28), 9711–9718. https://doi.org/10.1021/acs.analchem.1c00867.
- (289) Esfandiari, N.; Bagheri, Z.; Ehtesabi, H.; Fatahi, Z.; Tavana, H.; Latifi, H. Effect of Carbonization Degree of Carbon Dots on Cytotoxicity and Photo-Induced Toxicity to Cells. *Heliyon* 2019, 5 (12), e02940. https://doi.org/https://doi.org/10.1016/j.heliyon.2019.e02940.
- (290) Zulfajri, M.; Dayalan, S.; Li, W.-Y.; Chang, C.-J.; Chang, Y.-P.; Huang, G. G. Nitrogen-Doped Carbon Dots from Averrhoa Carambola Fruit Extract as a Fluorescent Probe for

- Methyl Orange. Sensors 2019, 19 (22). https://doi.org/10.3390/s19225008.
- (291) Pal, T.; Mohiyuddin, S.; Packirisamy, G. Correction to "Facile and Green Synthesis of Multicolor Fluorescence Carbon Dots from Curcumin: In Vitro and in Vivo Bioimaging and Other Applications." ACS Omega 2018, 3 (5), 5887. https://doi.org/10.1021/acsomega.8b00956.
- (292) Semeniuk, M.; Yi, Z.; Poursorkhabi, V.; Tjong, J.; Jaffer, S.; Lu, Z.-H.; Sain, M. Future Perspectives and Review on Organic Carbon Dots in Electronic Applications. *ACS Nano* **2019**, *13* (6), 6224–6255. https://doi.org/10.1021/acsnano.9b00688.
- (293) Mishra, L.; Behera, R. K.; Mondal, S.; Panigrahi, A.; Sarangi, M. K. Surface Charge Alteration in Carbon Dots Governs the Interfacial Electron Transfer and Transport. *J. Phys. Chem. C* **2021**, *125* (42), 23398–23408. https://doi.org/10.1021/acs.jpcc.1c06459.
- (294) Midekessa, G.; Godakumara, K.; Ord, J.; Viil, J.; Lättekivi, F.; Dissanayake, K.; Kopanchuk, S.; Rinken, A.; Andronowska, A.; Bhattacharjee, S.; Rinken, T.; Fazeli, A. Zeta Potential of Extracellular Vesicles: Toward Understanding the Attributes That Determine Colloidal Stability. ACS Omega 2020, 5 (27), 16701–16710. https://doi.org/10.1021/acsomega.0c01582.
- (295) Gaddam, R. R.; Mukherjee, S.; Punugupati, N.; Vasudevan, D.; Patra, C. R.; Narayan, R.; VSN Kothapalli, R. Facile Synthesis of Carbon Dot and Residual Carbon Nanobeads: Implications for Ion Sensing, Medicinal and Biological Applications. *Mater. Sci. Eng. C* 2017, 73, 643–652. https://doi.org/https://doi.org/10.1016/j.msec.2016.12.095.
- (296) Nguyen, H. A.; Srivastava, I.; Pan, D.; Gruebele, M. Unraveling the Fluorescence Mechanism of Carbon Dots with Sub-Single-Particle Resolution. ACS Nano 2020, 14 (5), 6127–6137. https://doi.org/10.1021/acsnano.0c01924.

(297) Dasog, M.; De los Reyes, G. B.; Titova, L. V; Hegmann, F. A.; Veinot, J. G. C. Size vs Surface: Tuning the Photoluminescence of Freestanding Silicon Nanocrystals Across the Visible Spectrum via Surface Groups. *ACS Nano* **2014**, *8* (9), 9636–9648. https://doi.org/10.1021/nn504109a.

- (298) Gutiérrez-Arzaluz, L.; Ahmed, G. H.; Yang, H.; Shikin, S.; Bakr, O. M.; Malko, A. V.; Mohammed, O. F. Correlation of Photoluminescence and Structural Morphologies at the Individual Nanoparticle Level. *J. Phys. Chem. A* 2020, 124 (23), 4855–4860. https://doi.org/10.1021/acs.jpca.0c02340.
- (299) Su, W.; Wu, H.; Xu, H.; Zhang, Y.; Li, Y.; Li, X.; Fan, L. Carbon Dots: A Booming Material for Biomedical Applications. *Mater. Chem. Front.* **2020**, *4* (3), 821–836. https://doi.org/10.1039/C9QM00658C.
- (300) Wang, Q.; Feng, Z.; He, H.; Hu, X.; Mao, J.; Chen, X.; Liu, L.; Wei, X.; Liu, D.; Bi, S.; Wang, X.; Ge, B.; Yu, D.; Huang, F. Nonblinking Carbon Dots for Imaging and Tracking Receptors on a Live Cell Membrane. *Chem. Commun.* **2021**, *57* (45), 5554–5557. https://doi.org/10.1039/D1CC01120K.
- (301) Tang, Y.; Wang, X.; Li, J.; Nie, Y.; Liao, G.; Yu, Y.; Li, C. Overcoming the Reticuloendothelial System Barrier to Drug Delivery with a "Don't-Eat-Us" Strategy. *ACS Nano* **2019**, *13* (11), 13015–13026. https://doi.org/10.1021/acsnano.9b05679.
- (302) Nie, S. Understanding and Overcoming Major Barriers in Cancer Nanomedicine Opsonization & Phagocytosis. **2010**, *5* (4), 523–528. https://doi.org/10.2217/nnm.10.23.Understanding.
- (303) Fleischer, C. C.; Payne, C. K. Nanoparticle–Cell Interactions: Molecular Structure of the Protein Corona and Cellular Outcomes. *Acc. Chem. Res.* **2014**, *47* (8), 2651–2659.

- https://doi.org/10.1021/ar500190q.
- (304) Wang, C.; Youle, R. J. The Role of Mitochondria in Apoptosis*. *Annu. Rev. Genet.* **2009**, 43, 95–118. https://doi.org/10.1146/annurev-genet-102108-134850.
- (305) Porporato, P. E.; Filigheddu, N.; Pedro, J. M. B.-S.; Kroemer, G.; Galluzzi, L. Mitochondrial Metabolism and Cancer. *Cell Res.* 2018, 28 (3), 265–280. https://doi.org/10.1038/cr.2017.155.
- (306) Bajpai, A.; Desai, N. N.; Pandey, S.; Shukla, C.; Datta, B.; Basu, S. Nanoparticle-Mediated Routing of Antibiotics into Mitochondria in Cancer Cells. ACS Appl. Bio Mater.
 2021, 4 (9), 6799–6806. https://doi.org/10.1021/acsabm.1c00527.
- (307) Cao, J. J.; Tan, C. P.; Chen, M. H.; Wu, N.; Yao, D. Y.; Liu, X. G.; Ji, L. N.; Mao, Z. W. Targeting Cancer Cell Metabolism with Mitochondria-Immobilized Phosphorescent Cyclometalated Iridium(Iii) Complexes. *Chem. Sci.* **2016**, 8 (1), 631–640. https://doi.org/10.1039/C6SC02901A.
- (308) Kim, S.; Palanikumar, L.; Choi, H.; Jeena, M. T.; Kim, C.; Ryu, J. H. Intra-Mitochondrial Biomineralization for Inducing Apoptosis of Cancer Cells. *Chem. Sci.* **2018**, *9* (9), 2474–2479. https://doi.org/10.1039/c7sc05189a.
- (309) Mertens, R. T.; Parkin, S.; Awuah, S. G. Cancer Cell-Selective Modulation of Mitochondrial Respiration and Metabolism by Potent Organogold(Iii) Dithiocarbamates. Chem. Sci. 2020, 11 (38), 10465–10482. https://doi.org/10.1039/d0sc03628e.
- (310) Zhu, S.; Song, Y.; Zhao, X.; Shao, J.; Zhang, J.; Yang, B. The Photoluminescence Mechanism in Carbon Dots (Graphene Quantum Dots, Carbon Nanodots, and Polymer Dots): Current State and Future Perspective. *Nano Res.* 2015, 8 (2), 355–381. https://doi.org/10.1007/s12274-014-0644-3.

(311) Pan, D.; Zhang, J.; Li, Z.; Wu, M. Hydrothermal Route for Cutting Graphene Sheets into Blue-Luminescent Graphene Quantum Dots. *Adv. Mater.* **2010**, 22 (6), 734–738. https://doi.org/https://doi.org/10.1002/adma.200902825.

- (312) Ji, C.; Zhou, Y.; Leblanc, R. M.; Peng, Z. Recent Developments of Carbon Dots in Biosensing: A Review. *ACS Sensors* **2020**, *5* (9), 2724–2741. https://doi.org/10.1021/acssensors.0c01556.
- (313) Ye, R.; Peng, Z.; Metzger, A.; Lin, J.; Mann, J. A.; Huang, K.; Xiang, C.; Fan, X.; Samuel, E. L. G.; Alemany, L. B.; Martí, A. A.; Tour, J. M. Bandgap Engineering of Coal-Derived Graphene Quantum Dots. *ACS Appl. Mater. Interfaces* **2015**, *7* (12), 7041–7048. https://doi.org/10.1021/acsami.5b01419.
- (314) Zhang, D.; Wen, L.; Huang, R.; Wang, H.; Hu, X.; Xing, D. Mitochondrial Specific Photodynamic Therapy by Rare-Earth Nanoparticles Mediated near-Infrared Graphene Quantum Dots. *Biomaterials* 2018, 153, 14–26. https://doi.org/10.1016/j.biomaterials.2017.10.034.
- (315) Shen, J.; Zhu, Y.; Yang, X.; Li, C. Graphene Quantum Dots: Emergent Nanolights for Bioimaging {,} Sensors {,} Catalysis and Photovoltaic Devices. *Chem. Commun.* **2012**, *48* (31), 3686–3699. https://doi.org/10.1039/C2CC00110A.
- (316) Li, H.; He, X.; Kang, Z.; Huang, H.; Liu, Y.; Liu, J.; Lian, S.; Tsang, C. H. A.; Yang, X.; Lee, S.-T. Water-Soluble Fluorescent Carbon Quantum Dots and Photocatalyst Design.

 Angew. Chemie Int. Ed. 2010, 49 (26), 4430–4434.

 https://doi.org/https://doi.org/10.1002/anie.200906154.
- (317) Zhou, Y.; Sun, H.; Wang, F.; Ren, J.; Qu, X. How Functional Groups Influence the ROS Generation and Cytotoxicity of Graphene Quantum Dots. *Chem. Commun.* **2017**, *53* (76),

- 10588-10591. https://doi.org/10.1039/C7CC04831A.
- (318) Yan, X.; Zhang, C.; Dong, Z.; Jiang, B.; Dai, Y.; Wu, X.; He, G. Amphiprotic Side-Chain Functionalization Constructing Highly Proton/Vanadium-Selective Transport Channels for High-Performance Membranes in Vanadium Redox Flow Batteries. ACS Appl. Mater. Interfaces 2018, 10 (38), 32247–32255. https://doi.org/10.1021/acsami.8b11993.
- (319) Lim, S. Y.; Shen, W.; Gao, Z. Carbon Quantum Dots and Their Applications. *Chem. Soc. Rev.* **2015**, *44* (1), 362–381. https://doi.org/10.1039/C4CS00269E.
- (320) Wang, Y.; Hu, A. Carbon Quantum Dots: Synthesis, Properties and Applications. *J. Mater. Chem. C* **2014**, 2 (34), 6921–6939. https://doi.org/10.1039/c4tc00988f.
- (321) Chen, W.-T.; Liao, Y.-H.; Yu, H.-M.; Cheng, I. H.; Chen, Y.-R. Distinct Effects of Zn2+, Cu2+, Fe3+, and Al3+ on Amyloid-Beta Stability, Oligomerization, and Aggregation: Amyloid-Beta Destabilization Promotes Annular Protofibril Formation. *J. Biol. Chem.*2011, 286 (11), 9646–9656. https://doi.org/10.1074/jbc.M110.177246.
- (322) Lu, W.; Gao, Y.; Jiao, Y.; Shuang, S.; Li, C.; Dong, C. Carbon Nano-Dots as a Fluorescent and Colorimetric Dual-Readout Probe for the Detection of Arginine and Cu2+ and Its Logic Gate Operation. *Nanoscale* **2017**, *9* (32), 11545–11552. https://doi.org/10.1039/C7NR02336G.
- (323) Kwon, N.; Hu, Y.; Yoon, J. Fluorescent Chemosensors for Various Analytes Including Reactive Oxygen Species, Biothiol, Metal Ions, and Toxic Gases. *ACS Omega* **2018**, *3* (10), 13731–13751. https://doi.org/10.1021/acsomega.8b01717.
- (324) Wang, J.; Qiu, J. A Review of Carbon Dots in Biological Applications. *J. Mater. Sci.* **2016**, *51* (10), 4728–4738. https://doi.org/10.1007/s10853-016-9797-7.
- (325) Gonçalves, M.; Simões, N.; Serra, C.; Flores-Colen, I. A Review of the Challenges Posed

- by the Use of Vacuum Panels in External Insulation Finishing Systems. *Appl. Energy* **2020**, *257*, 114028. https://doi.org/https://doi.org/10.1016/j.apenergy.2019.114028.
- (326) Sima, M.; Vrbova, K.; Zavodna, T.; Honkova, K.; Chvojkova, I.; Ambroz, A.; Klema, J.; Rossnerova, A.; Polakova, K.; Malina, T.; Belza, J.; Topinka, J.; Rossner Jr, P. The Differential Effect of Carbon Dots on Gene Expression and DNA Methylation of Human Embryonic Lung Fibroblasts as a Function of Surface Charge and Dose. *Int. J. Mol. Sci.* **2020**, *21* (13), 4763. https://doi.org/10.3390/ijms21134763.
- (327) Cui, L.; Ren, X.; Sun, M.; Liu, H.; Xia, L. Carbon Dots: Synthesis, Properties and Applications. *Nanomaterials* **2021**, *11* (12). https://doi.org/10.3390/nano11123419.
- (328) Abbaspour, N.; Hurrell, R.; Kelishadi, R. Review on Iron and Its Importance for Human Health. *J. Res. Med. Sci.* **2014**, *19* (2), 164–174.
- (329) An, Q.; Lin, Q.; Huang, X.; Zhou, R.; Guo, X.; Xu, W.; Wang, S.; Xu, D.; Chang, H.-T. Electrochemical Synthesis of Carbon Dots with a Stokes Shift of 309 Nm for Sensing of Fe3+ and Ascorbic Acid. *Dye. Pigment.* **2021**, *185*, 108878. https://doi.org/https://doi.org/10.1016/j.dyepig.2020.108878.
- (330) Li, J.; Cao, D.; Huang, Y.; Chen, B.; Chen, Z.; Wang, R.; Dong, Q.; Wei, Q.; Liu, L. Zinc Intakes and Health Outcomes: An Umbrella Review. *Front. Nutr.* **2022**, 9. https://doi.org/10.3389/fnut.2022.798078.
- (331) Gao, T.; Xing, S.; Xu, M.; Fu, P.; Yao, J.; Zhang, X.; Zhao, Y.; Zhao, C. A Peptide Nucleic Acid–Regulated Fluorescence Resonance Energy Transfer DNA Assay Based on the Use of Carbon Dots and Gold Nanoparticles. *Microchim. Acta* **2020**, *187* (7), 375. https://doi.org/10.1007/s00604-020-04357-w.
- (332) Feng, L.; Zhao, A.; Ren, J.; Qu, X. Lighting up Left-Handed Z-DNA: Photoluminescent

Carbon Dots Induce DNA B to Z Transition and Perform DNA Logic Operations. *Nucleic Acids Res.* **2013**, *41* (16), 7987–7996. https://doi.org/10.1093/nar/gkt575.

- (333) Kumar, R.; Kumar, V. B.; Gedanken, A. Sonochemical Synthesis of Carbon Dots, Mechanism, Effect of Parameters, and Catalytic, Energy, Biomedical and Tissue Engineering Applications. *Ultrason. Sonochem.* 2020, 64, 105009. https://doi.org/https://doi.org/10.1016/j.ultsonch.2020.105009.
- (334) Liu, Q.; Zhang, N.; Shi, H.; Ji, W.; Guo, X.; Yuan, W.; Hu, Q. One-Step Microwave Synthesis of Carbon Dots for Highly Sensitive and Selective Detection of Copper Ions in Aqueous Solution. *New J. Chem.* **2018**, *42* (4), 3097–3101. https://doi.org/10.1039/C7NJ05000C.
- (335) Chu, L.; Shi, J.; de Cursi, E. The Fingerprints of Resonant Frequency for Atomic Vacancy Defect Identification in Graphene. *Nanomaterials* **2021**, *11* (12). https://doi.org/10.3390/nano11123451.
- (336) Ma, C.-B.; Zhu, Z.-T.; Wang, H.-X.; Huang, X.; Zhang, X.; Qi, X.; Zhang, H.-L.; Zhu, Y.; Deng, X.; Peng, Y.; Han, Y.; Zhang, H. A General Solid-State Synthesis of Chemically-Doped Fluorescent Graphene Quantum Dots for Bioimaging and Optoelectronic Applications. *Nanoscale* **2015**, *7* (22), 10162–10169. https://doi.org/10.1039/C5NR01757B.
- (337) Liu, Y.; Zhou, L.; Li, Y.; Deng, R.; Zhang, H. Highly Fluorescent Nitrogen-Doped Carbon Dots with Excellent Thermal and Photo Stability Applied as Invisible Ink for Loading Important Information and Anti-Counterfeiting. *Nanoscale* 2017, 9 (2), 491–496. https://doi.org/10.1039/C6NR07123F.
- (338) Kozák, O.; Sudolská, M.; Pramanik, G.; Cígler, P.; Otyepka, M.; Zbořil, R.

- Photoluminescent Carbon Nanostructures. *Chem. Mater.* **2016**, 28 (12), 4085–4128. https://doi.org/10.1021/acs.chemmater.6b01372.
- (339) Lu, D.; Gong, X.; Chen, Y.; Huang, J.; Lin, Y.; Luo, Z.; Huang, Y. Synthesis and Photoluminescence Characteristics of the LiGd_3(MoO_4)_5:Eu^3+ Red Phosphor with High Color Purity and Brightness. *Opt. Mater. Express* **2018**, *8* (2), 259. https://doi.org/10.1364/ome.8.000259.
- (340) Zhu, X.; Zhang, Z.; Xue, Z.; Huang, C.; Shan, Y.; Liu, C.; Qin, X.; Yang, W.; Chen, X.; Wang, T. Understanding the Selective Detection of Fe3+ Based on Graphene Quantum Dots as Fluorescent Probes: The Ksp of a Metal Hydroxide-Assisted Mechanism. *Anal. Chem.* 2017, 89 (22), 12054–12058. https://doi.org/10.1021/acs.analchem.7b02499.
- (341) Li, C.; Wang, Y.-T.; Chen, Y.; Wang, Y. Hyperbranched Poly(Amido Amine) Entrapped Tetraphenylethene as a Fluorescence Probe for Sequential Quadruple-Target Detection and Its Potential as a Chemical Logic Gate. *Anal. Chem.* **2020**, *92* (14), 9755–9763. https://doi.org/10.1021/acs.analchem.0c01155.
- (342) Barnoy, E. A.; Motiei, M.; Tzror, C.; Rahimipour, S.; Popovtzer, R.; Fixler, D. Biological Logic Gate Using Gold Nanoparticles and Fluorescence Lifetime Imaging Microscopy.

 ACS Appl. Nano Mater. 2019, 2 (10), 6527–6536.

 https://doi.org/10.1021/acsanm.9b01457.
- (343) Fricker, M.; Tolkovsky, A. M.; Borutaite, V.; Coleman, M.; Brown, G. C. Neuronal Cell Death. *Physiol. Rev.* **2018**, *98* (2), 813–880. https://doi.org/10.1152/physrev.00011.2017.
- (344) McKinnon, P. J. DNA Repair Deficiency and Neurological Disease. *Nat. Rev. Neurosci.* **2009**, *10* (2), 100–112. https://doi.org/10.1038/nrn2559.
- (345) Kumar, A.; Yegla, B.; Foster, T. C. Redox Signaling in Neurotransmission and Cognition

- During Aging. *Antioxid. Redox Signal.* **2018**, 28 (18), 1724–1745. https://doi.org/10.1089/ars.2017.7111.
- (346) Briffa, J.; Sinagra, E.; Blundell, R. Heavy Metal Pollution in the Environment and Their Toxicological Effects on Humans. *Heliyon* **2020**, *6* (9), e04691. https://doi.org/https://doi.org/10.1016/j.heliyon.2020.e04691.
- (347) Ding, R.; Cheong, Y. H.; Ahamed, A.; Lisak, G. Heavy Metals Detection with Paper-Based Electrochemical Sensors. *Anal. Chem.* **2021**, *93* (4), 1880–1888. https://doi.org/10.1021/acs.analchem.0c04247.
- (348) Tchounwou, P. B.; Yedjou, C. G.; Patlolla, A. K.; Sutton, D. J. Heavy Metal Toxicity and the Environment. *Exp. Suppl.* **2012**, *101*, 133–164. https://doi.org/10.1007/978-3-7643-8340-4_6.
- (349) Balali-Mood, M.; Naseri, K.; Tahergorabi, Z.; Khazdair, M. R.; Sadeghi, M. Toxic Mechanisms of Five Heavy Metals: Mercury, Lead, Chromium, Cadmium, and Arsenic. Front. Pharmacol. 2021, 12. https://doi.org/10.3389/fphar.2021.643972.
- (350) Barbier, O.; Jacquillet, G.; Tauc, M.; Cougnon, M.; Poujeol, P. Effect of Heavy Metals on, and Handling by, the Kidney. *Nephron Physiology*. 2005. https://doi.org/10.1159/000083981.
- (351) Bakulski, K. M.; Seo, Y. A.; Hickman, R. C.; Brandt, D.; Vadari, H. S.; Hu, H.; Park, S. K. Heavy Metals Exposure and Alzheimer's Disease and Related Dementias. *J. Alzheimers. Dis.* 2020, 76 (4), 1215–1242. https://doi.org/10.3233/JAD-200282.
- (352) Kim, H. S.; Kim, Y. J.; Seo, Y. R. An Overview of Carcinogenic Heavy Metal: Molecular Toxicity Mechanism and Prevention. *J. cancer Prev.* **2015**, *20* (4), 232–240. https://doi.org/10.15430/JCP.2015.20.4.232.

(353) Gu, J.; Zhang, X.; Pang, A.; Yang, J. Facile Synthesis and Photoluminescence

Characteristics of Blue-Emitting Nitrogen-Doped Graphene Quantum Dots.

Nanotechnology 2016, 27 (16), 165704. https://doi.org/10.1088/0957-4484/27/16/165704.

- (354) Yahaya Pudza, M.; Zainal Abidin, Z.; Abdul Rashid, S.; Md Yasin, F.; Noor, A. S. M.; Issa, M. A. Eco-Friendly Sustainable Fluorescent Carbon Dots for the Adsorption of Heavy Metal Ions in Aqueous Environment. *Nanomaterials*. 2020. https://doi.org/10.3390/nano10020315.
- (355) Santos, R. M. dos; Flauzino Neto, W. P.; Silvério, H. A.; Martins, D. F.; Dantas, N. O.; Pasquini, D. Cellulose Nanocrystals from Pineapple Leaf, a New Approach for the Reuse of This Agro-Waste. *Ind. Crops Prod.* 2013, 50, 707–714. https://doi.org/https://doi.org/10.1016/j.indcrop.2013.08.049.
- (356) Huang, G.; Chen, X.; Wang, C.; Zheng, H.; Huang, Z.; Chen, D.; Xie, H.
 Photoluminescent Carbon Dots Derived from Sugarcane Molasses: Synthesis, Properties, and Applications. *RSC Adv.* 2017, 7 (75), 47840–47847.
 https://doi.org/10.1039/C7RA09002A.
- (357) Mandal, A.; Chakrabarty, D. Isolation of Nanocellulose from Waste Sugarcane Bagasse (SCB) and Its Characterization. *Carbohydr. Polym.* 2011, 86 (3), 1291–1299. https://doi.org/https://doi.org/10.1016/j.carbpol.2011.06.030.
- (358) Jungnikl, K.; Paris, O.; Fratzl, P.; Burgert, I. The Implication of Chemical Extraction

 Treatments on the Cell Wall Nanostructure of Softwood. *Cellulose* **2008**, *15* (3), 407–418.

 https://doi.org/10.1007/s10570-007-9181-5.
- (359) Dilamian, M.; Noroozi, B. A Combined Homogenization-High Intensity Ultrasonication Process for Individualization of Cellulose Micro-Nano Fibers from Rice Straw. *Cellulose*

- **2019**, 26 (10), 5831–5849. https://doi.org/10.1007/s10570-019-02469-y.
- (360) Jiang, N.; Huang, M.; Li, J.; Song, J.; Zheng, S.; Gao, Y.; Shao, M.; Li, Y. Enhanced Bioelectricity Output of Microbial Fuel Cells via Electrospinning Zeolitic Imidazolate Framework-67/Polyacrylonitrile Carbon Nanofiber Cathode. *Bioresour. Technol.* 2021, 337, 125358. https://doi.org/https://doi.org/10.1016/j.biortech.2021.125358.
- (361) Wang, T.; Zhai, Y.; Zhu, Y.; Li, C.; Zeng, G. A Review of the Hydrothermal Carbonization of Biomass Waste for Hydrochar Formation: Process Conditions, Fundamentals, and Physicochemical Properties. *Renew. Sustain. Energy Rev.* 2018, 90, 223–247. https://doi.org/10.1016/j.rser.2018.03.071.
- (362) Mahmoud, D. A.; Hassanein, N. M.; Youssef, K. A.; Abou Zeid, M. A. Das Bau-SOLL Im Tunnelbau Wo Liegen Die Missverständnisse Wo Liegen Die Größten Irrtümer. *Braz. J. Microbiol.* **2011**, *42* (3), 1007–1016.
- (363) Mazzaglia, A.; Scala, A.; Sortino, G.; Zagami, R.; Zhu, Y.; Sciortino, M. T.; Pennisi, R.; Pizzo, M. M.; Neri, G.; Grassi, G.; Piperno, A. Intracellular Trafficking and Therapeutic Outcome of Multiwalled Carbon Nanotubes Modified with Cyclodextrins and Polyethylenimine. *Colloids Surfaces B Biointerfaces* 2018, 163, 55–63. https://doi.org/https://doi.org/10.1016/j.colsurfb.2017.12.028.
- (364) Kavanagh, N.; Ryan, E. J.; Widaa, A.; Sexton, G.; Fennell, J.; O'Rourke, S.; Cahill, K. C.; Kearney, C. J.; O'Brien, F. J.; Kerrigan, S. W. Staphylococcal Osteomyelitis: Disease Progression, Treatment Challenges, and Future Directions. *Clin. Microbiol. Rev.* 2018, 31 (2). https://doi.org/10.1128/CMR.00084-17.
- (365) Speechly-Dick, M. E.; Swanton, R. H. Osteomyelitis and Infective Endocarditis.

 *Postgrad. Med. J. 1994, 70 (830), 885–890. https://doi.org/10.1136/pgmj.70.830.885.

Green Synthesis of Carbon Nanodots and its Theranostic and Biosensing Applications

by Somedutta Maity

Librarian

Indira Gandhi Memorial Library UNIVERSITY OF HYDERABAD

Central University P.O. HYDERABAD-500 046.

Submission date: 22-Feb-2023 04:37PM (UTC+0530)

Submission ID: 2020369755

File name: Somedutta_Maity.pdf (7.36M)

Word count: 34010

Character count: 185303

Green Synthesis of Carbon Nanodots and its Theranostic and Biosensing Applications

ORIGINALITY REPORT 77% SIMILARITY INDEX INTERNET SOURCES STUDENT PAPERS PRIMARY SOURCES Somedutta Maity, Munendra Singh Tomar, Kirti Wasnik, Sukanya Patra et al. " Seed Derived Carbon Nanocapsules: Cell Imaging, Depolarization of Mitochondrial Membrane Potential, and Dose-Dependent Control Death of Breast Cancer ", ACS Biomaterials Sciencem. GHANASHYAM KRISH Centre for Advanced Studies in Electronics Science & Technology & Engineering, 2022 School of Physics, University of Hydera Publication HYDERABAD-500 046. Telangana, Ind Submitted to University of Hyderabad, Hyderabad Student's own Student Paper Submitted to Medizinischen Universität Wienf. M. GHAMASHYAM KRI Centre for Adva Ged Studies Electronics Science & Technol School of Physics, University of Hyd HYDERABAD-500 046. Telangana, Submitted to IIT Delhi Student Paper www.researchgate.net Internet Source www.mdpi.com

Internet Source

7	www.mayoclinic.org Internet Source	<1%
8	Xian Zheng, Wenyu Cheng, Chendong Ji, Jin Zhang, Meizhen Yin. "Detection of metal ions in biological systems: A review", Reviews in Analytical Chemistry, 2020 Publication	<1%
9	www.dovepress.com Internet Source	<1%
10	Submitted to Higher Education Commission Pakistan Student Paper	<1%
11	www.science.gov Internet Source	<1%
12	Submitted to Universiti Tenaga Nasional Student Paper	<1%
13	Submitted to University of Utah Student Paper	<1%
14	Koushi Kumar, Shanmukha Kumar Doddi, Marasanapalli Kalle Arunasree, Pradip Paik. " CPMV-induced synthesis of hollow mesoporous SiO nanocapsules with excellent performance in drug delivery ", Dalton Transactions, 2015 Publication	<1%

15	Internet Source	<1%
16	www.repository.cam.ac.uk Internet Source	<1%
17	Ge Gao, Yao-Wen Jiang, Hao-Ran Jia, Jingjing Yang, Fu-Gen Wu. "On-off-on fluorescent nanosensor for Fe 3+ detection and cancer/normal cell differentiation via silicondoped carbon quantum dots", Carbon, 2018	<1%
18	ihim.uran.ru Internet Source	<1%
19	WWW.rsc.org Internet Source	<1%
20	Lihong Shi, Bo Zhao, Xiaofeng Li, Guomei Zhang, Yan Zhang, Chuan Dong, Shaomin Shuang. "Eco-friendly synthesis of nitrogen- doped carbon nanodots from wool for multicolor cell imaging, patterning, and biosensing", Sensors and Actuators B: Chemical, 2016 Publication	<1%
21	engagedscholarship.csuohio.edu Internet Source	<1%
22	publications.iitm.ac.in Internet Source	<1%

<1%
<1%
<1%
<1%
<1%
<1%
<1%
<1%
<1%

	"Biosynthesis of Sulphur Nanoparticles and discovering its effectiveness for some biological applications", Journal of Physics: Conference Series, 2022 Publication	
33	Submitted to Midlands State University Student Paper	<1%
34	Submitted to Norfolk State University Student Paper	<1%
35	Rajendra K. Singh, Kapil D. Patel, Chinmaya Mahapatra, Min Sil Kang, Hae-Won Kim. "C- Dot Generated Bioactive Organosilica Nanospheres in Theranostics: Multicolor Luminescent and Photothermal Properties Combined with Drug Delivery Capacity", ACS Applied Materials & Interfaces, 2016 Publication	<1%
36	www.politesi.polimi.it Internet Source	<1%
37	ir.kluniversity.in Internet Source	<1%
38	mdpi-res.com Internet Source	<1%
39	scholarsmine.mst.edu	

Salam Jumah mashkoor, Nazar Khalaf Mahan,

Khetam Habeeb Rasool, Ahmed N. Abd.

32

<1%

Hari Krishna Sadhanala, Subrata Senapati, Karuna Kar Nanda. "Temperature sensing using sulfur-doped carbon nanoparticles", Carbon, 2018 <1%

Publication

Submitted to Marryatville High School Student Paper

<1%

Submitted to School of Business and Management ITB

<1%

Student Paper

Somasundaram Anbu Anjugam
Vandarkuzhali, Sampathkumar Natarajan,
Shanmugapriya Jeyabalan, Gandhi Sivaraman
et al. "Pineapple Peel-Derived Carbon Dots:
Applications as Sensor, Molecular Keypad
Lock, and Memory Device", ACS Omega, 2018

<1%

pure.tue.nl

Publication

<1%

Submitted to St Ives High School
Student Paper

<1%

kups.ub.uni-koeln.de

<1%

repositorium.sdum.uminho.pt

s-space.snu.ac.kr

<1%

Mei Han, Shoujun Zhu, Siyu Lu, Yubin Song, Tanglue Feng, Songyuan Tao, Junjun Liu, Bai Yang. "Recent progress on the photocatalysis of carbon dots: Classification, mechanism and applications", Nano Today, 2018

<1%

- Publication
- commons.und.edu

<1%

Gupta, Abhisek, Bikash Kumar Shaw, and Shyamal K. Saha. "Bright Green Photoluminescence in Aminoazobenzene-Functionalized Graphene Oxide", The Journal of Physical Chemistry C

<1%

Murugan Nagaraj, K. Sundramoorthy Ashok.
"Green synthesis of fluorescent carbon dots
from Borassus flabellifer flower for label-free
highly selective and sensitive detection of
Fe3+ ions", New Journal of Chemistry, 2018

<1%

hal.science
Internet Source

Publication

<1%

54	mail.scialert.net Internet Source	<1%
55	Barati, Ali, Mojtaba Shamsipur, and Hamid Abdollahi. "Metal-ion-mediated fluorescent carbon dots for indirect detection of sulfide ions", Sensors and Actuators B Chemical, 2016. Publication	<1%
56	Submitted to Southern Illinois University Student Paper	<1%
57	Tuba Iftikhar, Natalya V. Izarova, Jan van Leusen, Paul Kögerler. "The Polyoxotungstate Archetype {P4W27} and its 3d Derivatives", Chemistry – A European Journal, 2021	<1%
58	scholarbank.nus.edu.sg Internet Source	<1%
59	staff.ustc.edu.cn Internet Source	<1%
60	"Nanotechnologies for Environmental Remediation", Springer Science and Business Media LLC, 2017 Publication	<1%
61	Jun Zhang, Lian He, Can Guo, Ziyue Liu, Kumaravel Kaliaperumal, Balian Zhong, Yueming Jiang. "Evaluation of Aspergillus	<1%

aculeatus GC-09 for the biological control of citrus blue mold caused by Penicillium italicum", Fungal Biology, 2022

Publication

62	Submitted to University of Glasgow Student Paper	<1%
63	Wang, L "Cs"2"."5H"0"."5PWO"4"0/SiO"2 as addition self-humidifying composite membrane for proton exchange membrane fuel cells", Electrochimica Acta, 20070505	<1%
64	link.springer.com Internet Source	<1%
65	ufdcimages.uflib.ufl.edu Internet Source	<1%
66	vdocuments.net Internet Source	<1%
67	www.aisc.org Internet Source	<1%
68	Srinivasan Venkatesan, Asha Jhonsi Mariadoss, Kathiravan Arunkumar, Ashokkumar Muthupandian. "Fuel waste to fluorescent carbon dots and its multifarious applications", Sensors and Actuators B: Chemical, 2019	<1%

69	Mohd Fa	med M., Sher Baaisal, Abdullah Nanoparticles", Ir	Л "Chapter 3	Iron	<1%
70	Submitte Technole Student Paper		Institute of		<1%
71	reposito	ory.uwc.ac.za			<1%
72	scholar.	ufs.ac.za			<1%
	le quotes le bibliography	On On	Exclude matches	< 14 words	



pubs.acs.org/journal/abseba Article

Azadirachta indica Seed Derived Carbon Nanocapsules: Cell Imaging, Depolarization of Mitochondrial Membrane Potential, and Dose-Dependent Control Death of Breast Cancer

Somedutta Maity, Munendra Singh Tomar, Kirti Wasnik, Sukanya Patra, Monami Das Modak, Prem Shankar Gupta, Divya Pareek, Monika Singh, and Pradip Paik*



Cite This: https://doi.org/10.1021/acsbiomaterials.2c00463



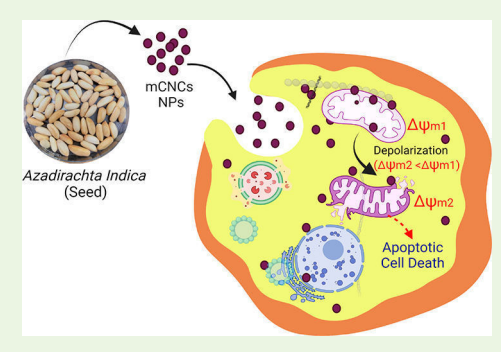
ACCESS I

III Metrics & More

Article Recommendations

Supporting Information

ABSTRACT: In this work, a series of mesoporous carbon nanocapsules (mCNS) of size below 10 nm have been prepared from *Azadirachta indica* seeds with a very easy and cost-effective approach. These nanocapsules can emit red and green light and are effective for cell imaging. Further, these carbon nanocapsules are biocompatible toward the normal healthy cells, however, they possess modest cytotoxicity against the MCF-7 (human breast cancer) and triple-negative breast cancer (TNBC) (MDA- MB-231 breast cancer cells), and the rate of killing cancer cells strongly depends on the dose of mCNCs. Further, the mitochondrial membrane potential and apoptosis assay were performed to analyze the therapeutic significance of these nanocapsules to kill breast cancer. Results showed that these carbon nanocapsules can depolarize the mitochondrial membrane potential alone (without using conventional drugs) and can change the physiological parameters



and cellular metabolic energy of the cancer cells and kill them. The apoptosis results confirmed the death of breast cancer cells in the form of apoptosis and necrosis. Moreover, the results suggested that the porous carbon nanocapsules (mCNCs) reported herein can be used as a potential candidate and useful for the theranostic applications such as for cancer cell detection and therapy without using any conventional drugs.

KEYWORDS: theranostics, carbon nanocapsules, porous, breast cancer, therapy, membrane potential

INTRODUCTION

A special type of nanoparticles exhibited fascinating properties for their usages in theranostic applications. 1-3 These nanoparticles possess the potential for molecular imaging and are effective in the treatment of the infected cells together with better molecular understanding.⁴ Further the advantages of these NPs are (1) they can monitor the response of the treatment very precisely, (2) can avoid the unnecessary side effects to the patients, and (3) they are potential for the costeffective treatment and ease the treatment procedures³ Another advantage of these NPs to use in theranostic applications, especially for cancer therapy, is that the cancer growth can be controlled even in the diagnostic steps, and in the subsequent steps, it becomes easier to treat cancer³⁻⁸ Apart from the nanoparticles, the biologically engineered cells can also be used for theranostic applications. However, every material and approach proposed to use in theranostic applications faces various challenges that must be overcome for safer clinical usages. 10 For instance, cancer cells grow faster and create leaky vascular systems in the surrounding tissues, and for the effective treatment with conventional chemotherapy drugs, the highly efficient drug delivery vehicles with enhanced permeability and retention (EPR) are required. 11,12

Developing such suitable material is always a challenging task. In the early stage of the concept "theranostics", the fluorophore (or fluorescent component) was usually attached with the drug delivery vehicles loaded with therapeutic components for the diagnostic purposes and found that the progress was very slow. We should also note that the cancer cells can efficiently interact with the surrounding immune cells, endothelial cells, neovasculature, and fibroblast. Further, they develop dangerous survival strategies with eight hallmarks, such as (1) selfsufficiency with growing signal, (2) evasion of apoptosis, (3) inactivate the antigrowth signal, (4) sustained angiogenesis, (5) metastasis, (6) rapid replication, (7) deregulation of cellular energetics, and finally (8) escape from immune regulation. The cancer cells can also develop severe genome instability and tumor promoting inflammation.¹⁶ Therefore, in such a situation, the better understanding of theranostics is required and it demands suitable materials to be developed.

Received: April 20, 2022 Accepted: July 22, 2022



Nanoscale



PAPER

View Article Online
View Journal | View Issue



Cite this: Nanoscale, 2017, 9, 14641

Mesoporous ZnO nanocapsules for the induction of enhanced antigen-specific immunological responses†

Sumbul Afroz, \$\bigcup_{\pm}^a\text{ Himadri Medhi,}\frac{t}{b}\text{ Somedutta Maity,}^b\text{ Gillipsie Minhas,}^a\text{ Srikanth Battu,}^a\text{ Jeevan Giddaluru,} \$\bigcup_{\pm}^a\text{ Koushi Kumar,}^b\text{ Pradip Paik} \$\bigcup_{\pm}^{\pm b}\text{ and Nooruddin Khan} \$\bigcup_{\pm}^{\pm a}\text{ Nooruddin Khan} \$\bigcup_{\pm}^{\pm a}\text{ Nooruddin Khan} \$\bigcup_{\pm}^{\pm} \text{ And Nooruddin Khan} \$\bigcup_{\pm}^{\pm a}\text{ And Nooruddin Khan} \$\bigcup_{\pm}^{\pm a}\text{ Sumbout Minham Nooruddin Khan} \$\bigcup_{\pm}^{\pm} \text{ And Noor

The application of nanotechnology in vaccinology has fuelled rapid advancement towards the design and development of nanovaccines. Nanoparticles have been found to enhance vaccine efficacy through the spatiotemporal orchestration of antigen delivery to secondary lymphoid organs and antigen-presentation by Antigen Presenting Cells (APCs) synchronized with stimulation of innate and adaptive immune responses. Metal based nanoparticles (MNPs) have been extensively engineered for the generation of nanovaccines owing to their intrinsic adjuvant-like properties and immunomodulatory functions. Furthermore, mesoporous nanocapsules of late have attracted researchers due to their precise size and exclusive capacity to encapsulate a wide range of biomolecules and their sustained release at the targeted sites. Herein, we have designed a novel mesoporous ZnO nanocapsule (mZnO) having a size of ~12 nm with an average pore diameter of 2.5 nm, using a surfactant-free sonochemical method and investigated its immunomodulatory properties by using Ova loaded mZnO nanocapsules [mZnO(Ova)] in a mice model. Our findings show that mZnO(Ova) administration steered the enhanced expansion of antigenspecific T-cells and induction of IFN-y producing effector CD4⁺ and CD8⁺ T-cells. Also, antigen-specific IgG levels were enriched in both the serum and lymph nodes of mZnO(Ova) immunized mice. Further, we noticed a substantial increase in serum IgG2a or IgG2b levels and IFN-γ secretion in Ova restimulated splenocytes from mZnO(Ova) immunized mice, indicating that mZnO(Ova) skew Th1 type immune response. Overall, the uniqueness of mZnO nanocapsules in terms of the defined particle to pore numbers ratio (maximum of three cavities per particle) allows loading antigens efficiently. Given these features in combination with its immunomodulatory characteristics reinforces the idea that mZnO could be used as an effective antigen-adjuvant platform for the development of novel nano-based vaccines against multiple diseases.

Received 24th May 2017, Accepted 24th August 2017 DOI: 10.1039/c7nr03697c

rsc.li/nanoscale

Introduction

The discovery of vaccines has been one of the greatest achievements of modern medicine in the war between humans and pathogens, yet the development of potent vaccines against several emerging and re-emerging diseases remains a formid-

able challenge. This could be attributed to several limitations such as antigen selection, proper antigen delivery and adjuvant engineering approaches employed towards vaccine development. Nanotechnology has gained significant importance in the past decades, both in industrial applications and in the field of biomedical sciences, especially in "nanovaccinology". As we cruise into an era of modern vaccines, the use of nanotechnology has allowed researchers to engineer nanoparticles varying in shape, size, composition and surface properties³ for improving the efficiency of antigen delivery and antigen immunogenicity by augmenting antigen processing/presentation and enhancing antigen stability and the sustained release of antigens.4 Nanovaccines are being used extensively as therapeutics for the treatment of various autoimmune diseases⁵ as well as degenerative diseases such as Alzheimer's,6 cancer treatment,7-9 cardiovascular diseases10 and nicotine addic-

^aSchool of Life Sciences, Department of Biotechnology and Bioinformatics, University of Hyderabad, Hyderabad-500046, Telangana, India. E-mail: noor@uohyd.ac.in, noorhcu@gmail.com

^bSchool of Engineering Sciences and Technology, University of Hyderabad, Hyderabad 500046, Telangana, India. E-mail: pradip.paik@gmail.com, ppse@uohyd.ernet.in, paik@uohyd.ac.in

 $[\]dagger\,\text{Electronic}$ supplementary information (ESI) available. See DOI: 10.1039/c7nr03697c

[‡]These authors contributed equally to this work.

Hollow mesoporous polymer capsules with Dihydroartemisinin and Chloroquine diphosphate for knocking down *Plasmodium falciparum* infection

Himadri Medhi^b, Somedutta Maity^b, Niranjan Suthram^c, Suresh Kumar Chalapareddy^d, Mrinal K. Bhattacharyya^c, Pradip Paik**^{a,b}

^aSchool of Biomedical Engineering, Indian Institute of Technology (BHU), Varanasi 220 051, India

^bSchool of Engineering Sciences and Technology, University of Hyderabad, 500 046, India

^cDepartment of Biochemistry, School of Life Sciences, University of Hyderabad, 500 046, India

^dDepartment of Biotechnology and Bio-informatics, School of Life Sciences, University of Hyderabad, 500 046, India

*E-mail: paik.bme@iitbhu.ac.in, ppse@uohyd.ernet.in, pradip.paik@gmail.com

RSC Advances



PAPER

View Article Online
View Journal | View Issue



Cite this: RSC Adv., 2018, 8, 37492

UCN-SiO₂-GO: a core shell and conjugate system for controlling delivery of doxorubicin by 980 nm NIR pulse†

Pradip Paik, **D** **A** K. Santhosh Kumar, **D** Monami Das Modak, ** Koushi Kumar U** and Somedutta Maity**

Herein, graphene oxide (GO) has been attached with core-shell upconversion-silica (UCN-SiO₂) nanoparticles (NPs) to form a GO-UCN-SiO₂ hybrid nanocomposite and used for controlled drug delivery. The formation of the nanocomposite has been confirmed by various characterization techniques. To date, a number of reports are available on GO and its drug delivery applications, however, the synergic properties that arise due to the combination of GO, UCNPs and SiO₂ can be used for controlled drug delivery. New composite UCN@SiO2-GO has been synthesized through a bioconjugation approach and used for drug delivery applications to counter the lack of quantum efficiency of the upconversion process and control sustained release. A model anticancer drug (doxorubicin, DOX) has been loaded to UCNPs, UCN@SiO₂ NPs and the UCN@SiO₂-GO nanocomposite. The photosensitive release of DOX from the UCN@SiO2-GO nanocomposite has been studied with 980 nm NIR laser excitation and the results obtained for UCNPs and UCN@SiO2 NPs compared. It is revealed that the increase in the NIR laser irradiation time from 1 s to 30 s leads to an increase in the amount of DOX release in a controlled manner. In vitro studies using model cancer cell lines have been performed to check the effectiveness of our materials for controlled drug delivery and therapeutic applications. Obtained results showed that the designed UCN@SiO2-GO nanocomposite can be used for controlled delivery based therapeutic applications and for cancer treatment.

Received 22nd August 2018 Accepted 24th October 2018

DOI: 10.1039/c8ra07030j

rsc.li/rsc-advances

Introduction

Upconversion nanoparticles (UCN) convert low-frequency light into high-frequency light. This phenomenon was observed in 1960 by Auzel Ovsyankin and Feofilov.¹ UCN NPs are used in various applications including fluorescent imaging for cancer diagnostics² and photodynamic therapy for treatment (PDT).³-6 These UCN materials can be inorganic or organic/polymer materials.¹ Inorganic UCN materials can be synthesized through thermal treatment of inorganic precursors, whereas polymer based UCN materials can be synthesized through various polymerization techniques, such as reversible addition fragmentation chain transfer (RAFT), ring opening polymerization (ROP) etc.² With these polymers NIR light sensitive cyanobased dyes can be conjugated. In PDT, after excitation by NIR laser light, UCN release drug/medicines loaded in the nanocapsules of polymers of inorganic materials.² During this

To date, a number of reports are available on the application of GO for drug delivery ¹¹⁻¹³ However, the loading of drug in GO is influenced by its electronic structure and electronic environment. A number of nanoparticles including UCN NPs are also reported for drug delivery and cancer therapy. ¹⁴⁻¹⁶ To the best of our knowledge, a nanocomposite of GO conjugated with UCN@SiO₂ NPs and its role in sustained drug delivery and therapeutic effects have never been reported.

It can be noted that appropriate design of nanomaterials¹⁷⁻¹⁹ or nanocomposites with suitable constituents tunes the sustained delivery and doses of drugs for various treatment procedures.²⁰⁻²² Depending on the functional behaviour of GO the effective delivery of drug can also be varied. Furthermore, photodynamic therapy (PDT) is an efficient approach to kill

process, NIR excites lower state electrons to the higher energy levels and subsequently converts lower-energy light to higher-energy light and influences the release of drugs at the targeted sites. However, the efficiency of the PDT process depends on the constituent materials (e.g., polymer, peptide, hydro gel etc.) and loaded photosensitizer. PDT has several advantages over more conventional cancer therapies such as, it is cost effective, able to treat/kill the infected cells at highly localized sites and is specific for tumor treatments and exhibits a higher cure rate for some tumors. 5,6,9

[&]quot;School of Biomedical Engineering, Indian Institute of Technology (BHU), Varanasi 221 005, UP, India. E-mail: paik.bme@iitbhu.ac.in; pradip.paik@gmail.com

^bSchool of Engineering Sciences and Technology, University of Hyderabad, Hyderabad-500046, Telangana, India. Tel: (+91)-(040) 2313 4457 (O)

[†] Electronic supplementary information (ESI) available: Table (EDAX) Fig. EDAX, TEM (core shell UCN@SiO₂) and UCN@SiO₂-GO. See DOI: 10.1039/c8ra07030j

RSC Advances



View Article Online

PAPER



Cite this: RSC Adv., 2019, 9, 38246

Self-assembled pearl-necklace patterned upconverting nanocrystals with highly efficient blue and ultraviolet emission: femtosecond laser based upconversion properties†

Monami Das Modak,^b Ganesh Damarla,^c Somedutta Maity,^b Anil K. Chaudhary^c and Pradip Paik (1)**ab

This work reports new findings on the formation of a pearl-necklace pattern in self-assembled upconverting nanocrystals (UCN-PNs) which exhibit strong upconversion emission under an NIR excitation source of a femtosecond laser (Fs-laser). Each nano-necklace consists of several upconversion nanoparticles (UCNPs) having a size $ca. 10 \pm 1$ nm. UCN-PNs are arranged in a self-organized manner to form necklace type chains with an average length of 140 nm of a single row of nanoparticles. Furthermore, UCN-PNs are comprised of UCNPs with an average interparticle separation of ca. 4 nm in each of the nanonecklace chains. Interestingly, these UCN-PNs exhibit high energy upconversion especially in the UV region on interaction with a 140 Fs-laser pulse duration at 80 MHz repetition rate and intense blue emission at 450 nm on interaction with a 900 nm excitation source is obtained. The preparation of self-assembled UCNPs is easy and they are very stable for a longer period of time. The emission (fluorescence/luminescence) intensity is very high which can make them unique in innumerable industrial and bio-applications such as for disease diagnosis and therapeutic applications by targeting the infected cells with enhanced efficiency.

Received 15th August 2019 Accepted 15th November 2019

DOI: 10.1039/c9ra06389g

rsc.li/rsc-advances

Introduction

Upconverting nanocrystals are attractive due to several unique properties and for their applications in materials, materials science, industrial applications for designing solar cells, sensors *etc.* and for biomedical medical applications.^{1,2} Rareearth upconverting materials have been demanded as they are the best energy upconverting (NIR-to-visible) materials ever known, therefore currently researchers are focusing on their design, synthesis and spectroscopic properties. Furthermore, upconverting materials possess potential uses in biological labeling and bio-assays and their extent of uses has increased remarkably with time.³⁻⁷ All these unique features drive us to synthesize self-assembled UCNPs having strong upconversion emission. To the best of our knowledge, self-assembled pearlnecklace type upconverting nanoparticles (UCN-PNs) are never known. A report was found where UCNPs were impregnated in

Self-assembled materials can be obtained from nature to the laboratory. Self-assembly in living system is biologically controlled whereas; self-assembly formation in laboratory is controlled artificially. The assembly of nanomaterials is purely represented by non-covalent bonding and controlled both by kinetic and thermodynamically. Inside laboratory self-

porphyrin dendrimers.8 In this work we are enabled to prepare self-assembled UCNPs in in situ condition without incorporating any external polymeric components. The as-prepared UCN-PNs have been formed by consuming all precursors into solid crystal nuclei as white precipitates at lower reaction temperature and then with increasing the reaction temperature crystal growth occurred followed by the formation of UCN-PNs. The as-prepared UCN-PNs have excellent dispersibility in nonpolar solvent (e.g., cyclohexane) and are stable for more than a year. As UCN-PNs exhibit excellent upconversion emission under 980 nm NIR excitation source and 140 femtosecond pulse duration at 80 MHz repetition rate, there is a vast ambit for using them in complex biolabeling by tuning their spectral properties. Further, for present available systems there are several draw backs in achieving good efficiency for the DNA detection,9 bio-imaging,10 sensors and fluorophores,11-13 analytes and several other important biomedical applications such as for the treatment of cancers14-17 which can be improved by using UCN-PNs.

[&]quot;School of Biomedical Engineering, Indian Institute of Technology, BHU, Varanasi 221 005, UP, India. E-mail: paik.bme@iitbhu.ac.in; pradip.paik@gmail.com

^bSchool of Engineering Sciences and Technology, University of Hyderabad, Hyderabad 500 046. Telangana, India

^cAdvanced Center of Research in High Energy Materials, University of Hyderabad, Hyderabad, Telangana, 500 046, India

[†] Electronic supplementary information (ESI) available. See DOI: 10.1039/c9ra06389g

Upconverting nanodots of NaYF4:Yb³+Er³+; Synthesis, characterization and UV-Visible luminescence study through Ti: sapphire 140-femtosecond laser-pulses

Monami Das Modak^a, Ganesh Damarla^b, K Santhosh Kumar^a, Somedutta Maity^a, Anil K Chaudhury^b and

Pradip Paik^{a,c*}

^a School of Engineering Sciences and Technology, University of Hyderabad, Hyderabad, Telangana, PIN: 500046

b. Advanced Center of Research in High Energy Materials, University of Hyderabad, Hyderabad, Telangana, PIN: 500046 Address here

^{c.}School of Biomedical Engineering, Indian Institute of Technology (IIT)-BHU, Varanasi, UP, PIN 221005

ABSTRACT: In this work, dot-sized upconversion nanocrystals (UCN-dots) with diameter c.a. 3.4 ± 0.15 nm have been synthesized. These UCN-dots exhibit visible emission (at $\lambda=497$, 527 and 545 nm) under the excitation with 980 nm CW-NIR laser. Further, these UCN-dots exhibit high energy upconversion emission (UV region, $\lambda=206$ to 231 nm) with Ti-Sapphire Femtosecond laser of 140-femtoseconds duration at 80 MHz repetition rate at different excitation, which has never been reported. This is interesting to report that the generation of high energy UV-Vis emission and their shifting from $\lambda=206$ to 231 nm for the UCN-dots by tuning the excitation wavelength ranging from $\lambda=950$ nm to 980 nm





http://pubs.acs.org/journal/acsodf

Article

Targeted and Enhanced Antimicrobial Inhibition of Mesoporous ZnO-Ag₂O/Ag, ZnO-CuO, and ZnO-SnO₂ Composite Nanoparticles

Monica Pandey, Monika Singh, Kirti Wasnik, Shubhra Gupta, Sukanya Patra, Prem Shankar Gupta, Divya Pareek, Nyshadham Sai Naga Chaitanya, Somedutta Maity, Aramati B. M. Reddy, Ragini Tilak, and Pradip Paik*



Cite This: ACS Omega 2021, 6, 31615-31631



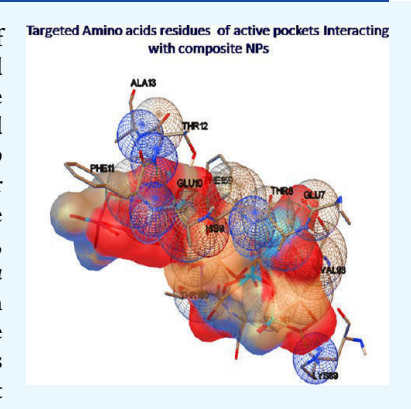
ACCESS

Metrics & More

Article Recommendations

Supporting Information

ABSTRACT: In this work, mesoporous (pore size below 4 nm) composite nanoparticles of ZnO-Ag₂O/Ag, ZnO-CuO, and ZnO-SnO₂ of size $d \le 10$ nm (dia.) have been synthesized through the *in situ* solvochemical reduction method using NaBH₄. These composite nanoparticles exhibited excellent killing efficacy against Gram-positive/negative bacterial and fungal strains even at a very low dose of 0.010 μ g/mL. Additionally, by applying the *in silico* docking approach, the nanoparticles and microorganism-specific targeted proteins and their interactions have been identified to explain the best anti-bacterial/anti-fungal activities of these composites. For this purpose, the virulence and resistance causing target proteins such as PqsR, RstA, FosA, and Hsp90 of Pseudomonas aeruginosa, Acinetobacter baumannii, Klebsiella pneumoniae, and Candida albicans have been identified to find out the best inhibitory action mechanisms involved. From the in vitro study, it is revealed that all the composite nanoparticle types used here can act as potent antimicrobial components. All the composite nanoparticles have exhibited excellent inhibition against the microorganisms compared to their constituent single metal or metal oxide nanoparticles. Among the nanoparticle types, the ZnO-Ag₂O/Ag



composite nanoparticles exhibited the best inhibition activity compared to the other reported nanoparticles. The microorganisms which are associated with severe infections lead to the multidrug resistance and have become a huge concern in the healthcare sector. Conventional organic antibiotics are less stable at a higher temperature. Therefore, based on the current demands, this work has been focused on designing inorganic antibiotics which possess stability even under harsh conditions. In this direction, our developed composite nanoparticles were explored for potential uses in the healthcare technology, and they may solve many problems in global emergency and epidemics caused by the microorganisms.

■ INTRODUCTION

Microbial contamination, adhesion, persistence colony formation on surfaces, and associated infections have become detrimental to public health and are causing massive alarm. The over usages of antibiotics lead to the development of resistant microbial strains which are the main cause of the antimicrobial resistance and persistent infection.² Thus, there is a high demand of efficient antimicrobial components that can resist the infection level. There are many organic, inorganic, and polymeric antibiotics, and each of them has their own advantages and disadvantages. Organic and polymeric antimicrobial agents are very much temperature sensitive, possess shorter lifetime, can degrade easily, and manifest various side effects in the long run.³ Therefore, constant efforts are necessary toward the development of new antimicrobial components to address these challenges with minimum side effects.

In the recent trends, nanoparticles (NPs) have also been explored as an efficient antimicrobial component mainly due to their unique mechanism of action, contact killing effect, the generation of reactive oxygen species (ROS), disruption of

DNA, disruption of cell membrane, and so forth.^{2,4–9} However, the field of material research is constantly progressing to accomplish the best antibiotics with optimum results. Materials such as metal and metal oxide NPs like ZnO (zinc oxide),⁵ CuO (copper oxide),¹⁰ SnO₂ (tin oxide),¹¹ and Ag₂O (silver oxide)^{12,13} NPs and different polymeric NPs have been reported and used for their antimicrobial properties. However, metallic/metal oxide NPs have been experimented and reported for the antimicrobial properties since time immemorial due to their unique way of interactions with the cellular components. By interacting with the thiol groups of enzymes, metallic/metal oxide NPs inactivate the cellular activities of proteins.¹⁴ Hence, further development of inorganic antimicrobial agents such as metal and metal oxide

Received: August 3, 2021 Accepted: November 8, 2021 Published: November 16, 2021





© 2021 The Authors. Published by American Chemical Society

RSC Advances



PAPER

View Article Online
View Journal | View Issue



Cite this: RSC Adv., 2022, 12, 1105

Targeted specific inhibition of bacterial and Candida species by mesoporous Ag/Sn-SnO₂ composite nanoparticles: in silico and in vitro investigation†

Monica Pandey,^a Kirti Wasnik,^b Shubhra Gupta,^b Monika Singh,^b Sukanya Patra,^b Premshankar Gupta,^b Divya Pareek,^b Somedutta Maity,^a Ragini Tilak^c and Pradip Paik **D** *

Invasive bacterial and fungal infections have notably increased the burden on the health care system and especially in immune compromised patients. These invasive bacterial and fungal species mimic and interact with the host extracellular matrix and increase the adhesion and internalization into the host system. Further, increased resistance of traditional antibiotics/antifungal drugs led to the demand for other therapeutics and preventive measures. Presently, metallic nanoparticles have wide applications in health care sectors. The present study has been designed to evaluate the advantage of Ag/Sn-SnO2 composite nanoparticles over the single oxide/metallic nanoparticles. By using in silico molecular docking approaches, herein we have evaluated the effects of Ag/Sn-SnO2 nanoparticles on adhesion and invasion responsible molecular targets such as LpfD (E. coli), Als3 (C. albicans) and on virulence/ resistance causing PgsR (P. aeruginosa), RstA (Bmfr) (A. baumannii), FoxA (K. pneumonia), Hsp90 and Cyp51 (C. albicans). These Ag/Sn-SnO2 nanoparticles exhibited higher antimicrobial activities, especially against the C. albicans, which are the highest ever reported results. Further, Ag/Sn-SnO₂ NPs exhibited interaction with the heme proionate residues such as Lys143, His468, Tyr132, Arg381, Phe105, Gly465, Gly464, Ile471 and Ile304 by forming hydrogen bonds with the Arg 381 residue of lanosterol 1 4α demethylase and increased the inhibition of the Candida strains. Additionally, the Ag/Sn-SnO2 nanoparticles exhibited extraordinary inhibitory properties by targeting different proteins of bacteria and Candida species followed by several molecular pathways which indicated that it can be used to eliminate the resistance to traditional antibiotics.

Received 13th October 2021 Accepted 15th December 2021

DOI: 10.1039/d1ra07594b

rsc.li/rsc-advances

1 Introduction

The multidisciplinary effort to develop new antimicrobial nanocomposites with efficient activities is one of the most promising advancements in composite science and has a tremendous societal and global health impact. The incorporation of known antimicrobial nanoparticles into polymeric, ceramic or metallic matrices has given rise to a new generation

of materials with improved properties/antibacterial activities.² Nanocomposites have great importance in the field of water treatment,³ food industry,⁴ biomedical and hospital management and in textile industries.⁵ Rapid development of these newly manufactured materials prevents microbial growth and is useful in resolving the current global health care crisis of antimicrobial resistance.⁶ Different nanoparticles (NPs) are increasingly used to target microbes as anti-microbial agents and are advantageous in preventing adhesion as well as treating microbial infections.

As an example, metallic or its oxide nanoparticles are in huge demand due to its physiochemical properties which are useful in fulfilling the various biomedical demands.⁷ Such as ZnO nanoparticles eliminate the possibilities of biofilm formation in medical instruments.⁸ Similarly, various types of nanomaterials are now extensively being explored as antimicrobial agents details of which have been reported by many research groups.^{9,10} These nanoparticles can bind to the any polymers, ligands, or

[&]quot;School of Engineering Sciences and Technology, University of Hyderabad, Telangana, 500046, India

^bSchool of Biomedical Engineering, Indian Institute of Technology, Banaras Hindu University (BHU), Varanasi, Uttar Pradesh, 221005, India. E-mail: paik.bme@ iitbhu.ac.in

Institute of Medical Sciences, Banaras Hindu University (BHU), Varanasi, Uttar Pradesh, 221005, India

[†] Electronic supplementary information (ESI) available: Fig. S1: EDS spectra, Fig. S2: results for antibacterial activities, Table S1: BET surface area analysis and average pore size distribution, Table S2 zeta potential analysis and Table S3 particle size analysis by zeta sizer. See DOI: 10.1039/d1ra07594b

ELSEVIER

Contents lists available at ScienceDirect

Materials Chemistry and Physics

journal homepage: www.elsevier.com/locate/matchemphys





Hollow mesoporous SiO₂–ZnO nanocapsules and effective *in vitro* delivery of anticancer drugs against different cancers with low doses of drugs

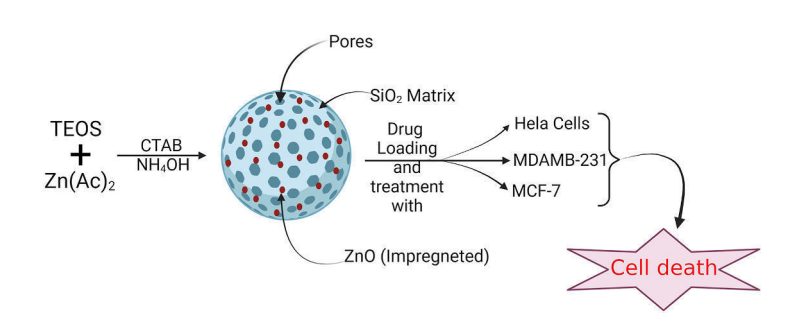
Gopabandhu Panigrahi^b, Himadri Medhi^b, Kirti Wasnik^a, Sukanya Patra^a, Premshankar Gupta^a, Divya Pareek^a, Somedutta Maity^b, Monica Mandey^b, Pradip Paik^a,*

^a School of Biomedical Engineering, Indian Institute of Technology, BHU, Varanasi, 221 006, UP, India

HIGHLIGHTS

- Biosafe spherical hollow and mesoporous SiO₂–ZnO nanocapsules.
- Formulation of SiO₂–ZnO nanocapsules with Imatinib and Paclitaxel.
- SiO₂–ZnO nanoformulation kill primary and triple negative breast cancer (TNBC).
- SiO₂–ZnO nanocapsules have huge clinical potential for targeted therapy.

GRAPHICAL ABSTRACT



ARTICLE INFO

Keywords: Hollow nanocapsules SiO₂–ZnO Imatinib Paclitaxel Sustained release Therapy

ABSTRACT

Spherical hollow and mesoporous SiO₂–ZnO nanocapsules were synthesized through sol-gel synthesis approach. Metabolic activity and biocompatibility of these nanocapules were tested and confirmed that SiO₂–ZnO nanocapsules are not toxic. Small biomolecules and drug can be loaded into the nanoparticles since they are mesoporous with hollow core. Further these nanocapsules are capable of loading a huge amount of anticancer drugs such as imatinib and paclitaxel. The sustained release of the drugs demonstrated that these functionalized nanocapsules are useful for various therapeutic applications with precise release of drugs such as for the cancer therapy with low doses. To check the therapeutic efficiency of these nanocapsules, HeLa cells (cervical cancer cell line), breast cancer cell lines such as MCF-7 (primary breast cancer) and MDA-MB-231 (triple negative breast cancer cell lines) were used for the study. For all cells the therapeutic efficiencies obtained are better than the treatment efficiencies obtained with the administration of the free drugs and it was found that the low doses are required for the treatment once the drug molecules are formulated with these nanocapsules. Results directed us that in future these nanocapsules may have a huge clinical potential to treat various diseases.

1. Introduction

Proper design of nanocapsules for sustained release of drugs to a

targeted area improves the pharmacodynamics and pharmacokinetic properties of various drug molecules as well as Therapeutic efficiency [1-12]. Sustained releases of drugs have many advantages over other

https://doi.org/10.1016/j.matchemphys.2022.126287

Received 26 January 2022; Received in revised form 10 May 2022; Accepted 16 May 2022 Available online 22 May 2022 0254-0584/© 2022 Published by Elsevier B.V.

^b School of Engineering Sciences and Technology, University of Hyderabad, Hyderabad, 500046, India

^{*} Corresponding author.

E-mail addresses: paik.bme@iitbhu.ac.in, pradip.paik@gmail.com (P. Paik).



A Review on Biodegradable Polymeric Materials for Bone Tissue Engineering (BTE) Applications

Prem S Gupta¹, Kirti Wasnik¹, Sukanya Patra, Divya Pareek, Monika Singh, and Somedutta Maity, School of Biomedical Engineering, Indian Institute of Technology (Banaras Hindu University), Varanasi, India Monica Pandey, University of Hyderabad. Hyderabad. India

Pradip Paik, School of Biomedical Engineering, Indian Institute of Technology (Banaras Hindu University), Varanasi, India

© 2021 Elsevier Inc. All rights reserved.

Introduction

Second-highest global burden is associated musculoskeletal condition with prevalence 61.6%. Worldwide 1.66 million people gone through hip fracture every year (Briggs et al., 2018; Kironde et al., 2019; Mondal et al., 2018; Yang et al., 2018). On the other hand, 20% people suffered from oral trauma, globally prevalent 117,402/years lived with disability (Lalloo et al., 2020; Bian et al., 2014). Current modernized approach in Bone tissue engineering (BTE) accelerates healing. BTE has clinical performances in treatment of complex skeletal defect arises due to traumatic injury, metabolic and/or genetic diseases. (Kim et al., 2016b).

Surgical orthopedic techniques improve osteogenic differentiation and avoids autograft-associated problems. However, this procedure is not satisfactory due to infections and chronic pain (Guerado and Caso, 2017). Tissue engineering (TE) promises new hope for future therapies of osseous defects. TE works on combinational approach between cells, scaffolds, growth factors and bioreactor (Sabir *et al.*, 2009; Dhandayuthapani *et al.*, 2011). A 3D-scaffold act as extracellular matrix (ECM), provides mechanical strength to surrounding tissue along with helping in adherence, stimulation, proliferation and differentiation of cells (Ghassemi *et al.*, 2018; Guo *et al.*, 2015a).

TE and regenerative-therapy although have promising secondary reconstruction technique but poses major challenges for achievement of biomechanically strong, well vascularized and physiologically-functional bone. Artificial bone materials should be biocompatible/ biodegradable, mechanical stable along with vascularization, osteoinductive, osteoconductive and regeneration properties. (Guerado and Caso, 2017; Lasanianos et al., 2010; Ghassemi et al., 2018). By incorporation of physiochemical and surface modification biodegradable polymer can mimic bone tissues and explicates great potential for providing ECM for cellular differentiation along with growth factors delivery potential to shorten healing time (de Gorter et al., 2011; Velasco et al., 2015). Advantages of using polymers have an advantage in BTE as its degradation product does not produce toxic substances (Kroeze et al., 2009). Further, biodegradable polymers can mimic to ECM and promote bone regeneration by stimulating immunomodulatory effects (Shi et al., 2016; Filippi et al., 2020).

Natural polymer mimics to bone components, presence of peptide enhance cellular adhesion but shows poor mechanical strength. However, synthetic biodegradable polymer shows advantages over natural polymers as they have excellent mechanical properties and are bioactive (Velasco et al., 2015). In this context different Biomaterials used in BTE along with their properties, advantages and disadvantages (Table 1).

Bone Microenvironment and Properties

Structurally, bones categorize into cortical (compact/dense) and cancellous (trabecular/spongy) bone. Cortical bone (80% of total bone mass) has osteon as functional unit house for bone forming cell osteoblast, osteocytes consists of central Haversian canal parallel to long axis of bone. Canal provides passage for nerve and blood vessels. Bone macro to Nano structure represented by (Fig. 1).

Natural bone is a composite material, consists of 60% minerals phase, 30% matrix phase and 10% water, which establish mechanical properties of bone. Presence of CaPO₄ called HAP (25–50 nm) nanocrystals along with inorganic compound provides compressive strength. Organic phase alters biochemical properties, composed of 90% of type I collagen and other materials mentioned (**Fig. 2**). ECM is responsible for calcification, where tiny bud in a matrix act as a nucleation site. (Velasco *et al.*, 2015; Razak, 2012; Qu *et al.*, 2019; Ste-Marie, 2012; Ott, 2018).

Bone Formation and Healing Mechanism

Skeletal/ craniofacial bone formation fallow the intramembranous ossification process for flat and lateral half clavicle bone and endochondral process for long bone formation. Nerve crest originates the intramembranous ossification especially appears in the calvarial and facial area. However, endosteal bone fallows both mechanism intramembranous and endochondral process. A mesenchymal cell is directly differentiated into blood capillaries, osteoblasts and creates the ossification center. Osteoblast produces osteoid (bone fibrous matrix tissue), and secreted osteoids accumulate in blood vessels and form random network of

¹Authors have contributed equally and can be considered both are as 1st authors.

Somedutta Maity

Email: someduhamity@uohyd.ac.in,someduttamaity31@gmail.com

Contact: +918919312233, +919492635233

LinkedIn:https://www.linkedin.com/in/somedutta-maity

Highly dedicated and devoted to work for achieving the proposed and desired goal. I ever excel myself by learning everything which comes in my way and helps me to work in a challenging environment. Pursue my research work in the challenging multidisciplinary advanced field of Nano science and Technology in order to be scientific, technical and innovative in upgrading my research-oriented knowledge by dedicated participation in the task.

Educational Details:

DEGREE	YEAR OF PASSIN G	Subjects	BOARD/University/Institute	% OF MARKS OBTAIN ED
Ph.D. (Pursuing)	2016- 2022	Nanobiotechnology	Hyderabad Central University (Working at School of Biomedical Engineering IIT BHU under the guidance of Dr. Pradip Paik)	
Post –graduation (M.Sc. biotechnology) (10+2+3+2)	2011- 2013	Cell Biology &genetics,Biomolecules &Biophysics,Microbiology,Biochemical tech&Biostatistics,Immunology,Enzymology,MolecularBiology,Bioenergetics, Genetic engineering,plantBiotechnology,AnimalBiotechnology,BioprocessEngineering,Bioinformatics,Medical&	GITAM Uuniversity Department Of Biotechnology	7.49(CGP A)
Canduction	2006	pharmaceutical Biotechnology.	The University Of Dyndyses	
Graduation B.Sc. Biotechnology (HONS.) (10+2+3)	2008- 2011	Chemistry of biomolecules, Genetics, microbiology, cell biology, Mathematics, commutative English, Physical& Organic chemistry, Molecular Biology, Cell & tissue culture, Recombinant DNA technology,Immunology,plantbiotechnology,An imalBiotechnology,Biostatistics& Bioinformatics	The University Of Burdwan Burdwan Institute of Management and Computer Science.	62.83%
Higher Secondary(10+2)	2007	Chemistry, Biological Science, physics, English, Bengali, Mathematics, Environmental Education.	West Bengal Council of Higher Secondary Education Durgapur Girls High School.	63.16%
Madhyamik (10)	2005	English, Bengali, Mathematics, Physical Science, Life Science, History, Geography.	West Bengal Board of Secondary Education Angadpur High School.	75%

Title of the Research Project Completed/Ongoing and highlights:

- 1.2020 "SITARE-Gandhian Young Technological Innovation (GYTI) Appreciations 2020" on Development of polymer based Nano medicine for the treatment of Cerebral Malaria.
- 2. Awarded/Selected CSIR-SRF, Year April-2020, under the project "Green synthesis of carbon dots from *Azadirahta indica*: in vitro and in vivo bio imaging and other applications".
- 3. As JRF: "Preparation of PLGA polymer Nano capsules delivery in domain III of envelope protein of all the four serotypes of Dengue virus" from school of Life Science, from Central University of Hyderabad. (December 2014 –August 2016).
- 4. M.Sc: "Cytotoxic Effects of Naproxen, Ketoprofen, Flubriprofen and Indomethacin on MDA-MB-231 Cell Line" (Cancer cell line) from Indian Association for the Cultivation of Science (Kolkata).
- 5. B.Sc.: "Extraction of ricin from castor seeds and its effects on micro-organisms".

Job Details: Worked at Thyrocare technologies Limited, Navi Mumbai from 29/08/2013 to 29/11/2014.

Projects Experiences

Preparation of polymer nanocapsules for drug delivery at school of Engineering Sciences and Technology (University of Hyderabad).(May2013-July 2013).

Technical Skills and Instruments Handled

Microbiology and cell biology: streaking and serial dilution methods, Staining techniques, MPN test, centrifugal techniques.

Biochemical Techniques: Estimation of proteins, glycine, carbohydrate.

Molecular Biology & Protein Techniques: Plasmid DNA isolation, Genomic DNA & m RNA isolation, PAGE, PCR(Polymerase Chain Reaction), ELISA, Protein isolation.

Cell Culture: Handled different explant cultures in Plant tissue culture, Cancer cell line.

Chromatography: Gel Filtration Chromatography, Thin Layer & Paper Chromatography, Column Chromatography, affinity chromatography.

Immunological Techniques: ELISA, Immunodiffusion, Electrophoresis techniques, handled various therapeutic kits, Agglutination test and latex.

Environmental biotechnology techniques: BOD, COD, OD.COD.

Bioinformatics tools: BLAST, SWISS Modeling, Phylogenetic tree construction methods, Gel Doc, PCR machines, UV Spectrophotometers, Calorimeters, Incubators, Centrifuges, Ultra centrifuges.

Animal Handling: Mice handle.

Computational skills: .Microsoft Word, Excel, PowerPoint.

Patent Filed:

- 1. A method of synthesizing carbon dots and a product thereof, Application No.: 202011018557, Dated: 30th April, 2020.
- 2. Reparation of carbon nanocapsules from azadirachtaindica seed for the treatment of breast cancer, application no.: 202111060434, dated: 23-12-2021.

Publications:

- 1. **Maity, Somedutta;** Tomar, Munendra; Wasnik, Kirti; Patra, Sukanya; Modak, Monami; Gupta, Prem Shankar; Pareek, Divya; Singh, Monika; Paik, Pradip. AzadirachtaIndica seed derived carbon nanocapsules: cell imaging, depolarization of mitochondrial membrane potential and dose dependent control death of breast cancer. **ACS Biomater. Sci. Eng.** 2022, 8, 8, 3608–3622.
- 2. Medhi, Himadri; **Maity, Somedutta**; Suthram, Niranjan; Chalapareddy, Suresh; Bhattacharyya, Mrinal; Paik, Pradip Hollow mesoporous polymer capsules with Dihydroartemisinin and Chloroquinediphosphate for knocking down Plasmodium falciparum infection, Biomed. Phys. Eng. Express, 2018, 4, 035006.
- 3. SumbulAfroz, HimadriMedhi, **Somedutta Maity**, GillipsieMinhas, SrikanthBattu, JeevanGiddaluru, Koushi Kumar, Pradip Paik and Nooruddin Khan; ZnOnanocapsules for the induction of enhanced antigen-specific immunological responses, **Nanoscale**.
- 4. Gopabandhu Panigrahi; HimadriMedhi; KirtiWasnik; SukanyaPatra; Premshankar Gupta; DivyaPareek; **Somedutta Maity**; Monica Pandey. Hollow Mesoporous SiO2-ZnO Nanocapsules and effective in vitro delivery of anticancer drugs against different cancers with low doses of drugs.
- 5. Pandey, Monica; Wasnik, Kirti; Gupta, Shubhra; Singh, Monika; Patra, Sukanya; Gupta, Prem Shankar; Pareek, Divya; **Maity, Somedutta**; Tilak, Ragini; Paik, Pradip, "Target specific inhibition of bacterial and Candida species by mesoporous Ag/Sn-SnO2

composite nanoparticles: in silico and in vitro investigation"

- 6. Pandey, Monica; Singh, Monika; Wasnik, Kirti; Gupta, Shubhra; Patra, Sukanya; c; Pareek, Divya; ChaitanyaNyshadhamsai Naga; **Maity, Somedutta**; Reddy, Aramati; Tilak, Ragini; Paik, Pradip, "Targeted and Enhanced Antimicrobial Inhibition of MesoporousZnO–Ag2O/Ag, ZnO–CuO, and ZnO–SnO2 Composite Nanoparticles".
- 7. Monami Das Modak, Ganesh Damarla, K. Santhosh Kumar, Somedutta Maity, Anil K. Chaudhury and Pradip Paik, Upconvertingnanodots of nayf4yb3er3 synthesis characterization and uv visible luminescence study through ti sapphire 140 femtosecond laser pulses,arXiv:2008.06783, (2020), 18th August, 2020,(http://arxiv.org/abs/2008.06783).
- 8. Monami Das Modak, Ganesh Damarla, **Somedutta Maity**, Anil K. Chaudhary and PradipPaik, "Self- assembled Pearl-necklace patterned upconvertingnanocrystals with highly efficient blue and ultraviolet emission: femtosecond laser based upconversion properties", RSC Adv., 2019, 9, 38246-38256 **RSC Adv.**
- 9. Pradip Paik, K. Santhosh Kumar, Monami Das Modak, Koushi Kumar U and **Somedutta Maity**, UCN–SiO2– GO: a core shell and conjugate system for controlling delivery of doxorubicin by 980 nm NIR pulse, RSC Adv., 2018,8, 37492-37502. RSC Adv.

Manuscript under Preparation:

- 1. Green synthesis of Carbon Nano dots from Kernel part of Azadirachta Indica seeds::selective detection of biologically relevant metal ions and drug delivery applications.
- 2. Detection and Seperation of heavy metals by Carbon nanoparticles (CDs) synthesized from Kernel part of Azadirachta Indica .
- 3. Revealing the structures of cellulose from bark Azadirachta indica, antimicrobial activity and Their Application: An in vitro study.

Book chapter

1.Gupta, Prem Shankar; Wasnik, Kirti; Patra, Sukanya; Pareek, Divya; Singh, Monika; **Maity, Somedutta**; Pandey, Monica; A Review on Biodegradable Polymeric Materials for Bone Tissue Engineering (BTE) Applications.

Presentation and proceedings/conferences:

1. <u>Somedutta Maity</u> and Pradip Paik, Synthesis and Novel properties of Carbon Nano dots and Its Applications Third International Conference on Advanced Materials (ICAM 2019) 9-11 August 2019 at Mahatma Gandhi University, Kottayam, Kerala, India. (Poster).

- 2. <u>Somedutta Maity</u> and Pradip Paik, Synthesis of poly (dl-lactide-co-glycolide) nanoparticles based on double emulsion method as a carrier system of protein delivery and its effect in immunological responses. Advances in polymer science and rubber technology, September 24-27, 2019 (APSRT,) IIT Kharagpur, India, (Poster).
- 3. <u>Somedutta Maity</u>, K. Santhosh Kumar, Monami Das Modak, Koushi Kumar U, Pradip Paik, UCN-SIO2– GO conjugate system for controlling delivery of doxorubicin by 980nm NIR pulse and intervention of cancer, 4th International Conference on "Nanotechnology for Better Living" April 6-7, 2019 IIT Kanpur. (Poster).
- 4. HimadriMedhi, SumbulAfroz, <u>Somedutta Maity</u>, Nooruddin Khan Pradip Paik, Nanostructured mesoporousZnO material for the enrichment of immunological response, NanoSciTech 2017, 9-10 Nov. 2017, (Poster).
- 5. Participated in the CME & Workshop on "Quality Forum For Bench Technologists Phase –II" Hyderabad on 3rd May 2019.
- 6. Participated in the **Frontiers in Nano science and technology** 6-7 April 2018, Centre for Nanotechnology University of Hyderabad.
- 7. Participated in one day **Workshop on Advanced Engineering materials: An Industry Perspective** on 25th November 2016, University of Hyderabad.
- 8. Participated in **Use of Radiation Technology In Agriculture, health And Research** University Of Hyderabad- Bhabha atomic Research Center, School of Life Sciences, University of Hyderabad 0n 13th November 2015
- 9. Participated in National **Applications of Atomic Energy** (February 22-23, 2012) GITAM University.
- 10. Participated in National Conference on **Present Relevance of Ancient Indian Sciences** (14-15 September 2011).

Research work referred in reputed newspaper and magazines:

- 1.THE HANS INDIA, Feb 25, 2018, has published a report entitled "Hyderabad varsity researchers develop nanomedicine" for malaria treatment".
- 2.DECCAN CHRONICLE, Feb 25, 2018, has published a report entitled "Nanomedicine for malaria treatment."
- 3.THE HINDU BUSINESS LINE, Feb 26, 2018 has published a report entitled "Hyderabad varsity team develops" nano-drug delivery system to neutralize malaria parasite."
- 4. THE INDIAN EXPRESS, Feb 25, 2018, has published a report entitled "University of Hyderabad team develops medicine to kill deadly malaria parasite."
- 5. NANO DIGEST May 2018 has published a report entitled "Polymer-based Nano medicine for the treatment of Malaria.".

Hobbies & Interest:

- Reading books and gaining knowledge.
- Athletic meet, gardening.
- Listening Music,
- Dancing, Surfing Net.

Strength

- Ability to work hard with punctuality and positive attitude.
- Ability to Face challenges.
- Forming a Team easily.
- Self motivator and high self Confidence.

Personal Information

Name : Somedutta Maity K
FatherName : Mr.Kashi Nath Maity
MotherName : Mrs. SuraviMaity
DateofBirth : 16thseptember1989

Gender : Female Passport/Nationality : Indian

LanguagesKnown : English, Hindi, and Bengali.

MobileNo : +918919312233

Email : <u>someduttamaity31@gmail.com</u>

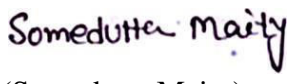
PermanentAddress : C/O: Mr. KashiNathMaity

Angadpur, Durgapur State: - West

Bengal, Pin No: - 713215

DECLARATION:

I do hereby declare that the above statement given by me is true to the best of my knowledge and belief and I look for a chance to prove my competency.



(Somedutta Maity)